UNIVERSIDAD
DE GRANADA

Doctoral Program in Earth Sciences

Department of Geodynamics

Geomorphological, seismic and geological interpretation of Neogene to recent deformations in northern Tunisia

Seifeddine GAIDI

Guillermo Booth Rea

Melki Fetheddine

University of GRANADA 2022

UNIVERSIDAD
DE GRANADA

Programa Doctorado
Ciencias de la Tierra

Editor: Universidad de Granada. Tesis Doctorales
Autor: Seifedine Gaidi
ISBN: 978-84-1117-560-9
URI: https://hdl.handle.net/10481/77675

Abstract

This Thesis analyses the tectonic evolution of Northern Tunisia from the Late Miocene to Present, using multiscale and multisource data analyses involving new technologies and approaches. Two orthogonal extensional systems with ENE- and SE-directed transport produced the extensional collapse of the Tell and Atlas thrust belts in northern Tunisia during the Late Miocene to Pliocene in a context of NW-SE plate convergence between Africa and Eurasia. This new hypothesis suggests for the first time the importance of crustal extension in the denudation of the Tunisian Atlas and Tell foreland thrust belts, which we related to deep mantle tectonic mechanisms, known as a common feature in other FTB´s in the western Mediterranean, i.e. Betics, Rif, Calabria and Apennines. Low-angle normal faults have extended and reworked the Tunisian Tell external foreland thrust belt, exhuming midcrustal epizonal Triassic metapelites and forming Late Miocene basins. This extension was followed by later Pliocene to Present tectonic inversion, developing the active shortening structures in Northern Tunisia. The main shortening structure is formed by different reverse and strike-slip fault segments, linked forming the 130 km long Alia-Thibar shear zone. Restored Plio-Quaternary deformation observed on reflection seismic lines indicates deformation rates around 0.6-0.8 mm/yr in the studied segments and larger amounts of shortening to the West of Northern Tunisia (16%) than to the East (7%), which suggests that tectonic inversion started earlier to the West and later propagated eastwards, reaching Northeastern Tunisia in the Late Pliocene. Due to the young age of tectonic this inversion, the present relief of Northern Tunisia is characteristic of a young thrust and fold belt, with dominating axial valleys along synforms and an incipient transverse drainage development propagating from West to East. New topographic development is favouring slope instabilities. Thus, in addition, we used a interdisciplinary approach, including Interferometric Synthetic Aperture Radar (InSAR) technologies to analyse the Chgega active landslide, or more specifically as vast rock spreading that evolved into a block slide, characterizing a progressive movement without clear episodic accelerations.

Key words

Active tectonics – Crustal extension – Eurasia-Africa Convergence – Northern Tunisia – Morphotectonics – Fault segmentation – InSAR technologies – Active Landslide – Plio-Quaternary

Abstract

En la presente Tesis doctoral analizamos la evolución tectónica del Norte de Túnez desde el Mioceno Superior hasta el presente, usando una metodología multidisciplinar que incluye el análisis tectónico y morfométrico de la región. El cinturón de pliegues y cabalgamientos del Tell tunecino fue adelgazado por dos sistemas extensionales ortogonales con transporte hacia el ENE y ESE, respectivamente, entre el Mioceneo Superior y el Plioceno en un contexto de convergencia NW-SE entre las placas Africana y Euroasiática. Esta nueva hipótesis sugiere por primera vez la importancia de la denudación extensional en el cinturón orogénico del Tell tunecino, en relación con mecanismos tectónicos profundos, como delaminación del manto litosférico subcontinental, descritos en otros cinturones de pliegues y cabalgamientos del Mediterráneo occidental como las Béticas, Rif, Calabria o los Apeninos. Fallas normales de bajo ángulo han extendido el cinturón de cabalgamientos exhumando rocas metamórficas situadas a la base del prisma orogénico a profundidades de corteza media, concomitántemente al desarrollo de cuencas sedimentarias del Mioceno Superior. Esta extensión fue seguida de una inversión tectónica contractiva desde el Plioceno, formándose las presentes estructuras transcurrentes y fallas inversas activas en el norte de Túnez. El principal zona de falla transcurrente de la region es la zona de falla de Alia-Thibar, con una longitud total de 130 km y compuesta por hasta 5 segmentos unidos, con diferente cinemática. La restauración del acortamiento observado en diversas lineas de sísmica de reflexión paralelas a la dirección de acortamiento indica tasas de acortamiento de 0,6-0,8 mm/año en los segmentos estudados y valores de acortamiento mayores al oeste de Tunez (16%) que hacia el este (7%). Esto podría indicar que la inversión tectónica se inició antes hacia el oeste y se ha propagado posteriormente hacia el este, afectando al NE de Túnez a partir del Plioceno superior. El relieve del norte de Túnez es característico de un cinturón de pliegues y cabalgamientos joven, con dominio de sistemas fluviales axiales a lo largo de sinformes y el desarrollo de un sistema de drenaje transverso incipiente, que se propaga de oeste a este. Este nuevo crecimiento topográfico está favoreciendo la inestabilidad de laderas. Por ello, hemos usado una metodología interdisciplinar, incluyendo el análisis interferométrico de radar (InSAR) para estudiar el deslizamiento activo de Chgega, caracterizado por un movimiento progresivo sin aceleraciones episódicas claras.

Palabras clave

Tectónica activa – Extensión cortical – Convergencia Africa-Eurasia – Norte de Túnez – Morfotectónica – Segmentación de fallas – Tecnología InSAR – Deslizamiento activo – Plio-Cuaternario

Résumé

La thèse présente et discute l'activité tectonique du nord de la Tunisie du Néogène, en se basant sur des analyses de données multi-échelles et multi-sources impliquant de nouvelles technologies et approches. Le présent manuscrit met en évidence deux systèmes d'extension orthogonaux avec un transport ENE et SE, produisantt l'effondrement des structures du Tell et de l'Atlas dans le nord de la Tunisie du Miocène supérieur au Pliocène dans un contexte de convergence des plaques NW-SE entre l'Afrique et l'Eurasie. Cette nouvelle hypothèse suggère pour la première fois l'importance de l'extension crustale dans la dénudation des limites de chevauchement de l'Atlas tunisien et de l'avant-pays du Tell qui est liée aux mécanismes tectoniques au niveau du manteau profond, connue comme une caractéristique commune pour d'autres FTB en Méditerranée occidentale, la Bétique et Rif. L'interprétation de la cristallinité de l'illite effectuée sur des métapélites du Trias correspond au modèle d'effondrement polyphasé orogénique tardif, mettant en cause l'évolution diapirique à longue durée de vie proposée précédemment dans des travaux antérieurs.

Les structures compressives actives dans le nord de la Tunisie se sont développées par inversion tectonique depuis le Pliocène. La déformation plio-quaternaire est mise en évidence à travers des lignes sismiques réflexions qui caractérisent, via restoration de coupes, des taux de déformation autour de 0,6-0,8 mm/an dans les segments étudiés et des raccourcissements plus importants du Nord-Ouest (16 %) vers le Nord-Est (7 %) de la Tunisie. De ce fait, l'inversion tectonique a commencé vers l'Ouest et s'est ensuite propagée vers l'Est, atteignant le Nord-Est de la Tunisie à la fin du Pliocène. En raison du jeune âge de cette inversion tectonique, le relief actuel du nord de la Tunisie est caractéristique d'un jeune ensemble de chevauchement et de plis, avec des vallées axiales dominantes le long des synformes et un début de développement de drainage transversal se propageant d'Ouest en Est. De plus, les technologies du radar interférométrique à synthèse d'ouverture (InSAR) ont révélé que la structure de Chgega est un glissement de terrain complexe actuellement actif, ou plus précisément comme un vaste étalement de roches qui a évolué en un glissement de blocs, caractérisant un mouvement progressif sans accélérations épisodiques claires identifiées.

Mots clés

Tectonique active – Extension – Convergence Eurasie-Afrique – Nord de la Tunisie – Morpho-tectonique – Segmentation des failles – Technologies InSAR – Glissement actif – Plio-Quaternaire, Néogéne.

Acknowledgments

This study was supported by research projects CGL2015-67130- C2-1-R, ***Erasmus Mundus External Cooperation*** *Window and by Scientific Cooperation Agreement 0534 between the* ***Office National des Mines (ONM)****, the* ***Tunis el Manar University*** *and the* ***Group for Relief and Active Processes Analysis (ARPA) from the University of Granada****. Proyecto del Ministerio de Ciencia e innovación PID2019-107138RB-I00 and P18-RT- 3632 of the Junta de Andalucia. We are grateful to the* ***Tunisian Company of Petroleum Activities (ETAP)*** *for sharing their Reflection Seismic Data.* ***Midland Valley Exploration Ltd*** *is gratefully acknowledged for supporting ASI (Academic Licence Initiative) and providing Academic licenses of* ***Move™*** *to the* ***Department of Geodynamics of the Granada University****.*

Chapter 1: Introduction

1. Background

Active tectonics is the study of the dynamic earth processes, how they shape the landscape and influence human society. Tectonic geomorphology is one of the principal tools used increasingly in a variety of applications including identification of active tectonic features, seismic hazard mapping and development of the earth's landscapes (Keller, E.A., and Pinter, 2002). Tectonic geomorphology has proven to be useful in these applications because landforms are created and preserved over time intervals ideal for recording details of tectonic activity (Keller, E.A., and Pinter, 2002).

The period necessary to study active tectonics, is more like several million years.
In order to predict tectonic events over time, we must study the proceses over a much longer time scale from several hundred years to several tens of thousands of years. The argument is that present tectonic activity and the tectonic framework (geometry and mode of operation of structures) controls the related deformation.

This discipline is growing due to the development of new geomorphological tools and new technologies, which facilitate the acquisition of accurate rates of different processes like uplift, incision, erosion, and fault slip, at variable time scales (Schumm et al., 2000; Keller, E.A., and Pinter, 2002; Bull, 2011; Burbank and Anderson, 2011).
Relief analysis is a good tool to detect and characterize active tectonic structures in regions with low to moderate tectonic activity (Keller and Pinter, 2002; Molin et al., 2004; Pedrera et al., 2009; Pérez-Peña et al., 2009b, 2010; Azañón et al., 2012). The combination of different morphotectonic indices allows differentiating uplifting from subsiding regions at different scales. This approach together with a geomorphological study and field ground-truthing work of the region helps to discriminate between different mechanisms that may influence topography and associated drainage networks in the north of Tunisia during the Neogene to quaternary.

The study of active structure needs the combinations of new technologies and classic methods like geological field data acquisition, very useful in this case for verifications and validations. Using Interferometric Synthetic Aperture Radar (InSAR) technologies and Uncrewed Aerial Vehicle UAV-DP will help us to prove the activity of structures in the study area.

The main objective of this PhD Thesis is to analyze the tectonic evolution of Northern Tunisia from the late Neogene until Present. For this, we revise and digitize the existing 1:50.000 geological maps of the region. A special effort was done to distinguish between extensional and contractive structures and to evaluate the role of extensional thinning in the Tunisian Tell present structure. Recent deformation in the region was analyzed by structural mapping and with the aid of morphotectonic relief analysis. We carried out a multidisciplinary approach mainly founded on the integration of different data sets. We employed structural fieldwork, morphometry GIS based methods and tools, Interferometric Synthetic Aperture Radar (InSAR) technologies and Uncrewed Aerial Vehicle UAV-DP in order to define the kinematics and most active structure in the north of Tunisia.

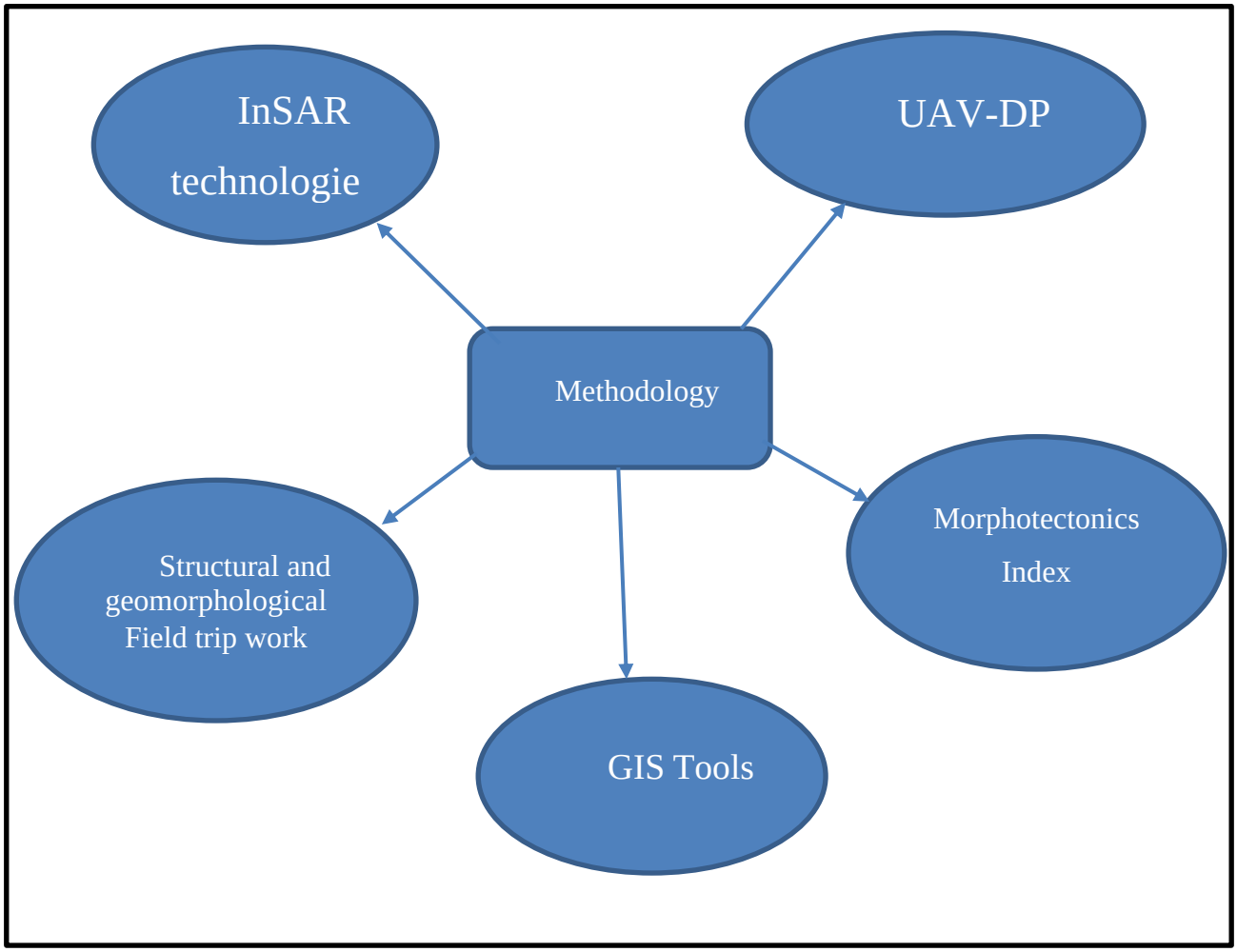

Figure 1-1 Shema of different technologies merged in this thesis into a single imaging system

2. Objectives of this thesis

The present thesis is the result of collaboration between the University of Tunis El Manar and the University of Granada. Through the following thesis work, we have analyzed the Late Neogene to recent deformation of Northern Tunisia combining different approaches: (1) field and structural geology analysis, (2) morphotectonics, (3) InSAR technologies, and (4) geophysical data interpretation.

The objectives of the thesis are summarized in two main points:

- Evaluation of the interplay between different mechanism that may influence the tectonic activity in Northern Tunisia at different scales, like upper-mantle structure and horizontal shortening related structures.
- Determination of the active tectonic structures in Northern Tunisia from Neogene to Quaternary.

Thus, this thesis presents a multidisciplinary focus from the beginning, on one hand using traditional Structural Geology tools to analyze the structure and tectonic evolution of Northern Tunisia during the late Neogene (i.e. field mapping, fault characterization, fault kinematic analysis, paleo stress analysis, interpretation, balancing and restoration of reflection seismic lines, illite crystallinity), together with morphotectonic analysis using geomorphic indices to aid in the determination of active deformation (Landslide, actives structures) and fault segmentation in the region. Following this approach, we map some of the possibly main active faults in the region and survey potential capture sites, wind gaps, and fluvial terraces, looking for evidence of recent deformation like striated pebbles in river terraces and seismogenic related structures.

In order to characterize an example of active landslide, we combined modern techniques, such as morphometrical analysis of DEMs and interpretation of aerial photographs, orthoimages and, hillshade model in a GIS environment, along with analysis of terrain 3D to extract virtual measurements. Additionally, we performed preliminary InSAR analysis to roughly estimate the regime and velocity of the landslide movement.

3. Outline of the thesis

This thesis was written as an article-based manuscript. It presents six independent chapters. Each chapter (2, 3, 4 and 5) has its own abstract, introduction, methodology, discussion and conclusion. Each chapter except chapter three (under preparation) was published in

international JCR journals corresponding to Tectonics, Journal of Structural Geology and Remote Sensing, respectively. Therefore, we will discuss and present our findings by a set of consecutive chapters as follows:

In the **introduction** (**chapter 1**), we provide some introductory notions and present the main objectives of the thesis and illustrate the aims and motivations behind this work.

Chapter 2: Provides the main result of the paper published in Tectonics entitled: Late Miocene Extensional collapse in the north of Tunisia. This paper proposes a new geological interpretation for northern Tunisia determined by its extensional collapse in the late Miocene.

Two orthogonal extensional systems produced the extensional collapse of the Tell and Atlas thrust belts in northern Tunisia during the Late Miocene to Pliocene in a context of NW-SE plate convergence between Africa and Eurasia. This new hypothesis shows for the first time the importance of crustal extension in the denudation of the Tunisian Atlas and Tell foreland thrust belts and its relation to deep mantle tectonic mechanisms.

Chapter 3: This chapter is not yet published and is submitted to be considered for publication in Tectonics with tittle: Halokinesis and ductile flow during Late Miocene extension in the Tunisian Tell and the thinning of Western Mediterranean Foreland Thrust Belts (FTB´s): We propose a new model explaining the presence of epizonal Triassic rocks in the core of three domal structures from northern Tunisia, which are classically interpreted as diapirs. We show that the deepest domal structures in the region are not diapirs, but are actually cored by greenschist-facies marbles and metapsamnites, exhumed by the activity of late Miocene low-angle normal faults, which have been imaged in seismic reflection profiles. Based on illite crystallinity of Triassic metapelites, the epizonal to anchizonal values impose a model of late orogenic collapse of the Tunisian Foreland Thrust Belt (FTB) from mid-crustal levels instead of a long-lived diapiric evolution since the Cretaceous. This late extensional collapse and exhumation of midcrustal rocks in foreland type settings is a common feature of other FTB´s in the Western Mediterranean, like the Betics, Rif and Apennines, which underwent a late stage tearing or delamination of their subcontinental lithospheric mantle at the edges of the subduction systems.

Chapter 4: Provides the main result of the paper published in the Journal of Structural Geology entitled: Active fault segmentation in northern Tunisia. In this paper, we propose

active shortening structures in northern Tunisia developed by tectonic inversion since the Pliocene.

Using restored and balanced seismic reflexion lines, we measured Plio-quaternary shortening rates around 0.6-0.8 mm/yr in the studied segments and larger amounts of shortening to the West of Northern Tunisia (16%) than to the East (7%). We suggest tectonic inversion started earlier to the West and after propagated to the East in the late Pliocene.

Using morphotectonic analysis with the aim of field fault mapping, we identify the main shortening fault system and its segmentation in Northern Tunisia, which shows a helicoidal geometry with five different segment including reverse, dextral and oblique faults with a total length of 130 km, named the Alia –Thibar fault. The present relief of Northern Tunisia is characteristic of a young thrust and fold belt, with dominating axial valleys along synforms and an incipient transverse drainage development propagating from West to East.

Chapter 5: Provides the main result of a paper where we study the influence of recent topographic growth in Tunisia on landslide development, published recently in a special issue: Slope Stability Monitoring and Investigation Using Remote Sensing Techniques in Remote Sensing, in the section: Remote Sensing in Geology, Geomorphology and Hydrology. This paper is entitled "Analysis of the geological controls and kinematics of the Chgega landslide (Mateur, Tunisia) exploiting photogrammetry and InSAR technologies".

We studied a large complex landslide identified in Northern Tunisia, which stands out for its singular characteristics. One of them is a spectacular graben structure that breaks the ridge of the hill affected by the mass movement, in the Chgega Mountain.

Using Interferometric Synthetic Aperture Radar (InSAR) technologies, we demonstrate that this complex landslide is currently active and shows progressive movement without clear episodic accelerations. The velocity of the limestone block is just above 2 mm/yr. These results were obtained through the analysis of a 3D model and a high-resolution orthoimage created from photographs acquired by an Uncrewed Aerial Vehicle (UAV). We may conclude that the landslide movement is determined by normal faults with directions N060◦E and N140–150◦E. This characterization of the Chgega landslide can serve as the basis for future studies about the origin of this slope movement.

Chapter 6: This final chapter will be a summary of the outcomes of the present research, with the discussion of our results integrating the various methods used to study different parts of the Tell of Tunisia and presentation of some future perspectives.

Chapter 2: Late Miocene Extensional Collapse of Northern Tunisia

Two orthogonal extensional systems produced the extensional collapse of the Tell and Atlas thrust belts in northern Tunisia during the Late Miocene to Pliocene in a context of NW-SE plate convergence between Africa and Eurasia. The older extensional system shows several low-angle normal faults (LANFs) and associated high-angle faults with ENE-directed transport that produced half-grabens and hanging-wall syncline basins during the late Tortonian to Messinian. The direction of extension swinged towards the SE during the Messinian, cutting into, and tilting the previous detachments. Extension was accompanied by the extrusion of 8-Ma rhyodacites and Messinian basalts, together with the development of mineralized fault breccias. Plio-Quaternary NW-SE directed shortening formed inversion arrowhead structures, reverse faults, refolded extensional rollover anticlines and folded the LANFs. ENE-directed extension is concomitant with the opening of the Tyrrhenian basin. We consequently think that both processes are related and that tearing of the Calabrian slab along the northern Tunisia coast drove the ENE-directed extension. Meanwhile, the SE-directed extension that followed was probably related to SE-directed peeling back of the Tunisian continental lithospheric mantle during NW subduction of the Maghrebian margin. This extension propagated eastwards from the late Tortonian until the Pliocene following the SE migrating subduction front and favored by lateral slab tearing along the Tunisian Atlas dextral Subduction Transfer Edge Propagator boundary. This new hypothesis for the tectonic evolution of northern Tunisia shows for the first time the importance of crustal extension in the denudation of the Tunisian Atlas and Tell foreland thrust belts and its relation to deep mantle tectonic mechanisms

* Most of the content of this chapter corresponds to the following article: Booth-Rea, Gaidi, S., Melki, F., Marzougui, W., Azañón, J.M., Zargouni, F., Galvé, J.P., Pérez-Peña, J. V., Al, 2018. Late Miocene extensional collapse of Northern Tunisia. Tectonics 37, 1626–1647. https://doi.org/10.1029/2017TC00484

1. Introduction

Extensional denudation has been described coeval to plate convergence in most of the circum Mediterranean orogens. It has contributed to the thinning of crustal domains and exhumation of meta-morphic rocks in the hinterland of the Alps, Cyclades, Betics, Appenines, and Rif, among others(Lister et al., 1984; Selverstone, 1988; Platt and Vissers, 1989; Carmignani and Kligfiel, 1990; Booth-Rea, 2012). Moreover, it has formed deep basins floored by oceanic crust or exhumed mantle in back arc settings like the Algerian or Tyrrhenian basins in the core of the orogenic arcs (Booth-Rea et al., 2007; Prada et al., 2016) (Figure 2.1). Fewer cases have been described of extensional denudation of foreland thrust belts (FTBs). Although, this may occur related to the particular dynamics of FTBs (McIntosh et al., 1993; Booth-Rea et Al, 2008; Jimenez-Bonilla et al, 2016) Extension of FTBs has also occurred at the edges of migrating subduction systems like the Gibraltar arc, when lithospheric tearing has propagated under the FTB continental crust region (Pérez-Valera et al., 2013; Mancilla et al., 2015). Inboard of Subduction Transfer Edge Propagator (STEP) boundaries(Govers and Wortel, 2005) continental crust can undergo peeling of its mantle lithosphere (Levander et al., 2014). This tectonic mechanism has been described as edge delamination in the Betics and Rif (Duggen et al., 2003; Martínez-Martínez et al., 2006; Mancilla et al., 2015). Delamination of the continental mantle lithosphere and its substitution by a hotter asthenospheric mantle can drive regional topo-graphic uplift, extension, and volcanism (Bird, 1979; Kay and Mahlburg Kay, 1993; Currie et al., 2005; Göğüş and Pysklywec, 2008; Göğüş et al., 2011; Mancilla et al., 2015).STEP boundaries have been defined in most of the branches of the Mediterranean orogens permitting the advance of narrow subduction zones like the Gibraltar or Calabrian arcs (Govers and Wortel, 2005; Argnani, 2009; Mancilla et al., 2015; Polonia et al., 2016), Figure 2.1. This is the case of the southern edge of the Calabrian arc that swiped eastwards through the north-ern Tunisian margin and Sicily from the Tortonian until present, during the development of the Tyrrhenian basin (Faccenna et al., 2005; Chiarabba and Palano, 2017). Extension in the western Mediterranean has been driven mostly by mantle tectonic mechanisms like slab rollback, slab tearing, and detachment or peeling of the continental mantle lithosphere during subduction, in a setting of NW-SE convergence between Africa and Eurasia (Lonergan et al., 1997; C. Maury et al., 2000; Faccenna et al., 2004; Spakman and Wortel, 2004; Mancilla et al., 2015). Thus, understanding the upper mantle evolution is crucial to explain the extensional processes that have affected the western Mediterranean.

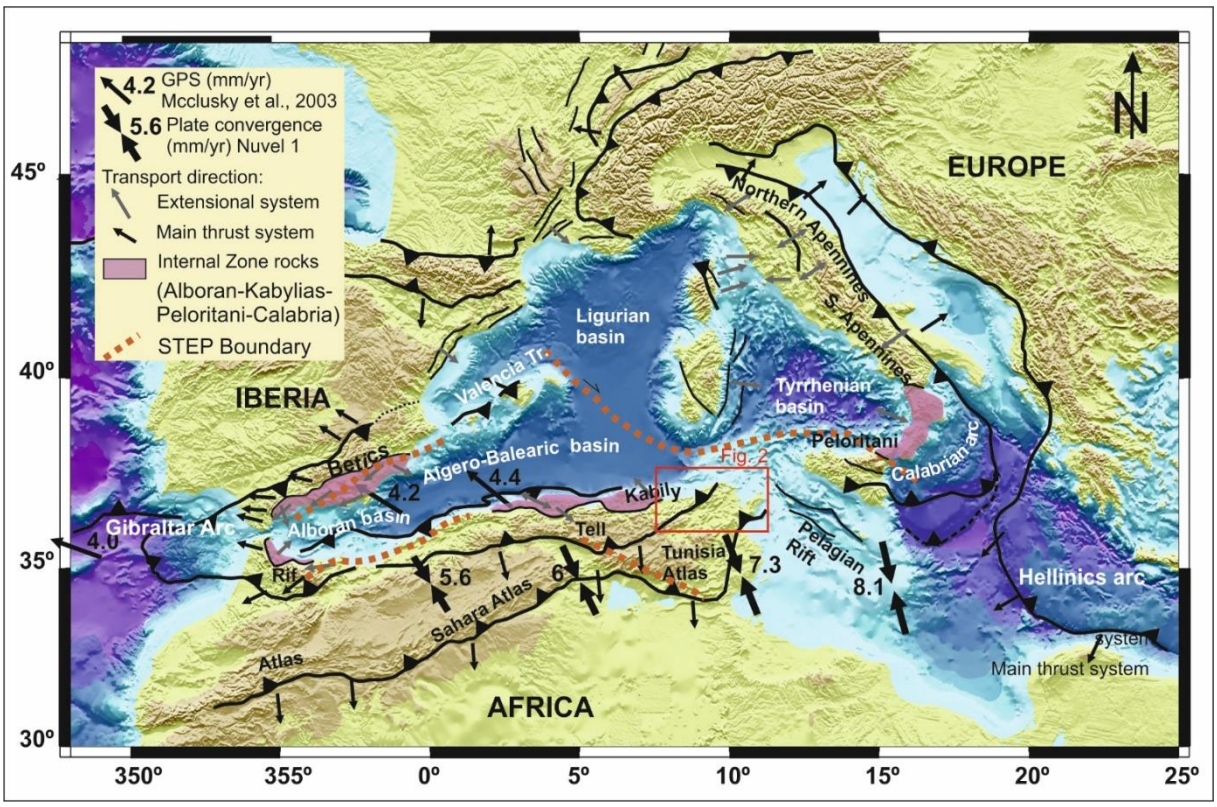

Figure 2-1 : *Tectonic sketch of the western Mediterranean basins and orogens. Modified from Booth-Rea et al. (2007).*

The tectonic evolution of northern Tunisia has been described in terms of the shortening and transcurrent structures developed under NW-SE convergence between Africa and Eurasia since the Paleogene(Zargouni.F, 1984; Frizon De Lamotte et al., 2000; Mzali and Zouari, 2006; Khomsi et al., 2009; Melki et al., 2010, 2011; Essid et al., 2016). Under this convergent setting the Tellian nappe stack developed, supposedly, together with important elongated diapiric structures cored by Triassic rocks parallel to NE-SW strike-slip and reverse faults. Normal faults in this setting are interpreted as subsidiary structures formed under SW-NE extension during the Pliocene-Quaternary or as very shallow extension affecting the Numidian units, related to FTB dynamics (Bouaziz et al., 2003; Khomsi et al., 2009; Belguith et al., 2011, 2013; Ramzi et al., 2015).

(Roure et al., 2012) have proposed the delamination of the African mantle lithosphere during the late Neogene under Algeria and Tunisia. However, the characteristic geological processes associated with lithospheric mantle delamination like extension, volcanism, and topographic uplift have not been described before in northern Tunisia, within this delamination scenario. Normal faults produced under an extensional regime are described in the Sicily Channel and in Central Tunisia (Tricart et al., 1994; Belguith et al., 2011, 2013). Furthermore, thinner crust is

observed towards the northern and eastern coast of Tunisia where the Moho depth decreases to 25 km from depths around 35 km in central Tunisia (Research group for lithospheric structure in Tunisia , Buness et al., 1992), suggesting some crustal extension of a previously thickened orogenic crust or shallowing of the Moho by some other tectonic cause. Hence, the geology of northern Tunisia needs revising to see if the most accepted model of continuous shortening from the Paleogene onwards in the region should be punctuated with a model where lithospheric continental mantle peeling, tearing, or other mantle tectonic mechanisms may play a role.

To analyze the role and importance of extension in northern Tunisia and its relation with mantle tectonic mechanisms we have carried out an extensive field campaign revising the structure of the region, distinguishing low-angle normal faults (LANFs) and associated listric fault systems from earlier thrusts. We have analyzed the nature, geometry, regime, crosscutting relationships and kinematics of the main structures, and the contacts between lithological units. Furthermore, we have analyzed the relationship between the main faults and the evolution and geometry of sedimentary basins and magmatism in the region. For studying the relation between extension and the development of sedimentary basins, we use ETAP industry reflection seismic lines. We show the relationship between fault geometry and syntectonic unconformities and fault-bend related folding. This work manifests the importance of extensional tectonic processes in northern Tunisia and explains them in the context of mantle mechanisms that have contributed to the Late Miocene to Pliocene tectonic evolution of the western Mediterranean.

2. Geological setting

Northern Tunisia has accommodated the shortening related to the northwestward subduction of the Nubian plate under Eurasia since the Paleogene (Frizon De Lamotte et al., 2000; Faccenna et al., 2005; Khomsi et al., 2009; Melki et al., 2011; van Hinsbergen et al, 2014). Under this convergent setting, the Tellian and Tunisian Atlas thrust belts are differentiated. The Tellian belt to the north is formed by the Flysch sedimentary cover of the Tethyan oceanic crust, thrusted over allochthonous nappes of the North-Mahgrebian Mesozoic to early Miocene passive margin. The Tunisian Atlas is the foreland thrust belt deforming the sedimentary cover of the north Maghrebian Mesozoic to Neogene passive margin(e.g., Khomsi et al., 2009; Melki et al., 2010, 2011) (Figure 2.1). Metamorphic rocks typical of a thick-skinned orogenic domain outcrop only locally off-shore in the La Galite Island (Belayouni et al., 2010) (Figure 2.2), and can also be found in the Kabilies region of Algeria where they are interpreted to represent part of the AlKaPeCa domain. This domain would be origin-ally formed by the internal zones of the Betics (Al), Kabilies (Ka), Peloritan (Pe), and Calabria (Ca) that are pro-posed to have formed an unique

collisional terrain in the western Mediterranean during the Paleogene(e.g.,Bouillin et al., 1986; van Hinsbergen et al, 2014) (Figure 2.1).

The deformation described up to date in both the Tell and Tunisian Atlas domains shows a transpressive component with the development of large NE-SW sinistral-reverse strike-slip structures like the Cap Serrat-Gardimaou, Ras El Korane-Thibar, El Alia-Teboursouk, Tunis-Ellès, and Zaghouan faults (Melki et al., 2012; Bejaoui et al., 2017) (Figure 2.2). Moreover, there are also conjugate dextral and normal NW-SE faults (Zargouni, 1978; Zouaghi et al., 2011; Melki et al., 2012). NW-SE plate convergence continues at present day (Mejri et al., 2010; Soumaya et al., 2015) (Figure 2.1).

This convergence is uplifting the Atlas and reactivating pre-existing faults (McClusky et al., 2003; Goes et al., 2004). WNW-ESE faults are reactivated with reverse dextral motion, while NE-SW ones are reactivated with pure to oblique reverse motion. This reactivation formed new folds with NE-SW axes (Mejri et al., 2010; Alyahyaoui and Zouari, 2014). Two unconformities related to folding have been related to late Tortonian to Quaternary shortening in northern Tunisia (Ramzi and Lassaad, 2017). Moreover, the southwestern boundary of the Tunisian Atlas is delineated by large NW-SE dextral structures like the Gafsa and Tozeur-Negrine faults (Zargouni, F. et Ruhland, 1981; Saïd et al., 2011b; Ben Hassen et al., 2014).In the surrounding peri Mediterranean orogens this late shortening is producing the tectonic inversion of many extensional structures developed by slab rollback or slab rupture dynamics, including the Algero-balearic and Tyrrhenian basins (e.g.,Booth-Rea et al., 2002; Bouillin et al., 2005; Kherroubi et al., 2009; Billi et al., 2011; Giaconia et al., 2015).

Normal faults active during the Plio-Quaternary, producing NE-SW directed extension are described in central Tunisia and in the Sicily Channel (e.g.,Civile et al., 2008, 2010; Belguith et al., 2011, 2013). These faults seem still active in the Sicily channel and with normal-oblique kinematics in the Pelagian foreland (Soumaya et al., 2015).

Middle to Late Miocene magmatism in northern Tunisia has been interpreted as postcollisional, related to the reactivation in a NW-SE convergent setting of shear zones and lineaments inherited from the Variscan orogeny (Piqué et al., 1998; Decrée et al., 2014b). The source of the potassic calcalkaline magmatism in Tunisia and Algeria is interpreted to be the subcontinental lithospheric mantle, metasomatized during an earlier sub-duction event (early Alpine or Variscan in age) mixed with partial melts from the African crust(Maury et al., 2000; Decrée et al., 2014b). This melting has been also related to a rise in the asthenospheric mantle as a result of lithospheric delamination (C. Maury et al., 2000; Abbassene et al., 2016).

3. Lithostratigraphy and geological map of Northen Tunisia

For this work we have compiled a raster map of Northern Tunisia based on the existing 1:50.000 maps published by Officine National de Mines (Batik P, 1980; Lamos, 1980, 1985; Biely et al., 1982; Rouvier, 1987, 1990; Fournet, 1994; Melki et al., 2002; Alouani et al., 2006; El Ghali, 2006) although, using a thorough revision and reinterpretation of the nature of the contacts between units and in some cases we have remapped or included data from (Marzougui et al., 2014) (Figure 2.3).

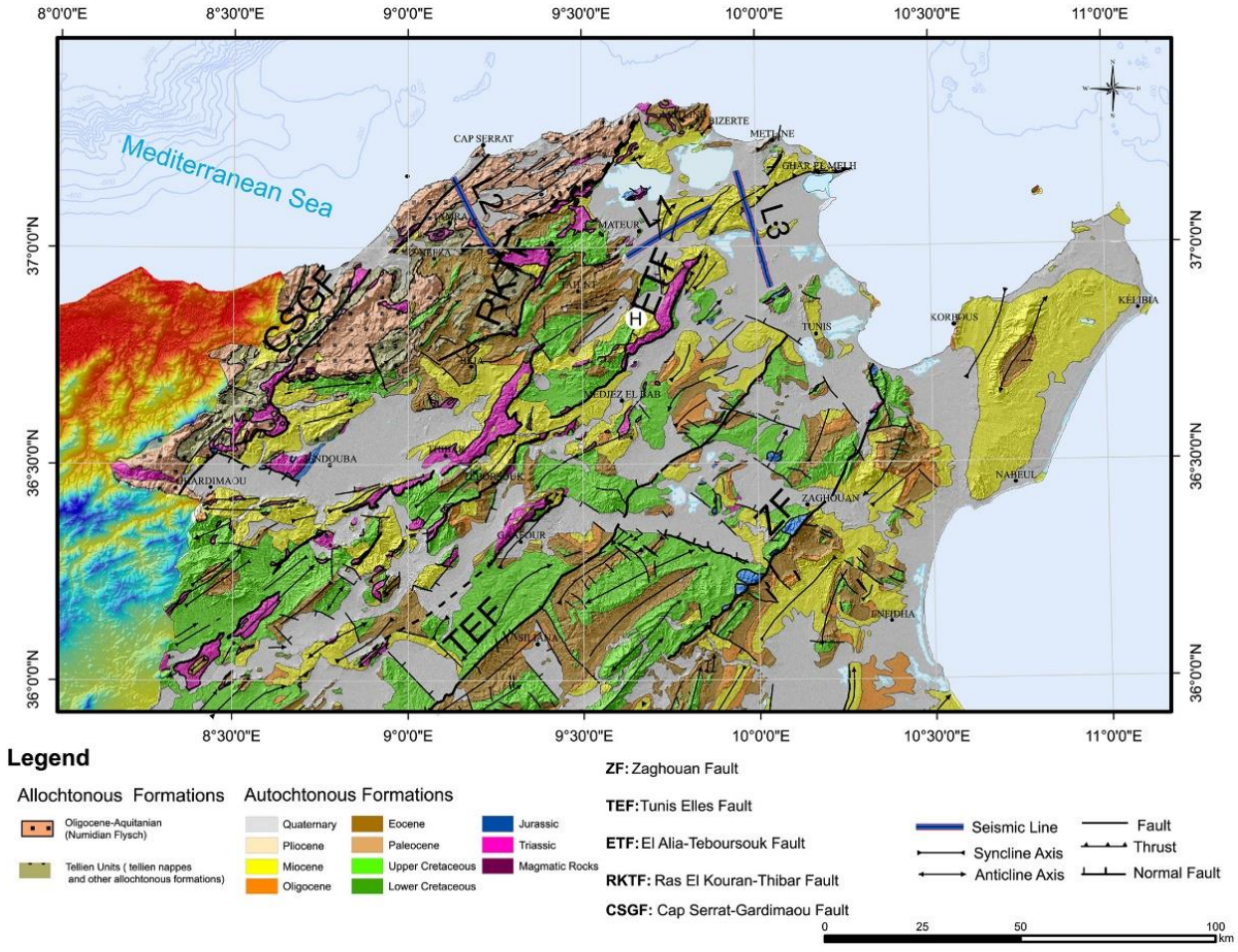

Figure 2-2: Tectonic map of northern Tunisia with the location of the studied area and seismic lines. Modified from Melki et al. (2012).

For aiding in the structural interpretation of the region, we have divided the mapped rocks into four tectonostratigraphic units that from top to bottom are as follows: (A) Neogene to Quaternary post-nappe sediments, tectonic breccias, and volcanic rocks; (B) Oligocene Numidian Flysch nappe. C) Infranumidian para-autochthonous nappes and D) Autochthonous north Maghrebian paleomargin sediments (Figures 2.3 and 2.4).

3.1 Late Neogene to Quaternary Post-Nappe Sediments and Volcanic Rocks

Several unconformable sedimentary formations from the Serravallian to Pliocene were cored in the Mateur basin (Alyahyaoui and Zouari, 2014)(Figures 2.3 and 2.4a). The Hakima formation (M1) composed of Serravallian lagoonal-marine shale, sandstone, clay, and gypsum forms the base of this sedimentary infilling. The overlying formations are unconformable upon this formation and include Tortonian clay and gypsum (Oued el Melah), followed by Tortonian sandstones and clay of the Kechabta Formation. The Oued Bel Khedim clays and gypsum together with lacustrine limestones and continental conglomerates of the Cheabet Tabala formation form the Messinian sedimentary sequence.

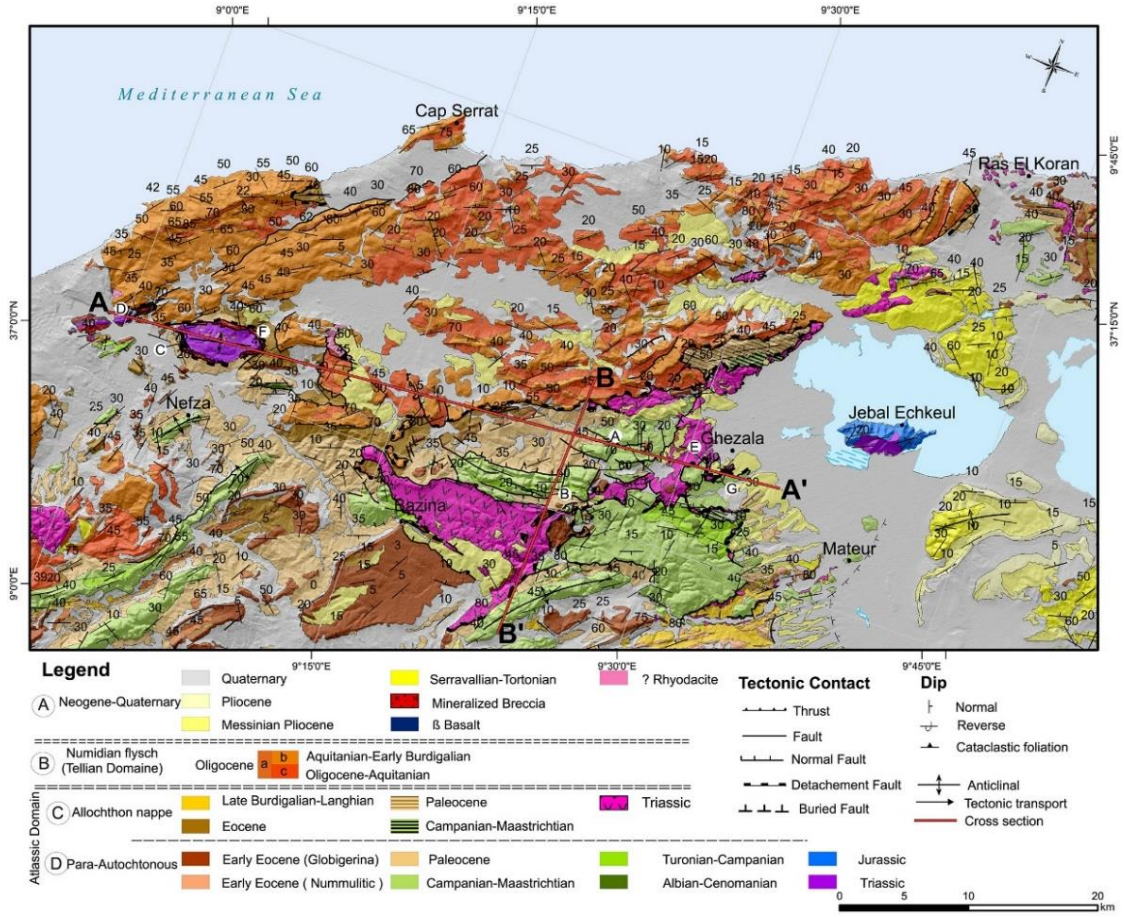

Figure 2-3: Geological map, including the location of cross sections

These Tortonian to Messinian formations have been included in sequence M2 in the seismic lines. Towards the west, these units show more proximal conglomeratic facies. Marine clays and sandstones, unconformable on the underlying sequence, characterize the Pliocene deposits in the Mateur basin. Further west, the Pliocene sediments are alluvial fans. Quaternary sediments are fluvial terraces, alluvial fans and colluvial cover, together with lacustrine sediments in the region

of Mateur. Marine and eolian Quaternary deposits occur also along the northern and northeastern coast of Tunisia.

Volcanic rocks in northern Tunisia include 13 Ma granodiorite (Oued Belif massif, (Decrée et al., 2014b)), 9.2 to 8.2 Ma rhyodacites (Oued Belif and Haddada massifs(Badgasarian, 1972; Faul and FOLAND, 1980; Decrée et al., 2014b) and cordierite-bearing rhyodacites (Ain Deflaia massif) in addition to rare 8.4- to 6.4-Ma basalts (Decrée et al., 2014b). The oldest Serravallian to Tortonian Nefza felsic magmatism results from the mixing at depth of an enriched mantle-derived calcalkaline magma with a predominant peraluminous crustal melt. The younger Messinian basalts essentially derive from the enriched mantle source and are nearly devoid of crustal participation (Decrée et al., 2014b).

3.2 Oligocene-Burdigalian Numidian Nappe

Oligocene to Burdigalian rocks form the northwestern succession of the Numidian Flysch. This formation is characterized by allochtonous turbidites deposited in the Tethys Ocean that include Oligo-Aquitanian clays of the Zouza member at the base and Aquitanian-Burdigalian sandstones and shales at the top, forming the Kroumirie and Babouch members (Riahi, 2010; Belayouni, H., 2013; Riahi et al., 2015).

3.3 Infranumidian para-autochthonous nappes

These units occur between the Numidian nappes and the autochthonous Atlas sediments. They include a complete sedimentary sequence from Triassic to Langhian that is characterized by important omissions of the series and lateral thickness variations. The most competent materials, comprising Eocene and Cretaceous limestones occur as discontinuous brittle boudin-type bodies embedded between an underlying Triassic gypsum-dolostone breccia and overlying Paleocene and late Eocene clays. Eocene limestones are characterized by deep-sea globigerine facies (Erraioui, 1994). A late Burdigalian to Langhian unconformable formation of glauconite marls and sandstones dates the tectonic emplacement of the Numidian nappes (Belayouni, 2013) (Figure 2.4).

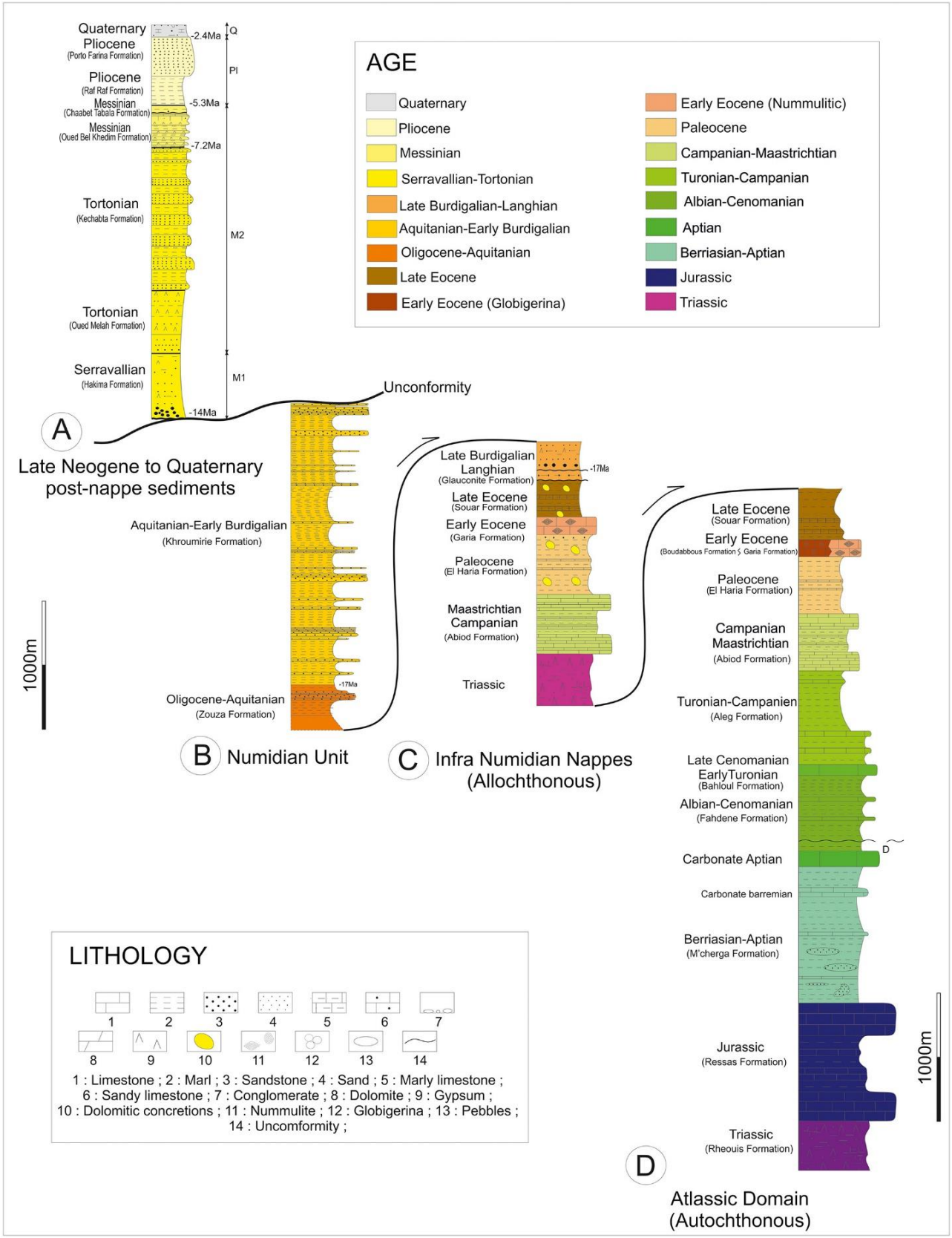

Figure 2-4: Lithological series in northern Tunisia.

3.4 Autochthonous North Maghrebian Paleomargin Cover

The Autochthonous Tunisian paleomargin sediments span from Triassic to Langhian (e.g.,Melki et al., 2012)(Figure 2.4). Gypsum, slates, carbonates and multicolor sandstones with chaotical structures conform the Triassic rocks. The Triassic evaporites often act as a detachment level of the thrust faults and present tectonic contacts with other formations in northern Tunisia. Jurassic carbonates show discontinuous outcrops with some marly intercalations, typical of deep-sea environments. The Cretaceous is represented by deep marine Santonian marls of the Aleg Formation, followed by upper Campanian-middle Maastrichtian limestone and marl-limestone alternations of the Abiod Formation. A sequence of 800–900 m of upper Maastrichtian to Paleocene marls of the El Haria Formation follows the above sediments. The El Haria Formation marls frequently form a neutral decollement level that accommodates the displacement of overlying faults. Early Eocene limestones produce positive reliefs in the region. Sandy, clayey and carbonate facies indicating a shallow marine to fluvial environment of the Fortuna Formation deposited during the Oligocene to Aquitanian.

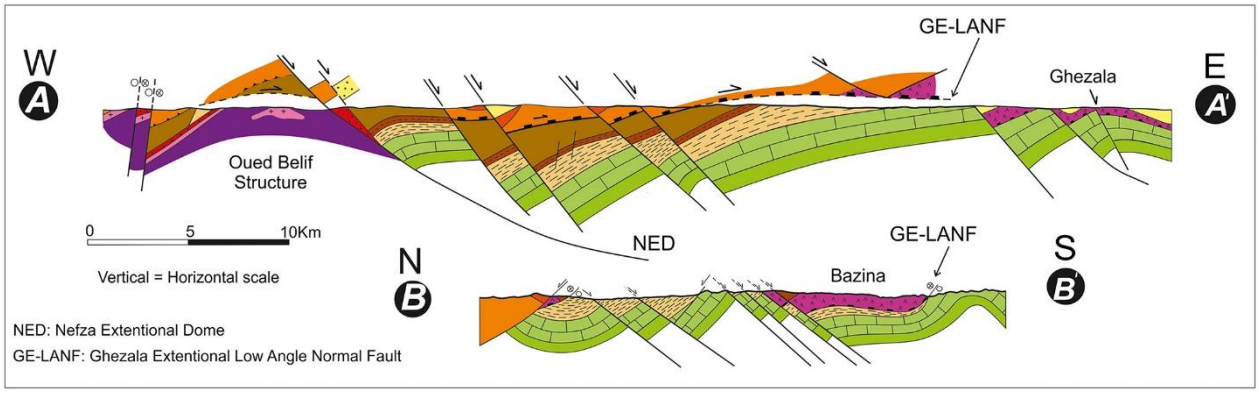

Figure 2-5: *Geological sections across the studied region. The sections are located in Figure 3. (a) East-west line showing the Nefza extensional detachment and associated listric fan, cutting and tilting the overlying Ghezala LANF. (b) N-S line showing the Nefza listric fan formed by low- angle normal faults with S- directed transport. Lithological legend as in Figures 2.3 and 2.4.*

4. Extensional systems in Northern Tunisia

We have identified two orthogonal sets of normal faults in northern Tunisia. Bothhigh-angle and LANFs that detach in the most plastic materials, like Triassic evaporites and Cretaceous, Paleocene and late Eocene marls, have accommodated extension. The main extensional faults identified in northern Tunisia detach in two LANFs, the Ghezala and Nefza faults that root within Paleocene marls and the infra-Numidian Triassic or in the autochthonous Atlas Triassic, respectively (Figures 2.5 and 2.6). The Ghezala normal fault system shows E-NE hanging-wall tectonic transport, whilst the Nefza extensional system shows S-SE hanging-wall transport sense (white arrows in Figures 2.6 and 2.10 represent the kinematics of the main faults). Both have

associated an extensional listric fan cutting and tilting the hanging-wall block. In some cases, the normal faults forming the listric fan also show low-angle geometry (Figures 2.5b and 2.7a and 2.7b). Locally, the LANFs separate very low-grade marbles or igneous plutonic rocks in the footwall, from diagenetic rocks in the hanging wall, defining regional detachment surfaces where the deeper autochthonous Triassic rocks crop out. Low-grade metamorphic rocks are described underlying the Chemtou marbles in northwestern Tunisia and in the Jebel Echkel Triassic outcrops in the Matteur basin (Ghorabi and Henry, 1992; Ouazaa et al., 2013) (Figure 2.2). Meanwhile the autochthonous Atlas Triassic rocks crop out also, deformed in the presence of high-temperature fluids and granodiorite magma in the Oued Belief anticline near Nefza (Decrée et al., 2013, 2014b)(Figures 2.5 and 2.10).

4.1 The Ghezala low-angle normal fault

The Ghezala low-angle normal fault (GE-LANF) shows a gentle footwall and hanging-wall ramp geometry that cuts down into the autochthonous Atlas unit, omitting most of the Paleogene sequence at its footwall from West to East, from Bazina towards Ghezala (Figure 2.3 and cross section 2.5a). The GE-LANF shows a shallow dip, practically horizontal at a regional scale, although, it shows segments dipping towards the NW that have been tilted by later, deeper-seated normal faults of the Nefza extensional system. In the region of Bazina it forms the contact between the Numidian nappe and the underlying Upper Eocene marls and towards the East it cuts down into the Cretaceous. To the East, near the region of Mateur, it forms the contact between the infra-Numidian Triassic and the autochthonous Cretaceous (Figure 2.6). In this region, a large segment of the LANF shows a flat geometry with strongly stretched Triassic evaporites in between Cretaceous or Paleogene marls (Figures 2.5a and 2.7g). Overlying the GE-LANF we found several extensional horses (Gibbs, 1984) formed by competent Eocene limestones that are bounded by LANFs with ENE hanging-wall transport sense. Extensional horses are also observed over the LANF in seismic line L1 (Figure 2.8). A N-S striking LANF ofthe overlying listric fan cuts through the whole hanging wall in Ghezala, bounding tilted Messinian sediments of the Mateur basin to the East. A segment of the LANF showing the Messinian half-graben crops out at the Ghezala mine (Figure 2.9). Here the Messinian sedimentary sequence, including continental conglomerates, gypsum, and lacustrine marls and silts is tilted 30° and detached over the LANF that dips 35° towards the E (Figure 9). These sediments are also cut by many small normal faults showing the same kinematics as the underlying master fault (Figures 2.6, 2.7e, and 2.9). The fault rock is developed in the infra-

Numidian Triassic and also shows foliated cataclasites formed from the comminution of Paleocene black marls. Kinematic indicators along the GE-LANF like slicken fibers on the fault surface, false S-C'structures, rotated porphyroclast tails show E-NE tectonic transport (white arrows in Figure 6, near Ghazela). This transport sense has also been measured on normal faults of the hanging-wall listric fan (Figure 2.6). Faults of the hanging-wall listric fan bound small sedimentary basins filled by Late Miocene to Pliocene sediments and alluvial fans in the Bazina region. The Late Miocene sediments host Pb-Zn extensional related mineralizations (Decrée et al., 2008b). The alluvial fans were fed from an exhumed Fe-mineralized breccia, leading to Pliocene Fe-rich conglomerates that have been exploited in the Sejanne and Tamra mines (Decrée et al., 2008a). To the south of the Bazina region, the GE-LANF is folded appearing as a dextral low-angle (30–40°) strike-slip fault (see southern end of cross-section B-B' in Figure 5).

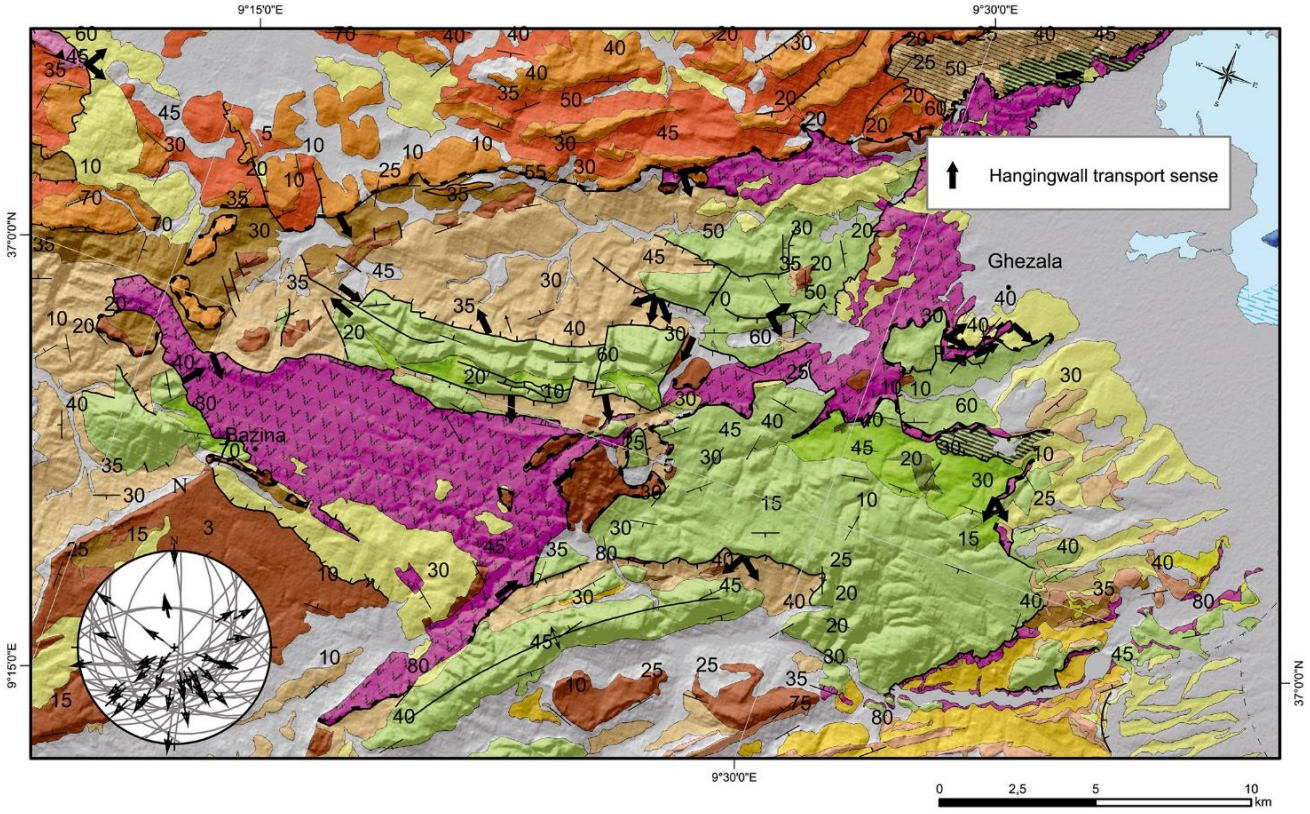

Figure 2-6: *Geological map and hanging-wall transport sense of extensional faults in the region of Bazina-Mateur. Modified from Marzougui et al. (2015). Included is a lower-hemisphere stereographic projection of fault data in the region. Lithological and structural data legend as in Figures 2.3 and 2.4.*

The westernmost segment of the GE-LANF has been traditionally interpreted as a thrust surface, representing the Numidian thrust front that superposes the Numidian unit over para-

autochthonous Paleogene sediments (e.g.,Khomsi et al., 2009; Marzougui et al., 2015; Essid et al., 2016). This contact must have been originally a thrust surface when the Numidian nappe was emplaced towards the SE over the African passive margin in the Early Miocene (Khomsi et al., 2009; Belayouni, 2013). However, the present contact shows ENE-transport sense and the fault surface cuts down into the structural pile towards the direction of transport, omitting most of the Paleogene sequence and reaching the Cretaceous in its footwall. Thus, the original thrust surface has been cut and probably omitted by later extensional tectonics and at present is a LANF (Figure 2.5a). LANFs affecting regions shortened by previous nappe tectonics can still separate older rocks over younger ones or higher metamorphic over low metamorphic ones, because extension does not change the stacking order produced by the previous thrusts (e.g.,Martínez-Martínez and Azañón, 1997; Platt, 1998)

The GE-LANF can be followed in reflection seismic line 1 where it shows a ramp-flat-ramp-flat geometry lead-ing to the development of a hanging-wall syncline basin (e.g.,Benedicto et al., 1999; Reston et al., 2007) and associated rollovers 1 and 2 in the hanging-wall Tortonian to Messinian sedimentary sequence (Figure 2.8). The LANF reaches depths of approximately 2.5–3 s Two-Way Traveltime (TWT) at the eastern end of Line 1, probably rooting in the autochthonous Triassic at a depth around 4–4.5 km for velocities between 2.7 and 3.0 km/s. Extensional horses, probably of the infranumidian unit carbonates, can be observed over the LANF in line 1 (Figure 2.8). The fault activity is well constrained by the development of a synrift unconformity between the Serravallian Hakima formation (M1) and the overlying Tortonian to Messinian sedimentary units (M2) that onlap the hanging-wall flat defined by the prekinematic M1 sediments (Figure 2.8). The postrift unconformity is marked by onlapping Pliocene marine sediments (P) that thin towards the limb of the rollover 1 anticline, evidencing that this structure has been further folded by Plio-Quaternary shortening. The main fault shows evidences of being inverted during the Plio-Quaternary with a small reverse fault component cutting the Pliocene sedimentary unit between line traces 1345 and 1505 (Figure 2.8). The Pliocene sediments show syntectonic features, thickening over the footwall of the thrust.

Dextral transfer fault structures with E-W to NE-SW orientation have also been identified in the field in the region of Bazina. These faults bound the infranumidian Triassic from autochthonous Cretaceous in Joumine and cut into the Cretaceous to the north of Bazina (Figure 2.6). These faults developed Fe-Zn-Ba mineralized dilatant breccias.

4.2 The Nefza extensional dome

The Nefza detachment exhumes authochthonous Triassic rocks in the footwall of the fault zone from under Numidian sandstones and Paleogene sediments in the hanging wall. This detachment is strongly folded, crop-ping out in the core of the Oued Belif Plio-Quaternary anticline (Figure 2.10). The Nefza detachment itself is defined by a thick sequence of mineralized tectonic breccia (Decrée et al., 2013) and locally by a marble mylonite where it exhumes syntectonic rhyodacites (Figures 2.7c and 2.7d). The breccia is cohesive and strongly miner-alized by iron oxide-LREE-U, implying fault-valve type behaviour of the shear zone during its activity (Sibson, 1987). Fluids during brecciation were high temperature (≥540 °C) with a mixed magmatic-basinal (salt related) origin (Decrée et al., 2013). The breccia shows an ill-defined cataclastic foliation with a poorly defined lineation, cut by extensional shear bands (Figure 2.7c). Striated surfaces within the breccia and at the top of it show mostly NE-SW to NW-SE mineralized slicken lines (Figure 2.7f). Tectonic transport shows mostly an easterly sense (stereoplot in Figure 2.10). The fault zone cuts the thrust contact between the Numidian flysch unit and Upper Eocene marls in its hanging wall (Figure 2.5a). In Oued Belif the Nefza detachment is folded, being reversed in the northern limb of the anticline where it presently shows dextral strike-slip kinematics. It dips 50° towards the west in the westward perianticlinal closure where it presently shows reverse kinematics (Figure 2.7c). Here the fault zone dips approximately 30° less than the hanging-wall Paleocene marls. The south-ern limb also shows strong dips of around 80° with sinistral-oblique strike-slip kinematics. Finally, in its eastern perianticlinal closure the detachment is cut by a later NW-SE sinistral-normal fault. Most of the kinematic indicators along the dome indicate northeastward transport sense, however at the eastward end of the dome the normal faults show mostly SE-directed hanging-wall transport (Figure 2.10). A 12-Ma granodiorite plug intruding the autochthonous Triassic is exhumed in the core of the Oued Belif Dome(Decrée et al., 2014). Moreover, 8- to 9-Ma rhyodacites intrude the dome structure. In some case, to the north of Oued Belif, the magmatic foliation at the top of a rhyodacite body is parallel to the detachment surface and to the foliation in carbonate fine-grained mylonites, indicating that the Nefza detachment was active very close to the surface at the time of rhyodacite dome extrusion (Figure 2.7d). The fault rock later evolved towards a cemented iron-jasper rich cat-aclastic breccia. Tortonian pyroclastic conglomerates occur in the hanging wall of the fault.

The Nefza detachment listric fan cuts through the autochthonous Cretaceous cropping out to the northeast of Bazina. Here the Cretaceous is tilted and cut by several low-angle (approx. 35°) normal faults (Figures 2.7a and 2.7b and cross section 2.5b). These faults show mostly S-

SE directed transport; however, in some cases two and three sets of oblique striae have been identified indicating S-, SE-, and NE-directed transport. In three dimensions, the normal faults are strongly segmented by N-S to NNE-SSW strike-slip faults that we interpret as transfer structures of the extensional system (Figure 2.6). These faults show contrary kinematics to the observed offset between the normal faults they link that is a normal characteristic of transfer faults in extension (e.g.,Gibbs, 1984; Giaconia et al., 2014).

Figure 2-7: *Photo panel. (a) S to SE-directed low-angle normal fault between Cretaceous carbonates and Paleocene marls in the Bazina region. (b) Low-angle normal fault scarp with well-defined striations and groves indicating S-directed transport in the region of Bazina. (c) Nefza detachment mineralized extensional breccia. (d) Rhyodacites in the footwall of the Nefza detachment, showing a magmatic foliation that is parallel to a mylonitic foliation in overlying dolomitic marbles. The detachment is defined by a brittle fault plane with SW-NE directed slickenlines that separates the footwall rhyodacites and breccias from hanging-wall Numidian flysch sediments. (e) Late Miocene conglomerates tilted over the Ghezala LANF, marked by cataclastic breccia affecting a Triassic and Paleogene protolith (f) Fault surface with slickenlines at the top of the Nefza detachment breccias. (g) Foliated cataclasites in a flat portion of the Ghezala LANF with a gypsum mylonitic matrix of Triassic protholith. (h) Fault zone of the Ghezala LANF marked by Triassic gypsum breccia, cutting down into Cretaceous Atlas sediments to the west. Early Miocene marine sediments, to the east, form the hanging wall of the fault, location in Figure 2.2. All photographs located in Figure 2.3, except (h)*

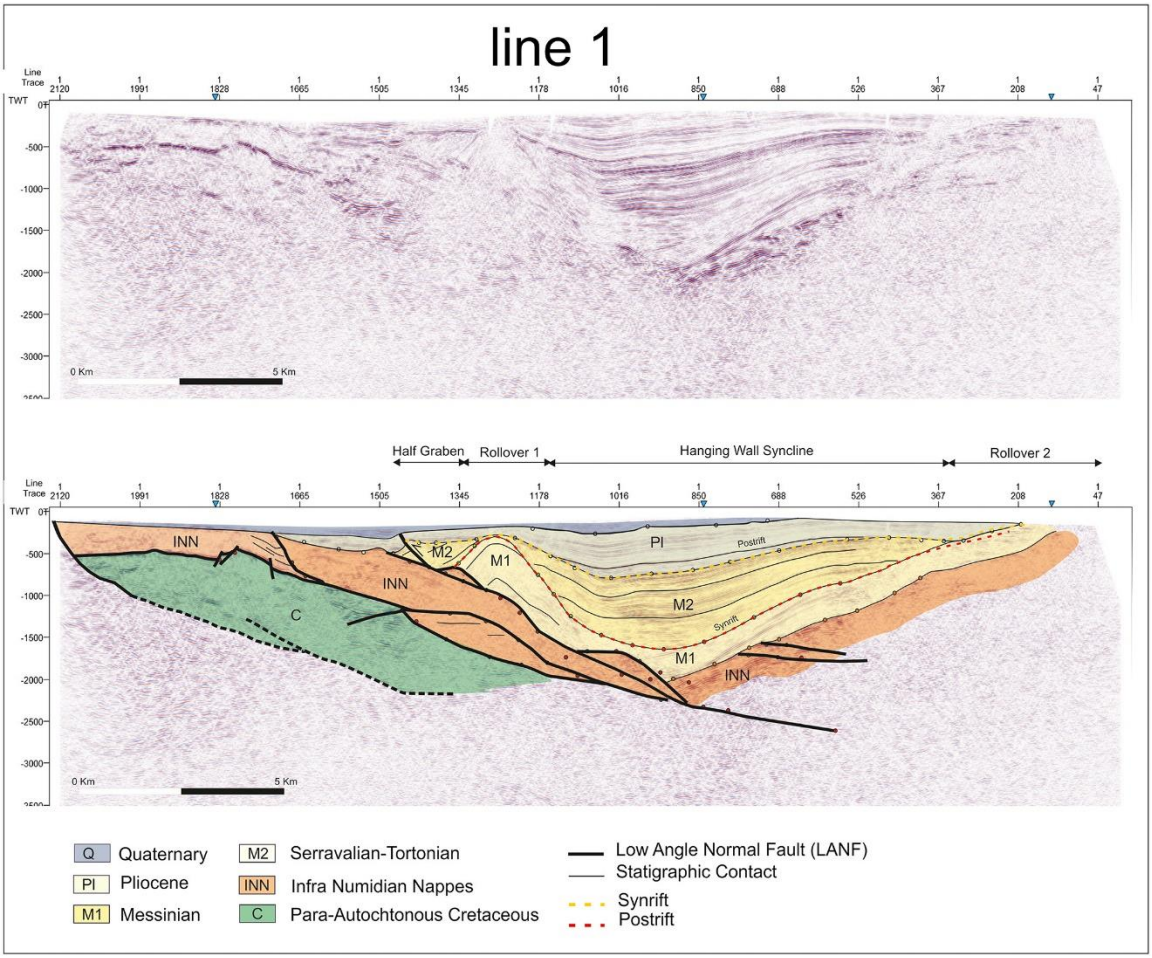

Figure 2-8: *Seismic line L1 across the Mateur basin showing a hanging-wall syncline basin filled in by Tortonian to Messinian synrift sediments. The postrift unconfor-mity is marked by the onlap of Pliocene marine sediments that have been later folded by NW-SE convergence.See location in Figure 3.*

At depth, seismic line L2 images the Nefza detachment as a low-angle fault that cuts down into the autochthonous Atlas series from northwest to southeast rooting in a flat detachment at a depth of 3 s TWT, in the Triassic series (Figure 2.11). At the northern end of Line L2 the detachment comes out to the surface being the contact between Upper Eocene infra-Numidian marls and strongly tilted Numidian sandstones on the hanging wall (Figure 2.10). Calcite fibers in the contact and in brittle shear zones within the Eocene marls show S-SE transport (Figure 2.10). The hanging wall of the detachment is a listric fan of normal faults that cuts and tilts the Numidian Flysch rocks (Figure 2.11). Furthermore, these faults cut other overlying LANFs, including the structurally higher Ghezala LANF. Finally, the shallower part of the section shows open folds shortening the Numidian Flysch.

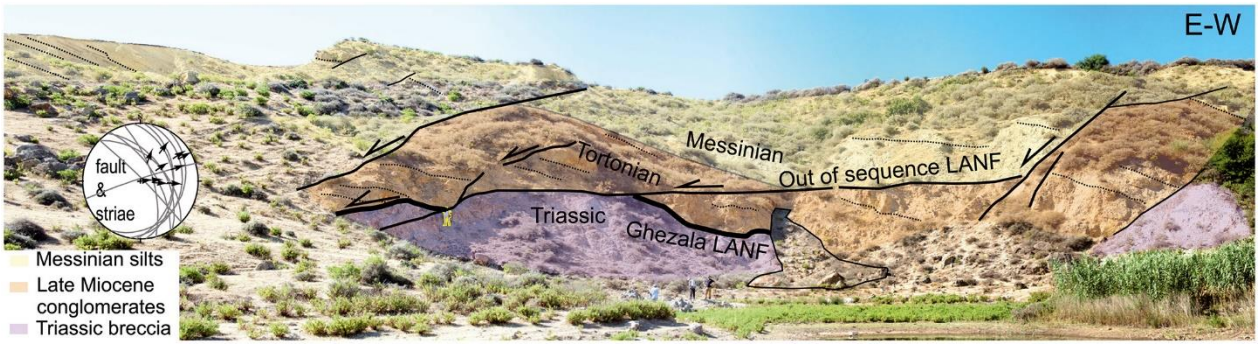

Figure 2-10: *Outcrop of the Ghezala LANF in a quarry at Ghezala (Figure 6). Notice the low-angle detachment at the contact between Late Miocene conglomerates and the underlying fault breccias, which is cut by later out of sequence faults that cut through Messinian silts. Faults and slickenlines are plotted in a lower- hemisphere stereoplot and show tectonic transport towards the E- NE.*

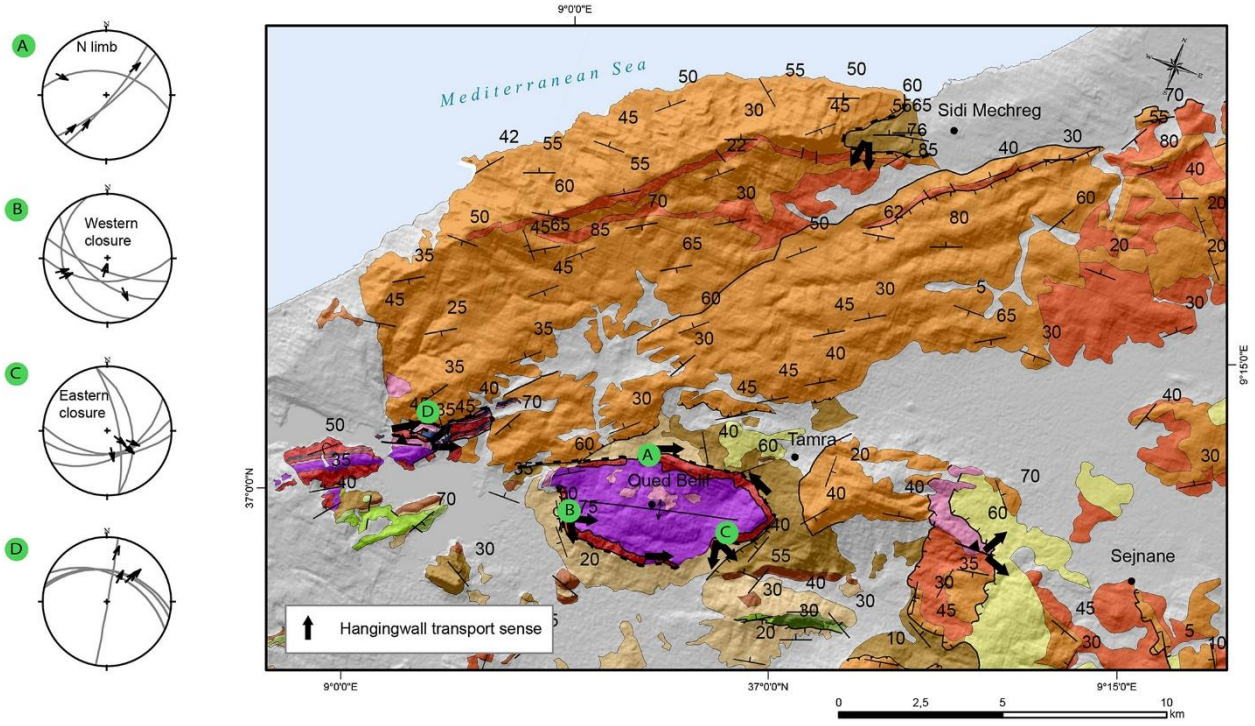

Figure 2-9: *Geological map and extensional kinematic data of the Nefza region, including a lower-hemisphere stereographic projection of faults and associated slickenlines. Lithological legend as in Figures 2.3 and 2.4*

4.3 Relationship between extensional systems

The extensional faults show mostly ENE and S-SE directed extension that we relate to the activity of two successive, orthogonal extensional systems. However, many individual faults, both high- and low-angle, show the two directions of extension with oblique striae. Indicating that the later SE-directed extension reused the same fault surfaces developed during the older ENE-directed extension. The relative age between extensional systems is clear as the SE-directed normal faults cut and tilt the main NE-directed extensional LANFs. This is especially evident in

the region of Bazina, where the Ghezala LANF, located here in the contact between the Paleocene and the overlying allochthonous infra-Numidian Triassic, is cut and tilted by SE-directed normal faults that exhume the Cretaceous Jebel Aouana massif (Figures 2.5b and 2.6). Further, east, however, in Ghezala the NE-directed extension was active until later, affecting Messinian sediments (Figures 2.8 and 2.9).

4.4 Extensional Systems versus Diapiric Structures in Northern Tunisia

The extensional structures we describe in northern Tunisia change the local tectonic structure interpreted so far in the region. Many of the Triassic outcrops interpreted to be related to Cretaceous to Recent diapiric processes are actually formed by a sheet of foliated breccias developed by extensional thinning of a previous nappe located at the base of the Infranumidian units. In some case this detachment has a flat geometry producing a neutral shear zone segment that was previously interpreted to be a Cretaceous salt canopy (Masrouhi et al., 2014). However, this shear zone separates different lithology, not only Cretaceous sediments; it is locally overlain by extensional horses of Eocene carbonate and shows continuous outcrops with ramp segments that have clear extensional kinematics (Figures 2.7g and 2.7h). Moreover, the Triassic outcrops that do correspond to the autochthonous Atlas unit, like in the core of the Oued Belief dome, were exhumed from depths of several kilometers by Tortonian extensional faults and not by diapiric processes. Finally, some of the large-scale sinistral strike-slip faults interpreted in northern Tunisia like the NE-SW Ras El Korane-Thibar fault are not so large, as many of their supposed fault outcrops are actually folded segments of LANFs that presently show dextral kinematics (Figure 2.6). Hence, including Late Miocene extension in the tectonic evolution of northern Tunisia requires the revision of many of the previously interpreted structures, to differentiate between recent contractive strike-slip and reverse faults like the Alia-Teboursouk fault, and associated folds, from extensional related structures.

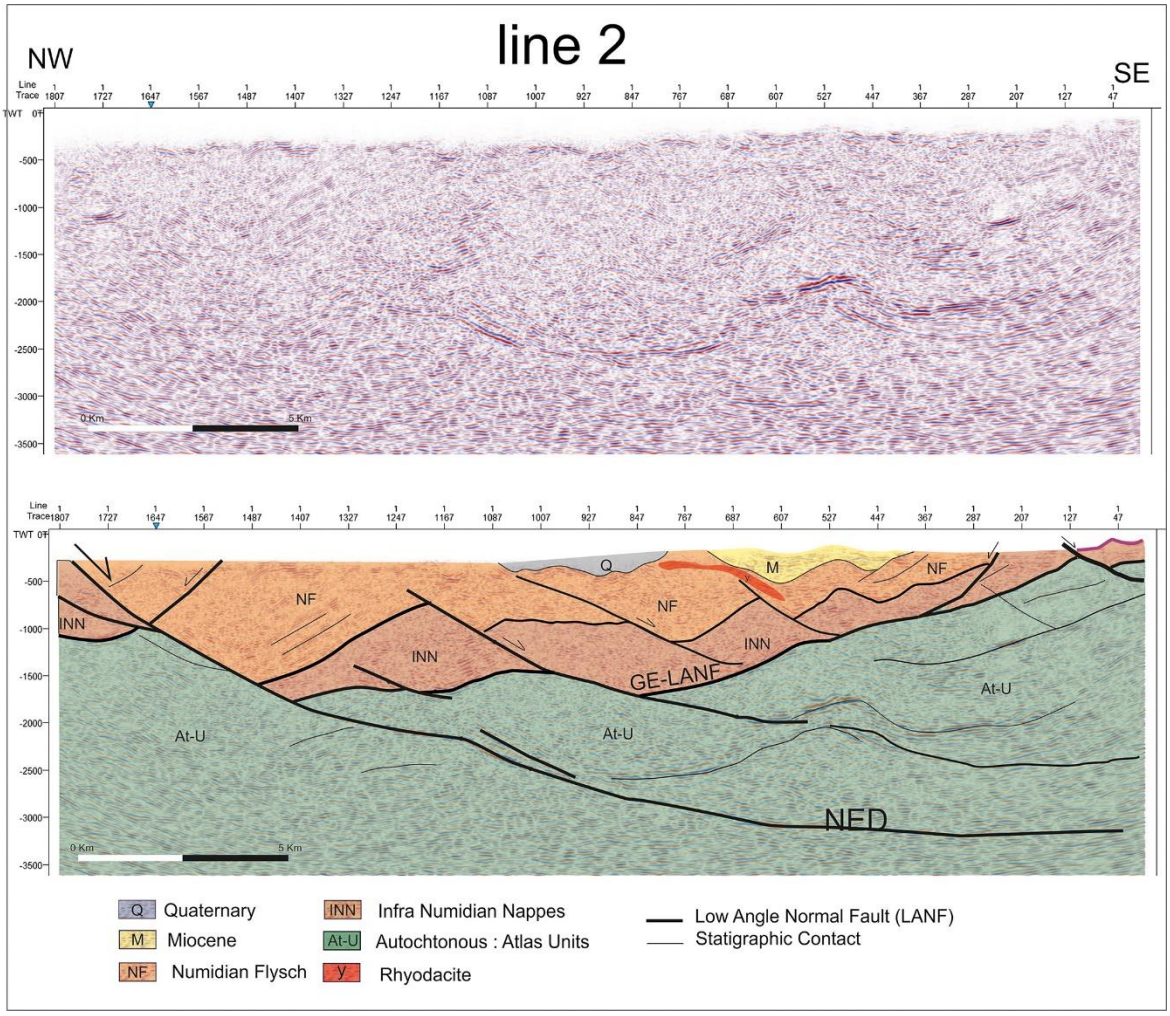

Figure 2-11:Seismic line L2 showing the Nefza detachment cutting into the infranumidian and Atlas units in the footwall. The hanging wall to the NW is formed by a thick sequence of Numidian Flysch tilted towards the NE. The line is located in Figure 3.

5. Plio-Quaternary Folding and Thrusting of Extensional Structures

The extensional faults and associated structures like rollovers are presently folded, cut by shortening structures, or inverted in relation to Pliocene to present shortening in northern Tunisia. This shortening is fully evident in the whole studied region, manifested presently by active seismicity (Soumaya et al., 2015), by the strain-field registered using fault kinematic data (Bouaziz et al., 2003), by the strike-slip and reverse kinematics of active or recent faults affecting the region, like the Alia-Teboursouk and Bled el Auana-Bizerte faults (Melki et al., 2011; Essid et al., 2016). Plio-Quaternary shortening has folded the Nefza detachment and refolded the extensional rollover anticlines and synrift unconformities developed in the Mateur basin region. Furthermore, reverse-oblique faults cut Quaternary sediments. Further work is necessary though

to measure the amount of shortening that has affected the region since the Pliocene. In some cases, where normal faults are suborthogonal to the Plio-Quaternary shortening direction, these have been inverted as thrusts, developing arrowhead-type structures where the wedge of synrift sediments has been elevated above regional(e.g.,McClay, K. R., & Buchanan, 1992). Furthermore, while synrift sediments show wedge-fanning geometries in the hanging wall of the structure, syn-thrusting sediments thicken above the footwall block (McClay,& Buchanan, 1992). This geometry is observed in the western end of line 1, where the Pliocene sediments thicken above the footwall of the Gezhala LANF.

Inversion tectonics in northeastern Tunisia is especially evident in seismic line L3 (Figure 2.12). This line runs in a NNW-SSE direction, perpendicular to the plate convergence and also to the SE-transport extensional system. The synrift basins developed during the Late Miocene have been later inverted, producing further folding of the hanging-wall rollovers, and Plio-Quaternary synclines that have sealed the main extensional faults. Hanging-wall sedimentary wedges thickening towards the normal faults characterize the Late Miocene synrift sequence. Meanwhile, thicker sediment sequences formed over the footwall of the normal faults during Plio-Quaternary shortening (Figure 2.12). Some of the normal faults have been later reused as thrusts, inverting the synrift wedges over the regional, for example, at line trace 982, Figure 2.12. The main LANF in this seismic line shows SE tectonic transport, probably exhuming authochthonous Triassic sediments in the footwall, which presently crop out to the west of the line in Jebel Echkeul. Meanwhile, the hanging wall of this LANF is strongly extended by conjugate listric faults showing NW hanging-wall transport. Towards the SE of the line, the authochtonous Mesozoic and Tertiary Tunisian Atlas sequence is tilted towards the NW over the LANF (Figure 2.12).

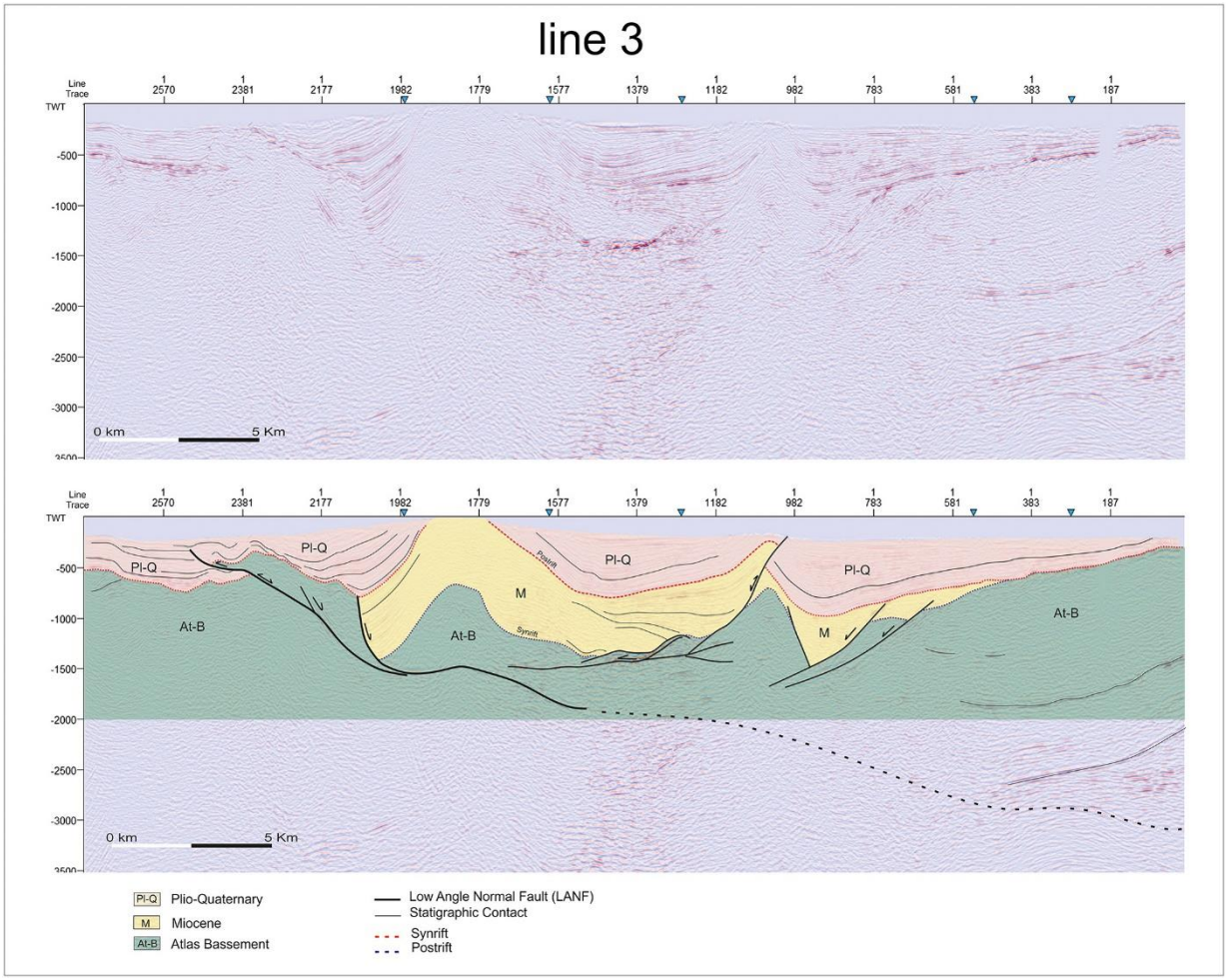

Figure 2-12: Seismic line L3 showing inversion tectonics in the norteastern end of Tunisia. This line is located in Figure 2.2. See explanation in the text

6. Discussion

The geometry of extensional faults in northern Tunisia is strongly controlled by a rheologically heterogeneous upper crust, formed during late Burdigalian to Langhian (17–14 Ma) thrusting in the Tellian Numidian Zone (Belayouni, 2013). This heterogeneous rheology with alternating plastic and competent layers has determined the development of superposed LANFs and detachments that root into the more plastic materials like Eocene, Paleocene and Cretaceous marls or in the Triassic evaporites. Meanwhile, the more competent Cretaceous or Eocene limestones, and Numidian sandstones occur as extensional riders (Gibbs, 1984) tilted over the detachments or as extensional horses forming lenses bounded by normal faults. This is a common feature of extended domains with contrasting rheologies, like in the Betics or the Apennines (Booth-Rea et al., 2004; Brogi, 2008).

We have differentiated two main LANFs, the Ghezala LANF and Nefza extensional detachment, and their associated hanging-wall listric fans. However, many other LANFs are

found in the region at different scales (Figures 2.7a and 2.7b). In the region of Nefza the age of extension is well constrained by the extrusion and deformation within the Nefza extensional detachment of 8- to 9-Ma rhyodacites (Figure 2.7d). However, extension here probably initiated before, during the Serravallian (12 Ma) intrusion of granodiorites (Decrée et al., 2014). Meanwhile, further east in the region of Mateur the extensional deformation is dated by tilted-syntectonic Upper Miocene sediments and by the development of a hanging-wall syncline basin and associated synrift unconformity of Tortonian to Messinian age (Figure 2.8). This diachronism in extensional ages suggests that extension propagated towards the East during the Late Miocene.

Geodynamic Evolution of Northern Tunisia

The extensional systems described here add new constraints on the tectonic evolution of northern Tunisia and on the geodynamic mechanisms driving deformation in the western Mediterranean since the Late Miocene. Furthermore, the direct relationship between crustal extension and peraluminous volcanism observed in the Nefza dome, where 8- to 9-Ma rhyodacites are deformed by an extensional detachment during their extrusion, suggests that deep mantle mechanisms leading to melting of the Maghrebian lower crust were driving extension. Moreover, the migration of the locus of extension towards the east-southeast during the late Neogene favors a southeastward-migrating mantle mechanism, like peeling back of the continental lithospheric mantle during subduction. The Thyrrenian basin, to the north of the studied region, opened at the same time related to the eastward rollback of the Calabrian slab that presently is hanging under the Calabrian arc (e.g.,Faccenna et al., 2004; Lucente et al., 2006). Thus, the ENE-directed extension we describe in northern Tunisia was most probably related to the Tortonian to Messinian opening of the Thyrrenian basin and to the concomitant eastward tearing of the Calabrian slab through the Tyrrhenian STEP (Govers and Wortel, 2005; Gallais et al., 2013; Barreca et al., 2014; Polonia et al., 2016). Furthermore, the process that drives the ENE-WSW extension appears to play on a larger scale, as it kinematically accommodates the counter-clockwise rotation of Adria relative to Eurasia, which is both seen in GPS data and paleomagnetic data (see (van Hinsbergen et al, 2014), and references therein).

Slab rupture occurred during the Middle Miocene in Algeria, producing postcollisional K-rich calc-alkaline magmatism dated at 17 Ma (Abbassene et al., 2016). Meanwhile, (Roure et al., 2012) suggested the delamination of the African continental mantle lithosphere under Tunisia in the late Neogene. According to (Faccenna et al., 2005) the rupture of the Calabrian slab along the northern coast of Tunisia produced Late Miocene volcanism with calc-alkaline granodiorites and rhyodacites dated between 14–8 Ma in Nefza and Galite island (Savelli, 2002) and alkali

basalts extruded at 8–6 Ma(Talbi et al., 2005). A very similar tectonic evolution, but with opposite kinematics, occurred in the Eastern Betics and Rif at the time, where westward-directed extension was accompanied by the extrusion of 8- to 9-Ma dacites. A process related to the westward rollback of the Betics-Rif slab and its lateral tearing off from the Iberian and Maghrebian continental lithospheric mantles (Duggen et al., 2004; Mancilla et al., 2015; Spakman et al., 2018).

Extension continued into the Messinian and probably Pliocene, after the tearing of the Calabrian slab off the northern coast of Tunisia. Furthermore, we observe a change in the kinematics of the main normal faults with the development of SE-directed extension. SE-directed normal faults in the region of Bazina and associated N-S transfer faults developed an alluvial fan system on their hanging wall. We relate the SE-directed extension with eastwards peeling back of the Tunisian continental lithospheric mantle in a subduction context during the Late Miocene. Peeling back of the African lithospheric mantle would have driven crustal extension, topographic uplift, and local Messinian alkaline magmatism coeval to the Middle to Late Miocene propagation of subduction related shortening. Topographic uplift initiated in the Late Miocene with the generalized continentalization of northerwestern Tunisia and migrated towards the E-SE with Pliocene marine sediments presently uplifted in the Bizerte-Cape Bon region (Salaj and B. Van Houten, 1988; Belayouni, 2013). In Central Tunisia, extension during the Late Miocene to Quaternary was mostly NE-directed forming half grabens filled by the continental Pliocene Segui formation (Belguith et al., 2011). NE-SW extension continued during the Quaternary in the Sicily channel accompanied by the still active Pantellaria peraluminous magmatism(Civile et al., 2008, 2010) and in the Pelagian foreland, where some oblique-normal faulting still occurs (Soumaya et al., 2015).

Extension must have affected the crustal structure of northern Tunisia, although few data exist about its deep lithospheric structure. Seismic refraction data show that the Moho depth decreases from approximately 35 km in central Tunisia to 25 km at the northern and eastern coastlines (Research group for lithospheric structure in Tunisia, 1992), supporting crustal thinning by extension near the coastlines, of a crust previously thickened during Tellian and Altas Alpine thrusting.

Peeling back of the continental lithospheric mantle during subduction produces a migrating belt of shortening, followed by extension, magmatism, and uplift. Thus, shortening related to SE peeling of the lithospheric mantle slab probably has occurred coeval to NW-SE shortening associated with plate convergence. The sum of these two shortening tectonic mechanisms could have induced higher strain rates in the region affected by mantle peeling producing an advance

of the Tunisian Atlas deformation front respect to the Algerian one and the development of a large NW-SE oriented dextral STEP boundary between western Tunisia and eastern Algeria, namely, the Tunisian Atlas STEP (Figure 2.12). As slab peeling and retreat in Tunisia was subparallel to the NW-SE convergence between Nubia and Eurasia it probably contributed to the southward propagation of the Tunisian Atlas belt, with an important component of left-lateral transpression (Melki et al., 2011). If some obliquity were present between the two shortening directions, two trends of shortening structures would be expected in Tunisia.

Slab detachment and the associated melting of the base of the African crust has been described in Northern Algeria, producing an important postcollisional Miocene magmatism in the Kabylies (Maury et al., 2000; Abbassene et al., 2016; Chazot et al., 2017) and extension (Saadallah and Caby, 1996; Aite and Gélard, 1997). The tectonic evolution we propose above is consistent with peeling back of the African continental lithospheric mantle initiating further west in the Kabylies during the Middle Miocene (Figure 2.12). Initial slab peeling or detachment is marked by the intrusion of 15-Ma peraluminous cordierite-bearing granodiorites and monzo-granites in the Bougaroun-Beni Toufout area BM, Figure 2.13; (Penven and Zimmermann, 1986; Chazot et al., 2017). K-rich shoshonitic series dacitic and rhyolitic dykes also occur in the Edough massif region (EM, Figure 2.13), dated between 16.8 and 14.3 Ma (Abbassene et al., 2016) (Figure 2.12). Thus, magmatism related to peeling or detachment of the African continental lithospheric mantle propagated from west to east from the Bougaroun massif around 15 Ma towards the Nefza region in Tunisia at 8.5–9 Ma.

The peeled back African lithospheric mantle is imaged by seismic tomography under Tunisia. Poor-resolution tomographic images of the mantle slabs under Algeria and Tunisia suggest that they are detached from the overlying lithosphere at ~150 km depth(Faccenna et al., 2014; Fichtner et al., 2015). Other tomographic models show the slab lying even deeper overlying the 660-km discontinuity (van der Meer et al., 2018). These tomographic models support a slab detached under Tunisia since the Late Miocene. These tomographic models have low-resolution due to poor seismological coverage and low-seismicity rates in the region. Thus, under SE Tunisia the slab may extend to shallower regions and be connected to the Nubia plate as indicated by the presence of a high-velocity reflector imaged by refraction seismics in the mantle at 87 km depth under central Tunisia, slightly north of the southern Atlasic deformation front (Research group for lithospheric structure in Tunisia, 1992). Furthermore, intermediate-depth seismicity occurs in the Sicily Channel reflecting a ridid body within the mantle at depths around 100 km (Calò and Parisi, 2014; Chiarabba and Palano, 2017). The slab probably has a curved geometry with NE-SW orientation under the South Atlassic Fault and N-S orientation under the North-

South Axis of Tunisia (Piromallo and Morelli, 2003) (Figure 2.13). The present stress field and seismicity in Tunisia also supports a slab connected to the African continental lithospheric mantle (Soumaya et al., 2015). Finally, most of the slab underlying Tunisia would be formed by stripped subcontinental lithospheric mantle, thus not having high-velocity eclogites derived from the metamorphism of oceanic crust. This lower-velocity continental slab may have also contributed to the low-resolution of the slab imaged under Tunisia. The continental nature of this slab would also explain the fact that the slabs imaged by (Fichtner et al., 2015) represent an area larger than the possible oceanic slab consumed by subduction since the Cretaceous (e.g.,van Hinsbergen et al, 2014).

Eastward peeling back of the African lithospheric mantle was bounded to the southwest by the Tunisian Atlas STEP boundary (Figure 2.13). This dextral transform boundary has NW-SE orientation and is presently active in the region of the Tunisian Atlas front (Figure 2.13). The surface expression of this transform boundary is represented by the dextral Gafsa and Tozeur-Negrine faults (Zargouni, F. et Ruhland, 1981; Saïd et al., 2011b; Ben Hassen et al., 2014).

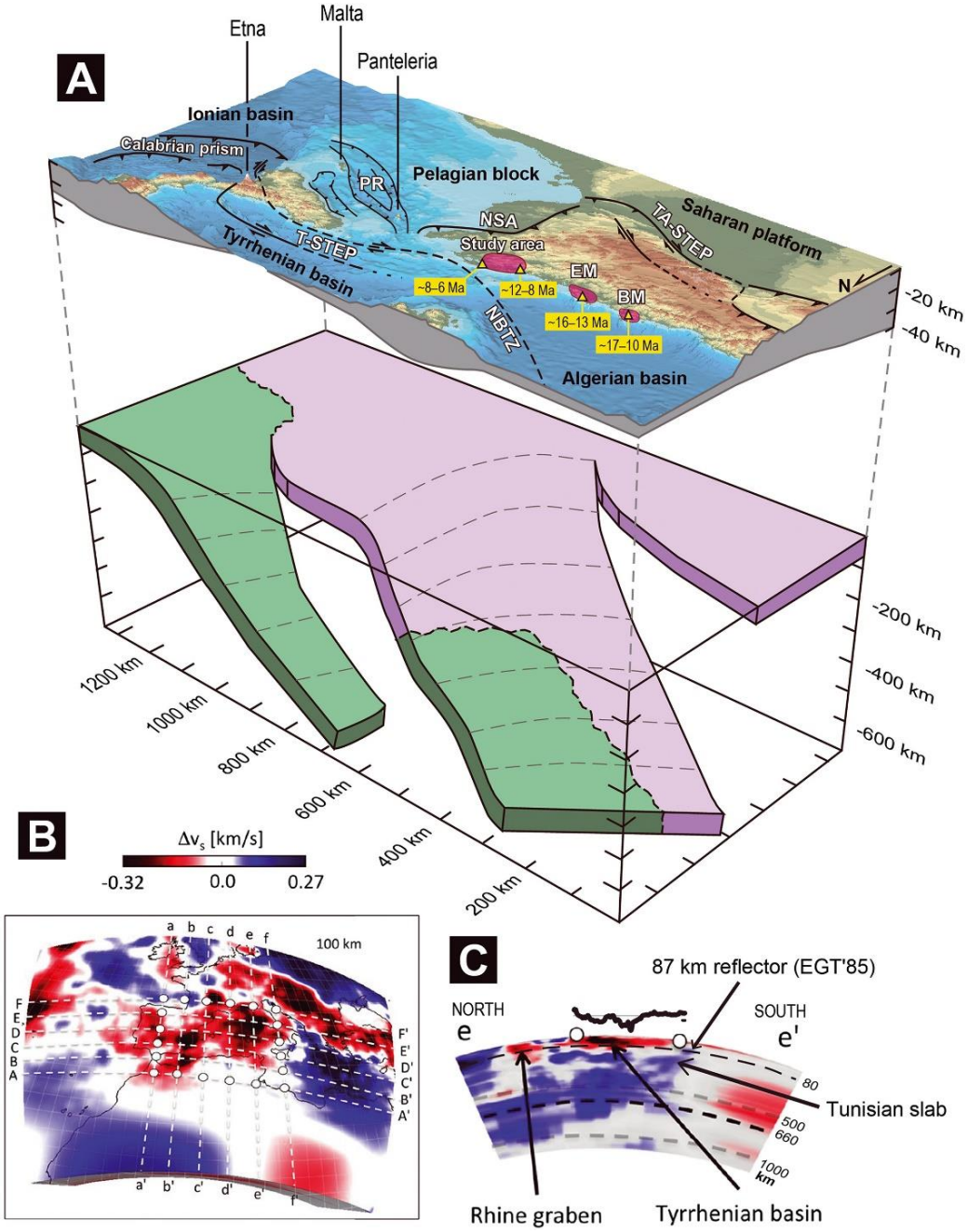

Figure 2-13: *((a) Tectonic sketch of the mantle structure under the Calabrian and Tunisian arcs. Green represents oceanic lithosphere subducted under the Tyrrhenian and Algerian basins. Pink represents stripped continental mantle litho-sphere of the Tunisian subducting slab. Notice that the Tunisian slab is bounded by two Subduction Transfer Edge Propagator (STEP) boundaries, the Tyrrhenian STEP (T-STEP) to the north (Govers & Wortel, 2005) and the Tunisian Atlas STEP (TA-STEP) to the SW. Furthermore, the age of volcanism related to subduction and delamination mechanisms together with regions where extension is described in Algeria and Tunisia, in red. See references in the discussion.NSA = north-south axis; BM = Bougaron massif; EM = Edough massif. (b) Tomographic model and N-S cross section through Tunisia and the Tyrrhenian basin showing the Tunisian slab and the location of the 87 km depth intramantle reflector detected by the EGT'85 seismic refraction experiment (Fichtner & Villaseñor, 2015; Research group for lithospheric structure in Tunisia, 1992).*

7. Conclusions

Northern Tunisia underwent extensional collapse during the Late Miocene by the contribution of two extensional systems with ENE- and SE-directed transport. These extensional structures exhumed the deep autochthonous Triassic sediments in the footwall of extensional LANFs like the Nefza extensional dome. Extension was accompanied by the extrusion of 8.5- to 9-Ma rhyodacites. Moreover, many of the Fe-Zn-Ba mineralizations present in northern Tunisia are hosted in the fault rock breccias or formed by the erosion and sedimentation of these breccias in alluvial fan systems.

Extension migrated towards the E-SE during the Messinian producing sedimentary depocenters with hanging-wall syncline geometry and associated synrift unconformities in the region of Mateur. Extensional structures in this region, including tilted half grabens, hanging-wall synclines and rollover anticlines, resulted from fault-bend folding over the ramp-flat-ramp geometry of the Ghezala LANF. The NE-transport extensional structures like the Ghezala LANF are cut by more recent SE-directed extensional faults.

The extensional structures in northern Tunisia appear folded and cut by Pliocene to Present contractional structures including NE-SW sinistral-reverse faults, WNW-ESE dextral faults and associated NE-SW to E-W folds. Plio-Quaternary shortening has refolded the previous fault-bend folds produced during extension. Furthermore, in some cases normal faults have been inverted as thrusts producing arrowhead tectonic inversion structures.

Deep mantle mechanisms that have migrated from Northern Algeria towards the East and Southeast since the Middle Miocene have probably driven extension. Tearing of the Calabrian mantle slab to the north of the Tunisian coast during the opening of the Tyrrhenian basin probably drove the Tortonian ENE-directed extension in northern Tunisia. Meanwhile, SE-directed extension could be related to the Late Miocene strip-ping of the African lithospheric mantle coeval to NW-directed subduction under northern Algeria and Tunisia.

Chapter 3: Halokinesis and ductile flow during Late Miocene extension in the Tunisian Tell and the thinning of Western Mediterranean Foreland Thrust Belts (FTB´s)

Extension in the Western Mediterranean has been mostly related to the dynamics of back-arc domains, where the main basins in the region formed since the Oligocene. However, extension also occurred away from the back-arc basins, propagating into the foreland domains of all the orogenic arcs bounding the Western Mediterranean. Here we analyze midcrustal extensional domes in the Tunisian Tell FTB, proposing a common tectonic mechanism for this extension in the rest of the Western Mediterranean foreland belts. The presence of Triassic rocks in the core of many geological structures of Northern Tunisia, classically interpreted as diapirs, has been the paradigm of the region's geology for decades. However, the deepest domal structures in the region are cored by greenschist-facies marbles and metapsamnites, stretched and exhumed in the footwall of extensional detachments, imaged in reflection seismic lines and outcropping in the field. Extension occurred sequentially by two sets of orthogonal normal faults during the Late Miocene. Illite crystallinity of Triassic metapelites in the region shows epizonal to anchizonal values favoring a model of late orogenic polyphasic collapse of the Tunisian Foreland Thrust Belt (FTB) from mid-crustal levels instead of a long-lived diapiric evolution since the Cretaceous as previously proposed. This late extensional collapse of the Tell FTB in Northern Tunisia and the consequent exhumation of orogenic middle crust in forearc type settings is a common feature of other FTB´s in the western Mediterranean, like the Betics and Rif, which underwent a late stage tearing or delamination of their subcontinental lithospheric mantle at the edges of the subduction system.

---

* Most of the content of this chapter not yet published and submitted to be considered for publication in Tectonics

1. Introduction

Northern Tunisia has been considered for decades as a paradigmatic region for the study of diapiric structures in an external foreland thrust belt context (Perthuisot, 1981; Vila, 1995; Bedir et al., 2001; Ben Chelbi et al., 2006; Melki et al., 2010; Ayed-Khaled et al., 2015; Troudi et al., 2017). Diapiric intrusions of Triassic evaporites are thought to have initiated in the Cretaceous during the rifting of the North Maghrebian passive margin, having been also extruded to the surface as thousand km^2 large salt glaciers (Vila, 1995; Vila et al, 1996; Ghanmi et al., 2001; Masrouhi and Koyi, 2012; Masrouhi et al., 2014; Ayed-Khaled et al., 2015; Amri et al., 2020). This Mesozoic extensional-diapiric structure would have evolved later in a convergent to transcurrent setting during the Cenozoic development of the Tell and Atlas Foreland Thrust Belts (FTB) that form part of the western Mediterranean alpine orogeny (Bouaziz et al., 2002; Melki et al., 2010; 2011; Amri et al., 2020)(Figure. 3.1). During thrusting, salt tectonics is interpreted to have played an important role, with the main decollements being located within the Triassic evaporites that presently are found at the base of the main Tellian thrust sheets (Khomsi et al., 2009,2016; Booth-Rea et al., 2018). Thus, some authors interpret the proposed salt canopies as over thrusted Triassic evaporites at the base of the Tellian nappes (Khomsi et al., 2009; Troudi et al., 2017).

Most authors consider that the present lithospheric structure of FTB´s in the Eastern Betics, Tell and Rif preserve the original thrust stack structure with only minor later extension, explaining the existing crustal thickness of these regions, below 30 km (Research group for lithospheric structure in Tunisia, 1992; Mancilla and Díaz, 2015), to the superposition of very thin nappes of the North Maghrebian and South Iberian passive margins, extended in the Mesozoic (e.g.Frizon de Lamotte et al., 1991; Gelabert et al., 1992; Platt et al., 2003 Crespo-Blanc & de Lamotte, 2006; ; Sàbat et al., 2011; Khomsi et al., 2016; Gimeno-Vives et al., 2019; Khelil et al., 2019). Alternatively, some authors suggest that these foreland domains have been strongly extended during the Middle to Late Miocene (Rodríguez-Fernández et al., 2011; Booth-Rea et al., 2012; 2018; Moragues et al., 2018; de la Peña et al., 2020;). According to the later hypothesis, evaporitic rocks at the base of the Tellian thrust sheets were reworked by extensional processes, localizing the main low-angle normal faults that thinned the Northern Tunisia FTB in the Late Miocene (Booth-Rea et al., 2018).

The Tell and Atlas belts are generally interpreted as external FTB´s comprising only sedimentary rocks, despite the presence of the Giallo Antico marbles, well known since Roman

times at the boundary between the two orogenic belts (e.g. Röder, 1988; Bugini et al., 2019). These marbles contain a WNW-ESE to WSW-ENE oriented magnetic fabric interpreted as a tectonic stretching (Ghorabi and Henry, 1992). Equivalent marbles also crop out in Jebel Ichkeul and the Oued Belif dome in the Tell belt (Booth-Rea et al., 2018; Khelil et al., 2019, Figure. 3.2). Moreover, Permo-Triassic epizonal rocks that underwent temperatures between 300 and 400ºC are described at the core of the Oued Belif dome (Mahdi et al., 2013).

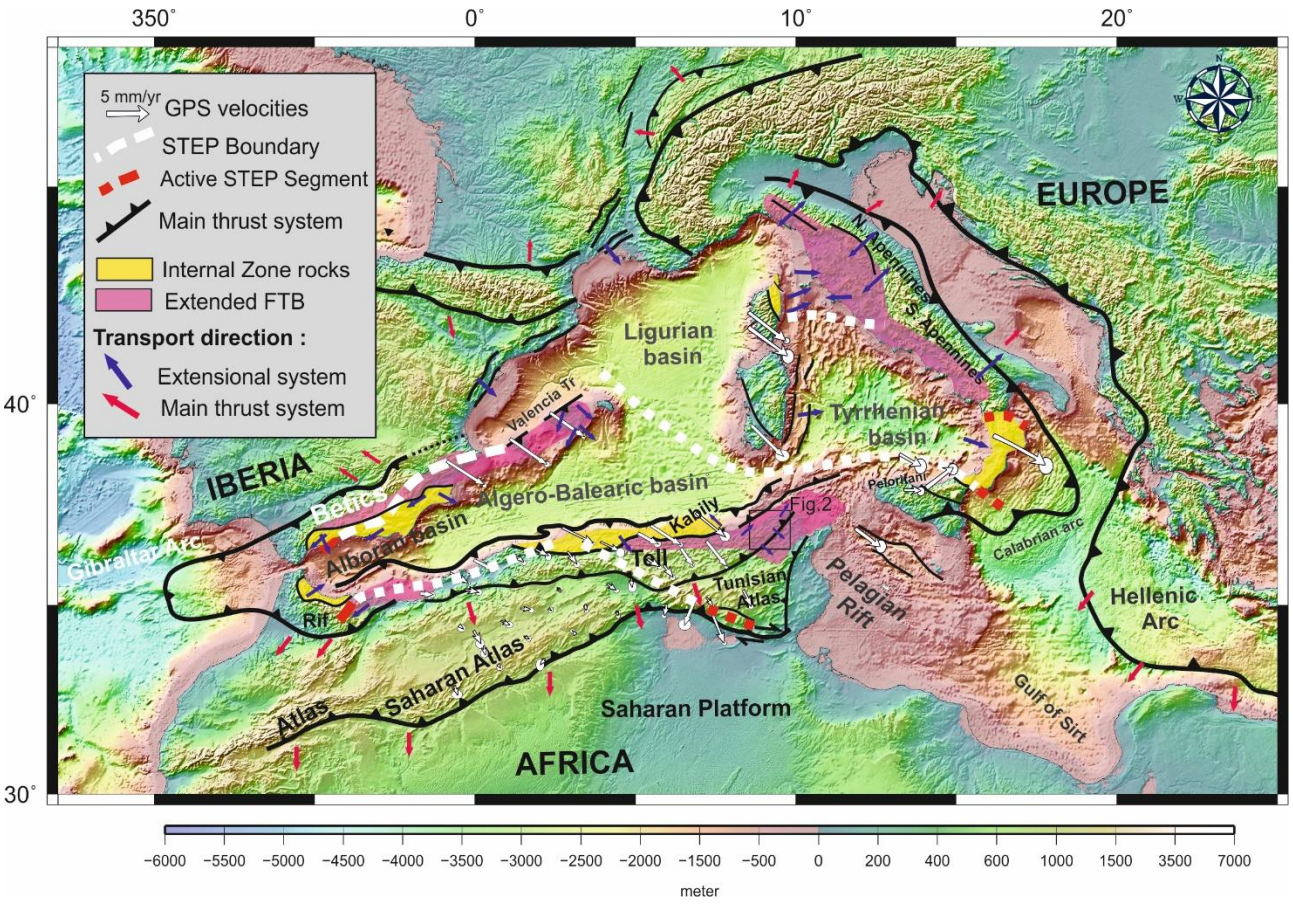

Figure 3-1: Tectonic boundaries, orogenic arcs and sedimentary basins of the Western Mediterranean. Figure modified from Booth-Rea et al. (2007; 2018) and Gaidi et al. (2020). GPS movement towards fixed Africa from Bougrine et al. (2019) and Nocquet,(2012).Fault patter along Algeria-Tunisia based on Kherroubi et al., (2009), Rabaute and Chamot-Rooke, (2014) and (Aïdi et al., 2018). Extended FTB domains from (Carmignani and Kligfiel, 1990), Ghisetti and Vezzani, (2002), Booth-Rea et al. (2012; 2018), Rodríguez-Fernández et al. (2013), Moragues et al., (2018)

Interestingly, some work has shown the importance of late Miocene extension in the region related to either the internal dynamics at the deformation front of the Tell accretionary wedge (Khelil et al., 2019) or to overall Late Miocene orogenic collapse of Northern Tunisia (Cohen et al., 1980; Booth-Rea et al., 2018; 2020), which could explain the exhumation of these rocks to the surface. However, the origin, exhumation and tectonic implications that these rocks have for

the tectonic evolution of the region, and at a larger scale, for the evolution of the western Mediterranean FTB´s, have not been satisfactorily analyzed until now.

Here, we show results of illite crystallinity for Triassic pelites and metapelites cropping out in the Tell FTB of Northern Tunisia, suggesting that they formed an overthickened orogenic wedge that reached epizonal metamorphic conditions. Together with extensive fieldwork and the analysis of multichannel seismic reflection lines, these data favor a model of mid-crustal extensional exhumation and crustal thinning of a previously thickened FTB, instead of a general protracted Mesozoic to Cenozoic diapiric evolution for Northern Tunisia. Finally, we integrate these findings in the tectonic evolution of FTB´s of the Western Mediterranean orogenic belts.

2. Geological setting

The Tell FTB in Northern Tunisia is part of the Alpine orogenic system that surrounds the Western Mediterranean Liguro-Provencal, Algero-Balearic, Tyrrhenian and Alboran basins that formed in a context of Nubia-Eurasia convergence since Late Cretaceous time (Dewey et al., 1989). This convergent setting favored the action of other tectonic mechanisms related to subduction, like slab roll back accompanied by slab tearing and detachment at the edges of the western Mediterranean arcs, which also contributed to the development of these basins and their surrounding orogenic belts (e.g. Lonergan and White, 1997; Carminati et al., 1998; Wortel and Spakman, 2000; Govers and Wortel, 2005; Booth-Rea et al., 2007; Chertova et al., 2014, van Hinsbergen et al., 2014; Romagny et al., 2020). Furthermore, particularly beneath continental domains like the South Eastern Betics, Northern Tunisia or the Central Apennines, delamination of the subcontinental lithospheric mantle driving crustal extension, magmatism and topographic uplift, has also been proposed (Duggen et al., 2003; Martínez-Martínez et al., 2006; Di Luzio et al., 2009; Roure et al., 2012; Levander et al., 2014; Mancilla et al., 2015; Booth-Rea et al., 2018; Camafort et al., 2020) (Figure. 3.1).

The Tell FTB in Tunisia is represented by the overthrusted nappes of the Maghrebian Tethys oceanic domain (Numidian Flysch) and by the underlying infra-Numidian and Atlassic sedimentary series that deposited along the North Maghrebian passive margin during the Mesozoic and Cenozoic (Khomsi et al., 2009; Riahi, 2010; Belayouni, 2013)(Figure. 3.2). The infra-Numidian domain is formed by several imbricated allochthonous nappes (Rouvier, 1993, 1992; Khomsi et al., 2009). Its Internal metamorphic domain is found to the NW in the Kabylies

in Algeria, where HP Eocene to Early Miocene rocks crop out (e.g. Bouillin et al., 1986; Bruguier et al., 2017). Metamorphic flysch successions also occur in la Galite island, North of Tunisia (Belayouni et al., 2010).

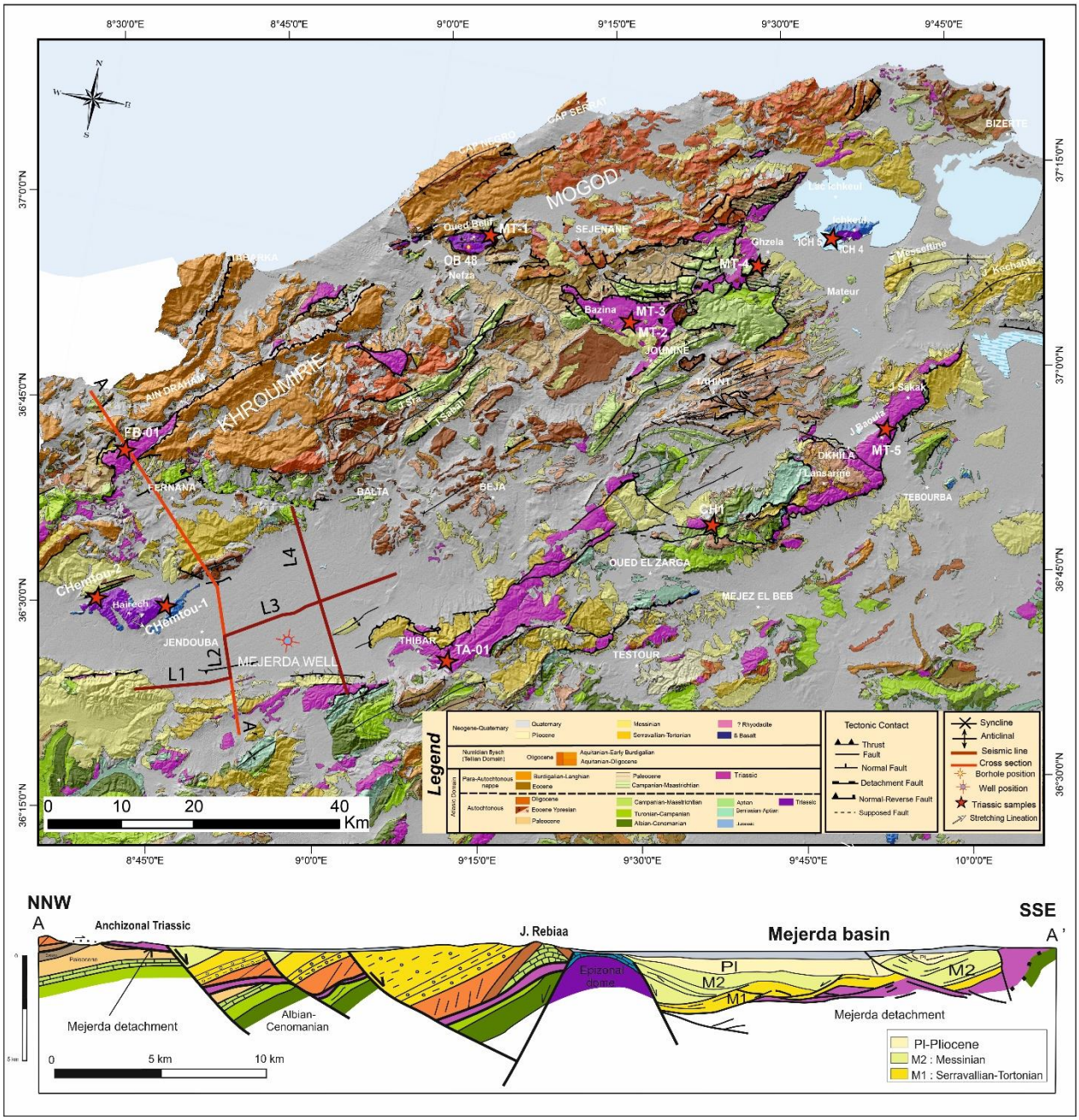

Figure 3-2: Geological map of Northern Tunisia and cross-section through the studied region. Notice the location of the analyzed Triassic pelitic samples together with the location of interpreted reflection seismic lines. OB 48 locality corresponds to bore hole where Mahdi et al. (2013) analyzed epizonal samples. Location in Figure. 4.1.

Tectonic shortening in the Tell FTB was first registered as a general angular unconformity between the Paleogene and Early Miocene series (Khomsi et al., 2009), and later by the overthrusting of Oligocene to Late Burdigalian Numidian Flysch series over Early Miocene foredeep sedimentary successions of Burdigalian to Langhian age (Riahi, 2010; Belayouni, 2013; Khomsi et al., 2009; 2016; Boukhalfa et al., 2020).

Most authors consider shortening in Northern Tunisia continued throughout the late Miocene producing folds (Melki et al., 2010, 2011; Ramzi and Lassaad, 2017). However, recent work has reinterpreted these folds as being extensional fault-bend related roll-overs and hanging-wall syncline structures produced during Tortonian to Messinian extensional collapse of the Tell FTB (Booth-Rea et al., 2018; 2020; Gaidi et al., 2020). Meanwhile, shortening at the time was accommodated further South, in the Tunisian Atlas (Bouaziz et al., 2002; Saïd et al., , 2011a, b).Tectonic inversion in Northern Tunisia occurred since the Pliocene-Quaternary, marked by a prominent angular unconformity in reflection seismic lines, developing new basin depocenters over the footwall of reverse faults and oblique strike-slip faults (e.g. Melki et al., 2010; 2011; Ayed-Khaled et al., 2015; Gaidi et al., 2020; Camafort et al., 2020a). Many of the reverse fault segments formed by tectonic inversion of earlier Late Miocene normal faults, especially those bounding sedimentary depocenters, such as the Mejerda and Mateur sedimentary basins (Booth-Rea et al., 2018; Gaidi et al., 2020). The main fault system accommodating this late Pliocene to Present-day convergence across Northern Tunisia is the Alia-Thibar dextral reverse fault zone, formed by the linking of at least five different fault segments (Gaidi et al., 2020).

3. Methods

For analyzing the structure of Northern Tunisia, together with the metamorphism undergone by the Triassic rocks of Northern Tunisia, we use a multidisciplinary approximation. We carried out field work with structural geology emphasis, and also to sample different Triassic evaporite bodies in the region. Our work is based on 1:50.000 geological maps of Northern Tunisia published by the Office National des Mines (ONM), which we digitized and revised (Booth-Rea et al., 2018; Gaidi et al., 2020). Furthermore, we interpreted several industry multichannel reflection seismic lines from the Tunisian Company of Petroleum Activities (ETAP) that cross through the Mejerda basin in Northwestern Tunisia. Triassic pelitic samples from different

massifs in Northern Tunisia we analyzed using X-ray diffraction techniques to determine their illite crystallinity.

3.1 X-ray diffraction

To avoid possible weathering effects, unaltered, clean samples were taken away from joints and well below the surface. Samples were washed and, after coarse crushing, homogeneous chips of the rocks were used for the X-ray diffraction (XRD) analyses. The clay fraction (<2μm) was extracted by repeated centrifugation and extraction of supernatant liquid subsequent to settling, according to the Stokes´s law. Oriented aggregates were prepared by sedimentation on glass slides. Whole and clay fractions were studied using a PANalytical X'Pert Pro diffractometer, with CuKα radiation, 45 kV and 40 mA, which is equipped with an X'Celerator solid-state linear detector. We used a step increment of 0.008° 2θ and an overall counting time of 10 s/step. For illite ‘‘crystallinity’’ determination, samples were prepared and Kubler Index (KI) measured according to the experimental conditions recommended by IGCP 294 IC Working Group (Kisch, 1991). Our KI values (x) were transformed into CIS values (y) according to the equation $y = 0.972x + 0.1096$ ($r = 0.970$), obtained in our laboratory using the international standards of Warr and Rice (1994). As the KI and CIS scales are not equivalent (Warr and Ferreiro-Mahlmann, 2015) anchizone limits for the latter are 0.32-0.52 ºΔ2θ. The b parameter of mica was obtained from the (060) peak measured on slices of rock cut normal to the sample foliation (Sassi and Scolari, 1974). Basal spacings (d_{001}) of micas and chlorites were obtained respectively from their peaks (00,10) and (004). For all the measurements of spacings, quartz from the sample itself was used as internal standard.

4. Results

4.1 Illite crystallinity

X-Ray diffraction results indicates quartz, white mica ± K-feldspar ± plagioclase ± hematite ± dolomite ± calcite (Table 3.1). Some of the samples from the Infranumidian Triassic also contain chlorite or cristobalite and one sample gypsum. Moreover, minerals usually linked to low-temperature alteration processes, like smectite, kaolinite or jarosite exist in the samples in very variable proportions.

Illite crystallinity (KI) of the Triassic metapelites cropping out in the Tunisian Tell shows two different populations (Table 3.1, see location in Figure. 3.2). Samples (Chemtou01,

Chemtou02, MT-1, ICH-04) picked from the deep autochthonous Triassic outcrops from Oued Belif, Hairech and Ichkeul anticlines are characterized by typical epizonal values between 0.26 and 0.30 (Table 3.1). Meanwhile, the allochthonous Triassic located at the base of the Infranumidian nappe is characterized by a range between diagenetic values (0.57, MT-5) and mostly anchizonal values between 0.33 and 0.47 (MT-2, MT-3, CH1, FB-01 and TA-01), together with an epizonal value in sample MT-4.

Tableau 3-1: Illite crystallinity results and mineralogy of the studied Triassic samples

		10Å		5Å			d_{001}	
Samples	**Minerals**	<2µ*	WF	<2µ	WF	b mica	mica	chlorite
CHemtou-1	quartz, mica, Kfds, hematite, smectite↑, kaolinite	0,26	0,26	0,26	0,26	9,032	9,978	
CHemtou-2	quartz, mica, plagioclase, hematite	0,30	0,28	0,28	0,27	9,038	9,971	
MT-1	mica, Kfds, quartz↓, jarosite	0,27	0,27	0,25	0,26			
ICH-04	calcite↑, kaolinite, mica, Kfds	0,29	0,26	0,30	0,25			
ICH-05	quartz, calcite, mica↓, plagioclase, smectite							
MT-2	quartz, mica, dolomite, cristobalite	0,32	0,32	0,32	0,29			
MT-3	quartz, mica, dolomite, cristobalite, Kfds↓	0,34	0,31	0,32	0,28			
MT-4	quartz, mica, smectite, Kaolinite, dolomite↑	0,31	0,32	0,32	0,28			
MT-5	quartz, mica, chlorite, gypsum	0,57	0,46	0,56	0,43			
CH1	quartz, mica, chlorite, hematite↓,Kfds↓↓	0,47	0,46	0,41	0,38	9,029	9,971	14,19
FB-01	dolomite↑, mica, chlorite, quartz↓	0,37	0,37	0,35				14,19
TA-01	quartz, mica, chlorite, Kfds, plagioclase	0,42	0,42	0,39	0,36	9.024 9.044	9,945	14,21
	↑, ↓, ↓↓ = qualitative indication of amount							
	*Anchizone limits (Warr and Ferreiro Mählmann, 2015) =		0,52	-	0,32			
	WF - Whole Fraction							

The number of mica b parameters in the metamorphic autochthonous Triassic outcrops is too low to get conclusions, however, it is between 9.032 and 9.038 Å, which would be characteristic of orogenic micas grown under an intermediate P/T metamorphic gradient (Guidotti and Sassi, 1986). Basal spacing of chlorites in the allochthonous Triassic is considerably high (14.19-14.20), which indicates high Si content (Nieto, 1997), which, in turn, suggests low temperature chlorites (Vidal et al., 2016 and references therein).

4.2 Extensional detachments in reflection seismics

Seismic lines across the Mejerda basin show a prominent reflection, namely the Mejerda detachment, cutting down at a low angle into the Atlas Cretaceous autochthonous sediments (Seismic lines Mejerda 1, 2, 3 and 4, Figures. 3.2, 4.3 and 3.4). The hanging-wall of the detachment is formed by Triassic rocks drilled in the Mejerda 1 drill hole (Troudi et al., 2017), which are overlain by tilted late Miocene sediments showing progressive angular unconformities and halokinetic intrusions over the evaporitic rocks. These extensional structures are overlain by an angular post-rift unconformity, sealed by folded Pliocene to Quaternary sediments. Meanwhile, the footwall of the Mejerda detachment, drilled in Mejerda 1 hole is formed by Middle Cretaceous marly limestones. Along lines 1, 2 and 3, the Mejerda detachment deepens towards the SW from 500 to 1800 ms at the SW border of the basin (Figure. 3.3).

Triassic evaporites form boudin type bodies together with highly-reflective packages, interpreted as Eocene limestones, cropping out nearby, above the detachment and below the Late Miocene sediments (Ayed-Khaled et al., 2015). Normal faults overlying the Mejerda detachment show listric geometry, with both SW- and NE-directed kinematics (Figure. 3.3). Overall, the normal faults cutting the Late Miocene sediments form a listric fan structure that roots into the Mejerda detachment. Few reflectors dipping smoothly towards the NE occur in the footwall of the Mejerda detachment, indicating a low-angle ramp geometry below the detachment. The low-angle detachment crops out to the South, uplifted in the hanging wall of the Pliocene to Quaternary thrust that deforms the southern margin of the basin (Gaidi et al., 2020, Figure. 3.2). The detachment fault zone is formed by a foliated cataclastic breccia affecting different Triassic lithologies, including red beds, dolostone and gypsum (Figure. 3.5a). This Triassic sequence that crops out largely along the Thibar anticline is itself detached over autochthonous Early Cretaceous marls (Mcherga Formation) that form the core of the anticlinal structure (see Geological map in Figure. 3.2).

The Chemtou marbles and underlying Triassic metapsamnites crop out in an anticlinal structure along the northwestern border of the Mejerda basin. This antiformal structure produces a prominent WSW-ENE oriented ridge with a positive gravimetric anomaly all along the border of the basin, coinciding with the Hairech and Rebiaa massifs (Amiri et al., 2011; Frifita et al., 2020)(See cross-section A-A´ in Figure. 3.2). These massifs are bounded by WSW-ENE trending normal faults that separate the metapsamnites and marbles in their core from strongly mineralized

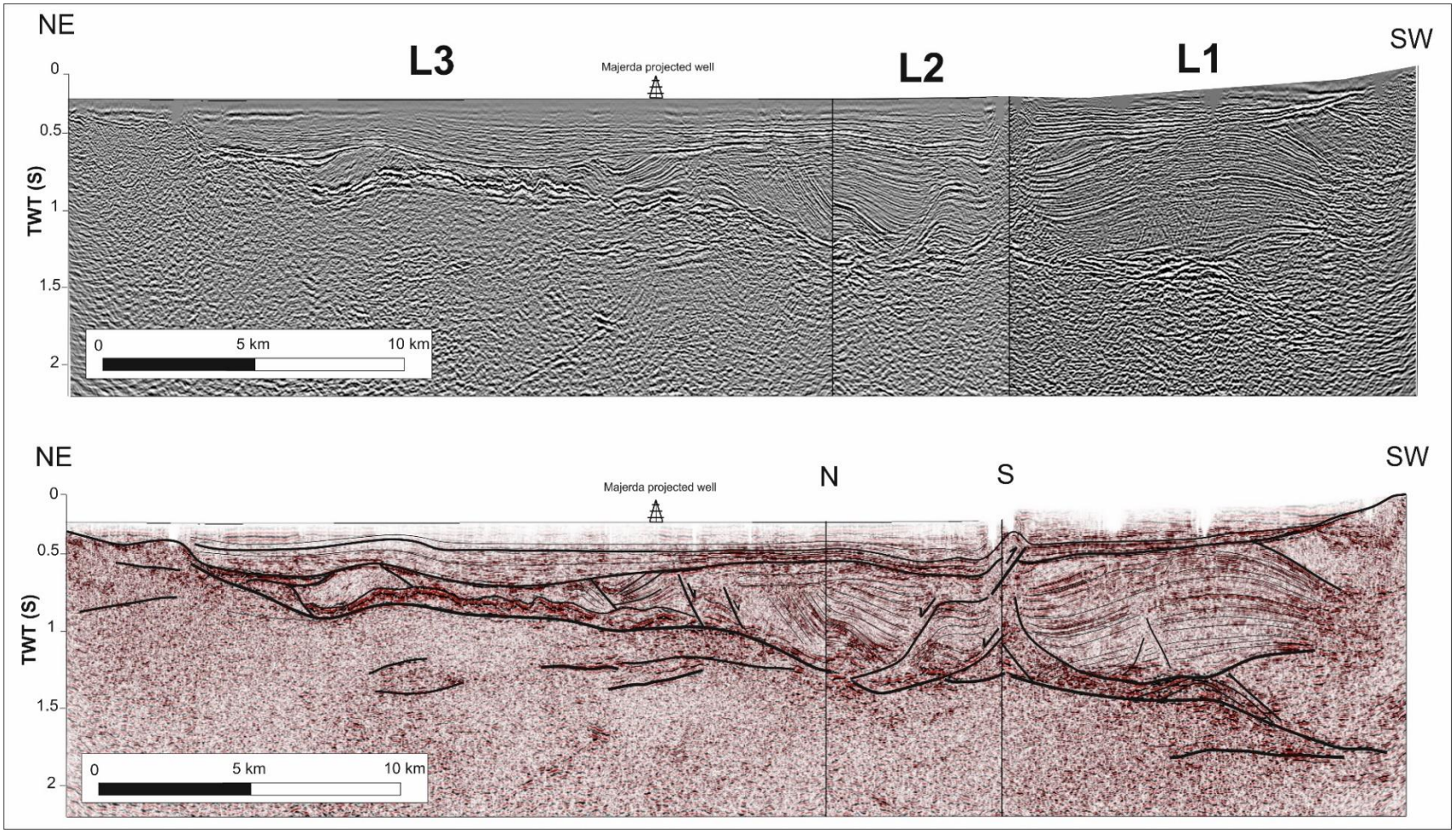

Figure 3-3: Seismic cross-section composition using multichannel reflection seismic lines L1, L2 and L3 through the Mejerda basin, showing normal fault listric fan cutting through Late Miocene sediments and rooting in the Mejerda detachment.

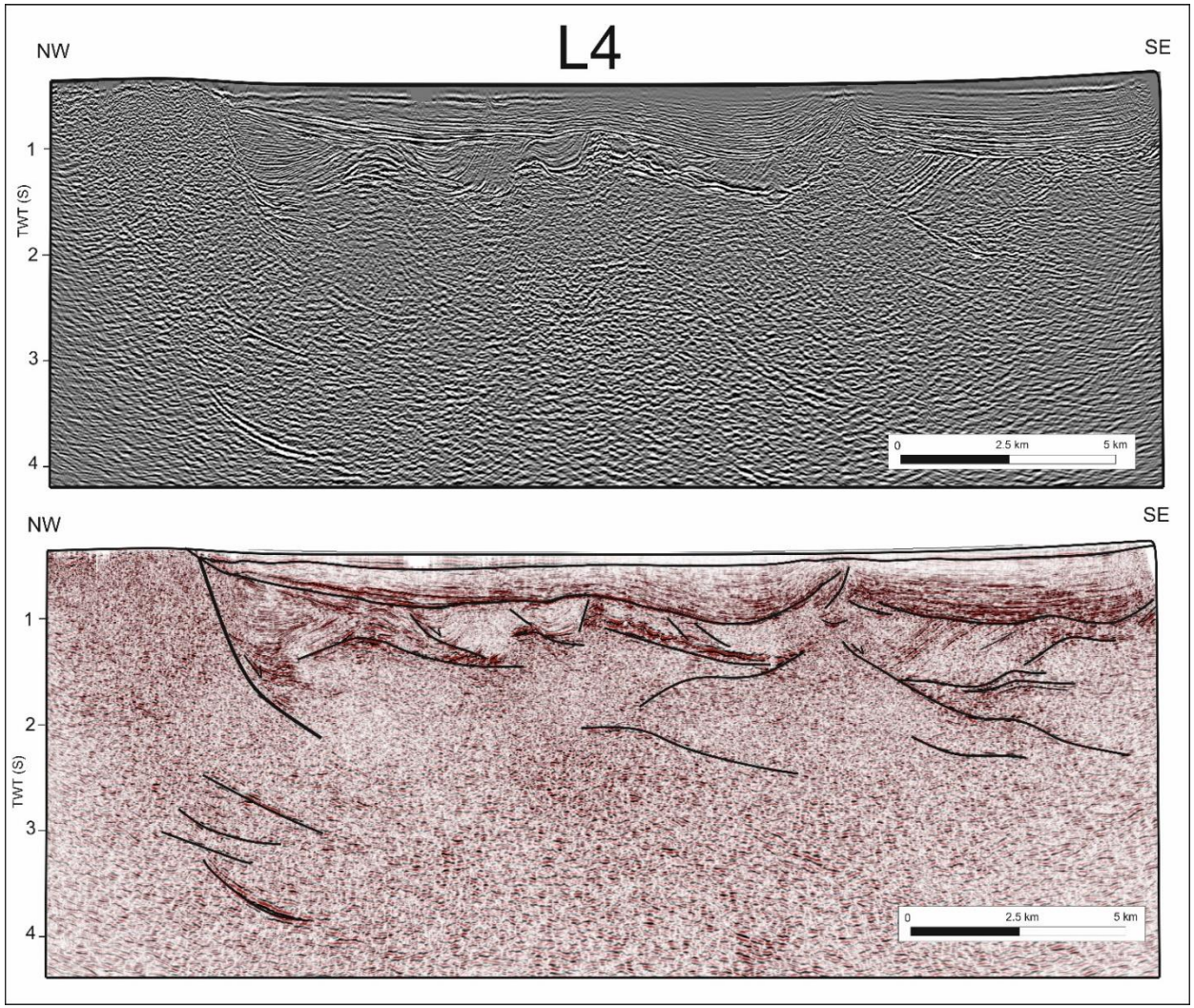

Figure 3-4: Seismic reflection line L4 across the Mejerda basin, showing high-angle faults exhuming the autochthonous Atlas rocks to the NW and tilted Late Miocene sediments overlying the Mejerda detachment. Late Plio-Quaternary folding is also evident in this line.

Eocene carbonates and Messinian sediments to the Northwest. Meanwhile, the southeastern border of the massifs also coincides with an WSW-ENE trending high-angle normal fault imaged in seismic line L4 (Figure. 3.4). This normal fault cuts through the whole structure described above rooting in low-angle reflectors at a depth of approximately 3000 ms TWT (Figure. 3.4).

4.3 Field outcrops

Epizonal rocks occur in the Hairech, Ichkeul and Oued Belif massifs in Northern Tunisia (Figure. 4.2). These rocks are marbles and metapsamnites formed by the metamorphism of Jurassic limestones and underlying Triassic red-beds. Samples from the Hairech and Ichkeul massifs show clear metamorphic foliations marked by the growth of mica and chlorite, together with chlorite pressure shadows around porphyroblasts. Marbles in the Ichkeul massif show a marked blastomylonitic foliation, containing a WSW-ENE stretching lineation, which in turn is cut by a penetrative system of NW-SE trending calcite veins (Figure. 3.5b). At microscopic scale, mica and chlorite growth define the mylonitic foliation (S_m) that cuts the older compositional banding (S_0) defined by pelite-carbonate layers (Figure. 3.5c, d). These structures are presently folded in the core of an anticline with a WSW-ENE oriented axis. The southern limb of the anticline is cut by E-W trending high-angle normal faults with SE-directed transport (Figure. 3.5e).

Marbles and metapsamnites from the Hairech massif also show a penetrative foliation, marked by the growth of white mica and chlorite parallel to the lithological banding (Figure. 3.5f). However, we did not observe an associated stretching lineation. These rocks do contain a magnetic fabric, related to a strong preferred crystallographic orientation in phyllosilicates, interpreted as a probable syn-metamorphic stretching lineation, with WNW-ESE to WSW-ENE orientation (Ghorabi and Henry, 1992). The Hairech massif shows an open antiformal WSW-ENE trending structure with its northern and southern limbs cut by high-angle normal faults with NW and SE directed transport, respectively (H. Rouvier, 1977)(cross-section, Figure. 3.2). These normal faults bound the Messinian sediments of the Mejerda basin, both to the North and South of the massif, and cut-mineralized outcrops of Eocene allochthonous rocks (cross section, Figure. 3.2). Anchizonal Triassic rocks crop out along both the Northern and Southern margins of the Mejerda basin (Samples FB-01 and TA-01, Figure. 3.2). These rocks crop out extensively in the region forming the base of the hanging-wall of the Mejerda detachment, for example, to the E-SE of Fernana, and in the region around Thibar (Figure. 3.2).

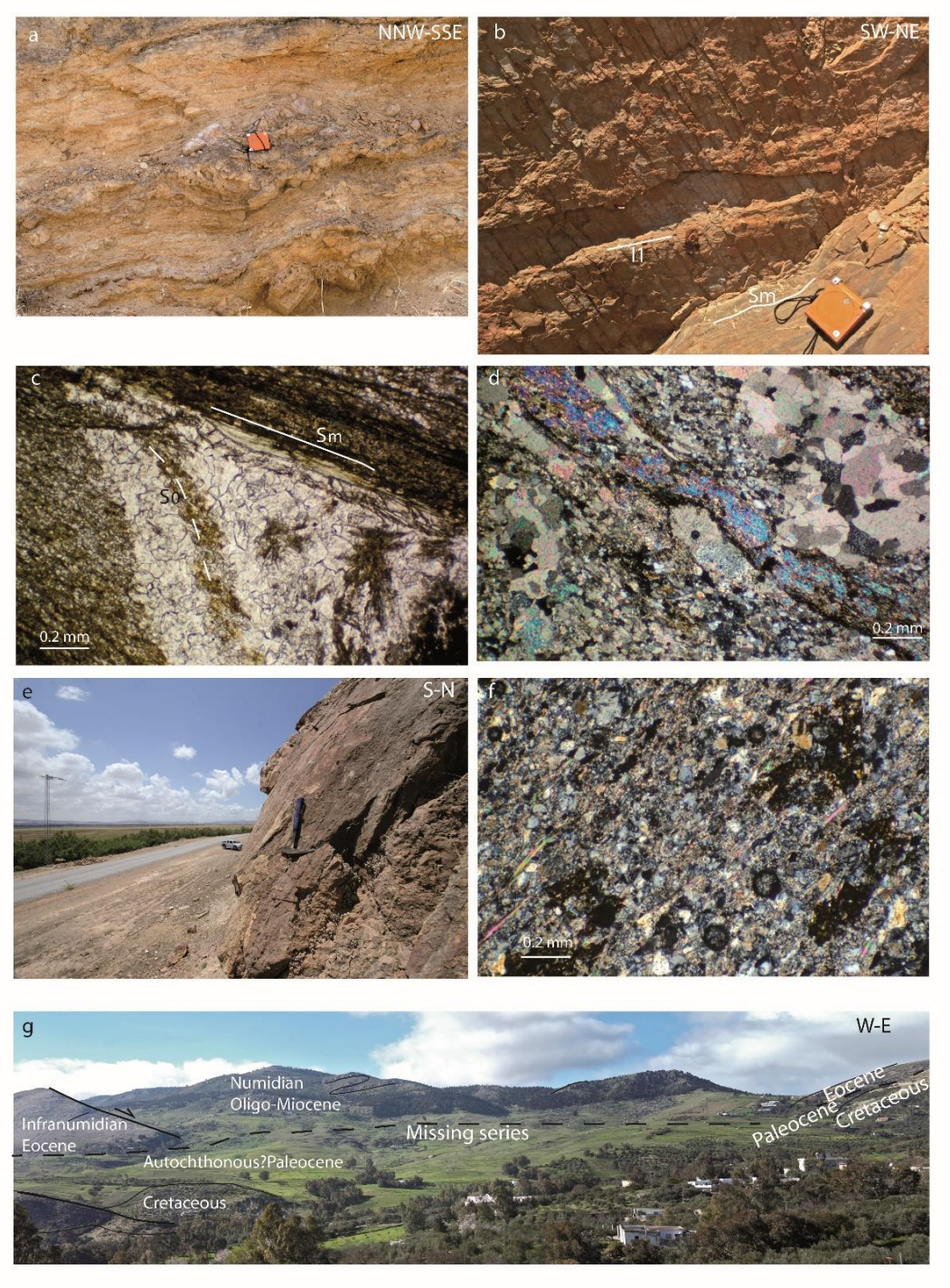

Figure 3-5: a) Foliated breccia affecting Triassic rocks in the Mejerda detachment. Notice cataclastic foliation and rotated porphyroclasts in the fault zone. b) Ichkeul marbles showing NW-SE oriented stretching lineation (L1) and mylonitic (Sm) foliation, later cut by calcite veins. c) Thin section of a greenshist metapelitic sample from the Ichkeul dome, notice Sm and S0 folitations and growth of large chlorite crystals parallel to the Sm fabric. d) Thin section showing a metapelitic band marked by white mica growth intercalated in calcite marble. e) Normal fault cutting through the southern limb of the Ichkeul dome, with SE-directed extension. f) Thin section of a metapsamnite from the Hairech dome, showing large white mica crystals defining a metamorphic foliation in these rocks. g) Panoramic view of the Tell-Atlas contact near Balta. Notice the missing infranumidian Eocene limestones, cut by a normal fault, along the supposed thrust contact between the Numidian Flysch and the underlying autochthonous series. We relate the missing series along this contact to extensional reworking of the original thrust contact by the activity of the Mejerda detachment.

These Triassic rocks, are directly overlain by extensional riders of diverse rocks like the Numidian Flysch, Eocene limestones or Cretaceous-Palaeogene Infra-Numidian sediments, and also by tilted Late Miocene sediments (see geological map and cross section, Figure. 3.2). These features are also observed in the seismic lines crossing the Mejerda basin (Figures. 3.3 and 3.4). To the East of Fernana, the Mejerda detachment shows a low-angle footwall ramp, cutting down towards the South from the Eocene to the Turonian-Santonian (cross section, Fig. 3.2). Finally, the detachment and overlying Triassic anchizonal rocks have been folded and thrusted over the whole sedimentary sequence of the Mejerda basin along its southern border during the Plio-Quaternary (Gaidi et al., 2020). This tectonic inversion also affected the Northern margin of the basin, along the Balta-Fernana thrust, a process the uplifted the Mejerda detachment in the hanging wall of the thrust, forming the southern contact of the Kroumerie Numidian Flysch outcrops and the Kasseb unit, over the autochthonous Atlas Cretaceous (Figure. 3.5g).

Outcrops of Triassic metapelites in the Oued Belif dome are strongly overprinted by mineralizations and magmatic related processes (Decrée et al., 2013, 2014b; Mahdi et al., 2013). These metamorphic rocks contrast with the overlying Paleogene and Eocene Infranumidian sediments, marking a pronounced metamorphic gap between epizonal and diagenetic rocks. Exhumation related structures in this region are particularly clear and intimately related to magmatic processes, with a well-defined brittle-ductile shear zone between the Triassic metapelites and overlying sediments, namely, the Nefza detachment (Booth-Rea et al., 2018). The main extensional detachment produced Eastwards directed extension during the extrusion of rhyodacites that show a magmatic foliation that is parallel to an overlying mylonitic foliation in marbles from the footwall of the Nefza detachment (Booth-Rea et al., 2018). Furthermore, the magmatic evolution evolves from plutonic intrusion of granodiorites in the Serravallian (12 Ma) to the shallower extrusion of volcanic rocks in the Tortonian (8-9 Ma) (Decree et al., 2014).

5. Discussion

5.1 Low-temperature metamorphism in the Tunisian Tell

The new illite crystallinity data we show in this study together with previous data in the region (Mahdi et al., 2013) manifests the presence of lower-greenschist epizonal rocks in the core of the structurally deepest domal Triassic outcrops of Northern Tunisia (Table 3.1). These Permo-Triassic rocks have been interpreted as forming the outcropping base of the authochthonous Mesozoic Atlassic sedimentary cover, deposited in the North Maghrebian passive margin (Rouvier, 1993, 1992; Booth-Rea et al., 2018). The fact that these minerals

show clear metamorphic textures and illite crystallinity values below the limit between anchizone and epizone imply they underwent temperatures above 300 ºC characteristic of mid-crustal depths (Frey, 1987; Merriman and Roberts, 1985; Merriman and Peacor, 1998).

Some samples contain variable proportions of smectite, kaolinite and jarosite, which are low-temperature minerals, incompatible with the metamorphic conditions described for the Triassic outcrops. The occurrence of these low-temperature minerals in rocks of higher diagenetic-metamorphic grades has been often described and interpreted as the result of retrograde diagenesis (Abad et al., 2003; Nieto et al., 2005), fluid-mediated retrograde processes occurring under diagenetic conditions. In particular, do Campo et al., (2017) linked the existence of jarosite in anchizonal/epizonal rocks of the Central Andes with the activity of hydrothermal fluids producing acid type alteration, related with the posthumous activity of the Ordovician volcanic arc; this alteration produced the widespread occurrence of retrograde diagenesis products as smectite and kaolinite in slates and metavolcanic rocks. Similar volcanic activity occurred in Northern Tunisia, especially obvious in the Oued Belif dome, which together with the hydrothermal activity related to extensional faulting can easily explain the presence of these retrograde mineral phases in the studied samples.

The infranumidian Triassic rocks cropping out above the Ghzela and Mejerda extensional detachments, below the Numidian nappes, reached anchizonal to diagenetic conditions below 300ºC. This scattering of KI values for the Infranumidian Triassic that crops out in a large area all along Northern Tunisia may represent original depth differences within the Tell orogenic wedge. The diagenetic value in sample MT-5 is located to the SE, theoretically, close to the Tell deformation front, where the Triassic is directly covered by Early Miocene fore-deep olistostromic sediments at the Lansarine ridge (Figure. 3.2). Meanwhile, most of the samples further towards the W or NW give anchizonal values, reflecting an original deeper position within the orogenic wedge. Sample MT-4 with epizone values is located at the footwall of the Ghzala extensional detachment a few meters below the fault zone, in the Jalta Pb-Zn mine. The high-temperature reached by this sample may reflect hydrothermal alteration around the fault zone, which has been dated as Tortonian (8-11 Ma) using Pb isotope compositions of galena (Jemmali et al., 2014).

Meanwhile, towards the SE of the Tell orogenic wedge at the tip of the deformation front the Triassic rocks underwent lower temperatures not surpassing diagenetic conditions. At present, the whole nappe stack, between epizonal rocks at the base and diagenetic Numidian series at the top has a total thickness around 3 s TWT (Booth-Rea et al., 2018) that would correspond to around 4 km depth using a velocity of 2.7 km/s for the sediments of the Tell belt.

Using an orogenic intermediate P-T gradient of 20ºC/km, as deduced from the micas b parameter, this means the original Tell nappe stack, was thinned from approximately 15 to 4 km during the Late Miocene extensional event, or that the epizonal Atlas Triassic domes have been exhumed from under 15 km overburden. This is probably a conservative estimation taking into consideration that P-T gradients determined from metamorphic rocks in the Betics and external Rif are closer to 15 ºC/km (e.g.Azañón et al., 1998; Booth-Rea et al., 2002; Negro et al, 2007) . This assertion is supported by the present structure of the Tell belt that shows extensional listric fans overlying extensional low-angle normal faults at least at two different structural levels, corresponding to the Ghzela and Mejerda detachments, and the deeper Nefza detachment that flattens around 3s TWT (Booth-Rea et al., 2018). The Ghzela and Mejerda detachments produced ENE-WSW directed extension cutting down into the Tell orogenic wedge and reaching anchizonal depths, whilst the Nefza detachment reached mid-crustal depths of approximately 15 km where deformation was governed by dynamic recrystalization creep, producing the mylonitic foliation and WSW-ENE stretching lineation observed in the Ichkeul massif marbles.

5.2 Halokinetic structures in Northern Tunisia

Concerning the diapiric origin of the Triassic outcrops in Northern Tunisia, our data indicates the necessity of reinterpreting some of the halokinetic structures described in the region. Some of the supposed diapirs have both geological and geophysical characteristics that are at odds with a standard diapiric structure. In this respect, gravity studies in the region show that some of the Triassic outcrops in Northern Tunisia, interpreted as diapirs, give positive gravimetric anomalies, and are modelled using higher densities than the surrounding rocks (Benassi et al., 2006; Amiri et al., 2011; Ayed-Khaled et al., 2012; 2015; Naouali et al., 2017). In other cases, diapiric boundaries coincide with faults that are forced to curve in such a way that the Triassic material that crops out at the surface above the underlying Atlas sedimentary sequence will be rooted underneath these sediments at depth (Ayed-Khaled et al., 2015; Marzoughi et al., 2015). Finally, the interpretation of seismic lines shows that many of the halokinetic structures are rooted in the Triassic material overlying low-angle extensional faults and detachments (Booth-Rea et al., 2018)(Figures. 3.3 and 3.4).

We find two main types of Triassic outcrops, the shallower of which, develop halokinetic structures related mostly to the late Neogene extensional phase, and the deeper ones are represented by exhumed middle crust formed by autochthonous Triassic redbeds and marbles. The first type of Triassic bodies outcrop extensively in the Thibar, Lansarine or Bazina regions and have traditionally been interpreted as salt canopies or glaciers overlying the Atlas

Cretaceous series (e.g. Masrouhi et al., 2014; Ayed-Khaled et al., 2015; Amri et al., 2020). However, these sheet-like bodies are not only overlain by Cretaceous sediments, but also by tilted extensional riders of Eocene limestones and Late Miocene sediments, for example in Ghzela, at the Jalta mine, and Mateur basin (Booth-Rea et al., 2018), Lansarine ridge (Gaidi et al., 2020) or in the Mejerda basin (Seismic lines and cross section, Figures, 3.2 and 3.3). We interpret that the shallower anchizonal to diagenetic infra-Numidian evaporites and redbeds were originally emplaced at the base of the Numidian and Infra-numidian nappes and were later reworked by the Mejerda and Ghzela extensional detachments and related normal faults, developing shallow depth halokinetic structures rooting in the extensional structures. These evaporitic outcrops form salt walls along the main high-angle normal faults, define the main extensional detachments, and also form small diapiric bodies rooting in the LANFs (Figure. 3.3). Moreover, these structures have been re-used and inverted during the later Plio-Quaternary shortening in the region (Gaidi et al., 2020). The deeper evaporitic bodies are found in antiformal dome-type outcrops, where the middle crust has been exhumed in the Oued Belif, Ichkeul and Hairech massifs (Figure. 3.2). These metamorphic domes were produced by ductile flow and extensional exhumation of the North Tunisian orogenic middle crust during the Late Miocene. Although, the age of the metamorphism has not been determined, final cooling of the system is constrained by the age of widespread hydrothermal activity and magmatism that has been dated by K-Ar and U-Pb between 12-6 Ma (Decrée et al., 2014; Jemmali et al., 2014). Meanwhile, under thrusting of the North Maghrebian passive margin in Tunisia occurred during the Burdigalian-Langhian (Belayouni et al., 2013), and thus, if the rocks where metamorphosed in the resulting orogenic wedge this must have been approximately between 20-14 Ma.

5.3 Extensional exhumation in Northern Tunisia

The extensional systems worked sequentially, the first system produced mostly eastwards directed extension during the Tortonian (≈11-8 Ma) with the development of brittle LANFs like the Mejerda, Ghzela and brittle-ductile detachments like the Nefza detachment that rooted in a region of mid-crustal ductile stretching that deformed the mostly psammitic and calcareous autochthonous Triassic series. However, the final exhumation of these midcrustal rocks to the surface was accomplished by a second orthogonal extensional system, producing mostly southwards directed extension during the Tortonian to Messinian ((≈8-5) Ma. High-angle normal faults of this later system are the structures that presently bound the mid-crustal domes in Northern Tunisia (Figure. 3.3, cross section in Figure. 3.2).

This work shows that the main tectonic boundaries present in the Tunisian Tell were strongly reworked during the late Miocene extensional collapse of Northern Tunisia. The

remains of the original Early to Middle Miocene nappe pile that formed the Tell orogenic belt are now cut and displaced by low-angle normal faults and extensional detachments that exhumed the Tunisian middle crust during the Late Miocene (Figure. 3.6). The late Miocene extension in Northern Tunisia propagated Southeastwards during the Pliocene to Quaternary, affecting large regions of Central Tunisia, the Sicilian Channel and the Pelagian domain offshore (Civile et al., 2010; Belguith et al., 2011; 2013; Arab et al., 2020)(Figure. 3.6).

5.4 Extensional tectonics and related geodynamic features of Tunisia

This tectonic model for Tunisia explains many geophysical characteristics of the region that are not explained by a model of protracted shortening since the Cretaceous and has to be taken into consideration when restoring and defining the main orogenic belts in Northern Tunisia. Our work shows that allochthonous anchizonal Triassic rocks we have attributed to the Infra-Numidian domain crop out to the South of the classical Tell boundary, indicating that the Tell orogenic wedge originally occupied a larger region towards the South than presently considered. Actually, the boundaries established for this orogenic belt coincide with the Present position of active shortening structures that formed since the Pliocene, like the Alia-Thibar fault system (Gaidi et al., 2020), which produces the main seismicity in the area (Soumaya et al., 2015) and accommodates most of the GPS measured shortening of the region (Bougrine et al., 2019).

Heat flow in Tunisia shows present-day values around 80-90 mW/m^2 with higher values towards the E of Tunisia (Lucazeau and Dhia, 1989). This heat flow is higher than observed in typical active FTB´s around the world (Morgan and James, 1989; Booth-Rea et Al, 2008; Lucazeau, 2019). Furthermore, lithospheric thickness shows a strong decrease from values above 180 km South of the Tunisian South Atlassic thrust and values around 140 (Globig et al., 2016) and probably less under the Southern Atlas STEP boundary where negative shear wave velocity anomalies are observed around 80-100 km depth (Radi et al., 2017). This relative thin lithospheric thickness in Tunisia is also accompanied by abundant hydrotermalism in the region (Dhia, 1987) and related high-temperature Fe-Zn-Pb mineralizations (>190 ºC) produced since the Late Miocene (e.g. Benchilla et al., 2003; Decrée et al., 2008; Jemmali et al., 2014; Aïssa et al., 2018), data that suggests even higher heat flow values in the Tortonian for the whole region. Several geophysical studies support the existence of a mantle slab underlying central Tunisia (Research group for lithospheric structure in Tunisia, 1992 ; Jallouli and Mickus, 2000; Piromallo and Morelli, 2003; Faccenna et al., 2014; Fichtner et al., 2015.)(Figure. 3.6).

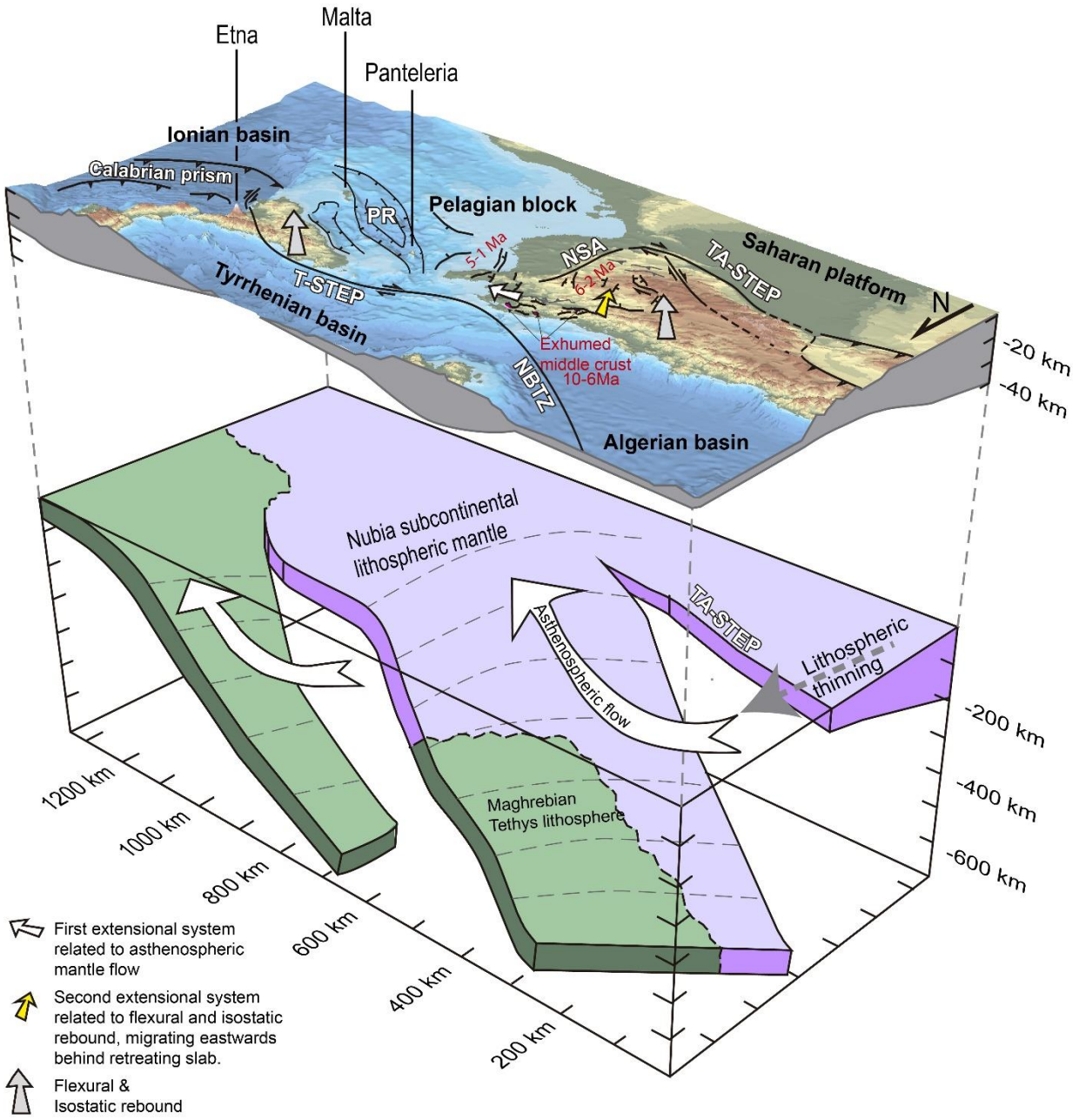

Figure 3-6: Cartoon of the tectonic mechanisms driving mid-crustal exhumation in Northern Tunisia and the location of exhumed middle crust in the region. Notice the age of crustal extension and thinning of the Tunisian lithosphere across the Southern Atlas STEP boundary. Modified from Booth-Rea et al., (2018).

Extension in Northern Tunisia has been related to the E to SE retreat and peeling-back of the slab body described above under Tunisia since the Late Miocene, which would represent Nubian continental lithospheric mantle (Roure et al., 2012; Booth-Rea et al., 2018; Camafort et al., 2020b). The older extensional system migrated eastwards, towards the direction of slab

retreat, and was thus, probably related to shearing at the base of the lithosphere through basal drag, by asthenospheric flow behind the retreating slab, as suggested for other retreating subduction systems like the Helenic and Calabrian arcs (Jolivet et al., 2018). Meanwhile, the later southwards directed extension was accompanied by important topographic uplift that migrated towards the E-SE in the late Miocene (Salaj and B. Van Houten, 1988), reaching the eastern coast of Tunisia in the Quaternary. This extension and the related topographic uplift we propose associated with flexural and isostatic rebound in response to the peeling back and tearing of the Algerian-Tunisian slab, a tectonic mechanism that followed behind the retreating slab. This tectonic mechanism drove active extension, magmatism, hydrothermalism and topographic uplift in the region. Slab retreat was favored by slab tearing or detachment at the edge of the system along the Southern Tunisian Atlas thrust front that has been interpreted as a dextral STEP boundary that continues active at Present day (Booth-Rea et al., 2018; Camafort et al., 2020b; Soumaya et al., 2020)(Figure. 3.6)

5.5 FTB extension in the Western Mediterranean

The structure of the Tell in Northern Tunisia resembles strongly the one observed in other external FTB´s of the Western Mediterranean, like the External Rif domain in Morocco, where middle crust was exhumed in the Temsamane massif during the Tortonian (Negro et al, 2007; Booth-Rea, 2012; Figure.3.1). The Betics FTB also has metamorphic rocks that underwent pumpellyite-actinolite facies metamorphism under approximately 300ºC and 4-5 kbar (Puga et al., 1988; Morata et al., 1994), which were probably exhumed through extensional tectonics (Azañón et al., 2012; Rodríguez-Fernández et al., 2013). At the same time, deeper HP/LT rocks from the subducted Iberian passive margin were also exhumed from mid-crustal depths, under the allochthonous hinterland rocks, by ductile-brittle detachments in the Betics (e.g. Jabaloy et al., 1993; Martínez-Martínez et al., 2002; Booth-Rea et al., 2005; 2015;). In all cases, the extensional structures affect the external FTB structure developed during the Early to Late Miocene in the Rif, Betics and Tell orogenic belts (Figure. 4.1). Extension propagated behind the FTB development, exhuming rocks from mid-crustal depths of the previously established accretionary wedge (Booth-Rea et al., 2012, 2020). Abridging, the structure observed in Northern Tunisia is comparable to other FTB´s in the Western Mediterranean that were extended between the Middle Miocene and Recent (e.g. Carmignani and Kligfiel, 1990; Ghisetti and Vezzani, 2002; Booth-Rea, 2012; Rodríguez-Fernández et al., 2013; Moragues et al., 2018, Figure.3.1). Although, several works suggest that extension in these FTB´s is related to the internal dynamics of the accretionary wedge, for example, to changes in the basal friction

related to the presence of underlying evaporites (Jimenez-Bonilla et al, 2016; Khelil et al., 2019), and this may be the case, in other cases, extension has resulted in a marked thinning of the crust under the FTB domain and exhumation of metamorphic rocks. In these later cases, where the crust shows thickness below 30 km, for example, in the eastern Betics and eastern Rif, Mallorca and northern Tunisia (Research Group for Lithospheric Structure in Tunisia, 1992; Mancilla et al., 2015; Mancilla & Diaz, 2015) we suggest extension was related to the propagation of the edge of the subduction system under the FTB domain. Thus, the same tectonic mechanisms corresponding to slab tearing and subcontinental lithospheric delamination determined the extensional collapse of FTB´s all around the Western Mediterranean in the Betics, Rif, Tell and Tunisian Atlas, mostly during the late Miocene (Figure. 3.6).

Future work should analyze the age and P-T conditions reached during the metamorphism of the Northern Tunisia extensional domes and the actual extent of the low-angle detachments described here, further South in the Atlas orogenic belt. Furthermore, deep geophysical soundings are necessary to understand the lithospheric structure of Tunisia and the existence or not of an attached lithospheric mantle slab under the region.

6. Conclusions

Our data support an alternative tectonic mechanism to diapirism and protracted shortening since the Cretaceous in Northern Tunisia, which corresponds to Late Miocene crustal extension of a previously overthickened orogenic wedge. Illite crystallinity shows that most of the Triassic outcrops in Northern Tunisia are made up by very low-grade metamorphic rocks that underwent epizonal or anchizonal conditions. We find two different types of Triassic outcrops, corresponding to overthrusted sheet type bodies intercalated in the remains of the extended Tellian thrust stack, which underwent mostly anchizonal metamorphism, and domal type bodies where the deeper autochthonous Atlas Triassic crops out metamorphosed under epizonal conditions. These second rooted outcrops show evidence of ENE-WSW directed ductile shearing under lower-greenschist facies metamorphism at temperature above 300 ºC in the footwall of extensional detachments.

Seismic reflection lines in the Mejerda basin show a conspicuous reflector reworking the Infra-Numidian Triassic that corresponds to the Mejerda detachment. The hanging wall of the Mejerda detachment is formed by Infra-Numidian, Numidian and Late Miocene sedimentary

rocks cut by a listric fan of normal faults. The footwall shows a low-angle ramp geometry cutting down into the autochthonous Atlas Cretaceous sediments. This extensional system is cut by later normal faults that root at depths of 3s TWT that finally exhume the folded Triassic epizonal Ichkeul, Hairech and Oued Belif metamorphic domes.

Shortening during the Late Pliocene to recent inverted the Late Miocene extensional systems, folding the extensional domes and inverting previous normal faults, driving the development of the present topography of Northern Tunisia and establishing the present thrust boundaries between the Tell and Atlas orogenic belts.

The mid-crustal exhumation observed in Northern Tunisia is analogous to the one described in other FTB´s of the western Mediterranean like the Betics and Rif, where delamination and tearing of the lithospheric mantle propagated under the continental FTB domains. Extension of the Western Mediterranean orogenic arcs propagated out of the back arc basins, affecting the external foreland domains of the Gibraltar, Calabrian and Tunisian arcs. Extension was polyphasic, with two orthogonal systems. The older system extended towards the direction of slab retreat and was probably driven by asthenospheric drag at the base of the lithosphere. Meanwhile, the later system, producing extension transverse to the direction of slab retreat was related to isostatic and flexural rebound that trailed behind the retreating slabs.

Chapter 4: Active Fault Segmentation in Northern Tunisia

Active shortening structures in Northern Tunisia have developed by tectonic inversion since the Pliocene, after Late Miocene extensional collapse of the whole region. Restored Plio-Quaternary deformation observed on reflection seismic lines indicates deformation rates around 0.6-0.8 mm/yr in the studied segments and larger amounts of shortening to the West of Northern Tunisia (16%) than to the East (7%), which suggests tectonic inversion started earlier to the West and later propagated eastwards, reaching Northeastern Tunisia in the Late Pliocene. This shortening is registered on striated pebbles in Quaternary alluvial terraces and fault-slip data giving two populations of strain ellipsoids with N-S and WNW-ESE maximum shortening. Morphometric analysis in combination with field fault segmentation mapping show that topographic uplift and drainage rejuvenation occurs in relation to 20-30 km long ENE-WSW reverse fault segments and related antiforms that are offset and linked by E-W to WNW-ESE dextral and NE-SW-oriented sinistral faults. The largest fully linked fault system is the Alia-Thibar fault. This 130 km long fault zone shows an helicoidal geometry with five different fault segments, including reverse, dextral, sinistral and oblique faults. Due to the young age of tectonic inversion, after late Miocene extensional collapse of the region, the present relief of Northern Tunisia is characteristic of a young thrust and fold belt, with dominating axial valleys along synforms and an incipient transverse drainage development propagating from West to East.

* Most of the content of this chapter corresponds to the following article: Gaidi, S., Booth-Rea, G., Melki, F., Marzougui, W., Ruano, P., Pérez-Peña, J. V., ... & Galve, J. P. (2020). Active fault segmentation in Northern Tunisia. Journal of Structural Geology, 104146. https://doi.org/10.1016/j.jsg.2020.104146

1. Introduction

Morphotectonic analysis has greatly advanced the capacity to investigate the relationships between active tectonics, geomorphic processes and landscape development. Tectonic-driven rock uplift will favor erosion, driving channel incision, headwards stream advance, fluvial captures and in general producing landscape rejuvenation processes (e.g. Ouchi, 1985; Jackson and Leeder, 1994; Whipple and Tucker, 1999; Keller, E.A., and Pinter, 2002; Pérez-Peña et al., 2010). The use of morphotectonics in tectonically active regions is a powerful tool for mapping fault segmentation patterns, obtaining relative rates of tectonic uplift, among fault segments, or related to particular structures like folds and faults.(e.g. Bull, W.B., and McFadden, L., 1977; Dumont et al., 2005; Pérez-Peña et al., 2009; Giaconia et al., 2012a; 2012b; 2013). Furthermore, morphometry can be used for differentiating between active and inactive mountain fronts in regions with changing tectonic settings (e.g.Ferrater et al., 2015). An empirical relationship has been found between power-law scaling rules for rivers and denudation rates in several active orogens (Kirby and Whipple, 2012; Azañón et al., 2015), which permits the use of channel normalized steepness index (Ksn) as a proxy for denudation rates (e.g. Kirby and Whipple, 2012; Azañón et al., 2015; Wang et al., 2018) . Consequently, the use of morphotectonic tools like topographic metrics of hillslope and catchment and channel morphology are appropriate for analyzing the relationships between channel incision and the geometry, segmentation and activity of tectonic structures like folds and fault systems in orogenic regions like the Western Mediterranean.

The active fault segmentation pattern of Tunisia has been analyzed under two different scientific approaches. Geophysical data like seismicity, focal mechanisms inversion and GPS movement suggest that the main active fault systems in Tunisia are large E-W and NW-SE oriented, 500-600 km long, dextral fault zones with minor reverse and sinistral fault splay terminations (Rabaute and Chamot-Rooke, 2014; Soumaya et al., 2018; Bougrine et al., 2019). These are the NW-SE Gafsa and the E-W Gardimau-North Constantine fault systems that explain well the GPS movements measured in Algeria (Bougrine et al., 2019). However, the more traditional view on fault segmentation in Northern Tunisia based on field mapping proposed that the main active and recent faults, are 100-150 km long NE-SW oriented sinistral-reverse faults (e.g. Bouaziz et al., 2002; Melki et al., 2010, 2011; Essid et al., 2016), together with conjugate NW-SE dextral 100-200 km long faults like the Gafsa fault in SW Tunisia (e.g. Zargouni and Ruhland, 1981; Saïd et al., 2011a; Ben Hassen et al., 2014). In some case these

faults are suggested to be longer, entering Algeria, like the Tebessa-El Alia fault that would be 270 km long (Bejaoui et al., 2017).

Active faults in Tunisia formed and are related to the continuous convergence between Africa and Eurasia since the Late Cretaceous-Palaeogene. The Tunisian Tell and Atlas thrust and fold belts formed in this general convergent setting with main shortening phases in the Eocene, Early and Late Miocene and the Quaternary (Zargouni, 1984; Frizon De Lamotte et al., 2000; Mzali and Zouari, 2006; Mashrouhi et al., 2007; Khomsi et al., 2009, 2016; Melki et al., 2010, 2011; Saïd et al., 2011a, b; Essid et al., 2016). Large NE-SW sinistral-reverse strike-slip faults like the Alia-Teboursouk, Cap-Serrat Gardimau, Ras El Korane-Thibar, Tunis-Ellés and Zagouan faults are proposed as the main structures accommodating this convergence, together with associated folds, supposedly cored by Triassic evaporites (e.g. Perthouisot and Jauzein, 1974, Melki et al., 2012; Bejaoui et al., 2017).

The most accepted tectonic model for Northern Tunisia suggests that the sinistral-reverse strike-slip faults nucleated along previous Mesozoic diapiric structures probably inverting Jurassic-Cretaceous rifting-phase normal faults (Perthouisot et al., 1999; Hatira et al., 2000; Bedir et al., 2001; Ben Chelbi et al., 2006; Melki et al., 2010; Ayed-Khaled et al., 2015; Naouali et al., 2016). This Cretaceous extension and associated diapirism also resulted into Triassic evaporitic bodies interlayered between Cretaceous sediments, which were interpreted as salt canopies (Vila, 1995; Vila et al, 1996; Ghanmi, M., 2001; Masrouhi et al., 2012, 2013, 2014; Ayed-Khaled et al., 2015).

Although, tectonic inheritance from the Mesozoic rifting phase must be an important factor determining the geometry of present-day tectonic structures in Northern Tunisia, other work proposes that these contractive structures formed during Plio-Quaternary tectonic inversion after extensional collapse in a NW-SE convergent setting during the late Miocene (Booth-Rea et al., 2018; 2019). This late Miocene extension produced extensional fault-bend related roll-overs and hanging-wall synclines, which had been previously interpreted as shortening structures (e.g. Frizon de Lamotte, et al., 2000; Ramzi and Lasaad, 2017). This extension was driven by mantle slab dynamics related to the SE-directed retreat of the underlying Algerian-Tunisian continental mantle lithospheric slab (Roure et al., 2012; Booth-Rea et al., 2018). Continued Pliocene to Present Africa-Eurasia convergence folded and inverted the extensional structures, leading to the development of classical tectonic inversion features (Booth-Rea et al., 2018).

The objective of this contribution is to use a combined morphotectonic and structural geology analysis to re-evaluate the geometry, displacement, activity and tectonic segmentation

of the main active shortening structures accommodating NW-SE plate convergence North of the Mejerda valley in northern Tunisia. To constrain the active fault segment network and its influence on local rock-surface uplift we have carried out a morphotectonic and drainage analysis using GIS based morphometric tools like gridded hypsometry analysis and channel steepness index (Ksn). Furthermore, we carried out several field campaigns with structural emphasis in the region, taking fault-slip data and determining the geometry and kinematics of the main faults. We digitized the geological maps of northern Tunisia, mapping in some cases new undescribed faults and folds that affect Plio-Quaternary sediments. This work was supported by the re-interpretation of industry reflection seismic profiles and a restoration of Pliocene to Quaternary folding and reverse thrusting deformation using MOVE^{TM} software. Finally, we distinguish the active fault system from the earlier folded Late Miocene extensional faults and detachments. The combination of morphometry, structural analysis and seismic reflection interpretation has helped elucidating the structure, segmentation geometry and displacement of the main active faults presently accommodating NW-SE convergence in northern Tunisia.

2. Geological and geodynamic settings

The Tunisian Tell and Atlas foreland thrust belts form the southeastern end of the Western Mediterranean orogenic system (Figure. 4.1). Thus, these belts share many common features with other orogenic belts in the region like the Betics, Rif, or the Calabrian arc. The western Mediterranean orogenic system has formed in response to Africa-Eurasia convergence since the late most Cretaceous (e.g. Dewey et al., 1989), together with the contribution of other tectonic mechanisms related to lithospheric dynamics like slab roll-back, slab tearing, or peeling back of the continental lithospheric mantle (e.g. Lonergan et al., 1997; Carminati et al., 1998; Faccenna et al., 2004, 2014; Spakman and Wortel, 2004; Govers and Wortel, 2005; Fichtner et al., 2015; Mancilla et al., 2015). This seems to have occurred also in the Tunisian Tell-Atlas arc, which has an underlying high-velocity anomaly interpreted as a mantle slab (Piromallo and Morelli, 2003; Faccenna et al., 2014; Fichtner et al., 2015).

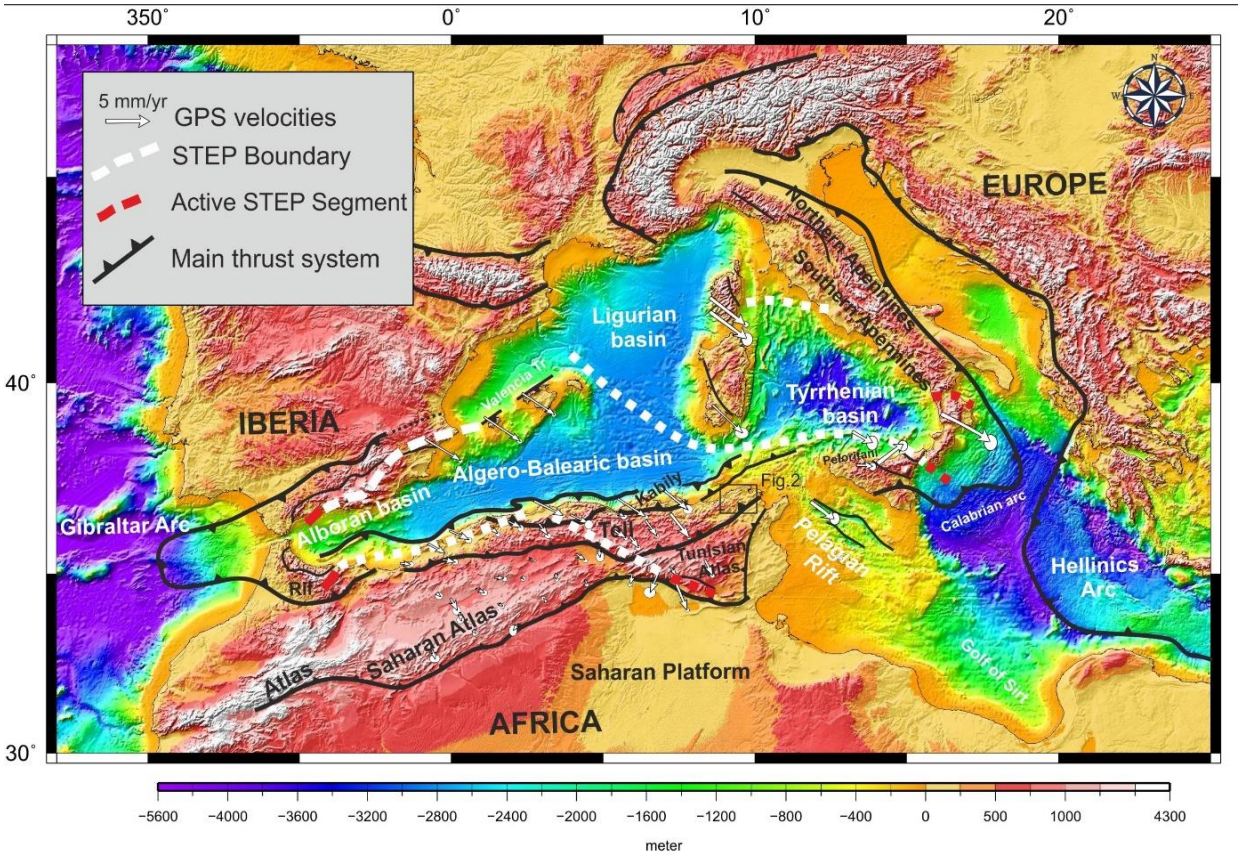

Figure 4-1: Tectonic map of the western Mediterranean with its main basins and orogenic arcs, modified from Booth-Rea et al. (2018, 2018). GPS movement towards fixed Africa from (Bougrine et al., 2019) and (Nocquet, 2012). Fault pattern along Algeria-Tunisia based on Kherroubi et al., 2009, Rabaute and Chamot-Rooke (2014) and Aïdi et al., 2018.

This slab underlies a wide section of the autochthonous African Atlas foreland region and thus, is interpreted to be partly of continental lithospheric mantle nature (Roure et al., 2012; Booth-Rea et al., 2018).

Crustal shortening is recorded in Tunisia since the latemost Cretaceous, with folds and thrust faults sealed by Oligo-Miocene sediments in the Atlas and Tell domains (e.g. Frizon de Lamotte et al., 2009; Khomsi et al., 2009, 2016; Saïd et al., 2011b), however, the main thrusting related to the northwestwards subduction of the Tethys oceanic lithosphere under Eurasia is registered in the Tunisian Tell foreland thrust belt by the tectonic superposition of Oligocene to Early Miocene Numidian flysch sediments over the autochthonous sediments of the Maghrebian passive margin during the Burdigalian to Langhian (e.g. Riahi et al., 2010; Belayouni et al., 2013) . The thick-skinned domain and hinterland of this subduction system is preserved in northern Algeria where the Kabylies metamorphic rocks overlie the Numidian Flysch units (e.g. Monié et al., 1988; Saadallah and Caby, 1996). Meanwhile, shortening

propagated southeastwards into the Atlas foreland thrust belt during the Late Miocene to Present (Bouaziz et al., 2002; Saïd et al., 2011a, b) .

Late Miocene extension in Northern Tunisia produced the collapse of the Early Miocene thrust stack. Extensional Low-Angle Normal Faults (LANFs) cut and reworked the previous Early to Middle Miocene thrusts that formed the nappe structure in the Atlas-Tell belts. LANFs exhumed the underlying Atlas sedimentary sequence, including low-grade metamorphic rocks, from below the allochthonous Numidian Flysch and Infranumidian sedimentary sequences (Booth-Rea et al., 2020). Late Miocene extension in Northern Tunisia was coeval to crustal shortening further south in the southern Atlas foreland fold and thrust belt (e.g. Saïd et al., 2011b). Moreover, extension propagated southeastwards affecting offshore areas of the Gulf of Tunis during the Pliocene (Melki et al., 2010) and the Sicily channel, forming the Pantelaria rift in the Plio-Quaternary (Civile et al., 2010; Belguith et al., 2013) .

Tectonic shortening during the Plio-Quaternary inverted the late Miocene extensional systems in northern Tunisia, folding extensional low-angle normal faults and detachments and re-using normal faults (Booth-Rea et al., 2018). This shortening phase, frequently referred to as the Villafranchian event (Burollet et Al, 1978; Burollet, 1991), is well known in Tunisia, driving the activity of large NE-SW sinistral-inverse and E-W dextral faults (Bouaziz et al., 2002; Melki et al., 2010, 2011; Alyahyaoui and Zouari, 2014; Bejaoui et al., 2017) and continues at Present (Mejri et al., 2010b; Soumaya et al., 2015, 2018; Bougrine et al., 2019; Hamdi et al., 2019). Active seismicity and GPS movement data from Algeria suggest that the Tunisian Atlas foreland thrust belt is still propagating towards the SE, towards fixed Africa, coeval to dextral shearing along the NW-SE South-Atlassic STEP boundary, which active segment is the Gafsa fault, and also along E-W faults in Northern Tunisia (Soumaya et al., 2018; Bougrine et al., 2019) (Figure. 4.1).

Contrasting tectonic mechanisms affect the topography of Northern Tunisia at different wavelengths. At short wavelengths active thrusts are driving the development of transverse drainage basins with high hypsometric integrals, high Ksn values and associated nickpoints (Camafort et al., 2020) . Meanwhile, at larger wavelengths, the filtered topography of northern Tunisia shows an ENE-WSW gradient, transverse to the Africa-Eurasia convergence direction that could be related to mantle dynamics, i.e., slab pull processes under the Sicily channel and Gulf of Gabes and asthenospheric upwelling to the east under the South-Atlassic dextral STEP fault (Camafort et al., 2020).

3. Lithology and Geological basemap

Our work is based on the 1:50.000 Office National de Mines (ONM) geological maps of Northern Tunisia, later rasterized, revised and modified after the fieldwork carried out in collaboration with the ONM and the University Of Tunis El Manar. A smaller portion of this newly compiled map, its stratigraphy, tectonostratigraphic subdivisions and corresponding references were published in Booth-Rea et al. (2018). According to this work, and following (Rouvier, 1987, 1990) and Khomsi et al., (2009), the lithological sequence in northern Tunisia can be grouped in different domains corresponding from bottom to top to the autochthonous Atlas domain, the infra Numidian parautochthonous units, the Numidian Flysch units and the overlying Neogene to Quaternary sedimentary cover (Figure. 4.2 and Figure.4.3).

Generally, at a single locality, the rock sequences appear incomplete do to the late Neogene extensional phase that affected the region, producing lithological omissions (Figure. 4.3).

So, the sedimentary sequence columns are seldom complete, being instead, built by joining fragmentary information from different outcrops. Commonly, the most competent lithologies, like Jurassic and Eocene limestones form brittle boudin-like discontinuous outcrops, whilst the more plastic lithologies like Paleogene shales and Triassic gypsum form more continuous stretched outcrops and localize deformation related to extensional low-angle normal faults (Figure. 4.3). The sedimentary lithologies of Northern Tunisia are highly erodible, although there are some contrasts between less erodible rocks like, Triassic metamorphosed red beds, Jurassic marbles, Oligocene Numidian sandstones and Eocene or Cretaceous carbonates and the more erodible Cretaceous and Palaeogene clays and marls.

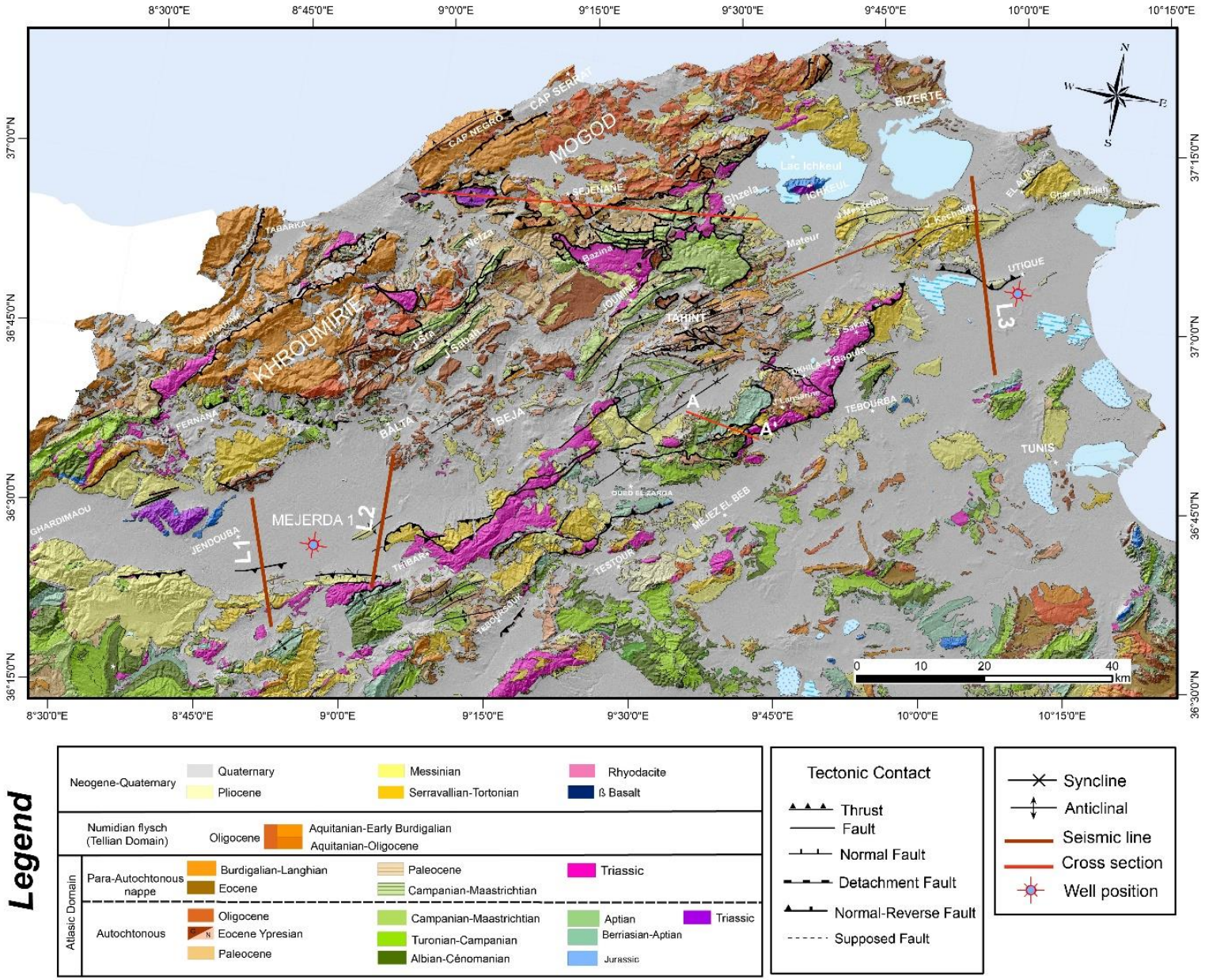

Figure 4-2: Geological map of the studied region in Northern Tunisia with the location of studied reflection seismic lines, wells and geological cross section. Location in Figure.3.1

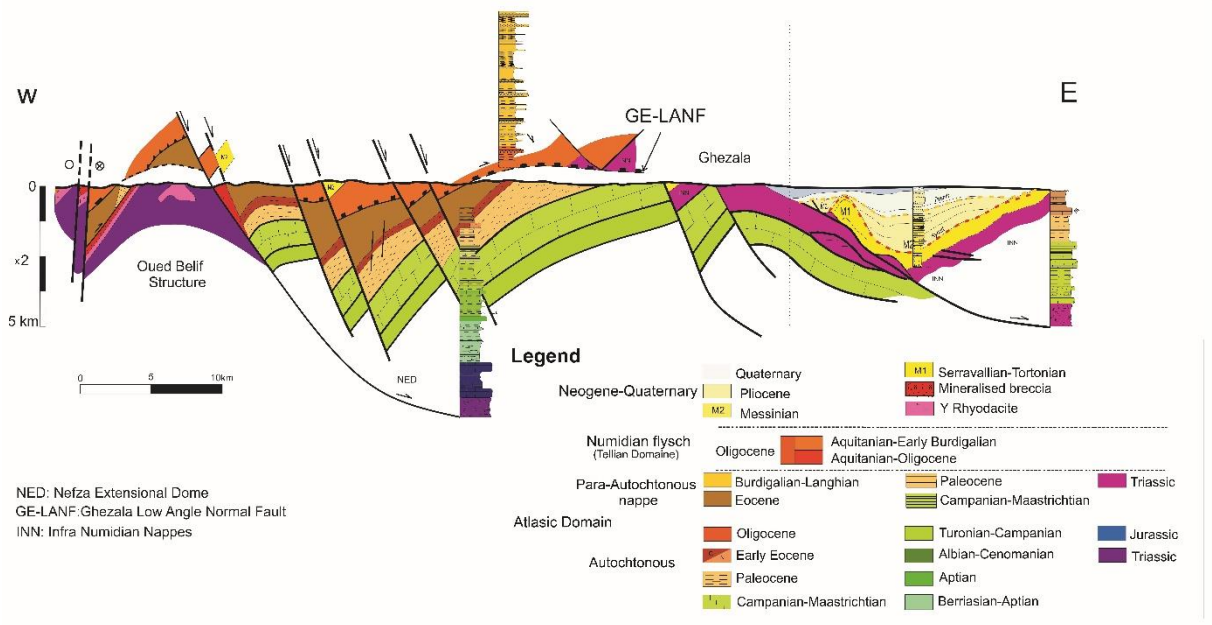

Figure 4-3: Lithological sequences in Northern Tunisia. Figure based on lithostratigraphy, cross-sections (AA′) and seismic line in Booth-Rea et al. (2018).

3.1 North Maghrebian passive margin units

The north-Maghrebian passive margin units, corresponding to the autochthonous Atlassic and parautochthonous Infranumidian units, include a complete Mesozoic to Cenozoic series from the Triassic up to the Early Miocene (Figure.4.3). The Triassic red beds and Jurassic limestones of the autochthonous Atlas domain are characterized by having low-grade metamorphism, which is not observed in the overlying Infranumidian evaporate rich Triassic sequence (Booth-Rea et al., 2018) . The Atlas domain Triassic to Early Jurassic sequence only crops out in three localities at the footwall of late Miocene extensional detachments in the Oued Belif, Jendouba and Ichkeul massifs (Figure. 4.2 and 4.3). The Cretaceous is formed from top to bottom by Early Cretaceous M´cherga marls, Aptian carbonates, Albian to Santonian marls (Fahdène and Kef formations) with intercalated Turonian carbonates. Campanian to Maastrichtian Abiod Formation carbonates culminate the series (Figure. 4.3). The Palaeocene is characterized by black clays of the El Haria formation. The Eocene starts with Ypresian carbonates of the Boudabbous/Garia formations that are formed respectively by deep globigerine facies and shallow nummulitic facies. Meanwhile, the rest of the Eocene sequence is represented by the Souar Lutetian to Priabonian marls. Oligocene fluvial quartz-rich sandstones of the Fortuna formation culminate the Palaeogene series (Figure. 4.3). Early

Miocene glauconitic marls with glauconitic sandstone intercalations deposited in the Atlas Domain during the main thrusting period in Northern Tunisia (e.g. Belayouni et al., 2013).

3.2. Numidian Flysch

The Numidian Flysch domain is characterized by Oligocene to Early Miocene turbiditic quartzarenites and clays (Riahi, et al., 2010; Belayouni et al., 2013) that formed the sedimentary cover of the Tethys ocean. Locally, this domain includes an underlying late Cretaceous to Eocene series (Riahi, 2010). Although, in most cases the Oligo-Miocene part of this domain is detached from its underlying sequence, mostly due to Late Miocene extension. The Oligo-Miocene Numidian formation reaches a thickness of up to 2.5 km with basal Oligocene-Aquitanian clays of the Zouza member, followed and interdigitated with the Aquitanian to Early Burdigalian Khroumirie Sandstone and clay member. This sequence is capped by Early to Late Burdigalian silexites and marls of the Babouch member (Riahi, 2010).

3.3. Neogene to Quaternary

The Neogene to Quaternary sedimentary cover in Northern Tunisia includes an Early Miocene, Late Burdigalian to Early Langhian, sequence of sandy marls with glauconitic sandstone intercalations that deposited coeval to the main thrusting event in Northern Tunisia (Mannaï-Tayech, 2006; Riahi, 2010) . Moreover, this formation occurs in piggy-back basins with an olistostromic sequence, including debris flows and large Eocene olistoliths in the region of Lansarine, which deposited upon the Infranumidian Triassic series. This glauconitic formation is followed by transitional-facies syn-rift molassic formations of Middle to Late Miocene age drilled to the East of the studied region in the Kechabta basin (e.g. Melki et al., 2011; Alyahyaoui and Zouari, 2014)(Figure. 4.3). Late Miocene syn-rift molassic sediments also occur in the Mejerda and Jendouba basins to the West of the studied region and along uplifted domains like the Lansarine ridge to the North of the Mejerda valley (Masrouhi et al., 2007). Early Pliocene marine clays of the Rafraf formation overlie the post-rift unconformity to the East of the studied region (Burollet et al, 1951; Melki et al., 2011). To the west in the Jendouba basin the Pliocene to Quaternary post-rift sequence is fully continental and not well dated. The Late Pliocene is represented by the Porto-Farina shallow marine sandstones with clay intercalations in northeastern Tunisia (e.g. Burollet et al, 1951; Melki et al., 2011; Bejaoui et al., 2017 and references therein).

The Quaternary is represented by unconformable alluvial conglomerates, fluvial terraces, calcareous crusts, aeolian sands and shallow marine terraces along the coastal areas (Oueslati, 1989; Mejri et al., 2010b; Melki et al., 2011; Bejaoui et al., 2017) .

4. Methods

To characterize the most active zone in the North of Tunisia we analyzed the drainage network through the study of morphometric patterns and gradient indices. Morphometry has been deemed as a useful tool to relate drainage anomalies and distinctive patterns to tectonic activity. In this paper, we have analyzed the drainage network through the Chi and ksn metrics and the landscape dissection by means of a gridded hypsometric analysis.

We use two different resolution DEMs, a high resolution 10 m DTM available for the northwest of Tunisia to extract the main drainage system, and a 30 SRTM DEM to analyze the hypsometry in a slightly wider area. Whereas drainage network and ksn metrics are sensitive to DEM resolution, hypsometric analyses yield similar results with different DEM resolutions (Pérez-Peña et al., 2009b).

4.1. Hypsometric analysis

The hypsometric curve and the hypsometric integral (HI) are valuable tools for characterizing topography because they are correlated with the stage of geomorphic development of the landscape (Strahler, 1952; Willgoose et al., 1998; Pérez-Peña et al., 2009a, 2009b). In this work, we followed the methodology proposed by Pérez-Peña et al. (2009b) to spatially analyze hypsometry. This methodology computes HI values for regular squares instead of values for basins and sub-basins and then applies spatial-autocorrelation techniques to recognize possible spatial patterns. Since we do not use drainage basins, HI values do not strictly represent a measure of dissection but instead, how rapidly elevation changes within each square (Van der Beek, P., & Braun, 1998). This method has shown to be very useful to analyze the topographic signal produced by active tectonic structures and it is thought to be capable to identify areas with different uplift rate (Pérez-Peña et al., 2009b; Siddiqui and Soldati, 2014), and it is more effective than analyzed individual hypsometric curves since it is capable to record spatial topographic variations.

We selected a grid size of 1 km and used a DEM of 30 m of pixel resolution to derive HI values. Once the HI values were computed from the grid squares, we performed a hot-spot analysis by calculating the Getis-Ord spatial statistics with a threshold search distance of 3.5 km. This distance corresponds with half the approximate width of the main structures in the region.

4.2. Chi and ksn metrics

Graded rivers show an exponential relationship between channel slope (S) and up-stream area (A) (Hack, 1957). This well-known relation is described by the power-law:

$$S = ks\, A^{-\theta}$$

where ks is the channel steepness-index and ϴ the concavity index (Flint, 1974). This power-law relation has been used in several tectonic studies, since different area-slope relations can be due to active tectonics, changes in river bed lithology, and/or climate (Wobus et al., 2006; Kirby and Whipple, 2012; Burbank et al., 2013; Whipple et al., 2013; Bellin et al., 2014; Scotti et al., 2014). Concavity index (ϴ) varies in natural channels in a narrow range, between 0.3 and 0.6 and is somehow less sensitive to differences in uplift rate, lithology and/or climate variations in steady state landscapes (Kirby and Whipple, 2012; Whipple et al., 2013). By the contrary, steepness index (ks) is highly sensitive to all the mentioned factors. As ksn and ϴ are highly auto correlated, in practice most studies have used the normalized steepness index (ksn). This index is computed by considering a reference concavity (θ_{ref}) (Wobus et al., 2006; Kirby and Whipple, 2012; Burbank et al., 2013; Whipple et al., 2013).

One of the most robust analysis to derive the ksn index is through the Chi metric (Perron and Royden, 2013). This metric result from the integration of the power-law equation mentioned above as follows:

$$z(x) = z(x0) + ksn * \chi$$

This linear equation relates the Chi (χ) metrics and river profile elevation by a linear equation, thus allowing the direct estimation of the ksn index as the slope of the line. This method considerably reduces the scattering that logarithmic area slope plots produce (Perron and Royden, 2013). In this work we have calculated ksn and chi indexes for all pixels of a drainage network extracted from a 10 meters resolution DEM with an area threshold of 0.5 km^2 (5000 cells) and a θ_{ref} of 0.45. The use of the latter value allows comparisons of results with previous works in the Betics(Bellin et al., 2014; Scotti et al., 2014; Azañón et al., 2015), being also a standard value taken in other studies (Kirby and Whipple, 2012; Perron and Royden, 2013; Willett et al., 2014). However, in this work we calculated the ksn index for each pixel in chi-elevation orthogonal space by using a moving window with 10 pixels up and down-stream, instead of calculating for river segments as in other studies (Bellin et al., 2014; Scotti et al., 2014; Willett et al., 2014). Moreover, the estimation of ksn is made by linear regression with the values of chi and elevation within the moving window, thus ensuring the best quadratic fit.

This approach ensures a minimum point sample of 20 pixels for each ksn estimation and also allow to estimate enough points to interpolate a ksn anomaly map for the study area.

4.3. Seismic reflection profiles

We interpreted industry multichannel seismic reflection lines from the Tunisian Company of Petroleum Activities (ETAP) for determining the deep structure of the Jendouba and Mateur-Utique basins in Northern Tunisia. We chose seismic lines transverse to the main active shortening structures so as to determine the seismic stratigraphy of the sedimentary infilling related to active thrusting, and the age and amount of shortening (Figure. 4.2).

Seismic interpretation was aided by the use of 2DMOVE software (®Midland Valley Exploration Ltd, 2011) to create balanced and restored cross sections. We extrapolated our mapping information at depth with the aid of deep drill holes in Northern Tunisia (Mej1 and UTQ1 boreholes), tied to our interpreted lines with crosscutting seismic lines (Figure. 4.2). Using the borehole information we obtained seismic velocities of 2200 m/s in the Jendouba basin and of 2100 m/s in the Utique basin for transforming the Plio-Quaternary sedimentary infilling to depth in the seismic lines.

4.4. Structural kinematic data

During several field missions, we have measured fault slip data and determined fault kinematics using rotated porphyroclast tails, riedel faults, fault offset, etc. Furthermore, we have measured several stations of striated pebbles in Quaternary fluvial and alluvial conglomerate deposits in the studied region.

For each striae on the pebble surface we measured the orientation of the striae and the tangent plane on the pebble surface that contains the striae, following the Ruano and Galindo-Zaldivar (2004) method. Fault-slip data and striated pebbles affecting Plio-Quaternary sediments were analyzed using the simple geometrical Right Dihedra method (Angelier, J., & Mechler, 1977) and the Search Grid Method, SGM (Galindo-Zaldívar, and González-Lodeiro, 1988), a stress inversion method based on the minimization of the deviation of real and theoretical striae for the fault population based on (Bott, 1959) equation. The use of different fault analysis methods guarantees the reliability of the obtained results. Stress tensors are given with orientation of maximum (σ_1), intermediate (σ_2), and minimum (σ_3) stress and the value of R (stress ratio in Bott's equation; (Bott, 1959),

$$R = (\sigma 2 - \sigma 3)/(\sigma 1 - \sigma 3).$$

5. Morphotectonic results

Northern Tunisia is mostly characterized by a smooth topography and low elevation with maximum altitudes around 1100 m. The main drainage system is the axial Mejerda River that runs from SW to NE from Northeastern Algeria towards the Sicily channel to the North of Tunis. This SW-NE directed axial drainage pattern is also followed by other smaller catchments like the Tine, Joumine and Sejnane Oueds that drain into the Ichkeul Lake (Figure. 4.4) and transverse short rivers draining towards the NW at the Northern coast of Tunisia.. During the Quaternary the Mejerda River has expanded its catchment area by capturing other parallel axial valleys like the Tine River to the North and also others rivers towards the S (Camafort et al., 2020). Short transverse rivers drain towards the NW along the Northern coast of Tunisia.

Ksn and gridded Hi results are generally low, especially in Northeastern Tunisia (Figure. 4.4 and 4.5). However, within the studied region there are some areas with high ksn and hypsometric integral high values. Some of these regions with high ksn and gridded Hi results coincide with the location of the hanging-wall of reverse faults and associated antiformal structures that affect Quaternary sediments (Figure. 4.5). Other anomalies however, occur over regions where faults are inactive and other processes like fluvial captures, may be influencing higher incision rates and drainage rejuvenation (Camafort et al., 2020).

The highest ksn values and larger clusters of high gridded-Hi values are obtained in two areas of the Kroumirie Tellian region, between the localities of Fernana and Nefza (anomalies 1 and 2 in Figures. 4.4 and 4.5). Although, this region is mostly formed by Numidian Flysch outcrops, the areas with high ksn values also occur over highly erodible rocks, like cretaceous marls, of the deeper infranumidian and Atlas domains. Anomaly 1 lies between Ain Draham and and Nefsa, mostly in an area of Kroumirie sandstones in the hanging wall of a Miocene normal fault that exhumes the Infranumidian sequence under the Numidian Flysch (Figures. 4.2, 4.5). Anomaly 2 with E-W orientation, slightly N of Balta-Fernana, does not follow the trace of the Tellian or Numidian thrust front, but also overlaps the underlying Atlas Cretaceous sequence (Figure. 4.2). Thus, although this anomaly has been previously related to a lithological contrast (Camafort et al., 2020), it probably reflects the activity of a reverse fault unmapped up to date, although with present thrust-related seismicity (Soumaya et al., 2015). This fault could be related with the Jbel Sra and Jbel Sabbah anticlines to the NE (Figure. 4.5). The drainage in this area describes hairpin loops around anticlinal closures in Infranumidian Eocene limestones of the Kasseb unit and also related to fluvial captures (Figure. 4.4).

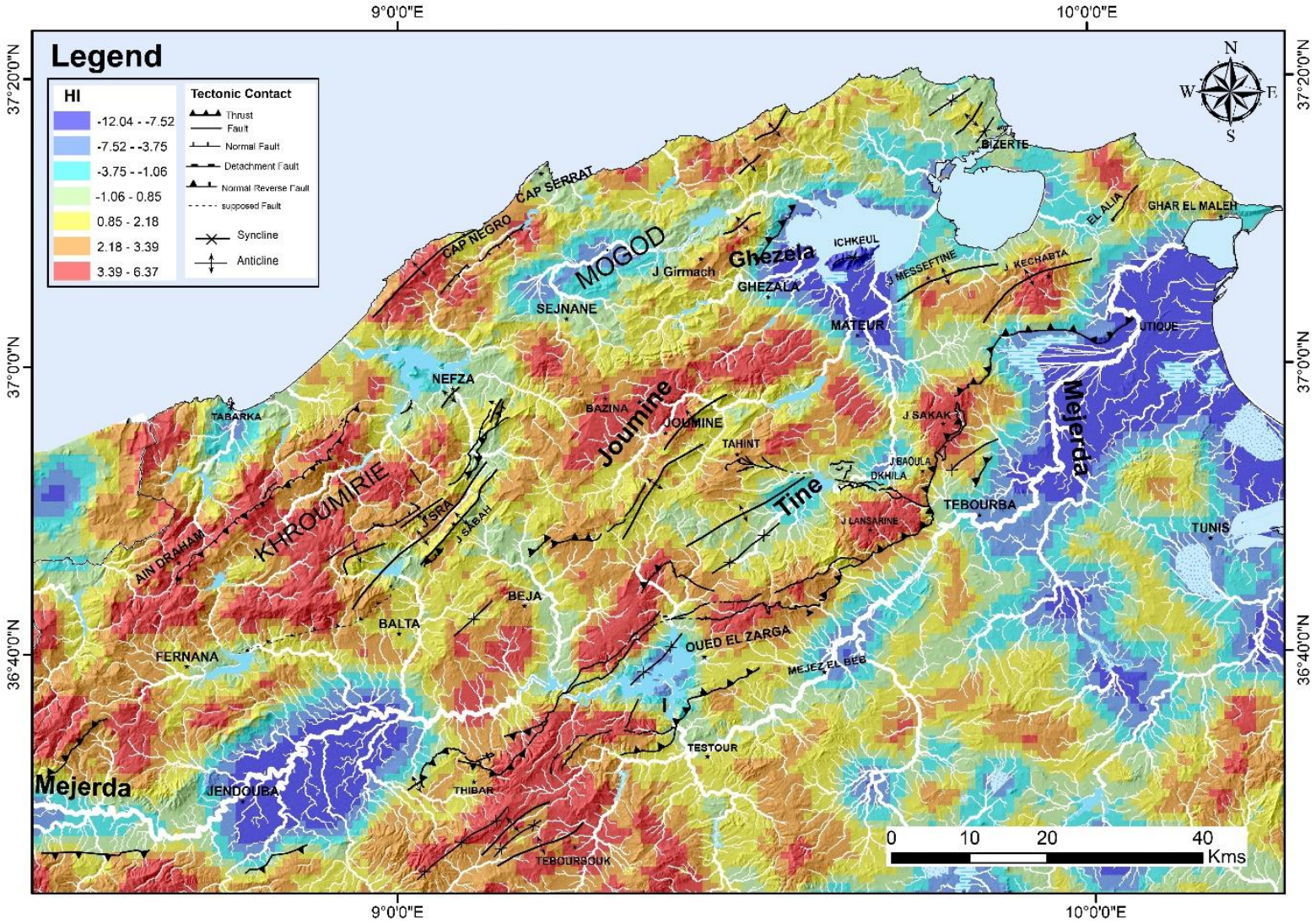

Figure 4-4: Gridded hypsometric integral (Hi) results for Northern Tunisia, together with the drainage network and active faults in the region.

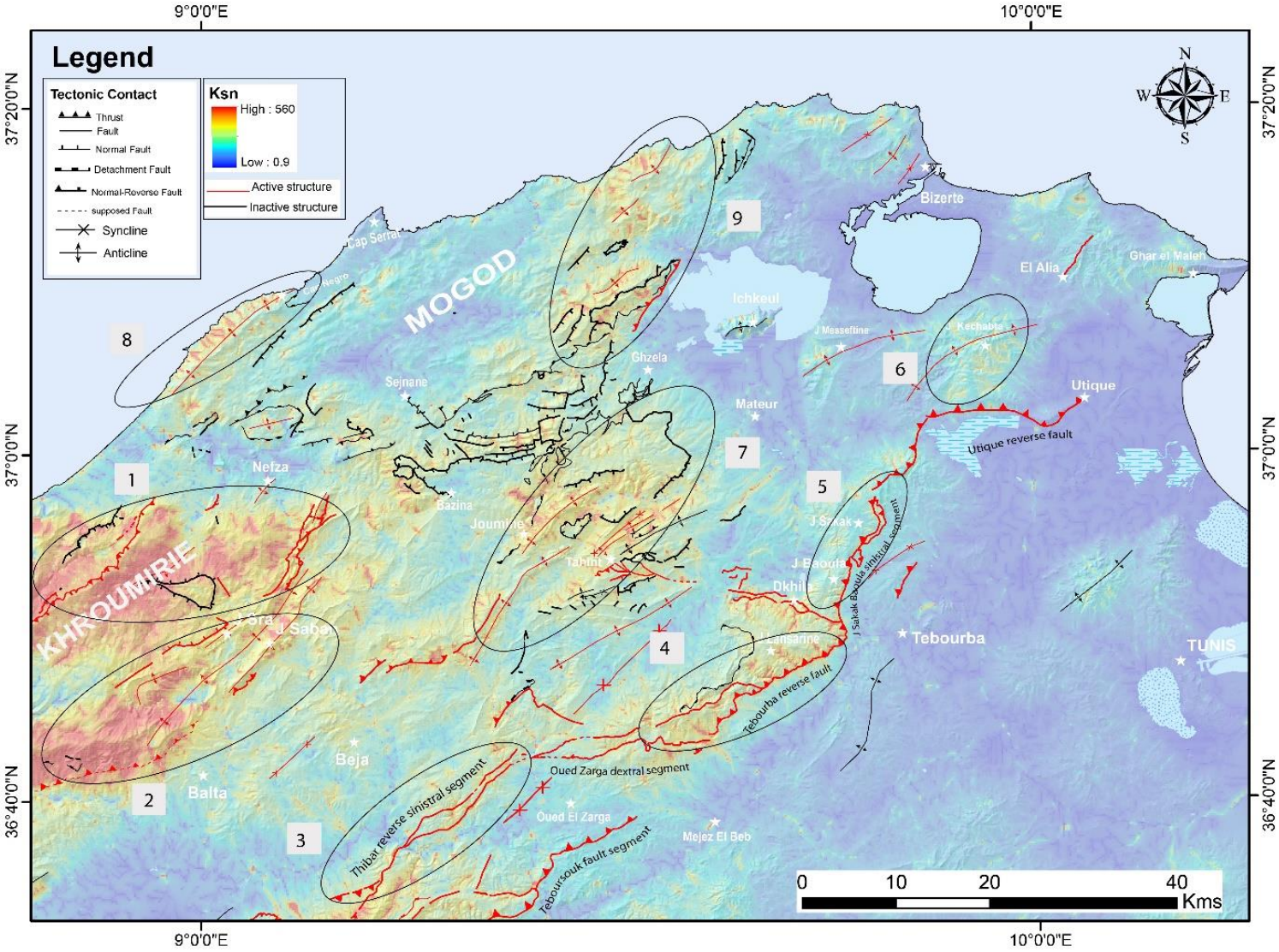

Figure 4-5: Normalized steepness index (ksn) results in Northern Tunisia, together with the main active faults in the region, in red and inactive ones, mostly extensional in black

Furthermore, transverse drainage basins of the Mejerda River cut across the anomaly 2, capturing previous basins that drained towards the NE (Camafort et al., 2020, Figure. 4.4).

Northern Tunisia is crossed from SW to NE by a domain with high ksn and gridded Hi values running from the locality of Thibar-Teboursouk in the S to Ghar El Melh to the NE (anomalies 3, 4, 5, 6 and 7 in Figures. 4.4 and 4.5). The anomalies 4, 5, 6 and 7 match the northern segments of the Alia-Teboursouk but anomaly 3 appears displaced to the NW of the main fault trace (Figures. 4.4 and 4.5) towards the Thibar ridge.

Other smaller-scale regions with high ksn and hypsometric integral values occur in the studied area. In most cases they show SW-NE orientation, parallel to anticlinal ridges cored by Cretaceous Atlas sediments and sinistral-reverse faults in the center of the studied region nearby Tahint and Joumine (region 8 in Figures. 4.4 and 4.5). Similar domains also occur near the coastline in Cape Negro and in Sidi Mechreg, associated to folds in the Numidian Flysch units (anomaly 9 in Figures. 4.4 and 4.5) and to the Northwest of lake Ichkeul in Jebal Girmach in relation with a reverse fault and associated anticlinal ridge (anomaly 10 in Figures. 4.4 and 4.5).

6. Structural and fault segmentation results for Northern Tunisia

We present a new map of active shortening structures in Northern Tunisia (Figure. 4.2 and 4.5). This map has resulted from the combination of a morphotectonic study with fault analysis and new structural mapping. In red, we differentiate active structures from older inactive extensional faults marked in black (Figure. 4.5). The faults mapped as active in most cases cut Quaternary alluvial fans and fluvial terraces and have associated high morphometric anomalies.

6.1. Fault kinematic data and striated pebbles

Fault and striated pebble kinematics were determined in many of the main active fault segments and deformed Quaternary fluvial terraces and are shown in stereographic projections, and in some cases with kinematic arrows in Figure. 4.6.We have measured striated pebbles in many of the faulted and folded Quaternary fluvial terraces that support a recent N-S to NW-SE shortening event in Northern Tunisia (Camafort et al., 2020, together with new data herein, Figure. 4.7). The obtained stress tensors are compatible with the orientation of observed pebble solution pits in the field. In some stations (e.g. 28 in Figure. 4.7), two stress tensors were obtained.

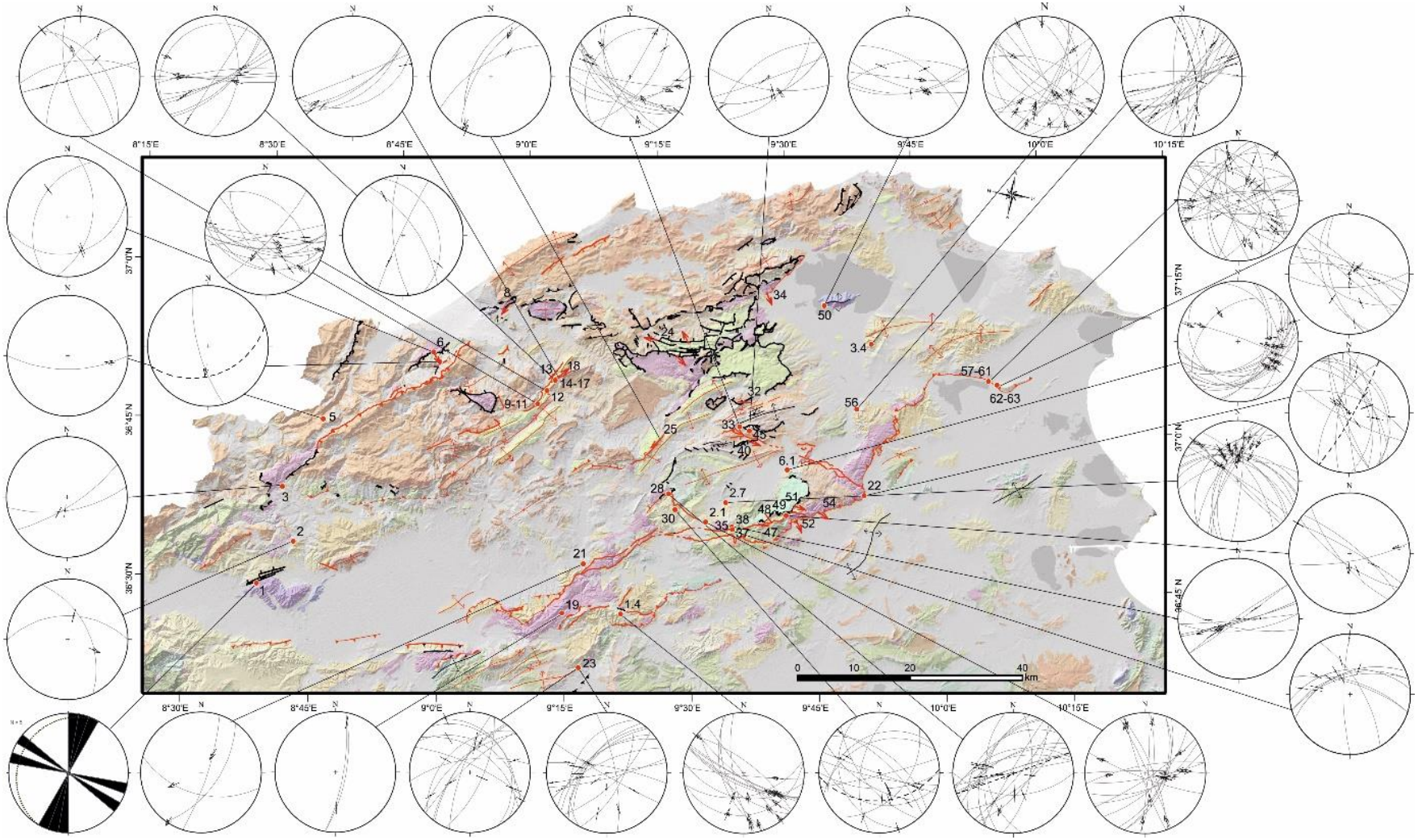

Figure 4-6: Faults and striated pebbles slip data and joints measured in Northern Tunisia. Lower hemisphere stereographic projections. Active structures in red. Legend in Figure. 3.2

The order of the stress tensors depends only on the abundance of striae corresponding to each faulting phase and it is not related to its age. In some locations, the striated pebbles where measured on folded fluvial conglomerates, for which we have determined stress tensor calculations both without and rotating the strata to horizontal.

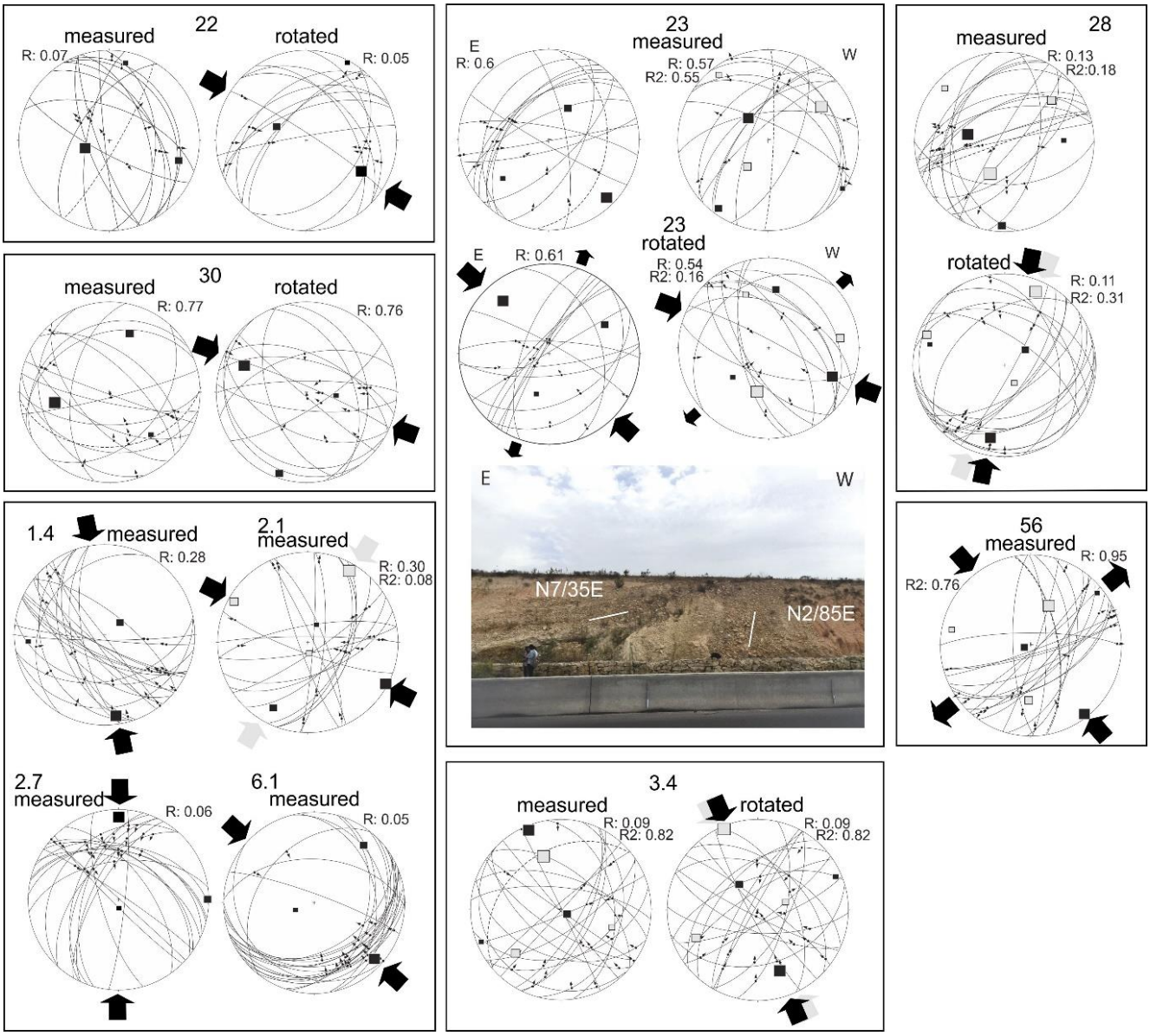

Figure 4-7: Stress field for Northern Tunisia determined from striated pebble data measured on Plio-Quaternary and Miocene sediments. Notice, progressive PlioQuaternary deformation registered by two different stress tensors in single stations in some station. R, axial ratio (R = (σ2 - σ3)/(σ1 - σ3)). Station location in Figure. 3.6

Striated pebble stations in the strongly dipping Quaternary sediments show vertical pit solutions indicating a prolate stress ellipsoid with vertical σ_1 and resulting in radial extension (Figure. 4.7). This suggests that the striated pebbles have been rotated towards vertical during folding at the footwall of the thrust. When the stratification is rotated to horizontal, these stations give mostly NW-SE sub horizontal shortening (Figure. 4.7). For stress-inversion we have also analyzed striated-pebble stations measured by (Camafort et al., 2020). Furthermore, in some case we have analyzed striated pebbles on the two limbs of an outcrop-scale anticline (station 23, Figure. 4.7; Tab. 4.1).

The stress inversion of the slip data in pebbles from fold limbs give two different stress tensors, with the main shortening axis plotting along a great circle normal to the fold axis (stations 23, 28 and 3_4, Figure. 4.7). These two stress tensors may reflect that the pebbles were striated during Quaternary progressive folding of the strata.

Tableau 4-1: Summary of stress tensors and stress orientations obtained from striated pebble analysis. Locations in Figure. 4.6. Successive columns indicate: Station name and their geographical coordinates (latitude and longitude); age of the rocks; phase number (Ph)

Station	Lat	Long	rock age	Ph	σ_1	σ_2	σ_3	R	N	NT	S_0
22	36.8234	9.7720	Pleistocene	1	252/67	106/20	12/12	0.07	10	13	120/82
22_Rotated	36.8234	9.7720	Pleistocene	1	119/30	295/60	028/02	0.05	10	13	
23_E	36.4660	9.2725	Pleistocene	1	135/09	031/56	230/33	0.6	11	14	097/35
23_e_Rotated	36.4660	9.2725	Pleistocene	1	319/22	062/30	198/51	0.61	10	14	
23_W	36.4660	9.2725	Pleistocene	1	318/63	216/06	123/26	0.57	9	13	092/85
				2	058/30	218/59	323/09	0.55	6	13	
23_W_Rotated	36.4660	9.2725	Pleistocene	1	114/23	007/34	231/47	0.54	9	13	
				2	195/48	082/20	337/35	0.16	8	13	
28	36.7737	9.3874	Pleistocene	1	282/55	182/07	088/34	0.13	13	18	160/90
				2	205/58	048/30	312/10	0.18	11	18	
28_Rotated	36.7737	9.3874	Pleistocene	1	190/17	057/66	285/16	0.11	13	18	
				2	024/12	291/16	150/70	0.31	9	18	
30	36.7504	9.4049	Pleistocene	1	260/38	018/32	136/36	0.77	12	14	176/40
30_Rotated	36.7504	9.4049	Pleistocene	1	294/24	200/08	093/65	0.76	11	14	
56	36.9577	9.7288	Miocene	1	142/02	250/84	52/06	0.95	14	20	080/65
				2	025/50	182/38	281/11	0.76	11	20	
1.4*	36.5680	9.3301	Pleistocene	1	172/09	051/72	265/15	0.28	17	23	
2.1*	36.7388	9.4692	Pleistocene	1	118/01	208/18	026/72	0.3	13	17	
				2	030/08	299/06	173/80	0.08	7	17	
2.7*	36.7750	9.4992	Pleistocene	1	000/08	090/00	180/82	0.06	15	21	
3.4*	37.0617	9.7384	Pleistocene	1	338/06	124/83	248/04	0.09	12	21	320/35
				2	342/37	226/30	109/39	0.82	10	21	
3.4_Rotated	37.0617	9.7384	Pleistocene	1	160/29	324/62	067/07	0.09	12	21	
				2	337/04	245/26	075/64	0.82	10	21	
6.1*	36.8397	9.6153	Pleistocene	1	133/08	041/16	248/72	0.05	18	22	

6.2. Results from the interpretation and balancing of reflections seismic lines

ETAP reflection seismic lines shot along the NW-SE direction of regional convergence image very clearly an Early Pliocene post-rift unconformity that is cut and folded by the active shortening structures (Figure. 4.8 and 4.9). Furthermore, both the seismic data and field analysis show that late Miocene extensional faults are presently being inverted under strike-slip and reverse kinematics. This tectonic inversion has been described in the Mateur basin region (Booth-Rea et al., 2018), but it is also evident to the SW in the Jendouba basin. Line L1 runs with N-S orientation across the Jendouba basin, cutting the main bounding fault to the south of the basin, namely the dextral strike-slip Ghardimaou fault (Hamdi et al., 2019). This line shows a clear post-rift erosive angular unconformity between the late Miocene sediments and the Plio-Quaternary (Figure. 4.8). The Plio-Quaternary shows a wedge-type geometry, thickening towards the south where it is cut by a reverse fault located at the base of a thick package of tilted late Miocene sediments, corresponding to an extensional rider. Thus, this reverse fault inverts and re-uses a previous low-angle normal fault. Meanwhile, the late Miocene sedimentary sequence shows several tilted blocks cut by normal faults with ramp-flat geometries and both northward and southward tectonic transport. These normal faults root in a detachment in Triassic evaporite, which overlays autochthonous Cretaceous Atlas sediments, drilled in the Mejerda 1 drill hole (Figure. 4.2, (Troudi et al., 2017). This line shows that shortening along the southern margin of the Jendouba basin is partitioned by both vertical dextral strike-slip and a low-angle reverse fault that inverts a late Miocene southward directed extensional normal fault. However, shortening is minor and has not undone the Late Miocene extension. A similar structure is observed in the N-S oriented Line L2, although, the Plio-Quaternary depocenter shows a thicker infilling, reaching depths of 1s TWT that correspond to approximately 1100 m. Line L2 shows clearly the erosive nature at the base of the Plio-Quaternary, which directly overlies Triassic evaporites drilled in Mejerda 1 bore hole (Troudi et al., 2017). A second angular unconformity marks the base of the Quaternary sequence that shows only very gentle folding and is cut by the reverse faults along the South of the Jendouba basin (Figure. 4.9).

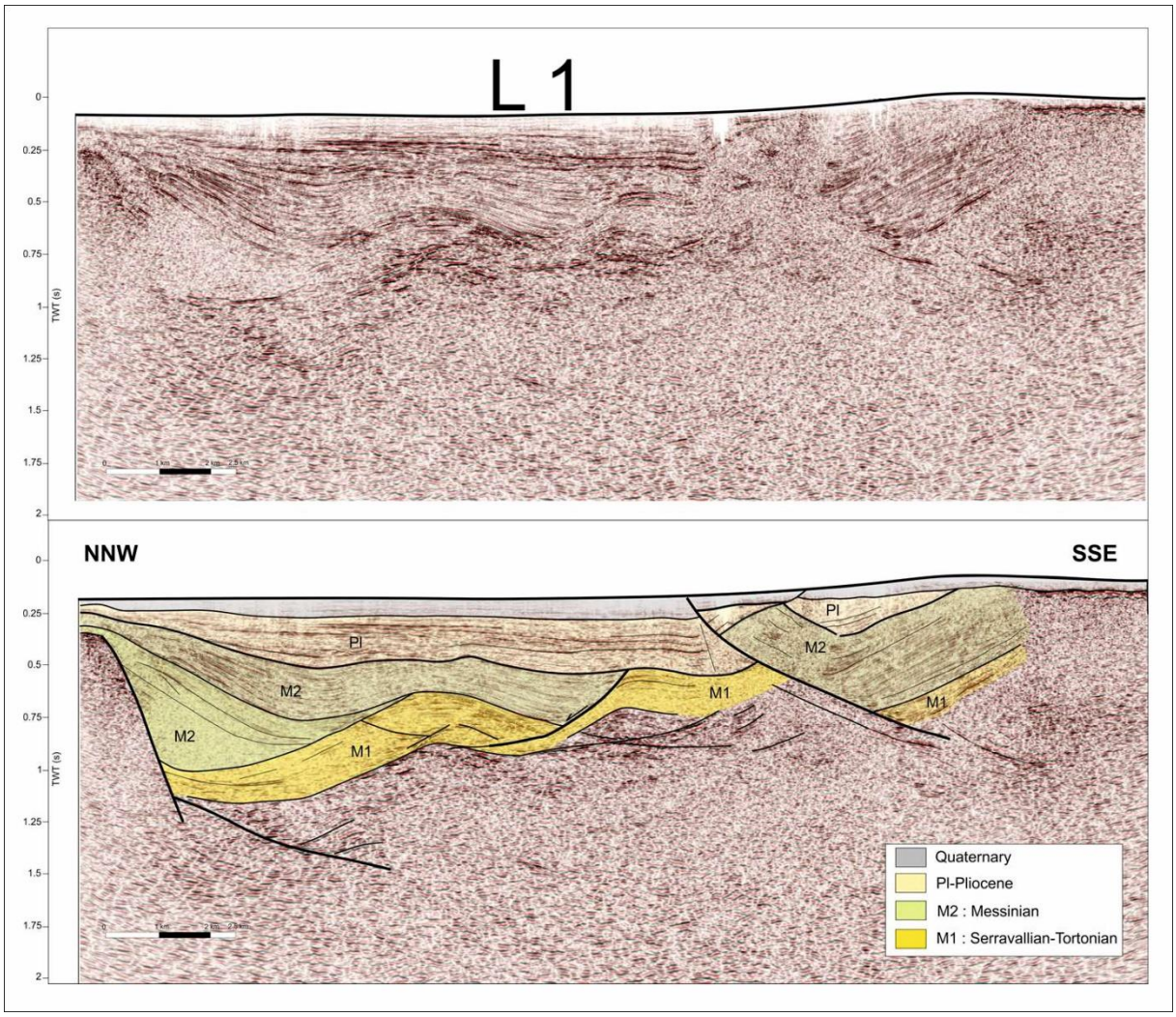

Figure 4-8: ETAP multichannel reflection seismic line L1 that runs across the Jendouba basin showing the synrift M2 late Miocene sediments and the later Pliocene

The age of Plio-Quaternary shortening can be well established to the East of Northern Tunisia, where the stratigraphy of this sequence is well known from bore-holes and field work (e.g. Burollet et al, 1951; Melki et al., 2011; Harrab et al., 2013; Alyahyaoui and Zouari, 2014; Ramzi and Lassaad, 2017) . The basal post-rift Early Pliocene unit, corresponding to the Raf-Raf formation, shows a tabular geometry, with no evidence of syn-depositional deformation related to shortening or extension (Booth-Rea et al., 2018). Meanwhile, the Late Pliocene Porto Farina and overlying Quaternary sediments do show thickness variations and onlap relationships that are related to the activity of folds and reverse faults. Thus, tectonic inversion in Northeastern Tunisia must have initiated in the late Pliocene after 3.2 Ma.

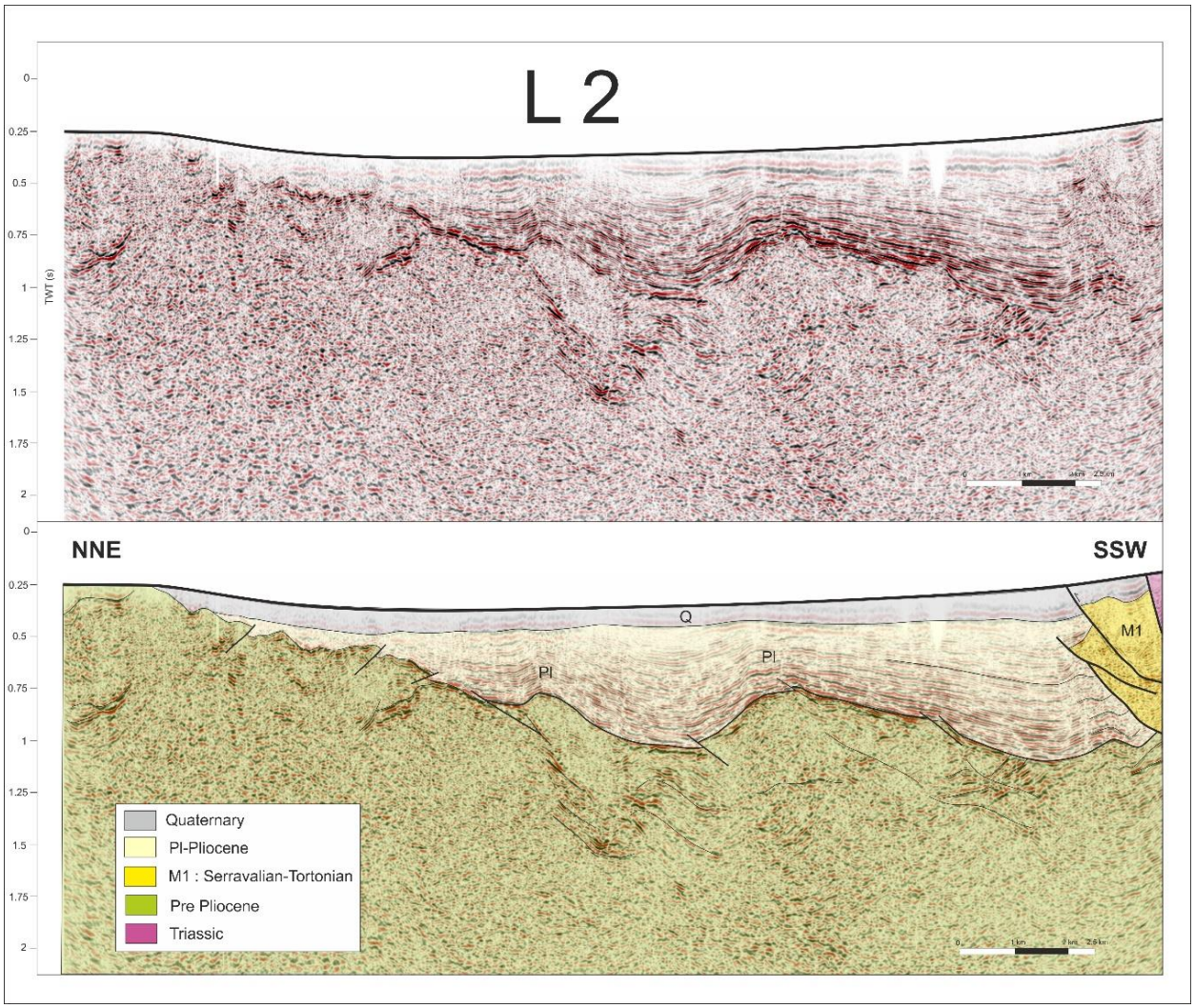

Figure 4-9: ETAP Multichannel reflection seismic line L2 showing shortening structures and the Early Pliocene folded post-rift unconformity. Location in Fig. 3.2.

We have determined the amount of Late-Pliocene to present shortening restoring two NW-SE to N-S oriented seismic lines in Northern Tunisia using MOVE software. In the first place we have chosen line 3 from Booth-Rea et al. (2018) that is parallel to the direction of shortening and shows clearly the geometry of the sedimentary infilling and reverse faults inverting previous Late Miocene normal faults and related folds (Figure. 4.10a). This line has a total length of 34.5 km and we obtain 2.5 km of shortening after restoring the line to its Early Pliocene geometry, before being inverted. This represents 7 % Late Pliocene to present shortening in the region traversed by Line 3, without considering layer-parallel shortening, and a shortening rate of approximately 0.8 mm/yr since 3.2 Ma for this segment of Northern Tunisia. In second place, we restored the Plio-Quaternary shortening in Line L2 that crosses the Jendouba basin from North to South (Figure. 4.2 and 4.10b). Here, the general wedge geometry of the Plio-Quaternary infilling, fanning towards the reverse faults at the southern margin of the basin, suggests their deposit

coeval to N-NW directed thrusting. The age at the base of the post-rift sediments, corresponding to the Segui Formation, is not well constrained although, most probably latemost Messinian to Early Pliocene (Mannaï-Tayech, 2006). This line shows several reverse blind faults and associated anticlines that invert late Miocene normal faults within the Jendouba basin. Furthermore, two large reverse faults occur to the south of the seismic line, bounding the southern margin of the basin. The line has a total length of 19.2 km and we obtain a total shortening of 3.1 km since the Early Pliocene. This represents 16 % shortening across the Jendouba basin and a tentative shortening rate of 0.6 mm/yr since 5.3 Ma.

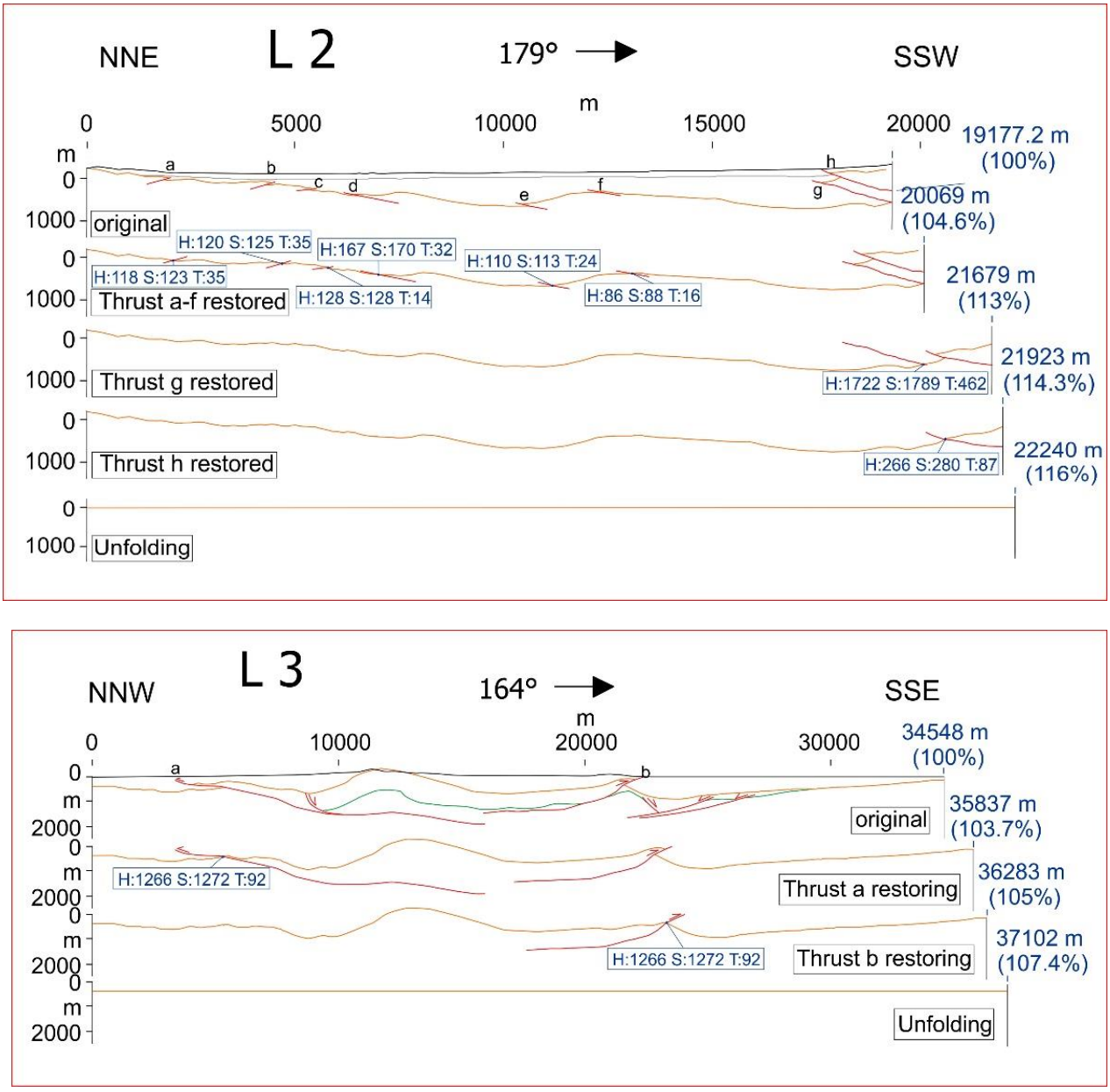

Figure 4-10: MOVE™ restoration of Pliocene to Quaternary shortening in seismic lines L2 (A) and L3 (B). See text for explanation. H, Heave; S, Slip; T, Throw

6.3. Fault segmentation pattern

The active faults in Northern Tunisia show a strong segmentation, forming long fault systems, of linked fault segments with variable orientation and kinematics. The main fault system coincides partly with the previously proposed Alia-Teboursouk sinistral-reverse fault (Melki et al., 2011). Especially in its northern segments, but towards the SW, we observe a dextral offset in the morphometric anomalies to the North of Oued Zarga, together with a lack of a morphometric anomaly further south, between Mejez el Beb and Oued Zarga (Figures. 4.4 and 4.5). Furthermore, we have identified a dextral strike-slip fault, namely the Zarga fault, which links two uplifting regions with related morphometric anomalies, corresponding to the Thibar and Lansarine ridges. These data suggest a different active fault segmentation pattern to the previously proposed Alia-Teboursouk fault, which is depicted quite clearly by the morphotectonic analysis that indicates active uplift along the northern limb of the Thibar anticline. Moreover, this model is further supported by the large thickness of syntectonic Plio-Quaternary sediments on the footwall of the Thibar reverse fault system in the Jendouba basin (Ayed-Khaled et al., 2015; Khelil et al., 2019), sediment thickness that is not found on the footwall of the Teboursouk fault segment. Following these results, we have renamed the fault system to Alia-Thibar fault. This fault zone, which we analyze in more detail below, shows an overall helicoidal geometry with a length of 130 km (Figure. 4.5).

The central segments of the fault zone are subvertical dextral transcurrent faults that occur near the locality of Oued Zarga (Figure. 4.2 and 4.5; 4.11A). Meanwhile, towards the SW these segments link with the SE-dipping Thibar sinistral-reverse fault segments and towards the NE it shows three different segments, starting with the NW-dipping Tebourba reverse fault segment (4.11A), following the NW-SE sinistral Jebel Baouala segment (Figure. 4.11B) and ending towards the North in a horstail-splay structure with several ENE-WSW to E-W oriented reverse-dextral faults like the Ghar el Melah and Utique fault segments (Figure. 4.11C). Overall, this fault system shows an helicoidal geometry, with a dextral vertical segment in the middle and terminating in reverse fault segments dipping in opposite senses towards the NW and SE. This is a relatively common geometry of transcurrent faults described in other regions (e.g. Booth-Rea et al., 2004; Giaconia et al., 2013). Towards the north, the Tebourba fault also links with the E-W dextral Dhkila fault (Camafort et al., 2020).

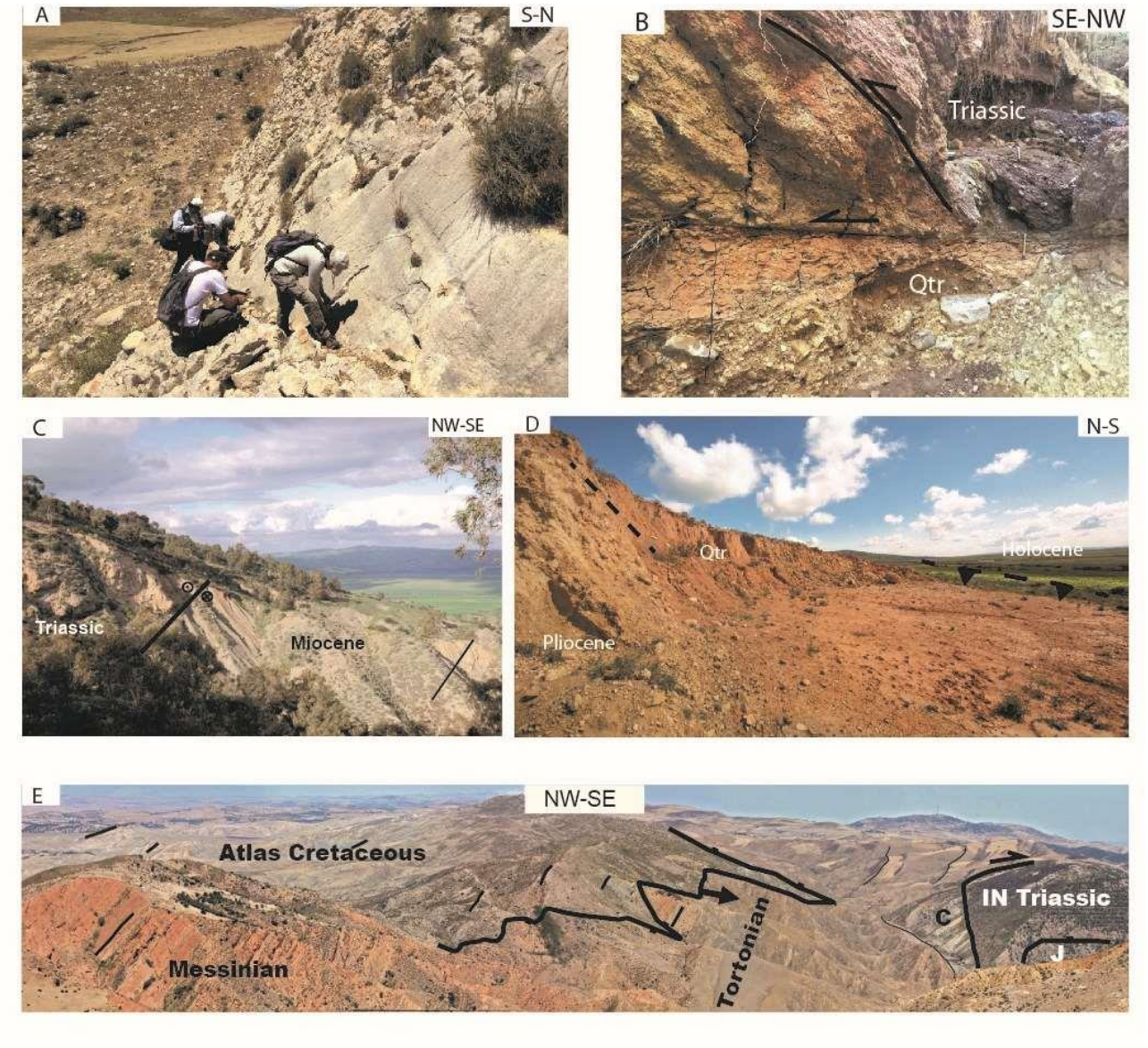

Figure 4-11: A) Dextral fault plane from the Oued Zarga fault zone, cutting through Eocene limestones. B) Tebourba reverse fault segment, with Triassic gypsum overthrusted over Quaternary alluvial conglomerates. C) Jebel Sakak sinistral-reverse fault segment of the Alia-Thibar fault zone. Notice Triassic Infranumidian rocks overthrusting reversed Miocene sediments. D) Folded Plio-Quaternary sediments in the hanging-wall of the Utique dextral-reverse fault, with the Utique depression to the right, at the footwall of the fault. E) Lansarine extensional detachment. Notice tilted Tortonian to Messinian sediments tilted over SE-dipping extensional detachment cutting down into a footwall ramp formed by Cretaceous Atlassic sediments (C). To the SE you can see a dextral strike-slip segment of the Oued Zarga fault cutting Infranumidian Triassic rocks that overlie Jurassic Atlassic sediments (J).

6.3.1. Ghar el Melah-Utique reverse segments

These fault segments form the northern termination of the Alia-Thibar fault system. They occur in a low-land region with active sedimentation at the mouth of the Mejerda River. Thus,

they cut and deform a complete sequence of Pliocene to Present sediments, which facilitates dating and restoring the shortening in this region (e.g. Mejri et al., 2010). Two reverse faults with SE-directed transport cut the surface near the localities of Ghar el Melah and Utique, respectively (Figure. 4.5, 4.11 C). A third reverse fault and associated blind fold also occurs further south, only observable on reflection seismics. The Ghar el Melah has an onshore length of 34 km, although probably continues towards the East, offshore. The faults show a NE-SW to E-W orientation. Measured striae along the E-W segment of the Ghar el Melah fault indicate reverse-dextral oblique kinematics (Figure. 4.6). The Utique reverse fault clearly inverts a previous NW-dipping normal fault (Seismic line L3, Booth-Rea et al., 2018). Finally, the structure of the largest Jebel Kechabta anticline is resolved to the north with a NW-directed blind thrust observable also on Line L3. These reverse faults merge towards the west into a NNE-SSW oriented sinistral fault segment bounding Jebel Sakak-Baoula (Figure. 4.5).

6.3.2. Jebel Sakak-Baoula sinistral segment

The Jebel Sakak segment shows subvertical and NW dipping strands with nearly pure sinistral strike-slip kinematics with a length of approximately 25 km. It separates Triassic Infranumidian sediments to the northwest from Neogene to Quaternary sediments in a synformal structure to the East (Figure. 4.11 B). (Amri et al., 2020)

6.3.3. Tebourba reverse segment

The Tebourba reverse fault segment runs with a NE-SW orientation for 22 km from the West of Tebourba until Oued Zarga to the SW. This fault dips strongly towards the NW, thrusting Triassic and Cretaceous rocks over Plio-Quaternary sediments of the Mejerda valley (Figure. 4.11 D). Early Pleistocene alluvial fan sediments are verticalized in the footwall of the fault. The hanging-wall of the fault defines a NE-SW oriented ridge cored by the autochthonous Atlas Cretaceous. Erosion at the core of this uplifting anticlinal ridge has exhumed the underlying structure that developed during the late Miocene extensional phase. This fold affects a Late Miocene extensional low-angle normal fault with E-SE tectonic transport and overlying extensional riders (Gibbs, 1984) formed by Early Miocene to Messinian sediments deposited over the allochthonous Infranumidian nappe (Figure. 4.11E). The LANF shows a gentle footwall ramp geometry cutting down into the Early Cretaceous-Jurassic sedimentary sequence (Cross-section A-A´, Figure. 4.12). Meanwhile, the hanging-wall of the LANF includes Late-Miocene syn-rift sediments overlying a tilted Early to Middle Miocene olistostromic piggy-back basin and its allochthonous infranumidian nappe Triassic basement. The Tebourba fault rock is mostly formed by strongly sheared Triassic gypsum and red beds over-thrusting Quaternary alluvial and colluvial sediments (Booth-Rea et al., 2018) (Figure. 4.11 D).

6.3.4. Oued Zarga dextral segment

The Oued Zarga fault segments run with a WNW-ESE orientation linking two oblique-reverse fault zones with opposite vergence. This fault zone with dextral kinematics is formed by several parallel fault segments that cut and displace the folded Oued Zarga Plio-Quaternary synclinal basin and the Mejerda valley. The fault zone has both dextral reverse and dextral-normal fault segments, thus developing both positive and negative flower structures (e.g. Figure 4.12). The fault zone is marked by elongated outcrops of Triassic rocks within autochthonous Atlas Cretaceous and Palaeogene sediments (Figure. 4.2).

6.3.5. Thibar reverse-sinistral segment

The Thibar fault segment runs with a NE-SW orientation along the southern margin of the Jendouba basin. It reaches 34 km length from Thibar towards the NE. Near Thibar it shows a dextral offset along a lateral ramp of approximately 5 km that probably takes advantage of a Late Miocene normal fault. Along most of its trace it separates Triassic red-beds on its hanging-wall from late Miocene sediments or Plio-Quaternary ones on its footwall. It shows several sets of striae with both pure reverse and oblique sinistral kinematics, with NW-directed hanging-wall transport. This reverse fault system continues, offset to the southwest of Thibar, with a more easterly direction and with dextral-reverse kinematics (Hamdi et al., 2019). However, the seismic reflection lines that cut the southern border of the Jendouba basin further East show that the main fault is a low-angle reverse fault that inverts a previous southward directed normal fault (Figure. 4.8).

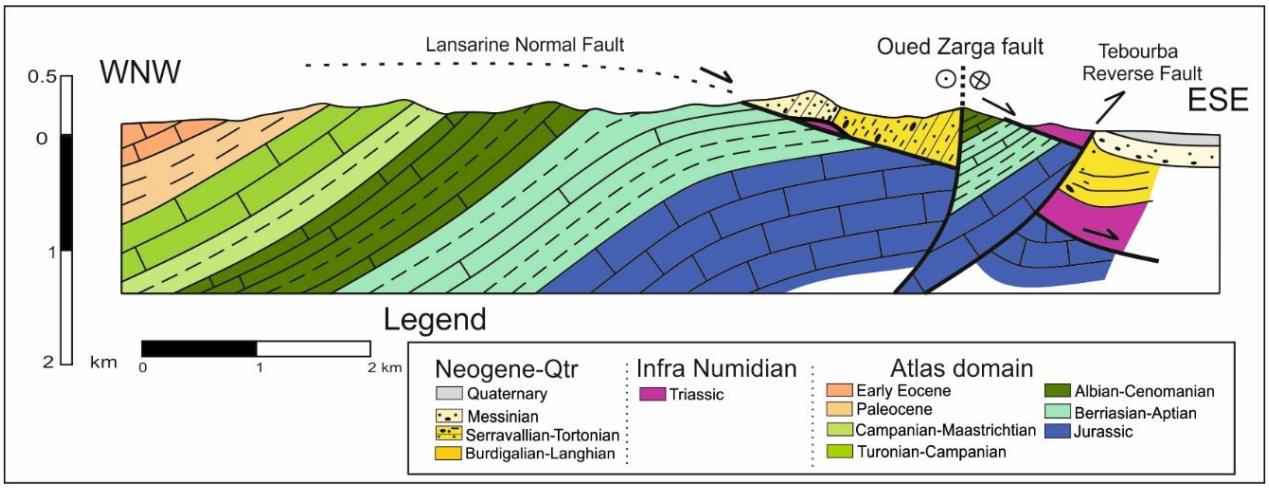

Figure 4-12:Cross-section across the Lansarine uplifted block, showing exhumed extensional detachment and overlying tilted late Miocene sediments cut by the later

7. Discussion

Combining field structural analysis, mapping, reflection seismics and morphometric indices we have obtained a new map of active tectonic structures and their segmentation in Northern Tunisia (Figure. 4.2, 4.5). This map offers a different pattern of fault segmentation than previously established and supports a present fully transpressive tectonic setting in response to Africa-Eurasia NW-SE convergence for the region, in accordance with stress inversion of focal mechanism solutions (Soumaya et al., 2015, 2018). A tectonic context that is further supported by the stress ellipsoids determined from striated pebbles in Quaternary alluvial fans and fluvial terraces that give maximum horizontal N-S to WNW-ESE shortening (Camafort et al., 2020 and our own results, Figure. 4.7). We actually obtain two different populations of strain ellipsoids with N-S and NW-SE main shortening axis. WNW-ESE shortening is obtained in the proximity of dextral strike-slip faults like the Oued Zarga and Dkhila faults (stations 2_1, 6_1 and 30, Figure. 4.7), suggesting that these faults may produce stress rotation in their proximity, as observed in oceanic transform faults (e.g.Angelier et al., 2004).

We have identified new active faults that influence the landscape of Northern Tunisia by cutting drainage basins and affecting rock uplift rates. These shortening structures developed after a phase of Late Miocene crustal extension that strongly modified the Tell and Atlas Early to Middle Miocene foreland fold and thrust belts (Booth-Rea et al., 2018). This change in tectonic setting is marked by the development of a Pliocene erosive post-rift unconformity that was later folded in the Late Pliocene to Present in Northeastern Tunisia (Figure. 4.8 and 4.9). Many of the Pliocene to Present reverse faults are inverting previous Late Miocene normal faults. For example, along the southern Margin of the Jendouba basin and also in the Mateur-Utique region to the East (Figure. 4.8).

The active faulting segmentation and folding pattern of Northern Tunisia, characterized by 20 to 30 km long SW-NE oriented fault segments, is mimicked by both ksn and gridded Hi morphometric results, which draw positive morphometric anomalies located over active shortening structures (Figure. 4.4 and 4.5). The morphometric analysis has highlighted especially the increase in incision rates produced in the hanging-wall of reverse and oblique reverse faults and active antiformal ridges. Anomaly 1 in the Kroumirie massif shows SW-NE high ksn values that run parallel to some segments of the sinistral strike-slip Cap Serrat-Gardimau fault zone. However, no anomaly follows the full published length of this fault zone. Furthermore, reflection seismics and field work has shown that this fault is a low-angle normal fault with SE-directed transport that was active during the late Miocene (Booth-Rea et al., 2018) . The geometry of the morphometric anomaly suggests that only a short segment of this fault, West of Nefza, is

presently being inverted as a reverse fault with NW-directed transport. The main active faults in the Kroumirie region related to anomaly 2 (Figures. 4.4, 4.5) do not coincide with the previously mapped thrusts bounding the main tectonostratigraphic Tellian and Atlas domains. On the contrary, the main fault uplifting this domain is out of sequence respect to older thrusts and steps up through the Atlas domain towards the NW (Ould Bagga et al., 2006). It shows an E-W orientation between the localities of Balta and Fernana within the Atlassic domain and later turns to a NE-SW orientation, parallel to the Jebel Sabah and Jebel Sra antiforms, which are locally bounded by sinistral-reverse faults (Figures. 4.2, 4.5). Thus, the Kroumirie region is being uplifted as a pop-up between two reverse faults with NW transport to the north and SE-directed transport to the S (Figure. 4.5).

The morphometric analysis has also shed light into the effects of transverse drainage development on topographic dissection in Northern Tunisia. Several domains with high ksn and gridded Hi values occur headwards of capture sites and 90º deflections in the drainage system formed in relation to headward erosion across antiformal ridges or the hanging wall of reverse faults. This is the case of high ksn values in the Joumine River basin, near Joumine. A process that has also been described at a larger scale in catchments at the South of the Mejerda basin (Camafort et al., 2020). The Mejerda river also has a transverse affluent across the Balta-Fernana reverse fault that has captured a basin that drained towards the NE, with high ksn and gridded Hi values in its headwaters (anomaly 2, Figure. 4.5).

The higher order rivers in Northern Tunisia like the Mejerda, Tine or Joumine rivers mostly follow regions with low gridded Hi and ksn values, at the footwall of the main thrust faults, forming large axial valleys that run from SW to the NE (Figure. 4.4). This drainage pattern with dominant longitudinal valley development is characteristic of young foreland thrust belts (e.g. Babault et al., 2012) . A feature that supports the young Pliocene age for tectonic inversion and development of the presently active shortening structures in Northern Tunisia, even though plate convergence across the region initiated in the Cretaceous (e.g. Dewey et al., 1989).

Our study shows that the general model of several parallel 100 km long NE-SW sinistral reverse faults and associated anticlines cored by diapirs, active since the Early Miocene, generally established for Northern Tunisia, must be revised. Also, tectonic models that use long 500-600 km fault zones to fit GPS measured horizontal movement do not agree with our observations. Instead, our analysis shows the existence of many shorter, reverse, sinistral and dextral faults, together with related folds, developed since the Pliocene, which are accommodating the present NW-SE shortening in the region. Only in one case we find a 130 km long highly-segmented fault system, namely the Alia-Thibar fault. This fault system shows an

helicoidal geometry with at least five different 20 to 30 km long fault segments. Overall, the fault zone shows a central E-W dextral segment corresponding to the Oued Zarga fault that links two domains with opposing reverse kinematics. To the West, the NE-SW Thibar reverse fault segment bounding the southern border of the Jendouba basin shows NW-directed transport. Meanwhile, towards the East the Oued Zarga fault links with mostly SE-directed reverse faults like the Tebourba fault and the Ghar el Maleh-Utique horse tail splays (Figure. 4.5). The Alia-Thibar fault zone determines the position of the main Plio-Quaternary sedimentary basins in Northern Tunisia that occur at the footwall of its reverse fault segments along the Mejerda depression.

The restoration of the Pliocene to Present shortening in Northern Tunisia using reflection seismic lines L2 and L3 indicates differential shortening from W to E. We obtain 16 % shortening across Line L2 in Northwestern Tunisia and 7% across line L3 in Northeastern Tunisia. This difference in amount of shortening probably reflects a younging of contractional inversion from West to East (Figure. 4.13). Tectonic inversion in Northeastern Tunisia started in the Late Pliocene during the deposit of the Porto-Farina marine formation. To the West, however, we do not have an age constraint of the base of the Plio-Quaternary Segui continental formation that could probably be older, even Messinian-Early Pliocene (Mannaï-Tayech, 2006). This younging towards the East of the tectonic inversion phase may have followed after the phase of late Miocene extension that also propagated from the West towards the East (Booth-Rea et al., 2018). Our morphotectonic results also show a higher degree of topographic dissection towards the Northwest of Tunisia where the maximum ksn values are obtained, together with larger domains of high gridded Hi values (Figure. 4.4 and 4.5). Results that also may reflect the younging of tectonic inversion towards the Northeast of Tunisia.

Reverse faults in a 35 km section (Line L3, Figure. 4.10B) through Northeastern Tunisia are accommodating shortening rates of approximately 0.8 mm/yr since 3.2 Ma. These values are lower than the predicted 1.5 mm/yr from GPS displacement analysis (Bougrine et al., 2019). However, our work shows that shortening is not accommodated along a single fault, but instead, it occurs across different shorter fault segments distributed in a wider region. Meanwhile, E-W displacement rates along dextral segments like the Oued Zarga fault are probably larger as they link regions with opposite displacement senses (Figure. 4.13).

The combination of reverse and dextral linked fault segments in Northern Tunisia can probably explain the observed GPS displacements, without the necessity of the single 500 km Gardimau-North Constantine dextral-oblique fault zone that was used for modeling them (Bougrine et al., 2019). Thus, NW-SE shortening and E-W dextral displacements required in

Northern Tunisia to explain GPS-measured displacements is distributed along a wide region with multiple short 20 to 30 km long faults and related folds.

This pattern of shortening and dextral shearing, along short 20-30 km long fault segments distributed throughout Northern Tunisia instead of along a single 500-600 km long dextral-reverse fault as modelled from GPS displacement results, probably fits better the moderate seismic risk predicted for Northern Tunisia with seismic magnitudes below 7 and a designed ground acceleration range between 0.154 and 0.3 g (Mourabit et al., 2014).

The tectonic evolution observed in Northern Tunisia since the Late Miocene shows many parallelisms with the rest of the Western Mediterranean, where recent tectonic inversion is affecting areas previously extended in the Late Miocene (e.g. Billi et al., 2011). Although, in this case, tectonic inversion initiated in the Late Pliocene, later than along more western regions of Algeria and the Southeastern Betics, where renewed shortening initiated in the latemost Tortonian to Messinian (e.g. Booth-Rea et al., 2004; Déverchère, 2005; Domzig et al., 2006; Mauffret, 2007; Giaconia et al., 2015), but earlier than further East in the Thyrrenian basin where tectonic inversion is younger than 2 My (Billi et al., 2011; Zitellini et al., 2019). Shortening structures in Northern Algeria propagated offshore, further North in the Plio-Quaternary, suggesting a northward migration of deformation, probably explained by in-sequence north-verging propagation of deformation (Recanati et al., 2019).This westwards younging of tectonic inversion also seems to be observable at the scale of Northern Tunisia and it must have initiated after the end of crustal extension, which also propagated in a similar fashion during the late Miocene, probably following the SE retreat of the peeling-back African lithospheric mantle ((Roure et al., 2012; Booth-Rea et al., 2018)

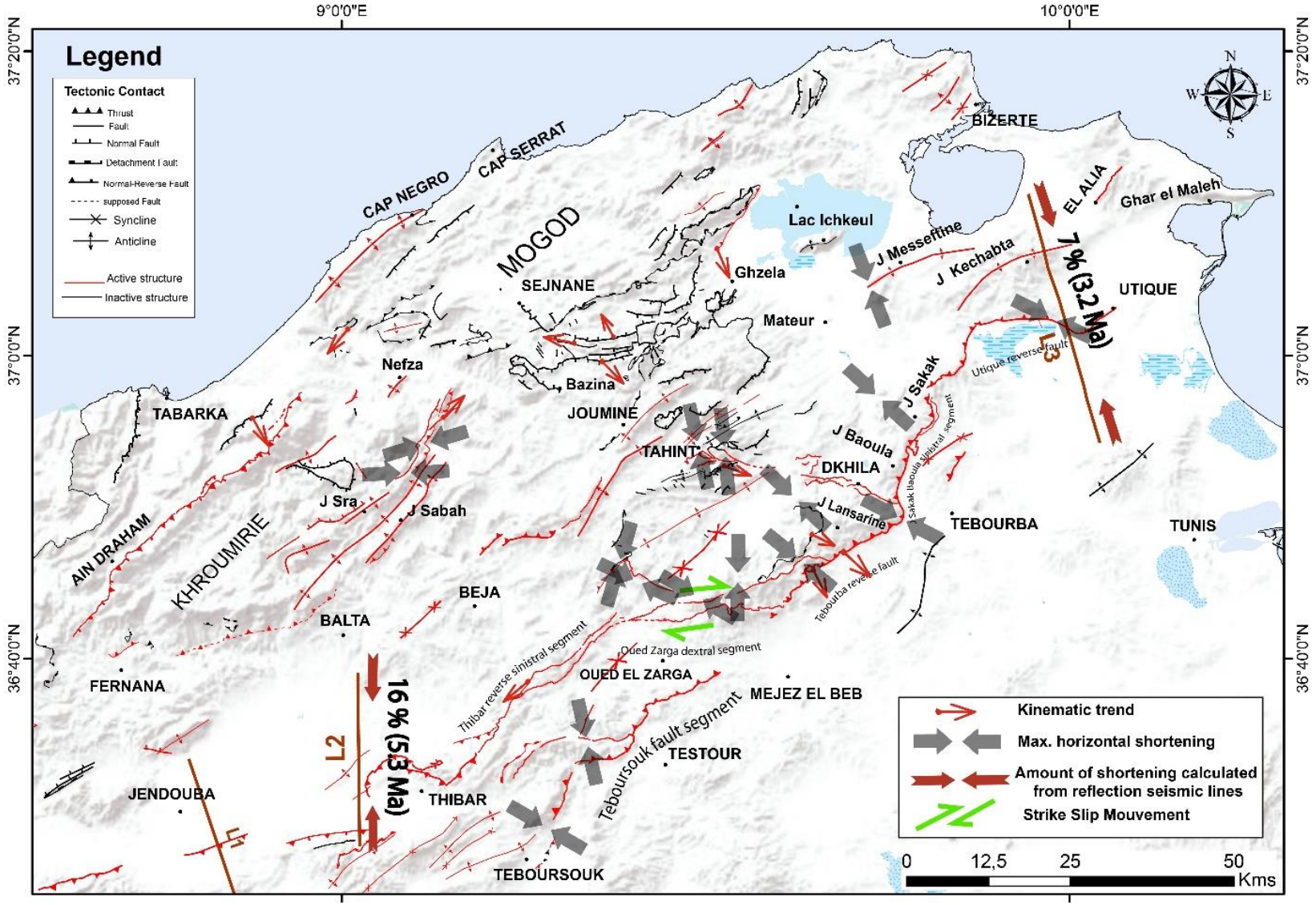

Figure 4-13: Active fault segmentation in Northern Tunisia together with max. Horizontal compression and amount of shortening since the Pliocene along two balanced sections

8. Conclusions

Northern Tunisia is accommodating a great part of the present NW-SE Africa-Eurasia convergence in the region. Most of the active shortening structures in Northern Tunisia developed since the Pliocene in a tectonic inversion phase that propagated from West to East, reaching Northeastern Tunisia in the Late Pliocene. Thus, many of the active thrusts in the region reuse Late Miocene normal faults. Furthermore, enhanced erosion in the uplifting hanging-wall of the main shortening structures has favored the exhumation of the Late Miocene extensional detachments and associated structures. Shortening ranges between 16 and 7 %, decreasing from W to E. The fault system accommodating plate convergence in Northern Tunisia is strongly segmented with ENE-WSW to NE-SW reverse faults, E-W to NW-SE dextral faults and NNE-SSW sinistral ones. The individual fault segments range between 10 and 30 km long. The largest linked fault system is the Alia-Thibar fault zone that reaches a length of 130 km and includes at least 5 different fault segments with an overall helicoidal geometry. We have characterized the landscape response to this convergent tectonic setting by topographic metrics of hillslope and catchment morphology calculating the normalized steepness index (ksn) and gridded hypsometric integral. The distribution of high ksn values and gridded Hi in the region strongly mimic the fault segmentation in Northern Tunisia, especially, defining the regions overlying reverse faults and related anticlinal ridges. Furthermore, both ksn and Hi maps show an East to West gradient in the degree of topographic dissection compatible with the increase in tectonic shortening and age of the inversion structures towards the West. In some case the high ksn and Hi clusters occur headwards of fluvial captures and 90º deflections in the fluvial channels, indicating higher fluvial dissection in response to the development of transverse drainage. The landscape of Northern Tunisia is characteristic of a young fold and belt region with dominant axial valleys coinciding with the footwall of the main faults and/or along syncline structures. This current young topography related to Pliocene to Present shortening in Northern Tunisia, in a convergent setting since the Cretaceous, indicates that Late Miocene extension completely dismantled the previous foreland thrust belt structure and associated topographic features. A process that resulted in a new SW-NE topographic gradient towards the main direction of extension and crustal thinning at the end of the Messinian. Tectonic inversion and development of new shortening structures accommodating NW-SE plate convergence in Northern Tunisia followed the trend observed at a larger scale in the western Mediterranean, with shortening propagating from central Algeria towards the East, from the late Miocene up to the Quaternary in the Tyrrhenian.

Chapter 5: Analysis of the Geological Controls and Kinematics of the Chgega Landslide (Mateur, Tunisia) Exploiting Photogrammetry and InSAR Technologies

---

Exploration of territories not previously analyzed by landslide experts provides interesting findings. The Chgega landslide, in northern Tunisia, represents a paradigmatic mass movement. It can be classified as a complex landslide, or more specifically as vast rock spreading that evolved into a block slide. It involves a great block of limestone (about 900 m long and 400 m wide) sliding over ductile clays and marls. The viscoplastic creep of the clays drives the landslide and creates, in its crown, a graben ~800 m long and ~120 m wide that breaks the summit of Chgega Mountain. Using Interferometric Synthetic Aperture Radar (InSAR) technologies, we demonstrate that this complex landslide is currently active and moreover shows progressive movement without clear episodic accelerations. The velocity of the limestone block is just above 2 mm/yr. The occurrence of gravity-induced joints indicates that the movement has an orientation towards 333° of azimuth on average, conditioned by the landscape around Chgega. These results were obtained through the analysis of a 3D model and a high-resolution orthoimage created from photographs acquired by an Uncrewed Aerial Vehicle (UAV). We may conclude that the landslide movement is determined by normal faults with directions N060°E and N140–150°E. This characterization of the Chgega landslide can serve as the basis for future studies about the origin of this slope movement. Furthermore, the data provided here may support the recognition of Chgega as a singular geological point that deserves to be declared a geosite.

---

* Most of the content of this chapter corresponds to the following article: Gaidi, S.; Galve, J.P.; Melki, F.; Ruano, P.; Reyes-Carmona, C.; Marzougui, W.; Devoto, S.; Pérez-Peña, J.V.; Azañón, J.M.; Chouaieb, H.; Zargouni, F.; Booth-Rea, G. Analysis of the Geological Controls and Kinematics of the Chgega Landslide (Mateur, Tunisia) Exploiting Photogrammetry and InSAR Technologies. *Remote Sens.* 2021, *13*, 4048. https://doi.org/10.3390/rs13204048.

1. Introduction

The development of landslide research in countries not traditionally involved in this topic, together with continuous exploration of further territories, will surely shed new light on mass movements and emblematic landslides. The largest known landslide in the world was recently described along the coast of Kara-Bogaz-Gol lagoon (Turkmenistan) (Aslan et al., 2021). In this paper we present another outstanding landslide, identified in Northern Tunisia, on Chgega Mountain. It can be considered paradigmatic of its kind in the Mediterranean basin because of the particular landscape it creates, classified by (Gaidi et al., 2020) as a "rock spreading". According to (Pasuto and Soldati, 2013) , there are two types of rock spreading phenomena: one developed in homogeneous rock masses and another that involves rigid rock formations overlying ductile terrains, as in this case. Still, the classification of this landslide is complex, as we explain in this paper. It may be categorized as a Deep-seated Gravitational Slope Deformation (DGSD) according to (Pasuto and Soldati, 2013) or as a rock spreading that evolves into a large rock planar slide. The latter can also be called block slide according to the recent classification developed by (Hungr et al., 2014). These terms describe slow-moving landslides that involve large slopes and that produce peculiar gravity-induced landforms. The areas where such landslides occur typically show persistent joints, double ridges, uphill-facing scarps, infilled troughs, trenches, gulls, grabens, pseudo-karst features, and bulges (Pasuto and Soldati, 2013). In the subsurface, this type of landslide also generates crevice caves (term used by (Halliday and McKelvey, 2004)). Good examples can be found in the non-karstic cavities described in the flysch units of the Western Carpathians (Lenart et al., 2014).

The Crimean Mountains (Ukraine) harbor some examples of mass movements similar to the one described in this paper namely, large-scale slope movements with blocks of limestone of great dimensions mobilized by sliding over marl and claystone units. This phenomenon creates an unusual rugged relief formed by lateral spreading and block sliding processes (Pánek et al., 2008). Other places where large lateral spreading and block-type slope movements of carbonate rock formations overlie clayey-marly rocks can be found include Malta (Soldati et al., 2019; Devoto et al., 2021), Sicily (Di Maggio et al., 2014), and Roccalbegna-Mt.Labbro (Italy) (Iotti, A.; Tarchiani, 1996). The combination of morphological features produced by this type of movement can create landmark sceneries, even regional symbols for the local population (e.g., the Trotternish landslides on the Isle of Skye, Scotland (Fenton et al., 2015)) and some are

nominated as geosites (e.g., crevice caves generated by mass movements in the UK (Cooper, 1983)).

In the case described in this paper, the landforms associated with the landslide could qualify as a geosite. One singular characteristic is a spectacular graben structure that breaks the ridge of the hill impacted by the mass movement, Chgega Mountain. The local name of this structure is "Kef Chgega" (كاف الشقاق), which means "the open fracture of Chgega Mountain". Although the site is a well-known landmark in the region of Mateur and forms a remarkable spot from different standpoints, only brief descriptions of it can be found in the scientific literature (Gaidi et al., 2019; Galve et al., 2019; Camafort et al., 2020).

This paper completes previous contributions by describing in greater detail the characteristics of this large landslide, its main singularities, and the conditions favoring the geomorphological evolution of this impressive DGSD. Our description of Chgega Mountain has benefited from new data gathered through up-to-date remote sensing (RS) techniques: landscape analysis, Uncrewed Aerial Vehicle Digital Photogrammetry (UAV-DP), and advanced Satellite InSAR techniques. The combination of the two latter techniques has already proven its usefulness for landslide characterization elsewhere (see for example the studies of (Cigna et al., 2017) in Ireland, (Mateos et al., 2018) in Spain, or (Martins et al., 2020) in Timor-Leste). The focus here, in turn, is on a region where RS methods are not yet common. Indeed, the use of InSAR techniques in North Africa is scarcely documented in the literature: (Fonseca, 2014) investigated failure mechanisms of DGSDs in the Rif Mountains (North Morocco) and (Beladam et al., 2019) correlated surface displacements detected by InSAR with known landslides in Constantine (Algeria). Photogrammetry has been applied to aerial photographs to study the El Biar Landslide in Algiers, Algeria (Laribi et al., 2015), but no other publication about North Africa used UAV images until the very recent paper by (Bounab et al., 2021). They undertook a study similar to ours in northern Morocco, integrating UAV-DP, InSAR, and geophysics to analyze a slow-moving landslide by the coast of the Alboran Sea. This paper complements the aforementioned case studies providing two new innovative aspects for UAV-DP and InSAR analyses: (1) we took advantage of a cloud-computing platform to perform the InSAR analyses. This platform provided us with displacement maps with no need for software or SAR images to develop the analysis. (2) We exploit the capacity of UAV-DP to generate a 3D model, an orthoimage, and a digital elevation model (DEM) to perform structural analysis in a virtual environment, enriching the information gathered in the field. The use of UAV-DP and its products considerably reduced both the fieldwork time and the resources needed to carry out our survey.

Thus, by combining the above technologies, it was possible to maximize the yield of the available study resources. They allowed us to gather a considerable volume of data within a limited time frame, to characterize the Chgega landslide without sacrificing the quality of the results. This research might therefore serve as a benchmark for similar investigations that need to optimize time and funding when applying new technologies. At the same time, the results of UAV-DP and InSAR enabled us to carry out not only a general portrayal of the mass movement but also a comprehensive characterization of its kinematics. This characterization should prove useful for future research into the origins of the Chgega landslide and to explain why it takes place in a region having low relief.

2. Geological and Geomorphological Setting.

Chgega is a mountain culminating at 553 m.a.s.l. located in the Mateur region of Northern Tunisia, near Tahint village (Figure 5.1). From the geological viewpoint, Chgega forms part of the reliefs created by the Tell belt, formed by the Mesozoic and Cenozoic sedimentary cover of the Maghrebian Tethys realm, overthrusted and folded (Frizon De Lamotte et al., 2000; Khomsi et al., 2009). This belt, together with the Atlas belt further south, was produced in a context of NW-SE to N-S plate convergence between Africa and Eurasia since the late Cretaceous.

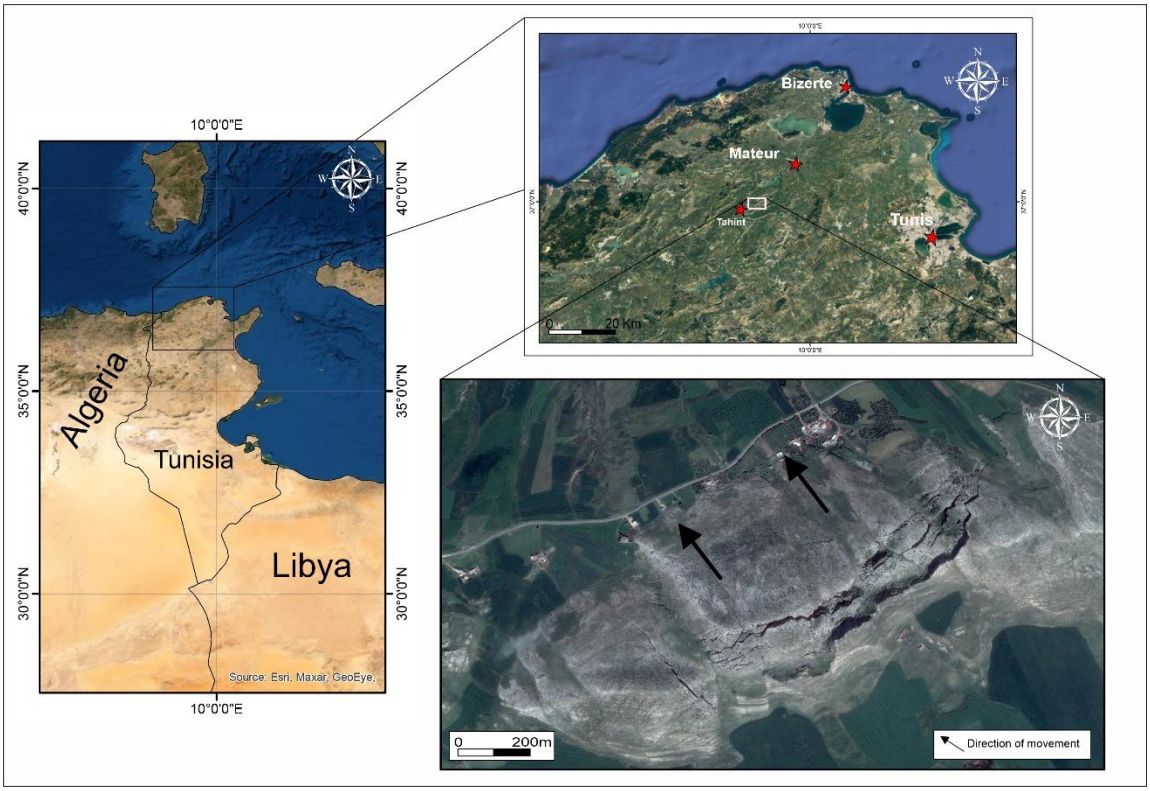

Figure 5-1: Location of the Chgega landslide.

The topography of Northern Tunisia is therefore strongly influenced by this general convergent setting. However, it does not show the landscape characteristics of a mature orogenic belt with a well-developed transverse drainage system (DeCelles and Giles, 1996; Babault et al., 2012; Camafort et al., 2020). A smooth and low relief largely characterizes the entire region. Over this structural landscape, the greatest reliefs coincide with anticlinal ridges or the hanging wall of shortening structures; in turn, the topographic depressions and axial valleys occur in relation to synforms and the footwall of reverse faults (Melki et al., 2011; Camafort et al., 2020; Gaidi et al., 2020). Large NE-SW oriented axial valleys such as the Mejerda, Tine, Joumine, and Ghezala river valleys run parallel to the main shortening structures, e.g., the Alia-Thibar fault zone (Gaidi et al., 2020). The landscape is furthermore influenced by rheological contrasts between competent and incompetent lithologies respectively, limestones and pelites. For instance, the folded region where Chgega Mountain is situated shows a differential relief marked by the erodibility contrast between the Early Eocene nummulitic limestones of the Garia Formation and the Palaeogene or Late Eocene clays and marls of the Haria and Souar Formations, respectively (Burollet, 1956; 1977 Rouvier, 1977) (Figures 5.2 and 5.3). Miocene half-grabens subparallel to the fold hinges in the region further stand out against the Eocene limestones in the uplifted footwall of the normal faults (Cohen et al., 1980).

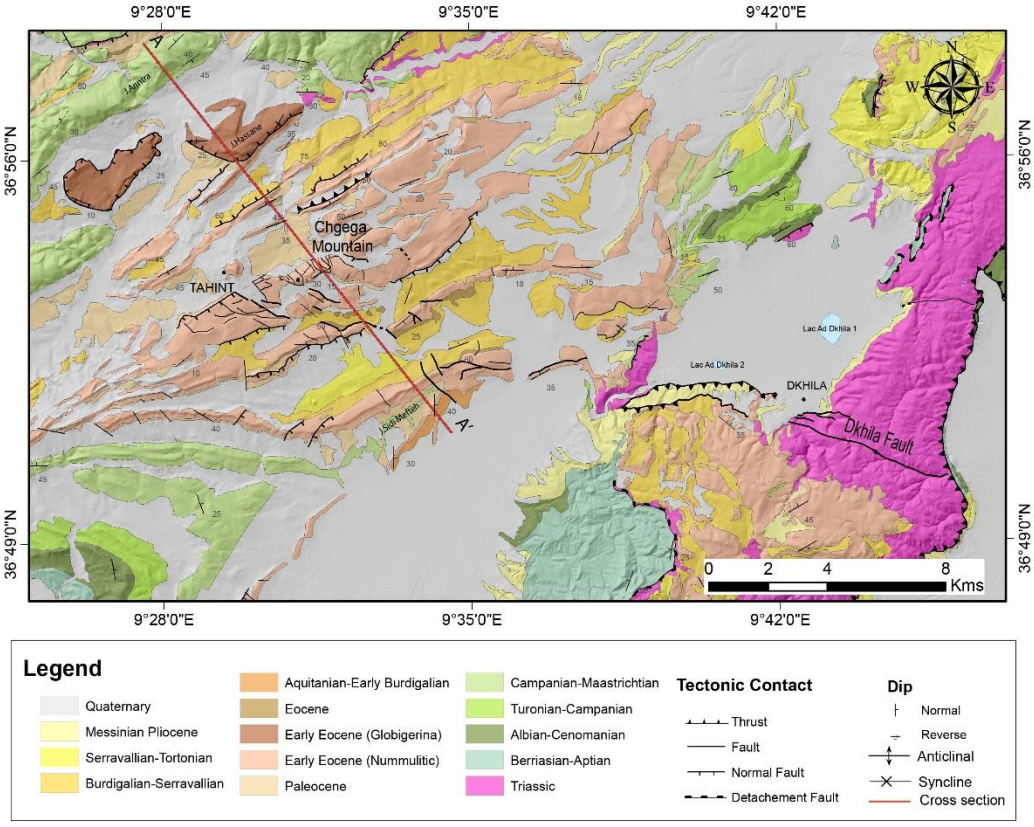

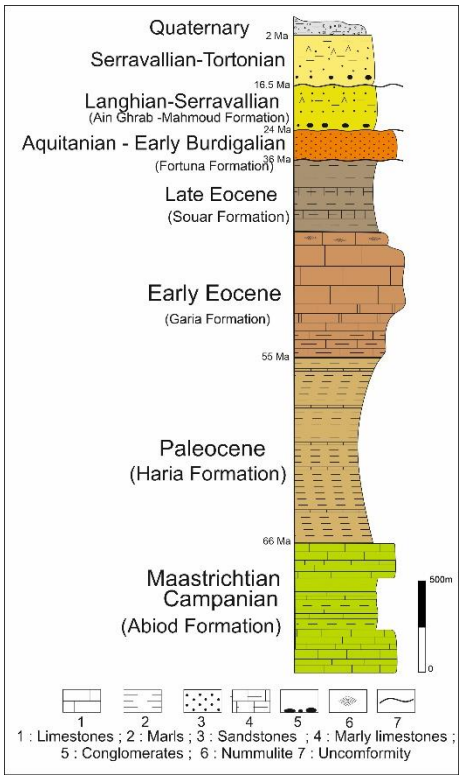

Figure 5-2 : Geological map based on existing 1:50,000 maps published by Office Nationale des Mines and stratigraphic column of the Chgega landslide region.

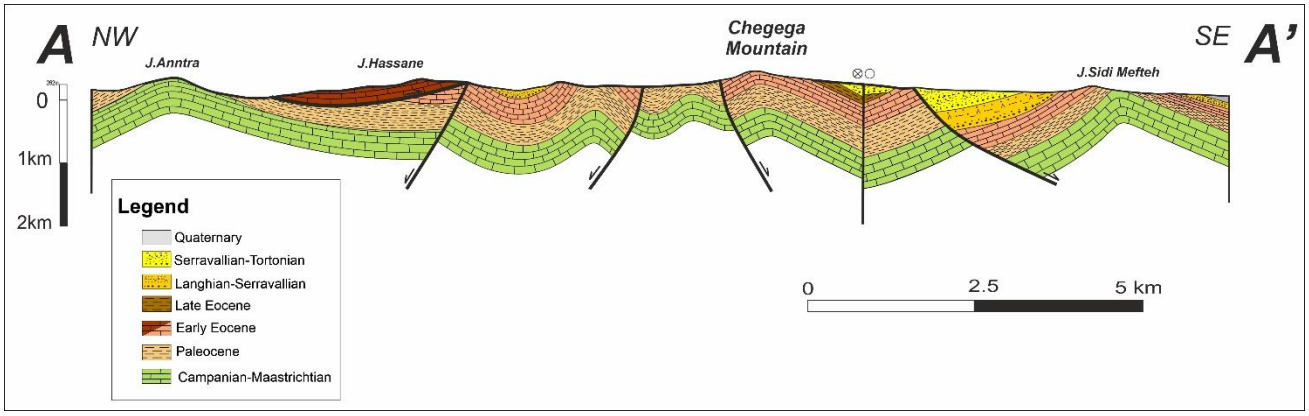

Figure 5-3 : Figure 4.3: NW-SE cross-section highlighting the main structures of the study area (AA'). Position of AA' is given in Figure 2.

Since the Late Pliocene topographic incision and rejuvenation in Northern Tunisia, the landscape evolution is mostly driven by NW-SE directed tectonic shortening, accommodated along reverse and strike-slip faults and associated folds, which favor the development of incipient transverse drainage through recent fluvial captures (Camafort et al., 2020; Gaidi et al., 2020).

This active tectonic shortening is the cause of damaging earthquakes (the 410 AD Utique and the 856 AD Tunis seismic events) related to the activity of the Alia-Thibar fault system

(Mejri et al., 2010a; Bahrouni et al., 2014). The maximum observed seismic intensity maps for Tunisia indicate higher intensity registered in the proximity of the western end of the fault system, near the village of Thibar (Kharrat et al., 2018). The seismic hazard map of Tunisia indicates the highest hazard in the region near Tunis, including our studied area (Soumaya et al., 2016) (Figure 5.4). The Chgega landslide occurs within the horsetail splay zone of one of the Alia-Thibar fault segments, corresponding to the Dhkila dextral fault (Camafort et al., 2020) (Figure 5.2). In addition to the Dhkila fault, the region of Chgega Mountain is well known for the presence of an imbricate fold and thrust stack that involves mostly the Tertiary Atlassic sedimentary cover (Kujawski, 1967; Cohen et al., 1980; Marzougui et al., 2014; Atawa et al., 2019) that is overprinted by late Miocene half-grabens (Fournet, 1994; Booth-Rea et al., 2018). One of the normal faults forming these half-grabens determines the Chgega landslide, as we shall see.

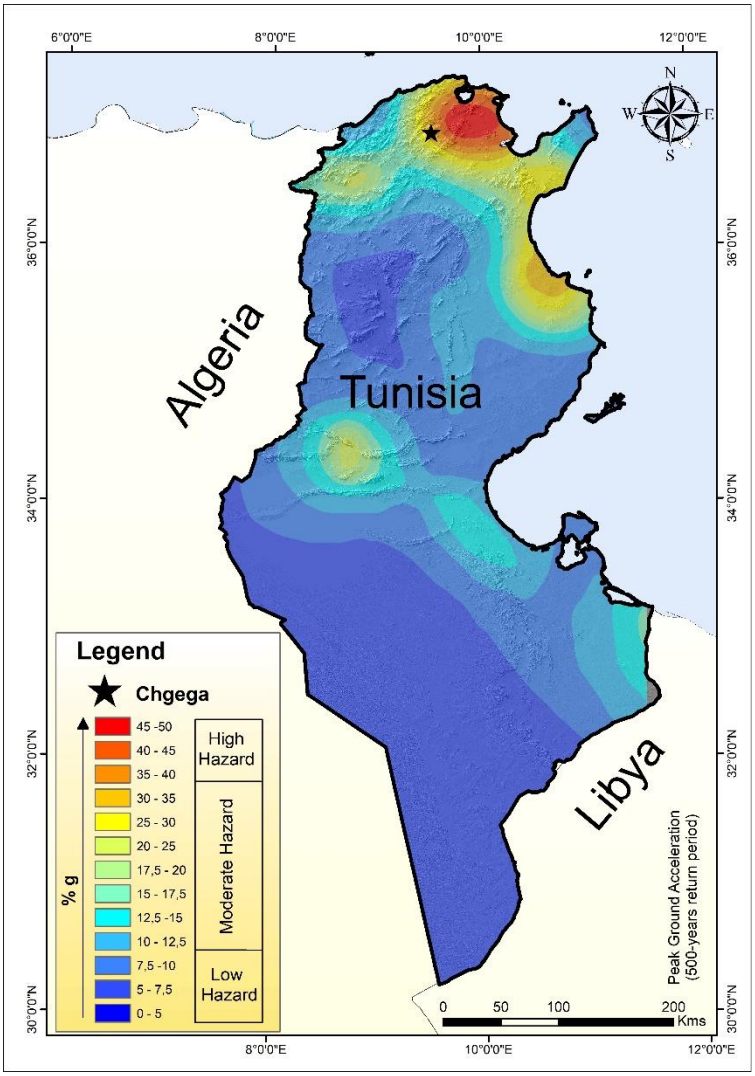

Figure 5-4: Seismic hazard of Tunisia according to (Soumaya et al. 2016).

The landslides in the region are commonly associated with clays and marls of the Haria Formation. The most common type would be slow-moving flows forming long tongues of clay materials moving downhill through low-angle slopes (Figure 5.5B–D). Less common are rockfalls, present only in a few cliffs amid the limestones of the Garia Formation (Figure 5A). Landslides similar to that of Chgega can be found in the hill right in Tahint village, where limestones of the Garia Formation slide over the clays of the Haria Formation and in the relief SW of Tahint, where rock spreading of smaller dimensions was recognized by us.

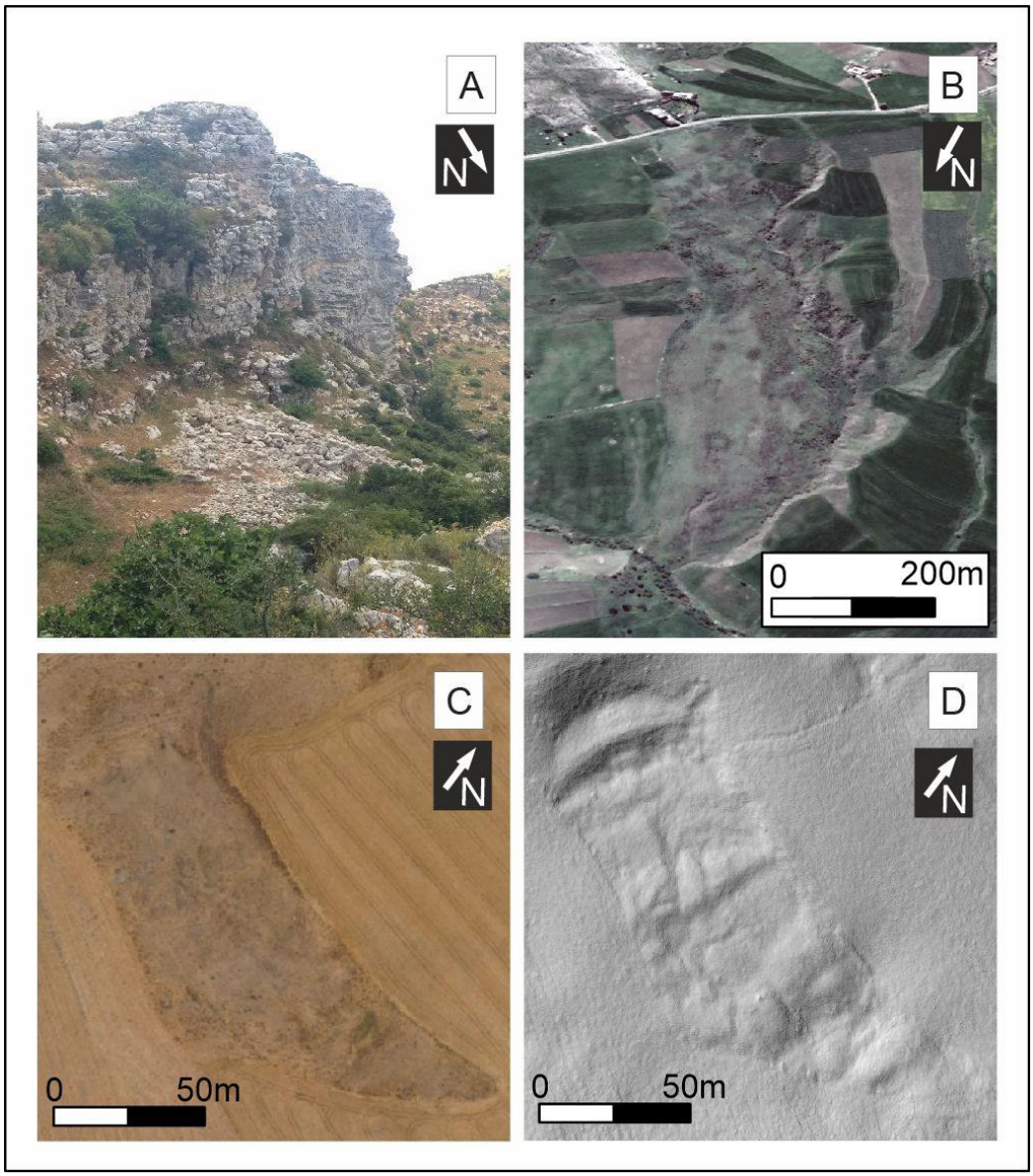

Figure 5-5 : Landslide types Landslide types observed in the region of Mateur. (**A**) Rockfall deposits at the foot of a scarp in the limestones of the Garia Formation. (**B**) Slow-moving flow developed in clays of the Haria Formation (Source: Google Earth™). (**C**,**D**) Orthoimage (**C**) and hillshade model (**D**) of a flow that occurred in a cereal crop adjacent to Chgega Mountain. Images obtained from the 3D model created in this study (see following sections for more details).

The area of Chgega Mountain features a warm climate, which is dry in summer and mild and wet in winter. July and August are the months of maximum temperature, evapotranspiration, and hours of sunshine, while humidity and precipitation are minimal. Average annual temperatures in the area targeted by the study are approximately 17 to 20 °C, with a monthly average of 27 to 29 °C; the average maxima is 33 to 34 °C in July–August. Total annual rainfall is around 521 mm and the average annual potential evaporation is between 1300 and 1800 mm. The average annual relative humidity is 60 to 68%, with maxima of 75 to 85% in the rainy season, from December to January, and lows of 49 to 60% in July–August. During historical times (Late to 4500 B.P), the Maghreb, hence Northern Tunisia, had a more humid climate than the present one, as attested by paleo-vegetation, sedimentological, and geomorphological studies (Paskoff and Sanlaville, 1986; Brun, 1989; Leveau, 2012). Within this interval, four dry episodes are identified (4700, 3000, 1600, and 400 B.P) (see reviews in (Leveau, 2012).

3. Methodology

In characterizing the Chgega landslide, we combined traditional methods and RS techniques. Classical methods included geological and geomorphological field surveys describing outcrops and landforms, with measurements of geological structures. Modern techniques encompassed morphometrical analysis of DEMs and interpretation of aerial photographs, orthoimages and hillshade models in a GIS environment, along with analysis of terrain 3D models to extract virtual measurements and better observe the morphological features. Additionally, we performed preliminary InSAR analysis to roughly estimate the regime and velocity of the landslide movement. The more innovative and specific techniques applied in Chgega landslide are detailed below.

3.1 Terrain 3D Model Production

Producing the 3D model of Chgega Mountain was a challenge because of the following main constraints: (1) the team involved in this research was unable to use its own UAV because introducing this equipment in Tunisia was prohibited; (2) at the time there were no professionals available in Tunisia specialized in performing this kind of task; and (3) there was a major constraint in the use of UAV due to the country's security situation. To overcome the administrative constraints, we leased a UAV service to a media professional and advised him how to project a mission of aerial photo acquisition aimed at creating 3D models. The flight was

performed in the early morning to avoid the strong wind that rises in the late morning in the study area. The UAV used in this work was a DJI Phantom 4 equipped with a three-axis stabilized camera having a resolution of 12.4 megapixels and a 1-inch 20 MP CMOS sensor. We designed the acquisition missions with the Pix4D Capture software. A normal double grid mission of 1200 × 750 m with multiple battery changes was designed because the range of the UAV was insufficient to cover the entire study area due to battery life issues. The elevation of flight was 100 m above the summit of Chgega Mountain. We programmed a 70% front and side overlap; the angle of the camera was 70°. Subsequently, we carried out a topographic survey to measure 9 ground control points (GCPs) on places easy to recognize in the UAV photo captures, such as artificial structures and targets (Figure 5.6).

The survey was performed using a GNSS LEICA GS07. The UAV surveys acquired 967 superposed images that we processed by means of Agisoft PhotoScan Professional software Version 1.4.3 to construct the 3D model and produce the DEM and orthoimage of the Chgega Mountain at high resolution. The Structure from Motion (SfM,(Ullman, 1979)) algorithms of Multiple-View Stereo (MVS, (Seitz et al., 2006)) images served to process UAV-based images using GCPs.

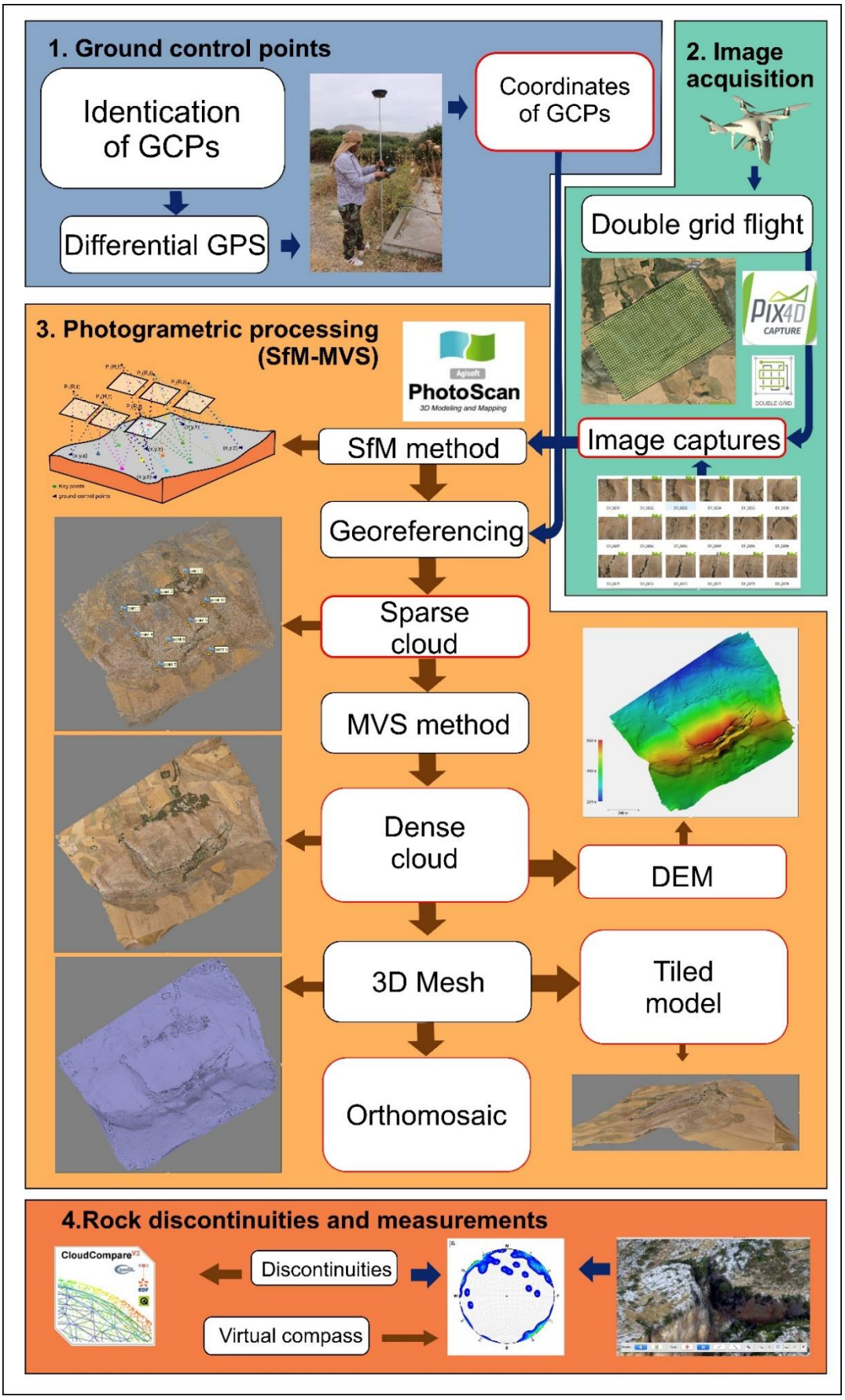

Figure 5-6 : Flow diagram of the UAV survey, 3D model production, and discontinuity investigations

We applied the conventional workflow with the following steps, in this order: (1) preliminary image selection and alignment; (2) import GCPs as markers, georeferencing and automatically allocated markers due to image matching by the scale invariant feature transform (SIFT) operator (Lowe, 1999); (3) manual marker matched in each image; (4) alignment optimizations, refinement that obtained a sparse cloud from tie points (SfM); (5) construction of a high-quality 3D dense-cloud with 107 million points (Point density: 47 points/m^2; Point spacing: 14.6 cm) and Mesh generation and refinement using a par depth map (Arbitrary 3D) and Multiview Stereo (i.e., Fast method; (Semyonov, 2011)); (6) building a DEM with a 16.4 cm/pix resolution and tiled model based on the dense cloud; and (7) deriving an orthomosaic with 8.19 cm/pix resolution.

It is worth noting that there is no high-resolution topographic information in the study area to compare with and validate our results using photogrammetry. The most precise topography available for this region is a 1:25,000-scale topographical map. To evaluate the accuracy of our results, we first compared the produced orthoimage with the high-resolution imagery available through Google Earth™. Secondly, we checked the elevation with a DEM generated using contours and elevation points extracted from the 1:25,000-scale topographical map. Third, we evaluated the 3D model comparing our measurements in the field with those taken in the virtual environment. We verified that our 3D model, orthoimage, and DEM fit the mentioned data.

3.2 DInSAR Analysis

We carried out DInSAR analysis by taking advantage of a powerful SAR image-processing tool implemented in a web platform of the European Space Agency (ESA). This tool is the Parallel Small Baseline Subset (P-SBAS) processing service of the Geohazards Exploitation Platform (GEP) (Casu et al., 2014; De Luca et al., 2015; Manunta et al., 2019). We selected from this platform SAR images with a descending orbit, as the corresponding geometry proves most adequate to obtain sound results for the Chgega landslide. The landslide is moving towards the NW and the Line of Sight (LOS) of the satellite has roughly the same orientation.

We processed 24 Sentinel-1A images acquired between 15 April 2015 and 19 January 2020 (4.7 years) by means of a multi-temporal method. The mean temporal sampling was 70 days, the coherence threshold was set at 0.95, and the reference point was situated 3 km away from Chgega Mountain at the following coordinates: Latitude 36.92511, Longitude 9.5369546 (WGS84 projection).

Before the aforementioned multi-temporal analysis, we ran several preliminary processing trials with the following objectives: to check if the slope was in motion in the analyzed period of time and if so, to know the approximate velocity of the movement, and finally, to fine-tune the processing. When we found that Chgega landslide appeared to be in motion but at a very-low velocity (because we were able to recognize the pattern of the movement, but below the common error range of this kind of analysis with Sentinel-1 images (i.e., ±5 mm/yr)) we decided to increase the precision of our measurements through two strategies: (1) selecting a reference point close to the landslide that showed great coherence and stability; and (2) defining a high coherence threshold. Thus, we reduced the error range to ±2 mm/yr, increasing the sensitivity of our analysis.

The rapid processing performance of GEP was well suited to make these adjustments. We checked different numbers and combinations of images in order to improve the quality of the results. SAR image processing was performed in the cloud, without downloading SAR images and no need to own specific software to perform the image analysis. This greatly facilitated our work.

The results provided by GEP conformed a CSV table with information about the location of the measured points, the mean velocity in the analyzed period, and a time series of displacements. Velocity and displacements are referred to the satellite LOS direction. The velocity of this movement may be underestimated owing to the different geometry between the acquisition of the satellite and the general direction and orientation of the movement. Therefore, we estimated an approximation of the real velocity through the Vslope method that transforms LOS velocity to the velocity along the slope(Notti et al., 2014). The difference between those two types of velocities was found to be below a tenth of millimeter per year in the case of Chgega landslide. Therefore, we used the LOS velocity as a good approximation of the real velocity. We also obtained time series to identify accelerations in the movement related to rainfall or seismic shakes, so as to constrain what kind of phenomena might trigger or reactivate the mass movement. However, the precision of the measurements with regard to the velocity of the movement was insufficient to detect temporal correlations with those phenomena.

The reliability of the InSAR results was checked by trying different values in the processing parameters and different SAR images, discovering that the displacements appear in all cases. Furthermore, InSAR techniques and the GEP platform have already demonstrated reliability in their results through a test period of 6 years (https://geohazards-tep.eu, accessed on 31 April 2021). We are moreover convinced of the active movement of the landslide because of field evidence pointing to displacements, e.g., open gravity-induced joints with a fresh appearance.

Indeed, we were surprised by the slow motion of the landslide, having expected a greater velocity according to the features observed in the field.

3.3 Geological Study Taking Advantage of Cutting-Edge Techniques

As mentioned above, we carried out a detailed geological and geomorphological field survey taking structural measurements and describing outcrops and landforms. In addition to that classical work, we took full advantage of the UAV-DP products (3D model, DEMs, orthoimages, aerial photographs) to derive and extract useful data for a comprehensive description of the Chgega landslide. Accordingly, we complete our in-situ structural data with measurements taken in the 3D model using the virtual compass implemented in the Cloud Compare open-source software (https://www.danielgm.net/cc/, accessed on 10 May 2021). This tool was used (manually) to measure the orientation of planar surfaces mostly related to rock discontinuities (Thiele et al., 2017). The high resolution DEM and the orthoimage produced using the UAV-DP techniques served to take planimetric measurements and accurately map structures, gravity induced joints, and landforms using QGIS v. 3.10. In this sense, we developed a detailed study of the landslide displacement orientation in order to understand, in depth, the nature of this slope movement. Vectors were generated taking into account the joints opened to extract the orientation and magnitude of the movement in each sector of the landslide.

Figure 7 outlines the procedure used to calculate the mean vectors of movement. First, we recognized rock corners in the two margins of the joints that matched perfectly, and we measured the azimuth of the line connecting these corners. Second, we measured pairs of azimuths in complementary joints where clear corners were not present. These azimuths were those of the lines perpendicular to the joints. The mean azimuth of these lines marks the azimuth of the joint opening in this case. We measured discontinuities with openings clearly recognizable in the orthoimage (resolution: 8.19 cm/pix). The aperture is generally of more than 50 cm.

To grasp the big picture and gain a more complete understanding of the Chgega landslide setting, we also performed analyses of the Chgega's region relief. In this regard, we analyzed the topography and drainage network of the area through morphometric tools applied to a regional DEM derived from the 1:25,000-scale topographic map. We calculated the bulk erosion and local relief to compare the characteristics of the landscape surrounding Chgega landslide with those of the adjacent areas having the same rocks, noting the singularities of the place where the slope movement developed.

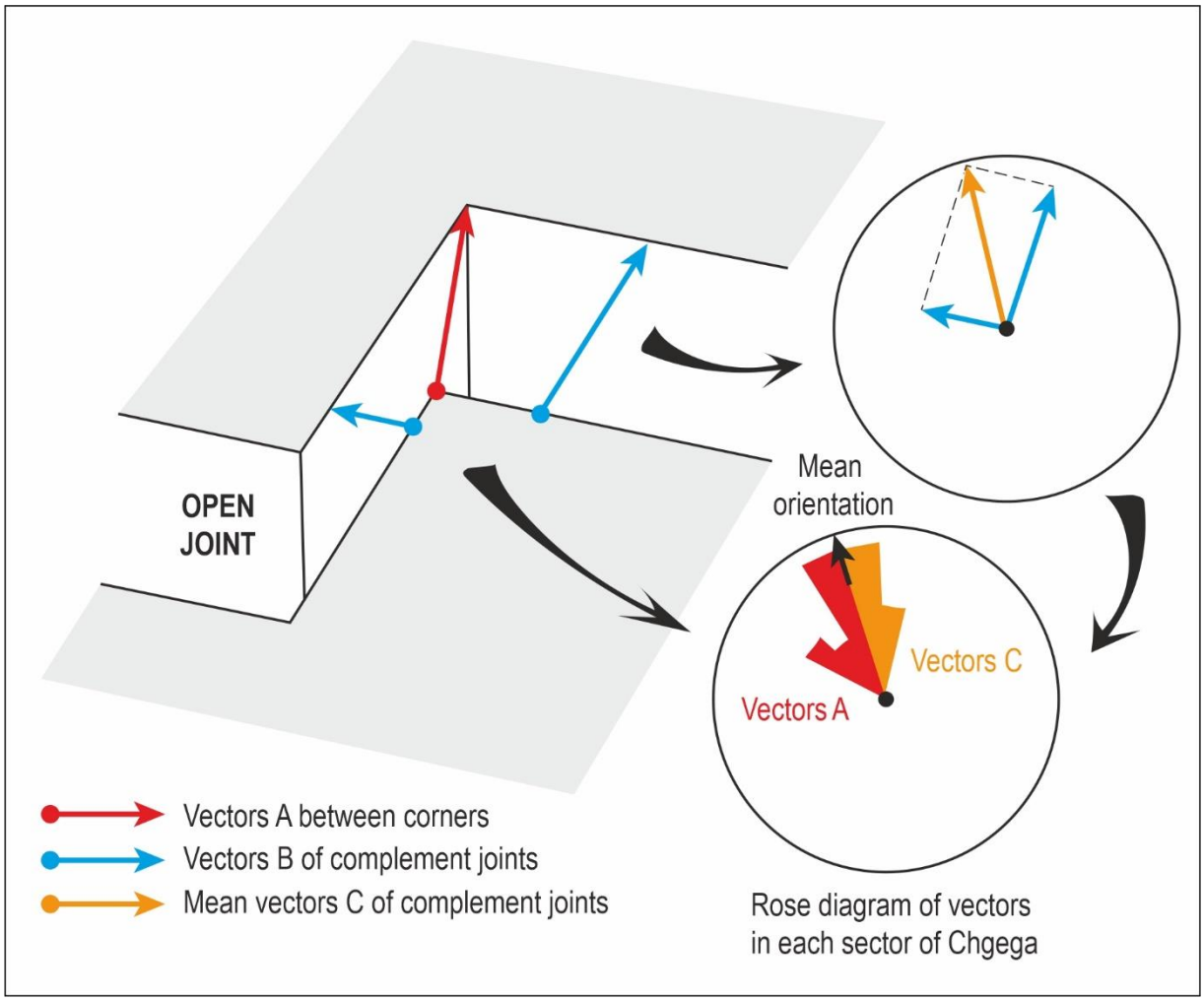

Figure 5-7: Graphic explanation of the measures taken in the open joints of Chgega and the data treatment performed. According to the scheme, we measured two types of vectors, A and B. Vectors A point out the orientation of the movement but they are scarce. To analyze more information, we added vectors B to calculate vectors C, which are an approximation of the orientation of the movement. Finally, we calculated the A and C average vectors in each sector of the mass movement.

4. Results

4.1 Geomorphology and Classification of the Chgega Landslide

The Chgega Mountain is impacted by a landslide that entails a large block of limestone from the Garia Formation, some 900 m long and 400 m wide, sliding over marls and clays of the Haria Formation. The lateral margins of this block are defined by several faults with N140°E direction that cut the Garia Formation in this sector. In turn, a N060°E normal fault puts the front of the moving limestone block in direct contact with the Haria Formation, allowing movement of the block downhill. In its current situation, the rigid limestone block can therefore push against the clays, deforming them. This plastic deformation explains the slight bulge observed in the Haria outcrop at the base of the mountain (Figure 5.8).

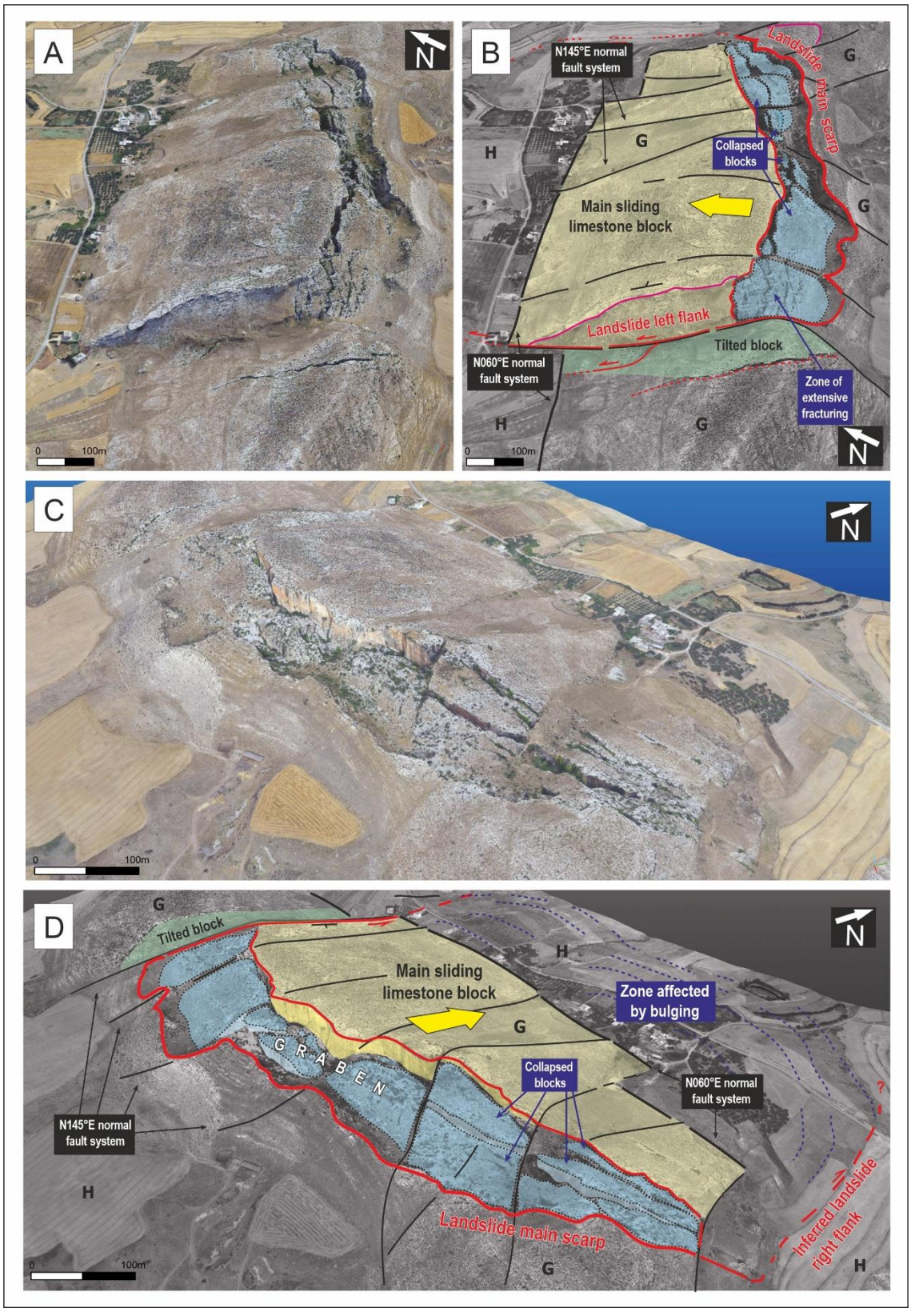

Figure 5-8 : Virtual oblique aerial views of Chgega landslide from the Southwest (A,B) and from the East (C,D). The main morphological features of the complex landslide and the geological structures are highlighted in B and D. G: Garia Formation; H: Haria Formation.The views were generated using the 3 D model produced by means od SfM methods.

The lateral movement of the limestone block produces a graben in the upper part of the relief. The graben forms a closed depression ~800 m long and ~120 m wide; its maximum depth is estimated to coincide with the Garia Formation thickness (~60 m (Rouvier, 1977)) (Figures 5.8 and 5.9B,C). The elongation of the graben follows a N060°E direction and has a slightly curved geometry. Its boundary in the NW sector is sharp, coinciding with the limits of the limestone block. A scarp (neither clear nor regular) limits the other side of the graben. Inside the graben are several limestone blocks having decametric to metric dimensions. These blocks are tilted towards the NW, giving an overall impression that they have collapsed into the graben or toppled within it.

Rockfall deposits, open joints, small rock pinnacles, and a ruiniform relief occupy the interior of the graben (Figure 5.9A–C). At the bottom of this landform there are cavities as well. The cavities are probably not of karstic origin, because they show angular sections and speleothems are not present. They can be considered as crevice caves that formed in large slope movements favored by the progressive opening of fractures (Figure 5.9E) (Halliday and McKelvey, 2004; Lenart et al., 2014). At either end of the graben the rock mass shows a complex network of open and deep fractures, finishing in the lateral faults that limit the main block of the mass movement (Figure 9D,F–H,K). All joints have directions of N040-060°E and N140–150°E (Figure 5.10) corresponding to the main discontinuity sets observed elsewhere in the Garia Formation (e.g., (Erraioui, 1994; Redhaounia et al., 2015); Figure 5.9A,I,J). Initially, these discontinuities correspond to joints inherited from the subsequent tectonic events affecting Northern Tunisia. Thus, a simple explanation for the opened cracks is that they represent reactivated joints during Chgega mass movement.

Figure 5-9 : Photographs of various sectors of the Chgega Mountain. (A) Open joints in the southwestern sector. (B) Deep trench in the northeastern sector. (C) Interior of the gravity-induced graben where tilted blocks and rockfall deposits are observed. (D) View of a deep open fracture from its bottom. (**E**) Entrance to crevice-type cavities. (**F**) Rock walls forming the boundary of the graben. The center cliff is formed by fault breccia. (**G**) Slickenside cropping out in the graben. (**H**) Deep open fracture in the eastern sector. (**I**,**J**) Main discontinuity sets observed in the Chgega Mountain. (**K**) Narrow passage through an open fracture.

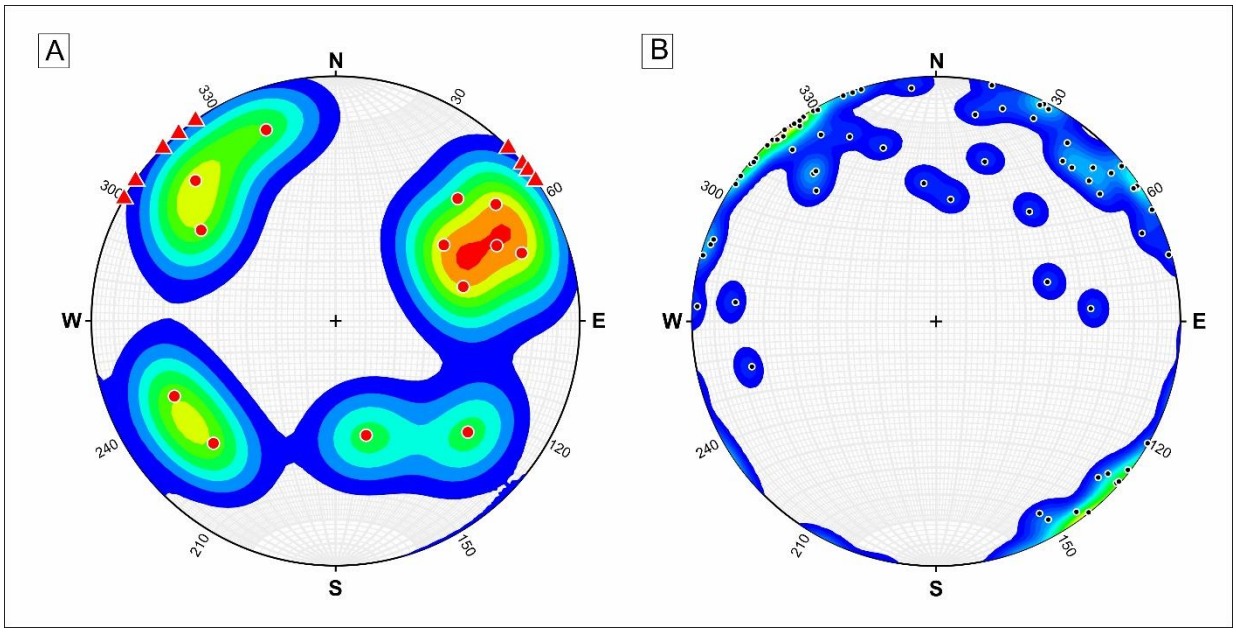

Figure 5-10 : Stereonets of the main rock discontinuities observed in the Chgega Mountain (pole faults in cir-cle and joints in triangle). The diagrams were elaborated on the basis of field measurements (A) and virtual measurements using a compass (B).

All the aforementioned characteristics indicate that the Chgega landslide can be classified as a "complex landslide" including a "rock planar slide" or a "block slide" according to the classification of (Hungr et al., 2014); and the upper part of the landslide can be described as a "lateral spreading" based on the Pasuto and Soldati descriptions (Pasuto and Soldati, 1996, 2013). Combining the mentioned classifications and also the "block slide" concept of (Ibsen, 1996), Chgega can be described as a "lateral spreading that evolves into a block slide".

4.1 Relief Conditions for the Chgega Landslide Occurrence

The relief of the Chgega region can partially explain the occurrence of the landslide. Our geomorphological analysis shows that the Chgega Mountain is located in the divide between the Joumin and Tine River basins, being the highest peak along this divide. Moreover, the slope impacted by block slide shows a highest local relief along the mentioned divide (Figure 11A) and the mountain flank of the river basin, where fluvial erosion processes have been more intense (Figure 5.11B). The ongoing erosion of the Joumine River comes just to the foot of Chgega Mountain, creating higher gradients on the NW side of the range than on the SE side. This condition, together with the geological structure of the Chgega Mountain, has generated an unfavorable situation for the relief's stability, promoting its sliding. For the same apparent reason, mass movement developed SW of Tahint (Figure 5.11A,B), where the gradient and the local relief are likewise steeper than in the surroundings.

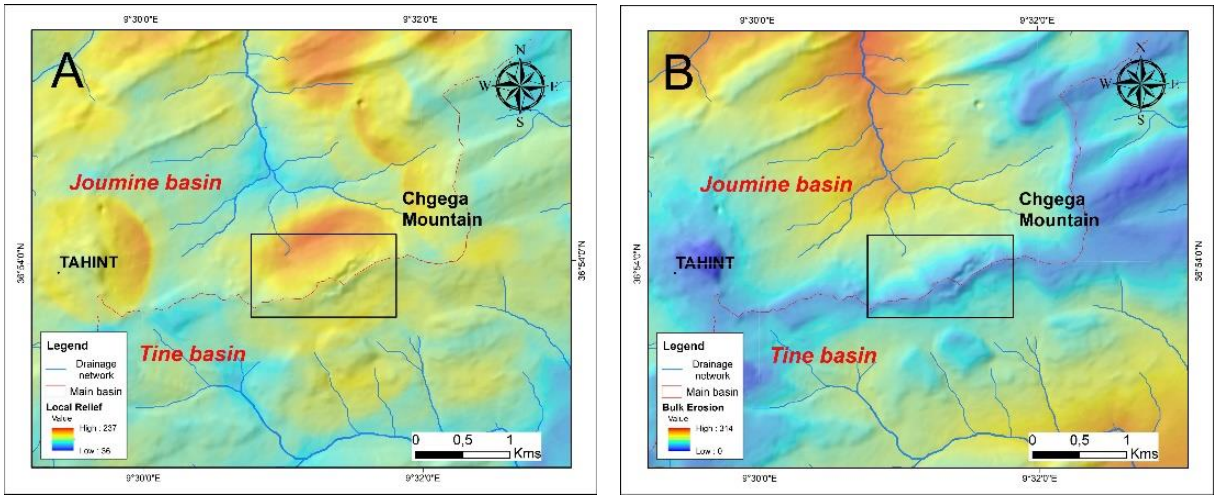

Figure 5-11 : (A) Map of the local relief of the Chgega surroundings. Local relief was calculated estimating the elevation range at 500 m of each point of the terrain. Note that Chgega shows the highest values in the ridge that define the limit be-tween the Joumine and Tine River basins. (**B**) Map of the bulk erosion volume (proxy for maximum potential erosion) of the Chgega surroundings.

4.3.Kinematics of the Chgega Landslide Derived from Open Joints

Regarding the kinematics of the landslide, the recent displacements recorded by the present open joints have a mean azimuth of 333° (Figure 5.12). This orientation is similar to the general one of the hillside, about 315–330°. However, we observe a slight decoupling between the orientation of the line of maximum slope and the mean vector of displacement. For this reason, we measured a mean displacement vector in the SW sector of the landslide oriented towards 340°, where the mean orientation of the slope is 310° (Figure 5.12B–D). This difference decreases towards the NE. In the northwestern sector of the graben, the opening of the joints indicates a movement oriented according to the line of maximum slope. In sum, the displacement has an orientation different than originally expected (Figure 5.12).

Associated with the landslide and adjacent to it is another block of limestone, limited by an open and deep fracture with a N140°E direction that evidences the rupture and slide of that block, probably triggered by the displacement of the main Chgega landslide. This could be considered a secondary failure. This block does not accompany the mobilized mass and its destabilization appears to be more recent. The measurements taken at the main joints indicate a movement towards 47° that does not match the orientation of the displacement in the main body of the Chgega landslide (Figure 5.12).

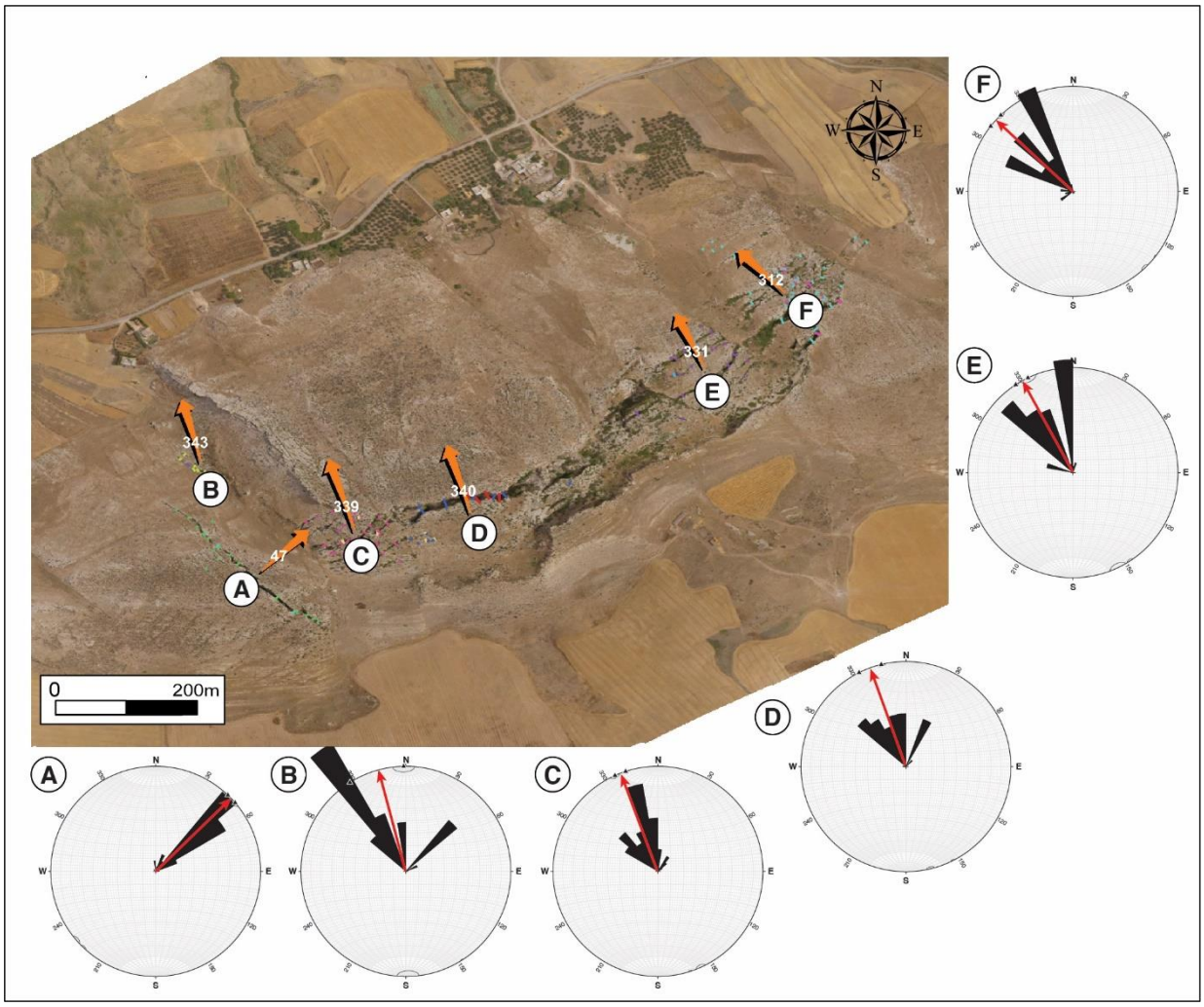

Figure 5-12 : Rose diagrams and orientation of the mean movement vectors for each sector of the Chgega landslide obtained through analysis of the open joints.

4.4 Estimated Velocity of Chgega Landslide by InSAR

Regarding the present displacements estimated with InSAR techniques, we show that the velocity of the slope movement is in the limit of our DInSAR analysis sensitivity. We set a very high coherence threshold (95%) in order to enhance the accuracy of our measurements, reducing the error range to 2 mm/yr. This means that we cannot recognize movements with velocities below 2 mm/yr. The maximum LOS velocity measured in the landslide is 4 mm/yr, while many points are just above 2 mm/yr and some are below this value. The pattern of the measured velocities seems to indicate that the entire limestone block is moving but at a very low speed, just above our measurement accuracy (Figure 5.13). The total LOS displacement during 4.7 years was on average ~1 cm, almost unnoticeable. The magnitude of the movements is so low that the temporal variations observed in the time series cannot be defined as accelerations or reductions of the displacement rate, being within the error range (Figure 5.14). Therefore, we lack sufficient

accuracy in the actual measurements to link the movements with triggering factors such as rainfall or seismic events.

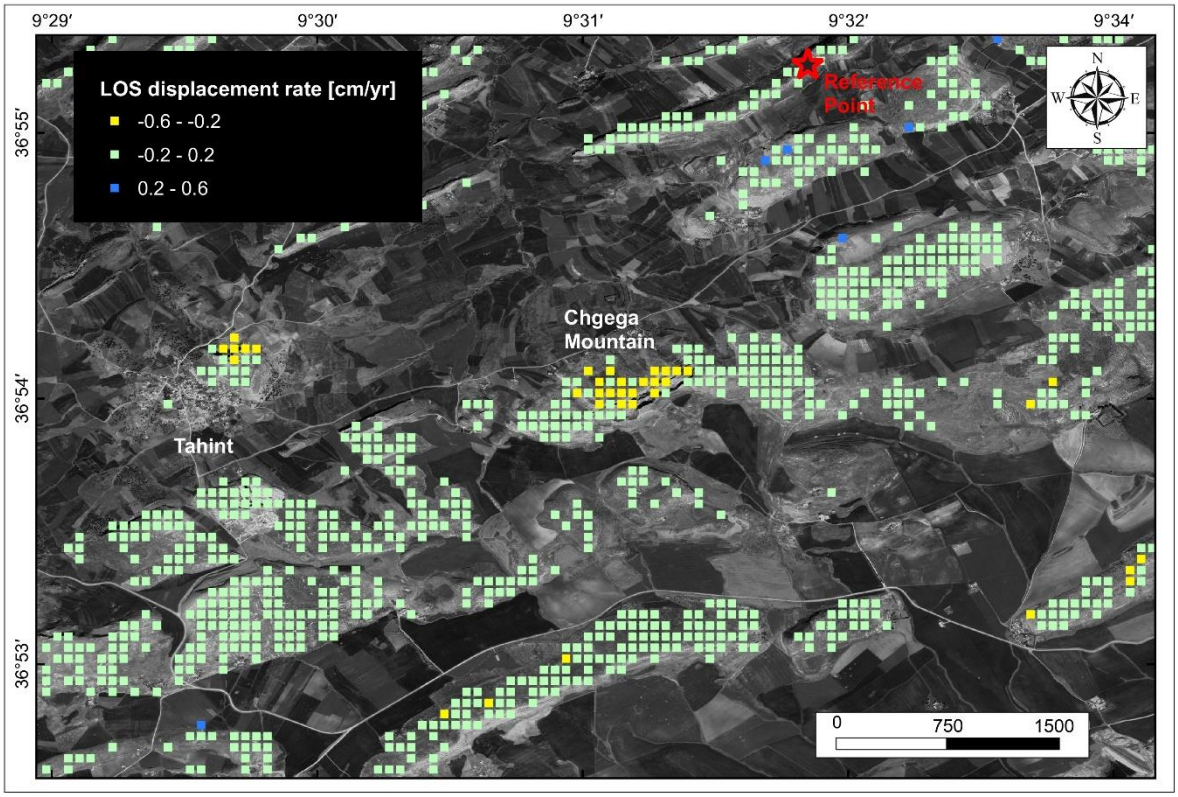

Figure 5-13 : LOS velocity map of the region of the Chgega Mountain using DINSAR. Note the movement detected in the Chgega landslide and in the northern slope of the hill adjacent to Tahint village.

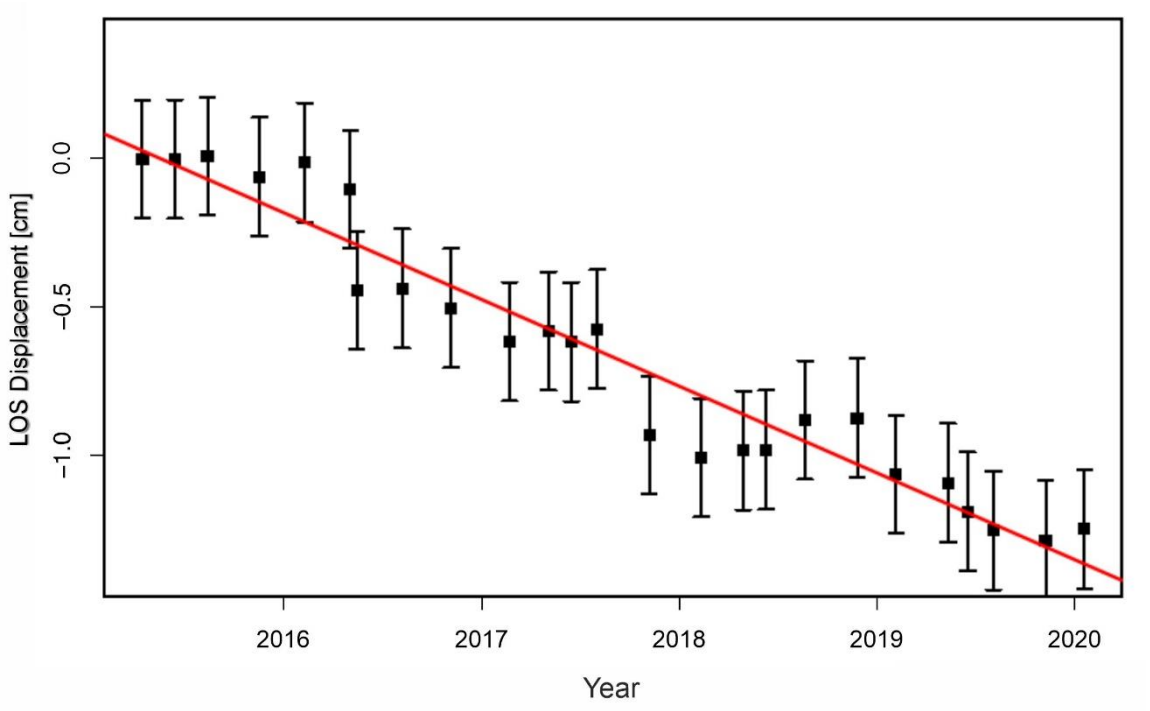

Figure 5-14 : Time series of LOS displacement in the Chgega landslide.

5. Discussion

5.1 Relationship between Chgega Landslide and the Geological Structure

The area where the Chgega landslide is located presents a hilly landscape configured by NE-SW trending bands of clays and marls of the Haria formation and limestones of the Garia Formation. The former form valleys and the latter form ridges. These alternations are due to the interference of two different types of structures (earlier NE-SW trending folds and more recent normal faults) that cut the series parallel to the previous fold axes (Cohen et al., 1980). The bands are further cut by a system of NW-SE trending normal faults. Finally, all these structures are cut by WNW-ESE to NW-SE dextral fault segments of the Dhkila fault´s northwestern splay termination (Figure 5.2). The lithologies cropping out in the area, along with all these faults and folds, clearly determine the development of the Chgega landslide. First, the common configuration of rock spreads described by Pasuto and Soldati (Pasuto and Soldati, 2013) is present: rigid rock masses (Garia Formation limestones) cap ductile terrains, such as clays and the marls of the Haria Formation (Bejaoui et al., 2017) (Figure 5.15). Second, the activity of the NE-SW normal fault system cut and tilted towards the NW the previously folded Garia limestone unit, producing the currently unfavorable conditions of slope instability, with the bedding inclined parallel to the hillslope (Figure 5.15). Third, these blocks are also configured by a different transverse set of NW-SE faults that appear to guide the movement of the main block. This block shows a motion towards 330° in correspondence with the N145°E direction of the mentioned faults (Figure 5.12). Such an effect would explain the decoupling between the line of maximum slope and the movement orientation inferred from open joints, as observed in the SW sector of the landslide.

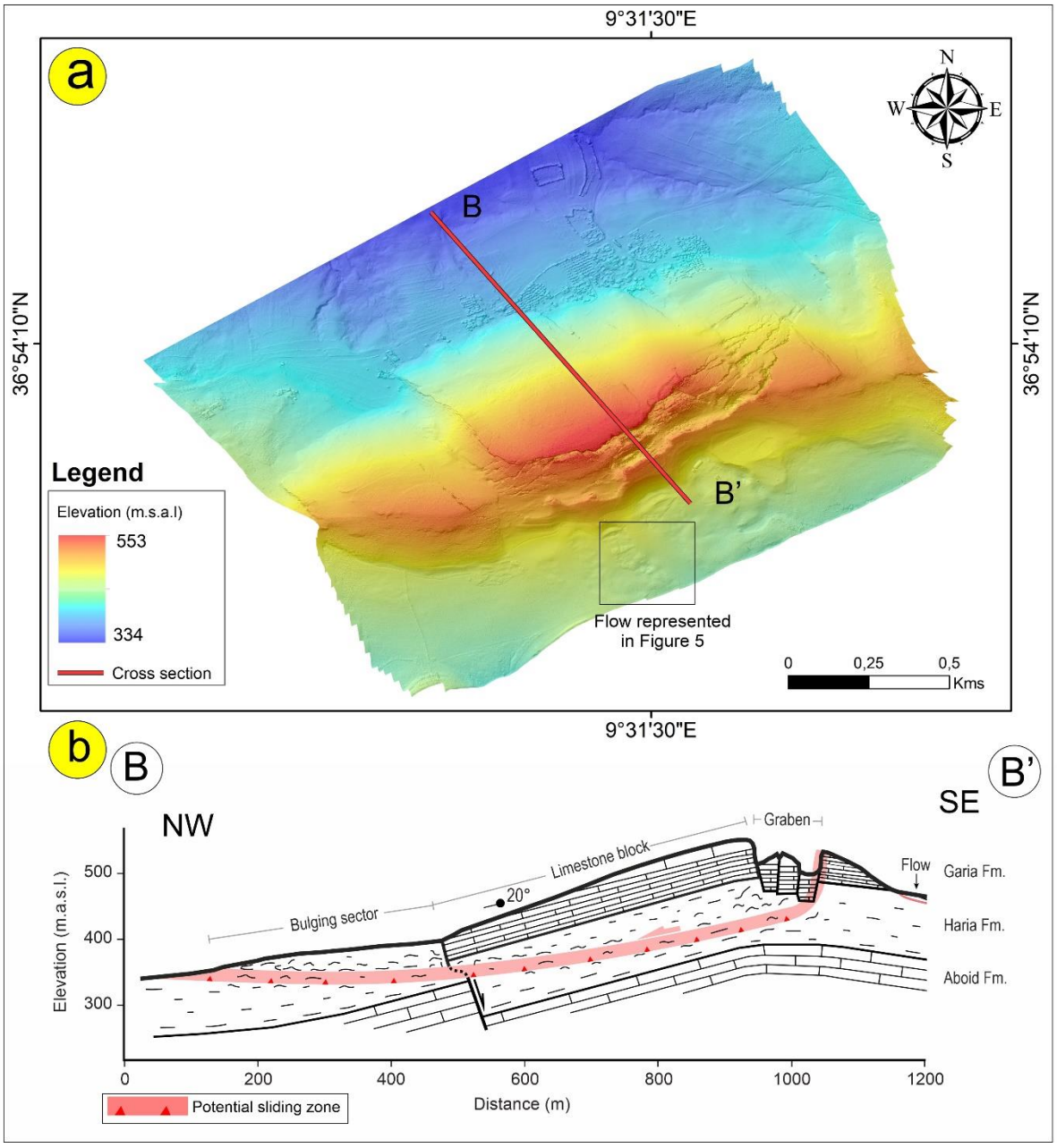

Figure 5-15 : (a) High resolution DEM generated using UAV-DP technique and (b) BB' detailed cross-section showing the Chgega Mountain.

We infer that the viscoplastic creep of the clay terrains of the Haria Formation subjacent to the limestones with 20° dip to the NW permitted the lateral expansion of the latter, creating the large graben in the landslide crown as well as the bulge at its two typical features of rock spreading according to (Pasuto and Soldati, 2013) (Figure 5.15). The failure plane would accordingly be located inside the Haria Formation and may crop out alongside the boundary of the bulge observed in the landslide toe (Figures 5.8 and 5.15). Therefore, it appears that (1) the soft terrains of the Haria Formation are the ones that have failed; (2) their movement caused the

fracturing process of the Garia limestone, producing the graben of the landslide crown and the individualization of a large limestone block; and (3) this limestone block was initially set in motion, i.e., dragged, by the underlying clay and marls to eventually become part of the slide mass (Figure 5.15).

Punctual events or periods of extreme rainfall often trigger or reactivate this kind of mass movement. The consulted paleoclimate data (Paskoff and Sanlaville, 1986; Brun, 1989; Leveau, 2012) indicate that the general climatic conditions prevailing were more humid than at present, a factor that may play a key role in the activation of the Chgega landslide. Yet neither this information nor our InSAR time series can demonstrate a direct relationship between precipitation and the Chgega landslide occurrence. On the other hand, (Gaidi et al., 2019) suggested there may be a relationship between the seismicity of the Dhkila fault and the initial opening of the Chgega joints. This is actually not a far-fetched hypothesis, because the map of (Soumaya et al., 2016) (Figure 5.4) demonstrates that the Chgega landslide is in a high seismic hazard region, surrounded by active faults, the closest being the Dhkila fault. Hence, the main open-fracture system bounding the landslide coincides with the directions of the Dhkila fault segments, having open tension joints trending N30–60°E, parallel to the direction of reverse faults and folds affecting Quaternary sediments in the region. These open joints are moreover linked by sinistral N130–150°E fractures, parallel to the main dextral Dhkila fault segments (Figure 2). Further research is needed to correlate the landslide origin with the regional

5.2 Motion Detected in Chgega and in Other Similar Landslide

The Chgega landslide has been moving at a little more than 2 mm/yr under the climatic conditions of the analyzed period (2015–2020). Although this is an extremely low velocity, it is in accordance with the velocities measured for other similar landslides, as for example, (Crosta et al., 2013) reported in the Alps. These authors show that most (75%) of the DGSD analyzed had a velocity below 5 mm/yr. Specifically, DGSDs developed in a geological setting similar to Chgega, with carbonate units overlying soft terrains, also show extremely slow motion. (Delgado et al., 2011) measured by InSAR rates resembling that of Chgega (2–4 mm/yr) in a compound rotational DGSD of large dimensions in the Sierra de Aitana (Spain).(Mateos et al., 2018) reported an average velocity of the same order of magnitude (5.2 mm/yr) in a large lateral spreading along the North coast of Majorca (Spain). Extensive lateral spreading and block sliding processes in a geological setting comparable to the Chgega landslide have been under investigation since 2006 in the North part of Malta (Mantovani et al., 2013, 2016; Soldati et al., 2019; Devoto et al., 2020, 2021). In this area, long-term differential GNSS monitoring outputs carried out gave displacement rates between 0.8 and 2.4 cm/yr in a limestone plateau affected by

lateral spreads and downslope blocks moved from block slides (Mantovani et al., 2013). InSAR analysis of ERS and Envisat satellite images covering a 20-year period measured, in the same area, velocities of less than 7 mm/yr (Mantovani et al., 2016). A comparison of our InSAR results with those of the cited studies confirms that the extremely slow motion identified in the Chgega landslide is not unusual for mass movements of its kind. Further research on Chgega, in greater detail, is required to determine if the observed motion is constant or if it changes due to external factors.

5.3 Significance of the Chgega Landslide

The Chgega landslide is an important spot for the landslide scientist community because it shows a paradigmatic rock spreading process in its crown. This type of landslide can be easily understood in places like Chgega given its dimensions and the fresh appearance of its morphological features. Good outcrops (that is, easily recognizable ones of convenient access) can be key to controlling movement magnitudes; such features make Chgega a potential natural laboratory for the study of these phenomena.

Chgega could also be a key place to analyze paleoseismicity in northern Tunisia. For this reason, the study of the relationship between this landslide with earthquakes must be addressed, as has been done in other DGSD (see, for example, the research of (Gutiérrez et al., 2008) in the Pyreness). New detailed analyses putting the focus on the recognition of features that evidence some participation of seismic shaking in the origin and in the displacement of the complex landslide must be developed. Once these features are found, their study using geochronological methods could offer useful information about the earthquake recurrence in a given region.

As we brought out in the “Introduction” section, significant rock spreading phenomena tend to become symbols for local cultures, and some of them have become geosites. In our opinion, Chgega is a sound candidate for geosite status. In addition to all the characteristics mentioned above, Chgega is interesting from an ecological viewpoint, since the graben creates local conditions permitting the presence of particular plant and animal species. It stands as a refuge for species not well adapted to the arid environment of the region and offers nesting cliffs for diverse raptors. The cultural significance of this place and the archaeological remains found there are likely to attract the attention of researchers in the near future. Chgega has many facets and all of them make it a special place deserving study and protection.

6. Conclusions

The Chgega landslide represents a spectacular example of a lateral spread that evolves into a block slide when a large block of limestone from the Garia Formation slides over the ductile clays and marls from the Haria Formation. For the presence of two different landslide mechanisms, this large landslide can be also classified as a complex landslide. The most prominent gravity-induced landform is a large graben ~800 m long and ~120 m wide that breaks the summit of the Chgega Mountain creating a double ridge. This landslide is currently active and shows a progressive movement without clear episodic accelerations. InSAR measurements show extremely slow speed, just above 2 mm/yr, with maximums of 4 mm/yr. The movement has an orientation towards 333° of azimuth; it is conditioned by the geological structure of the Chgega Mountain and more specifically by the normal faults with directions N060°E and N140–150°E that crosscut it. The latter fault system appears to guide the displacement of the main rock block. Further investigations are needed to elucidate why this large-scale movement was produced in a region of low relief and to determine the relationship between the landslide itself and the overall seismic activity of the region. Moreover, the presence of this large graben and several cavities make it a good candidate for becoming a geosite. The 3D model developed for this study could be used in future geological and paleoseismological investigations as well as to explain and divulge the unique landscape created by this large landslide.

Chapter 6: Discussion and Conclusion

6.1 Discussion:

The discussion is planned as a tentative synthesis of the observations made through this dissertation, discussions of the important ideas presented in the different sections mainly about extensional collapses, salt structures, active faulting and landslides. Thus, we aim to summarize some new developments on the tectonic model for Northern Tunisia, including the extensional collapse in the late Miocene and later Pliocene to Present tectonic inversion and its influence in the present topography and drainage network under continued convergence across the region. In addition, an example of a complex landslide is studied and discussed through this dissertation. These results are issued and improved collaborating with numerous specialists, which co-authored the multi-disciplinary papers presented exclusively in this *PhD* volume.

6.1.1 Late Miocene extensional collapse:

The new data and structural interpretation we published in Booth-Rea et al., (2018) contrasts with previous work where the tectonic evolution of northern Tunisia was mostly described in terms of the shortening and transcurrent structures developed under NW-SE convergence between Africa and Eurasia since the Paleogene, in an external foreland thrust belt setting (Zargouni.F, 1984; Frizon De Lamotte et al., 2000; Mzali and Zouari, 2006; Melki et al., 2010, 2012; Essid et al., 2016). We describe an important extensional phase that thinned the Tell fold and thrust belt. Extension was coeval to topographic uplift, K-Si rich magmatism and mineralization in Northern Tunisia, which we relate to continental lithospheric mantle delamination under the region, as proposed by Roure et al. (2012). Extension was polyphasic, with a first NE-directed extensional phase, followed by later S-SE directed extension during the Messinian. Normal faults in Northern Tunisia were alternatively interpreted as subsidiary structures formed under SW-NE extension during the Pliocene-Quaternary or as very shallow extension affecting the Numidian units, related to FTB dynamics (Bouaziz et al., 2003; Khomsi et al., 2009; Belguith et al., 2011, 2013; Ramzi et al., 2015; Khelil et al., 2019). The importance of Late Miocene extension had also been described by Cohen et al. (1980). This extension propagated towards the SE in the Plio-Quaternary being described in the Sicily

Channel and in Central Tunisia (Tricart et al., 1994; Belguith et al., 2011, 2013; Arab et al., 2020; Dhifaoui et al., 2021).

-There is a diachrony between extensional and shortening structures, since extension in Northern Tunisia occurred in the late Miocene, approximately between 9 and 5.3 Ma, after the main thrusting event, which in turn, occurred in the Early to Middle Miocene (i.e. 17-13 Ma), (Sami et al., 2010; Belayouni, 2013) and later propagated south-eastwards during the late Miocene to Present (Bouaziz et al., 2002; Saïd et al., 2011a, 2011b). These results published for the first time in Booth-Rea et al (2018) were contested by Khelil et al. (2019) proposing a simultaneous shortening and extension, leading to an interesting scientific discussion published in the Journal of Structural Geology: Booth-Rea et al. (2019) published as comment and Khelil et al. (2020) as reply. This discussion formed an interesting debate resulting in further research programs for both teams.

We describe two orthogonal extensional systems with extension parallel and transverse to the main direction of shortening. The older system with NE-SW directed extension, rooted in an extensional low-angle normal fault that detached in Triassic evaporites at the base of the Infra-Numidian thrust sheet. Meanwhile, the later extensional system, with mostly N–S to NW-SE directed transport cut deeper into the thrust stack, affecting the older low-angle normal faults and exhuming the autochthonous Atlas domain.

Triassic sheets located above the autochthonous Atlas domain in Northern Tunisia generally correspond to the base of the allochthonous infra-Numidian nappe, instead of being diapiric-related bodies coming from the base of the Atlas sedimentary sequence. These rocks were originally thrusted over the Atlas domain during the Early to Middle Miocene thrusting and have later been reworked by extensional structures. This is probably the case of the Triassic sequence drilled in the Mejerda-1 borehole (Troudi et al., 2017).

6.1.2 Halokinetic structures and extensional exhumation in Northern Tunisia

In the manuscript Gaidi et al. (under correction), we present new structural, mineralogical and geophysical data interpretation for the Tell and Atlas FTB´s of Northern Tunisia. The combination of X-Ray analysis allowed us to determine the illite crystallinity of different metapelite samples from Triassic bodies in Northern Tunisia, together with structural analysis in the field, and the interpretation of multichannel reflection seismics to revise the supposed diapiric structure of the region.

The results show the presence of very-low to low-grade metamorphic rocks in the Atlas and Tellian belts of Northern Tunisia. Anchizonal metamorphic conditions are reached by Triassic

pelites at the base of the Tellian nappe stack. Moreover, we find exhumed epizonal rocks in the core of three domal structures in Northern Tunisia, underlying well-imaged Late-Miocene extensional detachments. Although, the presence of low-grade metamorphic marbles is well known since roman times both in the Ichkeul and Hairech massifs (Röder, 1988; Bugini et al., 2019; Khelil et al., 2021), no previous study has described the petrology of these rocks, no proposed an explanation for their occurrence. Thus, the integration of our new data with previous results from other FTB´s in the Western Mediterranean permit us to propose a new tectonic paradigm for Northern Tunisia, where extensional tectonics exhumed rocks from mid crustal depths of the FTB, having undergone temperatures above 300 ºC. These data, together with the existence of anchizonal rocks at higher structural levels of the thrust stack suggests that the original nappe structure was thicker than presently preserved, and strongly modified by later extensional tectonics as proposed by Booth-Rea et al. (2018; 2019).

Two main types of Triassic outcrops are identified, the shallower of which, develop halokinetic structures related mostly to the late Neogene extensional phase, and the deeper ones are represented by exhumed middle crust formed by autochthonous epizonal Triassic red beds and marbles. The interpretation of seismic lines shows that many of the halokinetic structures are rooted in the Triassic material overlying low-angle extensional faults and detachments, which was originally emplaced at the base of overthrusted nappes (Troudi et al., 2017) and later extended. The shallower Triassic outcrops had been alternatively interpreted as “salt glaciers” (Vila, 1995; Ghanmi et al., 2001; Vila et al., 2002; Masrouhi et al., 2012, 2014), whilst the deeper Triassic outcrops where previously interpreted as diapiric domes (e.g. (Bolze, 1950; Perthuisot, 1978; Perthuisot et al., 1998; Jallouli et al., 2005; Benassi et al., 2006).

The proposed interpretation data support an alternative tectonic mechanism to diapirism and protracted shortening since the Cretaceous in Northern Tunisia proposed by previous authors (Perthuisot, 1981; Vila, 1995; Bedir et al., 2001; Ben Chelbi et al., 2006; Melki et al., 2010, 2012; Ayed-Khaled et al., 2015; Troudi et al., 2017) , which corresponds to Late Miocene crustal extension of a previously over thickened orogenic wedge. Late Neogene extension did favor the development of different types of halokinetic structures, above the main extensional detachments.

6.1.3 Active fault segmentation pattern

In the paper by Gaidi et al. (2020), we propose a new active fault segmentation pattern and evolution for Northern Tunisia combining structural geology field based data and morphometric results. We identify new active faults that influence the landscape of Northern Tunisia by cutting

drainage basins and affecting rock uplift rates. Previous fault segmentation patterns for Northern Tunisia assumed the main structures in the region, like the sinistral Alia-Teboursouk fault system, were active during most of the Tertiary after inverting Mesozoic or even Hercynian faults (e.g. (Perthuisot, 1974; Melki et al., 2011, 2012; Ayed-Khaled et al., 2015; Bejaoui et al., 2017). We, however, propose these shortening structures developed recently by tectonic inversion after a phase of Late Miocene crustal extension that strongly modified the Tell and Atlas Early to Middle Miocene foreland fold and thrust belts (Booth-Rea et al., 2018).

This process produced a Pliocene erosive post-rift unconformity that was later folded in the Late Pliocene to Present in Northeastern Tunisia. Many of the Pliocene to Present reverse faults are inverting previous Late Miocene normal faults. For example, along the southern Margin of the Jendouba basin and in the Mateur-Utique region to the East.

Most of the active shortening structures in Northern Tunisia developed since the Pliocene in a tectonic inversion phase that propagated from West to East, reaching Northeastern Tunisia in the Late Pliocene. Deformation observed on reflection seismic lines indicates deformation rates around 0.6-0.8 mm/yr in the studied segments and larger amounts of shortening to the West of Northern Tunisia (16%) than to the East (7%). The fault system accommodating plate convergence is strongly segmented with ENE-WSW to NE-SW reverse faults, E-W to NW-SE dextral faults and NNE-SSW sinistral ones. The individual fault segments range between 10 and 30 km long. The largest linked fault system is the Alia-Thibar fault zone that reaches a length of 130 km and includes at least five different fault segments with an overall helicoidal geometry.

The distribution of high ksn values and gridded Hi in the region strongly mimic the fault segmentation in Northern Tunisia, especially, defining the regions overlying reverse faults and related anticlinal ridges. Furthermore, both ksn and Hi maps show an East to West gradient in the degree of topographic dissection compatible with the increase in tectonic shortening and age of the inversion structures towards the West.

In some case the high ksn and Hi clusters occur headwards of fluvial captures and 90º deflections in the fluvial channels, indicating higher fluvial dissection in response to the development of transverse drainage. The landscape of Northern Tunisia is characteristic of a young fold and belt region with dominant axial valleys coinciding with the footwall of the main faults and/or along syncline structures. However, as proposed by Camafort et al. (2021), part of this W-E to NW-SE topographic dissection gradient may be related to dynamic topography due to negative buoyancy produced by an underlying lithospheric mantle slab body, still attached below the Sicily straits and parts of Central Tunisia (Booth-Rea et al., 2018).

This current young topography related to Pliocene-Present shortening in Northern Tunisia, in a convergent setting since the Cretaceous, indicates that Late Miocene extension completely dismantled the previous foreland thrust belt structure and associated topographic features. A process that resulted in a new SW-NE topographic gradient towards the main direction of extension and crustal thinning at the end of the Messinian. Tectonic inversion and development of new shortening structures accommodating NW-SE plate convergence in Northern Tunisia followed the trend observed at a larger scale in the western Mediterranean, with shortening propagating from central Algeria towards the East, from the late Miocene up to the Quaternary in the Tyrrhenian (Strzerzynski et al., 2010; Billi et al., 2011; Camafort et al., 2020; Zitellini et al., 2020; Leffondré et al., 2021; Loreto et al., 2021) , in a pattern symmetrical to tectonic inversion in the Betics-Rif and offshore areas of the western Algerian and Alboran basins (e.g. (Giaconia et al., 2015; Martínez-García et al., 2017).

6.1.4 Chgega Active Landslide

The Chgega Landslide represents a paradigmatic mass movement formed in a region with NE-SW trending bands of clays and marls of the Haria formation and overlying limestones of the Garia Formation. The former form valleys and the latter form ridges. These alternations are due to the interference of two different types of structures (earlier NE-SW trending folds and more recent normal faults) that cut the series parallel to the previous fold axes (Cohen et al., 1980). All these structures are cut by WNW-ESE to NW-SE dextral fault segments of the Dhkila fault´s northwestern splay termination (Gaidi et al.2020). The lithologies cropping out in the area, along with all these faults and folds, clearly determine the development of the Chgega landslide.

First, the common configuration of rock spreads described by Pasuto and Soldati (Pasuto and Soldati, 2013) is present: rigid rock masses (Garia Formation limestones) cap ductile terrains, such as clays and the marls of the Haria Formation (Bejaoui et al., 2017). Second, the activity of the NE-SW trending normal fault system cut and tilted towards the NW the previously folded Garia limestone unit, producing the currently favorable conditions for slope instability, with the bedding inclined parallel to the hillslope. Third, these blocks are also configured by a different transverse set of NW-SE faults that appear to guide the movement of the main block.

Therefore, it appears that (1) the soft terrains of the Haria Formation are the ones that have failed; (2) their movement caused the fracturing process of the Garia limestone, producing the graben of the landslide crown and the individualization of a large limestone block; and (3) this limestone block was initially set in motion, i.e., dragged, by the underlying clay and marls to eventually become part of the slide mass.

The Chgega landslide has been moving at a little more than 2 mm/yr under the climatic conditions of the analyzed period (2015–2020). A comparison of our InSAR results with those of others studies confirms that the extremely slow motion identified in the Chgega landslide is not unusual for mass movements of its kind. Further research on Chgega, in greater detail, is required to determine if the observed motion is constant or if it changes due to external factors.

The Chgega landslide is an important spot for the landslide scientist community because it shows a paradigmatic rock spreading process in its crown. This type of landslide can be easily understood in places like Chgega given its dimensions and the fresh appearance of its morphological features. Chgega could also be a key place to analyze paleoseismicity in northern Tunisia. For this reason, the study of the relationship between this landslide with earthquakes must be addressed, as has been done in other DGSD (see, for example, the research of (Gutiérrez et al., 2008) in the Pyrenees). Good outcrops (that is, easily recognizable ones of convenient access) can be key to controlling movement magnitudes; such features make Chgega a potential natural laboratory for the study of these phenomena.

Significant rock spreading phenomena tend to become symbols for local cultures, and some of them have become geosites. In our opinion, Chgega is a sound candidate for geosite status. In addition to all the characteristics mentioned above, Chgega is interesting from an ecological viewpoint, since the graben creates local conditions permitting the presence of particular plant and animal species. It stands as a refuge for species not well adapted to the arid environment of the region and offers nesting cliffs for diverse raptors. The cultural significance of this place and the archaeological remains found there are likely to attract the attention of researchers in the near future. Chgega has many facets and all of them make it a special place deserving study and protection.

6.2 Conclusion

The following final section presents a summary of the outcomes of the present dissertation:

- ✓ The Late Miocene extensional collapse in Northern Tunisia is characterized by extensional ENE- and SE-directed transport systems.
- ✓ The extensional structures in northern Tunisia are folded and cut by Pliocene to present contractional structures. The Plio-Quaternary shortening has reactivated the extensional faults into thrusts producing arrowhead tectonic inversion structures.

- ✓ The extension is driven by deep mantle mechanisms: (1) Tearing of the Calabrian mantle slab to the north of the Tunisian coast during the opening of the Tyrrhenian basin probably drove the Tortonian ENE-directed extension in northern Tunisia; meanwhile, (2) SE-directed extension could be related to the Late Miocene stripping of the African lithospheric mantle coeval to NW-directed subduction under northern Algeria and Tunisia.
- ✓ The extensional structures exhumed the deep autochthonous Triassic sediments in the footwall of extensional LANFs.
- ✓ Illite crystallinity shows that most of the Triassic outcrops in Northern Tunisia are made up by very low-grade metamorphic rocks that underwent epizonal or anchizonal conditions.
- ✓ The Late Miocene crustal extension of a previously over-thickened orogenic wedge is proposed as tectonic mechanism to explain the origin of some Triassic dome structures in Northern Tunisia, corresponding to ENE-WSW directed ductile shearing under lower-greenschist facies metamorphism in the footwall of extensional detachments.
- ✓ Seismic reflection lines in the Mejerda basin show a listric fan of normal faults affecting sedimentary rocks of the hanging wall of a low-angle ramp fault zone that cuts down into the autochthonous Atlas Cretaceous sediments of the footwall. This extensional system is cut by later normal faults that root at depths of 3s TWT that finally exhume the folded Triassic epizonal Ichkeul, Hairech and Oued Belif metamorphic domes.
- ✓ The erosion in the uplifting hanging-wall of the main shortening structures has favored the exhumation of the Late Miocene extensional detachments and associated structures. Shortening ranges between 16 and 7 %, decreasing from W to E.
- ✓ The fault system accommodating plate convergence in Northern Tunisia is strongly segmented with ENE-WSW to NE-SW reverse faults, E-W to NW-SE dextral faults and NNE-SSW sinistral ones.
- ✓ The distribution of high ksn values and gridded Hi in the region strongly mimic the fault segmentation in Northern Tunisia, especially, defining the regions overlying reverse faults and related anticlinal ridges. Furthermore, both ksn and Hi maps show an East to West gradient in the degree of topographic dissection compatible with the increase in tectonic shortening and age of the inversion structures towards the West. In some case, the high ksn and Hi clusters occur headwards of fluvial captures and 90º deflections in the fluvial channels, indicating higher fluvial dissection in response to the development of transverse drainage.
- ✓ The landscape of Northern Tunisia is characteristic of a young fold and belt region with dominant axial valleys coinciding with the footwall of the main faults and/or along syncline structures.
- ✓ The current young topography related to Pliocene to present shortening in Northern Tunisia, in a convergent setting since the Cretaceous, indicates that Late Miocene extension

completely dismantled the previous foreland thrust belt structure and associated topographic features.

- ✓ Tectonic inversion and development of new shortening structures accommodating NW-SE plate convergence in Northern Tunisia followed the trend observed at a larger scale in the western Mediterranean, with shortening propagating from central Algeria towards the East, from the late Miocene up to the Quaternary in the Tyrrhenian.
- ✓ The Chgega structure forms a spectacular example of landslide characterizing a large Ypresian limestone block gliding over the ductile clays and marls of Paleocene age. The identification of two different landslide mechanisms suggests to classify the Chegega as a complex landslide. This landslide is currently active and shows a progressive movement without clear episodic accelerations, characterized by an extremely slow speed as demonstrated using InSAR technologies. The movement of the main rock block is driven by the N140–150°E normal faulting system that crosscut the Chegega structure.
- ✓ A deep geophysical sounding are necessary to identify and clearly characterize the lithospheric structure of northern Tunisia.
- ✓ Future work should analyze the age and P-T conditions reached during the metamorphism of the Northern Tunisia extensional domes.
- ✓ Mores focus studies are also needed to characterize the active structures in Northern Tunisia and more specifics technologies and data like Height's DEM resolution and radar satellites images.

References

Abad, I., Nieto, F., Peacor, D.R., Velilla, N., 2003. Prograde and retrograde diagenetic and metamorphic evolution in metapelitic rocks of Sierra Espuna (Spain). Clay Minerals 38, 1–23.

Abbassene, F., Chazot, G., Bellon, H., Bruguier, O., Ouabadi, A., Maury, R.C., Déverchére, J., Bosch, D., Monié, P., Deverchere, J., Bosch, D., Monie, P., 2016. A 17 Ma onset for the post-collisional K-rich calc-alkaline magmatism in the Maghrebides: Evidence from Bougaroun (northeastern Algeria) and geodynamic implications. Tectonophysics 674, 114–134. https://doi.org/10.1016/j.tecto.2016.02.013

Aïdi, C., Beslier, M.O., Yelles-Chaouche, A.K., Klingelhoefer, F., Bracene, R., Galve, A., Bounif, A., Schenini, L., Hamai, L., Schnurle, P., Djellit, H., Sage, F., Charvis, P., Déverchère, J., 2018. Deep structure of the continental margin and basin off Greater Kabylia, Algeria – New insights from wide-angle seismic data modeling and multichannel seismic interpretation. Tectonophysics 728–729, 1–22. https://doi.org/10.1016/j.tecto.2018.01.007

Aïssa, L. Ben, Alouani, R., Aïssa, W. Ben, 2018. Tectono-magmatic events and genesis of Fe-Pb-Zn resources in Nefza area, NW Tunisia. Arabian Journal of Geosciences 11, 608.

Aite and Gélard, 1997. Distension néogène post-collisionnelle sur le transect de Grande-Kabylie (Algérie). Bulletin de La Société Geologique de France 168(4), 423-436.

Alouani, R., Melki, F., Tlig, S., Zargouni, F., 2006. Carte géologique de la Tunisie au 1/50.000, la feuille n◦ 6 de Menzel Bourguiba. Office National Des Mines, Tunis, Tunisie.

Alyahyaoui, S., Zouari, H., 2014. Synsedimentary folding process and transtensive tectonic during Late Miocene to Quaternary in northeastern Tunisia: case of Mateur-Menzel Bourguiba region. Arabian Journal of Geosciences 7, 4957–4973. https://doi.org/10.1007/s12517-013-1111-2

Amiri, A., Chaqui, A., Nasr, I.H., Inoubli, M.H., Ayed, N. Ben, Tlig, S., 2011. Role of preexisting faults in the geodynamic evolution of Northern Tunisia, insights from gravity data from the Medjerda valley. Tectonophysics 506, 1–10.

Amri, Z., Naji, C., Masrouhi, A., Bellier, O., 2020. Interconnection salt diapir–allochthonous salt sheet in northern Tunisia: The Lansarine–Baoula case study. Journal of African Earth Sciences 103876. https://doi.org/10.1016/j.jafrearsci.2020.103876

Angelier, J., & Mechler, P., 1977. Sur une méthode graphique de recherche des contraintes principales également utilisable en tectonique et en séismologie: la méthode des dièdres

droits. Bulletin de La Société Géologique de France, , 7(19), 1309-1318.

Angelier, J., Slunga, R., Stefansson, R., Homberg, C., 2004. Perturbation of stress and oceanic rift extension across transform faults shown by earthquake focal mechanisms in Iceland. Earth and Planetary Science Letters 219. https://doi.org/10.1016/S0012-821X(03)00704-0

Arab, M., Maherssi, C., Granjeon, D., Roure, F., Déverchère, J., Cuilhé, L., Hassaim, M., Mouchot, N., Doublet, S., Khomsi, S., 2020. On the origin and consequences of crustal-scale extension between Africa and Sicily since Late Miocene: insights from the Kaboudia area, western Pelagian Sea. Tectonophysics 228565.

Argnani, A., 2009. Evolution of the southern Tyrrhenian slab tear and active tectonics along the western edge of the Tyrrhenian subducted slab. Geological Society, London, Special Publications 311, 193 LP – 212. https://doi.org/10.1144/SP311.7

Aslan, G., De Michele, M., Raucoules, D., Bernardie, S., Cakir, Z., 2021. Transient motion of the largest landslide on earth, modulated by hydrological forces. Scientific Reports 11, 1–12.

Atawa, M., Boukerbout, H., Zouaghi, T., Mzali, H., Saibi, H., Abtout, A., 2019. Interpretation of gravity data using 3D inversion and 2D continuous wavelet transform in Hedil deformed structures, northern Tunisia. Journal of African Earth Sciences 151, 371–390.

Ayed-Khaled, A., Ayed-Khaled, A., Zouaghi, T., Atawa, M., Ghanmi, M., 2015. New evidence on the geologic setting of Medjerda Valley plain (northern Tunisia) from integrated geophysical study of Triassic evaporite bodies. Annals of Geophysics 58, S0326. https://doi.org/10.4401/ag-6567

Ayed-Khaled, A., Ghanmi, M., Zargouni, F., 2012. Filtering of the gravimetric anomalies to the study of the geological structures of Oued Zarga (Septentrional Tunisia): structural implications. Arabian Journal of Geosciences 5, 169–180.

Azañón, J.M., Galve, J.P., Pérez-Peña, J. V., Giaconia, F., Carvajal, R., Booth-Rea, G., Jabaloy, A., Vázquez, M., Azor, A., Roldán, F.J., 2015. Relief and drainage evolution during the exhumation of the Sierra Nevada (SE Spain): Is denudation keeping pace with uplift? Tectonophysics 663, 19–32. https://doi.org/10.1016/j.tecto.2015.06.015

Azañón, J.M., García-Dueñas, V., Goffé, B., 1998. Exhumation of high-pressure metapelites and coeval crustal extension in the Alpujarride complex (Betic Cordillera). Tectonophysics 285, 231–252.

Azañón, J.M., Pérez-Peña, J. V., Giaconia, F., Booth-Rea, G., Martínez-Martínez, J.M., Rodríguez-Peces, M.J., 2012. Active tectonics in the central and eastern Betic Cordillera through morphotectonic analysis: the case of Sierra Nevada and Sierra Alhamilla. Journal

of Iberian Geology 38, 225–238. https://doi.org/10.5209/rev_JIGE.2012.v38.n1.39214

Azañón, José Miguel, Roldán García, F.J., Rodríguez Fernández, J., 2012. Fallas y despegues extensionales en el Subbético Central: implicaciones en la evolución Neógena de las Zonas Externas de La Cordillera Bética.

Babault, J., Van Den Driessche, J., Teixell, A., Driessche, J. Van Den, Teixell, A., 2012. Longitudinal to transverse drainage network evolution in the High Atlas (Morocco): The role of tectonics. Tectonics 31, 1–15. https://doi.org/10.1029/2011TC003015

Badgasarian, G.P., 1972. Age radiométrique du volcanisme néogène du Nord de la Tunisie. Notes Serv. Géol. Tunisie 40, 79-85.

Bahrouni, N., Bouaziz, S., Soumaya, A., Ayed, N. Ben, Attafi, K., Houla, Y., El Ghali, A., Rebai, N., 2014. Neotectonic and seismotectonic investigation of seismically active regions in Tunisia: a multidisciplinary approach. Journal of Seismology 18, 235–256.

Barreca, G., Bruno, V., Cultrera, F., Mattia, M., Monaco, C., Scarfì, L., 2014. New insights in the geodynamics of the Lipari–Vulcano area (Aeolian Archipelago, southern Italy) from geological, geodetic and seismological data. Journal of Geodynamics 82, 150–167. https://doi.org/https://doi.org/10.1016/j.jog.2014.07.003

Batik P, 1980. Carte géologique de la Tunisie au 1/50.000, la feuille n° 11 de Hedhil. Office National Des Mines, Tunis, Tunisie.

Bedir, M., Boukadi, N., Ben Timzal, F., Zitouni, L., Alouani, R., Slimane, F., Bobier, C., Zargouni, F., Bédir, M., Ben Timzal received, F., 2001. Subsurface Mesozoic basins in the central Atlas of Tunisia: Tectonics, sequence deposit distribution, and hydrocarbon potential, AAPG Bulletin, v. https://doi.org/10.1306/8626CA2D-173B-11D7-8645000102C1865D

Bejaoui, H., Aïfa, T., Melki, F., Zargouni, F., 2017. Structural evolution of Cenozoic basins in northeastern Tunisia, in response to sinistral strike-slip movement on the El Alia-Teboursouk Fault. Journal of African Earth Sciences 134, 174–197. https://doi.org/10.1016/j.jafrearsci.2017.06.021

Beladam, O., Balz, T., Mohamadi, B., Abdalhak, M., 2019. Using ps-insar with sentinel-1 images for deformation monitoring in northeast Algeria. Geosciences 9, 315.

Belayouni, H., 2013. Paleogeographic and geodynamic Miocene evolution of the Tunisian Tell (Numidian and Post-Numidian Successions): Bearing with the Maghrebian Chain. International Journal of Earth Sciences 102, 831–855. https://doi.org/10.1007/s00531-012-0824-x

Belayouni, H., Brunelli, D., Clocchiatti, R., Staso, A. Di, Hassani, I.E.E.A. El, Guerrera, F.,

Kassaa, S., Ouazaa, N.L., Martín, M.M., Serrano, F., Tramontana, M., 2010. La Galite Archipelago (Tunisia, North Africa): Stratigraphic and petrographic revision and insights for geodynamic evolution of the Maghrebian Chain. Journal of African Earth Sciences 56, 15–28. https://doi.org/10.1016/j.jafrearsci.2009.05.004

Belguith, Y., Geoffroy, L., Mourgues, R., Rigane, A., 2013. Tectonophysics Analogue modelling of Late Miocene – Early Quaternary continental crustal extension in the Tunisia – Sicily Channel area Tunisia. Tectonophysics 608, 576–585. https://doi.org/10.1016/j.tecto.2013.08.023

Belguith, Y., Geoffroy, L., Rigane, A., Gourmelen, C., Ben, H., 2011. Tectonophysics Neogene extensional deformation and related stress regimes in central Tunisia. Tectonophysics 509, 198–207. https://doi.org/10.1016/j.tecto.2011.06.009

Bellin, N., Vanacker, V., Kubik, P.W., 2014. Denudation rates and tectonic geomorphology of the Spanish Betic Cordillera. Earth and Planetary Science Letters 390, 19–30. https://doi.org/10.1016/j.epsl.2013.12.045

Ben Chelbi, M., Melki, F., Zargouni, F., 2006. Mode of salt bodies emplacement in Septentrional Atlas of Tunisia. Example of a Bir Afou salt body. Comptes Rendus - Geoscience 338, 349–358. https://doi.org/10.1016/j.crte.2006.02.009

Ben Hassen, M., Deffontaines, B., Turki, M.M., Ben, M., Moncef, M., 2014. Recent tectonic activity of the Gafsa fault through morphometric analysis: Southern Atlas of Tunisia. Quaternary International 338, 99–112. https://doi.org/10.1016/j.quaint.2014.05.009

Benassi, R., Jallouli, C., Hammami, M., Turki, M.M., 2006. The structure of Jebel El Mourra, Tunisia: a diapiric structure causing a positive gravity anomaly. Terra Nova 18, 432–439.

Benchilla, L., Guilhaumou, N., Mougin, P., Jaswal, T., Roure, F., 2003. Reconstruction of palaeo-burial history and pore fluid pressure in foothill areas: a sensitivity test in the Hammam Zriba (Tunisia) and Koh-i-Maran (Pakistan) ore deposits. Geofluids 3, 103–123.

Benedicto, A., Séguret, M., Labaume, P., Duran, B., Jolivet, L., Horváth, F., Séranne, M., 1999. The mediterranean basins: Tertiary extension within the Alpine Orogen.

Biely, A., Maamouri, M., & Stranik, Z., 1982. Carte géologique de la Tunisie au 1/50.000, la feuille n° 18 de Beja. Office National Des Mines,Tunis, Tunisie.

Billi, A.N., Faccenna, C.L., Bellier, O.L., Minelli, L.I., Neri, G.I., Piromallo, C.L., Presti, D.E., Scrocca, D.A., Serpelloni, E.N., 2011. Recent tectonic reorganization of the Nubia-Eurasia convergent boundary heading for the closure of the western Mediterranean. Bulletin de La Societe Geologique de France 182, 279–303. https://doi.org/10.2113/gssgfbull.182.4.279

Bird, P., 1979. Continental delamination and the Colorado Plateau. Journal of Geophysical

Research: Solid Earth 84, 7561–7571. https://doi.org/10.1029/JB084iB13p07561

Bolze, J., 1950. Diapirs triasiques et phases orogéniques dans les monts de Téboursouk (Tunisie septentrionale). COMPTES RENDUS HEBDOMADAIRES DES SEANCES DE L ACADEMIE DES SCIENCES 231, 480–482.

Booth-Rea et Al, 2008. Heterogeneous deformation in the Cascadia convergent margin and its relation to thermal gradient (Washington , NW USA). 27, 1–15. https://doi.org/10.1029/2007TC002209

Booth-Rea, G., 2012. Upper-crustal extension during oblique collision : the Temsamane extensional detachment (eastern Rif , Morocco). 1–8. https://doi.org/10.1111/j.1365-3121.2012.01089.x

Booth-Rea, G., Azañón, J.M., García-Dueñas, V., 2004. Extensional tectonics in the northeastern Bethics (SE Spain): Case study of extension in a multilayered upper crust with contrasting rheologies. Journal of Structural Geology 26, 2039–2058. https://doi.org/10.1016/j.jsg.2004.04.005

Booth-rea, G., Azañón, J.M., García-Dueñas, V., Azan, J.M., 2004. Extensional tectonics in the northeastern Betics (SE Spain): case study of extension in a multilayered upper crust with contrasting rheologies. Journal of Structural Geology 26, 2039–2058. https://doi.org/10.1016/j.jsg.2004.04.005

Booth-Rea, G., Gaidi, S., Melki, F., Marzougui, W., Azañón, J.M., Galvé, J.P., Pérez-Peña, J. V, Ruano, P., 2020. Comment on “How to build an extensional basin in a contractional setting? Numerical and physical modelling applied to the Mejerda basin at the front of the eastern tell of Tunisia” by Mannoubi Khelil et al. Journal of Structural Geology 138, 103935. https://doi.org/https://doi.org/10.1016/j.jsg.2019.103935

Booth-Rea, G., Gaidi, S., Melki, F., Marzougui, W., Azañón, J.M., Zargouni, F., Galvé, J.P., Pérez-Peña, J. V, 2018. Late Miocene Extensional Collapse of Northern Tunisia. Tectonics 37, 1626–1647. https://doi.org/10.1029/2017TC004846

Booth-Rea, G., García-Dueñas, V., Azañón, J.M., 2002. Extensional attenuation of the Malaguide and Alpujarride thrust sheets in a segment of the Alboran basin folded during the Tortonian (Lorca area, Eastern Betics). Comptes Rendus Geoscience 334, 557–563. https://doi.org/https://doi.org/10.1016/S1631-0713(02)01794-7

Booth-Rea, G., Martínez-Martínez, J.M., Giaconia, F., 2015. Continental subduction, intracrustal shortening, and coeval upper-crustal extension: PT evolution of subducted south Iberian paleomargin metapelites (Betics, SE Spain). Tectonophysics 663, 122–139.

Booth-Rea, G., Ranero, C.R., Martínez-Martínez, J.M., Azañón, J.M., Giaconia, F., Gràcia, E.,

2013. Timing and Types of Extension in the Westernmost Mediterranean from Onshore-Offshore Studies.

Booth-Rea, G., Ranero, C.R., Martínez-Martínez, J.M., Grevemeyer, I., 2007. Crustal types and Tertiary tectonic evolution of the Alborán sea, western Mediterranean. Geochemistry, Geophysics, Geosystems 8. https://doi.org/10.1029/2007GC001639

Booth-Rea, G., Azañón, J.M., Martínez-Martínez, J.M., Vidal, O., García-Dueñas, V., 2005. Contrasting structural and P-T evolution of tectonic units in the southeastern Betics: Key for understanding the exhumation of the Alboran Domain HP/LT crustal rocks (western Mediterranean). Tectonics 24.

Bott, M.H.P., 1959. The mechanics of oblique slip faulting. Geological Magazine 96(2), 109-117.

Bouaziz, S., Barrier, E., Soussi, M., Turki, M.M., Zouari, H., 2002. Tectonic evolution of the northern African margin in Tunisia from paleostress data and sedimentary record. Tectonophysics 357, 227–253. https://doi.org/10.1016/S0040-1951(02)00370-0

Bouaziz, S., Jedoui, Y., Barrier, É., Angelier, J., 2003. Néotectonique affectant les dépôts marins tyrrhéniens du littoral sud-est tunisien : implications pour les variations du niveau marin Neotectonics in the Tyrrhenian marine deposits of the southeastern Tunisian coast : implications for sea level changes. C. R. Geoscience 335, 247–254. https://doi.org/10.1016/S1631-0713(03)00031-2

Bougrine, A., Yelles-chaouche, A.K., Calais, E., 2019. Active deformation in Algeria from continuous GPS measurements. Geophysical Journal International 217, 572–588. https://doi.org/10.1093/gji/ggz035

Bouillin, J.-P., DURAND-DELGA, M., OLIVIER, P., 1986. Betic-Rifian and Tyrrhenian Arcs : Distinctive Features, Genesis and Development Stages. In: WEZEL, F.-C.B.T.-D. in G. (Ed.), The Origin of Arcs. Elsevier, 281–304. https://doi.org/https://doi.org/10.1016/B978-0-444-42688-8.50017-5

Bouillin, J., Calais, E., Savoye, B., Kherroubi, A., Roy, P. Le, Pauc, H., Dan, G., 2005. Active thrust faulting offshore Boumerdes , Algeria , and its relations to the 2003 Mw 6 . 9 earthquake. 32. https://doi.org/10.1029/2004GL021646

Boukhalfa, K., Soussi, M., Ozcan, E., Banerjee, S., Tounekti, A., 2020. The Oligo-Miocene siliciclastic foreland basin deposits of northern Tunisia: Stratigraphy, sedimentology and paleogeography. Journal of African Earth Sciences 170, 103932.

Bounab, A., El Kharim, Y., El Hamdouni, R., Hlila, R., 2021. A multidisciplinary approach to study slope instability in the Alboran Sea shoreline: Study of the Tamegaret deep-seated

slow-moving landslide in Northern Morocco. Journal of African Earth Sciences 104345.

Brogi, A., 2008. Kinematics and geometry of Miocene low-angle detachments and exhumation of the metamorphic units in the hinterland of the Northern Apennines (Italy). Journal of Structural Geology 30, 2–20. https://doi.org/https://doi.org/10.1016/j.jsg.2007.09.012

Bruguier, O., Bosch, D., Caby, R., Vitale-Brovarone, A., Fernandez, L., Hammor, D., Laouar, R., Ouabadi, A., Abdallah, N., Mechati, M., 2017. Age of UHP metamorphism in the Western Mediterranean: insight from rutile and minute zircon inclusions in a diamond-bearing garnet megacryst (Edough Massif, NE Algeria). Earth and Planetary Science Letters 474, 215–225.

Brun, A., 1989. Microflores et paléovégétations en Afrique du Nord depuis 30 000 ans. Bulletin de La Société Géologique de France 25–33.

Bugini, R., Folli, L., Marchisio, R., 2019. "Giallo Antico" in Roman Architecture of Lombardy: A Preliminary Survey. Conference of the Arabian Journal of Geosciences. Springer, 107–109.

Bull, W.B., and McFadden, L., 1977. Tectonic geomorphology north and south of the Garlock Fault, California, in: Doering, D.O. (Ed.), Geomorphology in Arid Regions. University of New York, Binghamton,. 115-138.

Bull, W.B., 2011. Tectonically active landscapes. John Wiley & Sons.

Buness, H., Giese, P., Bobier, C., Eva, C., Merlanti, F., Pedone, R., Jenatton, L., Nguyen, D.T., Thouvenot, F., Egloff, F., 1992. The EGT-85 Seismic Experiment in Tunisia-a reconnaissance of the deep structures. Tectonophysics 207, 245–267.

Burbank, D.W., Anderson, R.S., 2011. Tectonic geomorphology. John Wiley & Sons.

Burbank, D.W., Anderson, R.S., Smith, R.P., 2013. Tectonic Geomorphology, Second Edition (Douglas W. Burbank and Robert S. Anderson) Review by: Richard P. Smith. XIX, 198–200.

Burollet et al, 1951. Étude géologique des bassins mio-pliocènes du Nord-Est de la Tunisie .

Burollet et Al, 1978. The geology of the Pelagian Block: The margins and basins off southern Tunisia and Tripolitania.

Burollet, P.F., 1991. Structures and tectonics of Tunisia. Tectonophysics 195(2–4), 359–369.

Burollet, P.F., 1956. Contribution à l'étude stratigraphique de la Tunisie centrale. Ann. Mines Géol. 18, 350.

C. Maury, R., El Azzouzi, M., Bellon, H., Coutelle, A., Cotten, J., Piqué, A., Réhault, J.-P.P., Fourcade, S., Ouabadi, A., Capdevila, R., Coulon, C., Semroud, B., Megartsi, M., Belanteur, O., Louni-Hacini, A., Hernandez, J., El Azzouzi, M., Bellon, H., Coutelle, A., Ouabadi, A.,

Semroud, B., Megartsi, M., Cotten, J., Belanteur, O., Louni-Hacini, A., Piqué, A., Capdevila, R., Hernandez, J., Réhault, J.-P.P., 2000. Post-collisional Neogene magmatism of the Mediterranean Maghreb margin: A consequence of slab breakoff. Comptes Rendus de l'Academie de Sciences - Serie IIa: Sciences de La Terre et Des Planetes 331, 159–173. https://doi.org/10.1016/S1251-8050(00)01406-3

Calò, M., Parisi, L., 2014. Evidences of a lithospheric fault zone in the Sicily Channel continental rift (southern Italy) from instrumental seismicity data. Geophysical Journal International 199, 219–225. https://doi.org/10.1093/gji/ggu249

Camafort, M., Melki, F., Gràcia, E., Azañón, J.M., 2019. Active tectonics and drainage evolution in the Tunisian Atlas driven by interaction between crustal shortening and mantle dynamics.

Camafort, M., Melki, F., Gràcia, E., Azañón, J.M.M., Pérez-Peña, J.V. V, Booth-Rea, G., Melki, F., Gràcia, E., Azañón, J.M.M., Galve, J.P.P., Marzougui, W., Gaidi, S., Ranero, C.R.R., 2020. Active tectonics and drainage evolution in the Tunisian Atlas driven by interaction between crustal shortening and mantle dynamics. Geomorphology 351, 106954. https://doi.org/https://doi.org/10.1016/j.geomorph.2019.106954

Carmignani and Kligfiel, 1990. Crustal extension in the northern Apennines: The transition from compression to extension in the Alpi. 9, 1275–1303.

Carminati, E., Wortel, M.J.R., Spakman, W., Sabadini, R., 1998. The role of slab detachment processes in the opening of the western – central Mediterranean basins : some geological and geophysical evidence. Earth and Planetary Science Letters 160, 651–665.

Casu, F., Elefante, S., Imperatore, P., Zinno, I., Manunta, M., De Luca, C., Lanari, R., 2014. SBAS-DInSAR parallel processing for deformation time-series computation. IEEE Journal of Selected Topics in Applied Earth Observations and Remote Sensing 7, 3285–3296.

Chazot, G., Abbassene, F., Maury, R.C., Deverchere, J., Bellon, H., Ouabadi, A., Bosch, D., Déverchère, J., Bellon, H., Ouabadi, A., Bosch, D., 2017. An overview on the origin of post-collisional Miocene magmatism in the Kabylies (northern Algeria): Evidence for crustal stacking, delamination and slab detachment. Journal of African Earth Sciences 125, 27–41. https://doi.org/10.1016/j.jafrearsci.2016.10.005

Chertova, M. V, Spakman, W., Geenen, T., Van Den Berg, A.P., Van Hinsbergen, D.J.J., 2014. Underpinning tectonic reconstructions of the western Mediterranean region with dynamic slab evolution from 3-D numerical modeling. Journal of Geophysical Research: Solid Earth 119, 5876–5902.

Chiarabba, C., Palano, M., 2017. Progressive migration of slab break-off along the southern Tyrrhenian plate boundary: Constraints for the present day kinematics. Journal of

Geodynamics 105, 51–61. https://doi.org/https://doi.org/10.1016/j.jog.2017.01.006

Cigna, F., Banks, V.J., Donald, A.W., Donohue, S., Graham, C., Hughes, D., McKinley, J.M., Parker, K., 2017. Mapping ground instability in areas of geotechnical infrastructure using satellite InSAR and Small UAV surveying: A case study in Northern Ireland. Geosciences 7, 51.

Civile, D., Lodolo, E., Accettella, D., Geletti, R., Ben-avraham, Z., Deponte, M., Facchin, L., 2010. Tectonophysics The Pantelleria graben (Sicily Channel , Central Mediterranean): An example of intraplate ' passive ' rift. Tectonophysics 490, 173–183. https://doi.org/10.1016/j.tecto.2010.05.008

Civile, D., Lodolo, E., Tortorici, L., Lanzafame, G., Brancolini, G., 2008. Relationships between magmatism and tectonics in a continental rift: The Pantelleria Island region (Sicily Channel, Italy). Marine Geology 251, 32–46. https://doi.org/https://doi.org/10.1016/j.margeo.2008.01.009

Cohen, C.R., Schamel, S., Boyd-Kaygi, P., 1980. Neogene deformation in northern Tunisia: Origin of the eastern Atlas by microplate—continental margin collision. Geological Society of America Bulletin 91, 225–237.

Cooper, R.G., 1983. Mass movement caves in Great Britain. Studies in Speleology 4, 37–44.

Crespo-Blanc, A., de Lamotte, D.F., 2006. Structural evolution of the external zones derived from the Flysch trough and the South Iberian and Maghrebian paleomargins around the Gibraltar arc: a comparative study. Bulletin de La Société Géologique de France 177, 267–282.

Crosta, G.B., Frattini, P., Agliardi, F., 2013. Deep seated gravitational slope deformations in the European Alps. Tectonophysics 605, 13–33.

Currie, B.S., Rowley, D.B., Tabor, N.J., 2005. Middle Miocene paleoaltimetry of southern Tibet: Implications for the role of mantle thickening and delamination in the Himalayan orogen. Geology 33, 181–184. https://doi.org/10.1130/G21170.1

de la Peña, L.G., Ranero, C.R., Gràcia, E., Booth-Rea, G., 2020. The evolution of the westernmost Mediterranean basins. Earth-Science Reviews 103445.

de Lis Mancilla, F., Diaz, J., 2015. High resolution Moho topography map beneath Iberia and Northern Morocco from receiver function analysis. Tectonophysics 663, 203–211.

De Luca, C., Cuccu, R., Elefante, S., Zinno, I., Manunta, M., Casola, V., Rivolta, G., Lanari, R., Casu, F., 2015. An on-demand web tool for the unsupervised retrieval of earth's surface deformation from SAR data: The P-SBAS service within the ESA G-POD environment. Remote Sensing 7, 15630–15650.

DeCelles, P.G., Giles, K.A., 1996. Foreland basin systems. Basin Research 8, 105–123.

Decrée, S., De Putter, T., Yans, J., Moussi, B., Recourt, P., Jamoussi, F., Bruyère, D., Dupuis, C., 2008a. Iron mineralisation in Mio-Pliocene sediments of the Tamra iron mine (Nefza mining district, Tunisia): Mixed influence of pedogenesis and hydrothermal alteration. Ore Geology Reviews 33, 397–410.

Decrée, S., Marignac, C., De Putter, T., Deloule, E., Liégeois, J.P., Demaiffe, D., 2008b. Pb-Zn mineralization in a Miocene regional extensional context: The case of the Sidi Driss and the Douahria ore deposits (Nefza mining district, northern Tunisia). Ore Geology Reviews 34, 285–303. https://doi.org/10.1016/j.oregeorev.2008.01.002

Decrée, S., Marignac, C., De Putter, T., Yans, J., Clauer, N., Dermech, M., Aloui, K., Baele, J.-M., 2013. The Oued Belif hematite-rich breccia: A Miocene iron oxide Cu-Au-(U-REE) deposit in the Nefza mining district, Tunisia. Economic Geology 108, 1425–1457.

Decrée, S., Marignac, C., Liégeois, J., Yans, J., Ben, R., Demaiffe, D., 2014a. Lithos Miocene magmatic evolution in the Nefza district (Northern Tunisia) and its relationship with the genesis of polymetallic mineralizations. LITHOS 192–195, 240–258. https://doi.org/10.1016/j.lithos.2014.02.001

Decrée, S., Marignac, C., Liégeois, J.P., Yans, J., Ben Abdallah, R., Demaiffe, D., 2014b. Miocene magmatic evolution in the Nefza district (Northern Tunisia) and its relationship with the genesis of polymetallic mineralizations. Lithos 192–195, 240–258. https://doi.org/10.1016/j.lithos.2014.02.001

Delgado, J., Vicente, F., García-Tortosa, F., Alfaro, P., Estévez, A., Lopez-Sanchez, J.M., Tomás, R., Mallorquí, J.J., 2011. A deep seated compound rotational rock slide and rock spread in SE Spain: Structural control and DInSAR monitoring. Geomorphology 129, 252–262. https://doi.org/10.1016/j.geomorph.2011.02.019

Déverchère, J., 2005. Active thrust faulting offshore Boumerdes , Algeria , and its relations to the 2003 Mw 6 . 9 earthquake. Geophysical Research Letters 32, 1–5. https://doi.org/10.1029/2004GL021646

Devoto, S., Hastewell, L.J., Prampolini, M., Furlani, S., 2021. Dataset of Gravity-Induced Landforms and Sinkholes of the Northeast Coast of Malta (Central Mediterranean Sea). Data 6, 81. https://doi.org/https://doi.org/10.3390/data6080081

Devoto, S., Macovaz, V., Mantovani, M., Soldati, M., Furlani, S., 2020. Advantages of using UAV digital photogrammetry in the study of slow-moving coastal landslides. Remote Sensing 12, 3566.

Dewey, J.F., Helman, M.L., Knott, S.D., Turco, E., Hutton, D.H.W., Knott, S.D., 1989.

Kinematics of the western Mediterranean. Geological Society, London, Special Publications 45, 265–283. https://doi.org/10.1144/GSL.SP.1989.045.01.15

Dhia, H. Ben, 1987. The geothermal gradient map of central Tunisia: comparison with structural, gravimetric and petroleum data. Tectonophysics 142, 99–109.

Dhifaoui, R., Strzerzynski, P., Mourgues, R., Rigane, A., Gourmelen, C., Peigné, D., 2021. Accommodation of compression and lateral extension in a continental crust: Analogical modeling of the Central Atlas (eastern Algeria, Tunisia) and Pelagian sea. Tectonophysics 817, 229052. https://doi.org/https://doi.org/10.1016/j.tecto.2021.229052

Di Luzio, E., Mele, G., Tiberti, M.M., Cavinato, G.P., Parotto, M., 2009. Moho deepening and shallow upper crustal delamination beneath the central Apennines. Earth and Planetary Science Letters 280, 1–12.

Di Maggio, C., Madonia, G., Vattano, M., 2014. Deep-seated gravitational slope deformations in western Sicily: Controlling factors, triggering mechanisms, and morphoevolutionary models. Geomorphology 208, 173–189. https://doi.org/10.1016/j.geomorph.2013.11.023

Do Campo, M., Nieto, F., Albanesi, G.L., Ortega, G., Monaldi, C.R., 2017. Outlining the thermal posdepositional evolution of the Ordovician successions of northwestern Argentina by clay mineral analysis, chlorite geothermometry and Kübler index. Andean Geology 44, 179–212. https://doi.org/10.5027/andgeoV44n2-a04

Domzig, A., Yelles, K., Le, C., Déverchère, J., Bouillin, J., Bracène, R., Mercier, B., Lépinay, D., Le, P., 2006. Searching for the Africa – Eurasia Miocene boundary offshore western Algeria (MARADJA ' 03 cruise). 338, 80–91. https://doi.org/10.1016/j.crte.2005.11.009

Duggen, S., Hoernle, K., van den Bogaard, P., Harris, C., 2004. Magmatic evolution of the Alboran region: The role of subduction in forming the western Mediterranean and causing the Messinian Salinity Crisis. Earth and Planetary Science Letters 218, 91–108. https://doi.org/https://doi.org/10.1016/S0012-821X(03)00632-0

Duggen, S., Hoernle, K., van den Bogaard, P., Rüpke, L., Phipps Morgan, J., 2003. Deep roots of the Messinian salinity crisis. Nature 422, 602–606. https://doi.org/10.1038/nature01553

Dumont J Santana E Vilema W, Dumont, J.F., Santana, E., Vilema, W., Dumont J Santana E Vilema W, Dumont, J.F., Santana, E., Vilema, W., 2005. Morphologic evidence of active motion of the Zambapala Fault, Gulf of Guayaquil (Ecuador). Geomorphology vol: 65 (3, pp: 223-239. https://doi.org/10.1016/J.GEOMORPH.2004.09.003

El Ghali, A., 2006. Carte géologique de la Tunisie au 1/50.000, la feuille n° 4 de Cap Negro. Office National Des Mines, Tunis, Tunisie.

Erraioui, L., 1994. Environnements sédimentaires et géochimie des séries de l'Eocène du Nord-

Est de la Tunisie. Tunis (Tunisia).

Essid, E.M., Kadri, A., Inoubli, M.H., Zargouni, F., 2016. Identification of new NE-trending deep-seated faults and tectonic pattern updating in northern Tunisia (Mogodos–Bizerte region), insights from field and seismic reflection data. Tectonophysics 682, 249–263. https://doi.org/10.1016/j.tecto.2016.05.032

Faccenna, C., Becker, T.W., Auer, L., Billi, A., Boschi, L., Brun, J.P., Capitanio, F.A., Funiciello, F., Horvàth, F., Jolivet, L., Piromallo, C., Royden, L., Rossetti, F., Serpelloni, E., 2014. Mantle dynamics in the Mediterranean. Reviews of Geophysics 52, 283–332. https://doi.org/10.1002/2013RG000444.Received

Faccenna, C., Civetta, L., D'Antonio, M., Funiciello, F., Margheriti, L., Piromallo, C., 2005. Constraints on mantle circulation around the deforming Calabrian slab. Geophysical Research Letters 32. https://doi.org/10.1029/2004GL021874

Faccenna, C., Piromallo, C., Crespo-Blanc, A., Jolivet, L., Rossetti, F., 2004. Lateral slab deformation and the origin of the western Mediterranean arcs. Tectonics 23. https://doi.org/10.1029/2002TC001488

Faul, H., FOLAND, K.A., 1980. L'âge des rhyodacites de Nefza-Sedjenane. Notes Du Service Géologique 47–49.

Fenton, C., Martin, P., Cheng, F., Murphy, B., 2015. Geomorphological analysis of large scale slope instability, Trotternish, Isle of Skye.

Ferrater, M., Booth-Rea, G., Pérez-Peña, J.V., Miguel, J., Giaconia, F., Masana, E., Azañón, J.M., Giaconia, F., Masana, E., 2015. From extension to transpression: Quaternary reorganization of an extensional-related drainage network by the Alhama de Murcia strike-slip fault (eastern Betics). Tectonophysics 663, 33–47. https://doi.org/10.1016/j.tecto.2015.06.011

Fichtner, A., Villaseñor, A., Fitchner and Villaseñor, 2015. Crust and upper mantle of the western Mediterranean - Constraints from full-waveform inversion. Earth and Planetary Science Letters 428, 52–62. https://doi.org/10.1016/j.epsl.2015.07.038

Flint, J.J., 1974. Stream Gradient as a Function of Order, Magnitude, and Discharge. 10, 969–973.

Fonseca, A.F. de P.S.C., 2014. Large deep-seated landslides in the northern Rif Mountains (Northern Morocco): inventory and analysis.

Fournet, A. et al, 1994. Carte géologique de la Tunisie au 1/50.000, la feuille n° 12 de Mateur. Office National Des Mines, Tunis,Tunisie.

Frifita, N., Mickus, K., Gharbi, M., 2020. Gravity contribution to the Mejerda foreland basin,

Northwestern region of Tunisia. Journal of African Earth Sciences 171, 103956. https://doi.org/https://doi.org/10.1016/j.jafrearsci.2020.103956

Frizon de Lamotte, D., Andrieux, J., Guezou, J.-C., 1991. Cinematique des chevauchements neogenes dans l'Arc betico-rifain; discussion sur les modeles geodynamiques. Bulletin de La Société Géologique de France 162, 611–626.

Frizon De Lamotte, D.F., Bezar, B. Saint, Bracène, R., Mercier, E., 2000. The two main steps of the atlas building and geodynamics of the Western Mediterranean. Tectonics 19, 740–761. https://doi.org/10.1029/2000TC900003

Frizon de Lamotte, D.F., Leturmy, P., Missenard, Y., Khomsi, S., Ruiz, G., Saddiqi, O., Guillocheau, F., Michard, A., 2009. Mesozoic and Cenozoic vertical movements in the Atlas system (Algeria, Morocco, Tunisia): An overview. Tectonophysics 475, 9–28. https://doi.org/10.1016/j.tecto.2008.10.024

Gaidi, S., Booth-Rea, G., Melki, F., Marzougui, W., Ruano, P., Pérez-Peña, J. V, Azañón, J.M., Zargouni, F., Chouaieb, H., Galve, J.P., 2020. Active fault segmentation in Northern Tunisia. Journal of Structural Geology 139, 104146. https://doi.org/https://doi.org/10.1016/j.jsg.2020.104146

Gaidi, S., Carmona, C.R., Arnedo, J.P.G., Pérez, J.V., Melki, F., Guillermo, B.R., Jabaloy, A., Marzougui, W., Azañón, J.M., 2019. Paradigmatic Examples of Lateral Spreading Phenomena in the Betic-Rif and Maghrebian Chains. 263–266. https://doi.org/10.1007/978-3-030-01455-1_57

Galindo-Zaldívar, J., & González-Lodeiro, F., 1988. Faulting phase differentiation by means of computer search on a grid pattern. In Annales Tectonicae. Vol. 2, No, 90–97.

Gallais, F., Graindorge, D., Gutscher, M.-A., Klaeschen, D., 2013. Propagation of a lithospheric tear fault (STEP) through the western boundary of the Calabrian accretionary wedge offshore eastern Sicily (Southern Italy). Tectonophysics 602, 141–152. https://doi.org/https://doi.org/10.1016/j.tecto.2012.12.026

Galve, J.P., Carrión, M., Carmona, C.R., Gaidi, S., Booth-Rea, G., Sánchez, A.J., Ruano, P., Peña, J.V.P., Hernández, J.M.A., Melki, F., 2019. Formas del relieve generadas por fenómenos de expansión lateral y deslizamiento de bloques: de fortalezas naturales y lugares sagrados a valiosos recursos arqueológicos y paisajísticos. XV Reunión Nacional de Cuaternario Bizkaia Aretoa-Bilbao, 1-5 Julio 2019 Libro de Resúmenes. Universidad del País Vasco/Euskal Herriko Unibertsitatea, 406–409.

Gelabert, B., Sabat, F., Rodríguez-Perea, A., 1992. A structural outline of the Serra de Tramuntana of Mallorca (Balearic Islands). Tectonophysics 203, 167–183.

Ghanmi, M., et al, 2001. Jebel Kebbouch halokinesis (NW Tunisia): Shallow water emplacement and evolution of an Albian" salt glacier". ECLOGAE GEOLOGICAE HELVETIAE 94, n, 153-160.

Ghanmi, M., Youssef, M. Ben, Jouirou, M., Zargouni, F., Vila, J.M., 2001. " Glacier de sel" du Jebel Kebbouch (NW Tunisie). Eclogae Geologicae Helvetiae 94, 153–160.

Ghisetti, F., Vezzani, L., 2002. Normal faulting, extension and uplift in the outer thrust belt of the central Apennines (Italy): role of the Caramanico fault. Basin Research 14, 225–236.

Ghorabi, M., Henry, B., 1992. Magnetic fabric of rock from Jebel Hairech (Northern Tunisia) and its structural implications. Journal of African Earth Sciences (and the Middle East) 14, 267–274. https://doi.org/https://doi.org/10.1016/0899-5362(92)90103-J

Giaconia, F., Booth-Rea, G., Martínez-Martínez, J.M., Azañón, J.M., and Pérez-Peña, J.V., 2012. Geomorphic analysis of the Sierra Cabrera, an active pop-up in the constructional domain of conjugate strike-slip faults: The Palomares and Polopos fault zones (eastern Betics, SE Spain),. Tectonophysics 580, 580, 27-42. https://doi.org/10.1016/J.TECTO.2012.08.028

Giaconia, F., Booth-Rea, G., Martínez-Martínez, J.M., Azañón, J.M., Pérez-romero, J., Villegas, I., Miguel, J., Pérez-romero, J., Villegas, I., 2013. Mountain front migration and drainage captures related to fault segment linkage and growth : The Polopos transpressive fault zone (southeastern Betics , SE Spain). Journal of Structural Geology 46, 76–91. https://doi.org/10.1016/j.jsg.2012.10.005

Giaconia, F., Booth-Rea, G., Martínez-Martínez, J.M., Azañón, J.M., Storti, F., Artoni, A., 2014. Heterogeneous extension and the role of transfer faults in the development of the southeastern Betic basins (SE Spain). Tectonics 33, 2467–2489. https://doi.org/10.1002/2014TC003681

Giaconia, F., Booth-Rea, G., Ranero, C.R., Gràcia, E., Bartolome, R., Calahorrano, A., Iacono, C. Lo, Cameselle, A.L., Costa, S., Gómez, L., Peña, D., Martínez-Loriente, S., Perea, H., Viñas, M., Lo Iacono, C., Vendrell, M.G., Cameselle, A.L., Costa, S., De La Peña, L.G., Martínez-Loriente, S., Perea, H., Viñas, M., Gómez de la Peña, L., Martínez-Loriente, S., Perea, H., Viñas, M., 2015. Compressional tectonic inversion of the Algero-Balearic basin: Latemost Miocene to present oblique convergence at the Palomares margin (Western Mediterranean). Tectonics 34, 1516–1543. https://doi.org/10.1002/2015TC003861

Gibbs, A.D., 1984. Structural evolution of extensional basin margins. 141, 609–620.

Gimeno-Vives, O., Mohn, G., Bosse, V., Haissen, F., Zaghloul, M.N., Atouabat, A., Frizon de Lamotte, D., 2019. The Mesozoic margin of the Maghrebian Tethys in the Rif belt (Morocco): Evidence for polyphase rifting and related magmatic activity. Tectonics 38,

2894–2918.

Globig, J., Fernàndez, M., Torne, M., Vergés, J., Robert, A., Faccenna, C., 2016. New insights into the crust and lithospheric mantle structure of Africa from elevation, geoid, and thermal analysis. Journal of Geophysical Research: Solid Earth 121, 5389–5424.

Goes, S., Giardini, D., Jenny, S., Hollenstein, C., Kahle, H.-G., Geiger, A., 2004. A recent tectonic reorganization in the south-central Mediterranean. Earth and Planetary Science Letters 226, 335–345. https://doi.org/https://doi.org/10.1016/j.epsl.2004.07.038

Göğüş, O.H., Pysklywec, R.N., 2008. Near-surface diagnostics of dripping or delaminating lithosphere. Journal of Geophysical Research: Solid Earth 113. https://doi.org/10.1029/2007JB005123

Göğüş, O.H., Pysklywec, R.N., Corbi, F., Faccenna, C., 2011. The surface tectonics of mantle lithosphere delamination following ocean lithosphere subduction: Insights from physical-scaled analogue experiments. Geochemistry, Geophysics, Geosystems 12. https://doi.org/10.1029/2010GC003430

Govers, R., Wortel, M.J.R., 2005. Lithosphere tearing at STEP faults: Response to edges of subduction zones. Earth and Planetary Science Letters 236, 505–523. https://doi.org/10.1016/j.epsl.2005.03.022

Guidotti, C. V, Sassi, F.P., 1986. Classification and correlation of metamorphic facies series by means of Miscovite b (o) data from low-grade metapelites. Neues Jahrbuch Für Mineralogie. Abhandlungen 153, 363–380.

Gutiérrez, F., Guerrero, J., Lucha, P., 2008. A genetic classification of sinkholes illustrated from evaporite paleokarst exposures in Spain. Environmental Geology 53, 993–1006.

HACK, J.T., 1957. Studies of longitudinal stream profiles in Virginia and Maryland. US Government Printing Office.

Halliday, G.S., McKelvey, R.J., 2004. Video-analysis of an extremely rapid rockslope failure, Nevis Bluff, New Zealand. Landslides: Evaluation and Stabilization. 1355–1360.

Hamdi, M.S., Soumaya, A., Kadri, A., Ayed, N. Ben, Braham, A., Shimi, N., 2019. Evolution of E-W strike-slip fault networks, the northwestern foreland of Tunisia. Journal of African Earth Sciences. https://doi.org/10.1016/j.jafrearsci.2019.02.024

Harrab, S., Mannai-Tayech, B., Rabhi, M., Zargouni, F., 2013. Study of a Neogene basin dynamics: The “Bizerte basin”, northeastern Tunisia: Relevance to the global Messinian Salinity Crisis. Comptes Rendus - Geoscience 345, 251–261. https://doi.org/10.1016/j.crte.2013.01.007

Hungr, O., Leroueil, S., Picarelli, L., 2014. The Varnes classification of landslide types, an

update. Landslides 11, 167–194.

Ibsen, M.-L.., 1996. Block Slide. In Landslide Recognition: Identifi cation, Movement and Courses;Dikau, R., Brunsden,D., Schrott , L., Ibsen, M.-L., Eds.; Wiley: hichester, UK. pp.64-77.

Iotti, A.; Tarchiani, U., 1996. Notes on Some Lateral Spreading Phenomena around Roccalbegna-Mt.Labbro (Tuscany, Italy). Geografia Fisica e Dinamica Quaternaria 19, 343–349.

Jabaloy, A., Galindo-Zaldívar, J., González-Lodeiro, F., 1993. The Alpujárride-Nevado-Fibábride extensional shear zone, Betic Cordillera, SE Spain. Journal of Structural Geology 15, 555–569.

Jackson, J., Leeder, M., 1994. Pergamon Drainage systems and the development of normal faults : an example from Pleasant Valley , Nevada. Journal of Structural Geology 16, 1041–1059.

Jallouli, C., Chikhaoui, M., Braham, A., Turki, M.M., Mickus, K., Benassi, R., 2005. Evidence for Triassic salt domes in the Tunisian Atlas from gravity and geological data. Tectonophysics 396, 209–225.

Jallouli, C., Mickus, K., 2000. Regional gravity analysis of the crustal structure of Tunisia. Journal of African Earth Sciences 30, 63–78.

Jemmali, N., Souissi, F., Carranza, E.J.M., Vennemann, T.W., Bogdanov, K., 2014. Geochemical constraints on the genesis of the Pb–Zn deposit of Jalta (northern Tunisia): Implications for timing of mineralization, sources of metals and relationship to the Neogene volcanism. Geochemistry 74, 601–613.

Jimenez-Bonilla et al, 2016. Changes in dip and frictional properties of the basal detachment controlling orogenic wedge propagation and frontal collapse: The external central Betics case. 3028–3049. https://doi.org/10.1002/2016TC004196

Jolivet, L., Menant, A., Clerc, C., Sternai, P., Bellahsen, N., Leroy, S., Pik, R., Stab, M., Faccenna, C., Gorini, C., 2018. Extensional crustal tectonics and crust-mantle coupling, a view from the geological record. Earth-Science Reviews 185, 1187–1209.

Kay, R.W., Mahlburg Kay, S., 1993. Delamination and delamination magmatism. Tectonophysics 219, 177–189. https://doi.org/https://doi.org/10.1016/0040-1951(93)90295-U

Keller, E.A., and Pinter, N., 2002. Active Tectonics: Earthquakes, Uplift, and Landscape, Prentice Hall, New Jersey.

Kharrat, S., Harbi, A., Meghraoui, M., Bouaziz, S., 2018. The Tunisian Homogenized

Macroseismic Database (Second Century–1981): First Investigations. Seismological Research Letters 90, 347–357. https://doi.org/10.1785/0220180237

Khelil, M., Khomsi, S., Roure, F., Arfaoui, M.S., Echihi, O., Zargouni, F., 2021. Late Miocene-Quaternary thrusting in the Utique-Kechabta foreland basin of the Tell, Northern Tunisia. Arabian Journal of Geosciences 14, 108. https://doi.org/10.1007/s12517-020-06388-2

Khelil, M., Souloumiac, P., Maillot, B., Khomsi, S., Frizon de Lamotte, D., 2019. How to build an extensional basin in a contractional setting ? Numerical and physical modelling applied to the Mejerda Basin at the front of the eastern Tell of Tunisia. Journal of Structural Geology 129, 103887. https://doi.org/10.1016/j.jsg.2019.103887

Kherroubi, A., Déverchère, J., Yelles, A., Mercier de Lépinay, B., Domzig, A., Cattaneo, A., Bracène, R., Gaullier, V., Graindorge, D., 2009. Recent and active deformation pattern off the easternmost Algerian margin, Western Mediterranean Sea: New evidence for contractional tectonic reactivation. Marine Geology 261, 17–32. https://doi.org/https://doi.org/10.1016/j.margeo.2008.05.016

Khomsi, S., Ben Jemia, M.G., de Lamotte, D.F., Maherssi, C., Echihi, O., Mezni, R., Ghazi, M., Jemia, B., Frizon, D., Lamotte, D., Maherssi, C., Echihi, O., Mezni, R., Ben Jemia, M.G., de Lamotte, D.F., Maherssi, C., Echihi, O., Mezni, R., 2009. An overview of the Late Cretaceous–Eocene positive inversions and Oligo-Miocene subsidence events in the foreland of the Tunisian Atlas: Structural style and implications for the tectonic agenda of the Maghrebian Atlas system. Tectonophysics 475, 38–58. https://doi.org/10.1016/j.tecto.2009.02.027

Khomsi, S., Lamotte, D.F. De, Bédir, M., Echihi, O., 2016. The Late Eocene and Late Miocene fronts of the Atlas Belt in eastern Maghreb : integration in the geodynamic evolution of the Mediterranean Domain. Arabian Journal of Geosciences. https://doi.org/10.1007/s12517-016-2609-1

Kirby, E., Whipple, K.X., 2012. Expression of active tectonics in erosional landscapes. Journal of Structural Geology 44, 54–75. https://doi.org/10.1016/j.jsg.2012.07.009

Kisch, H.J., 1991. Illite crystallinity: recommendations on sample preparation, X-ray diffraction settings, and interlaboratory samples. Journal of Metamorphic Geology 9, 665–670.

Kujawski, H., 1967. Resultats de nouvelles observations a l'est des Hedil (Tunisie septentrionale). Bulletin de La Société Géologique de France 7, 735–740.

Lamos, A., 1985. Carte géologique de la Tunisie au 1/50 000, la feuille n°5 de de Oued Sejnane. Office National Des Mines, Tunis, Tunisie.

Lamos, A., 1980. Carte géologique de la Tunisie au 1/50 000, la feuille n°1 de Kef Abed. Office

National Des Mines, Tunis, Tunisie.

Laribi, A., Walstra, J., Ougrine, M., Seridi, A., Dechemi, N., 2015. Use of digital photogrammetry for the study of unstable slopes in urban areas: case study of the El Biar landslide, Algiers. Engineering Geology 187, 73–83.

Leffondré, P., Déverchère, J., Medaouri, M., Klingelhoefer, F., Graindorge, D., Arab, M., 2021. Ongoing inversion of a passive margin: Spatial variability of strain markers along the Algerian margin and basin (Mediterranean Sea) and seismotectonic implications. Frontiers in Earth Science 365.

Lenart, J., Pánek, T., Dušek, R., 2014. Genesis, types and evolution of crevice-type caves in the flysch belt of the Western Carpathians (Czech Republic). Geomorphology 204, 459–476. https://doi.org/10.1016/j.geomorph.2013.08.025

Levander, A., Bezada, M.J., Niu, F., Humphreys, E.D., Palomeras, I., Thurner, S.M., Masy, J., Schmitz, M., Gallart, J., Carbonell, R., Miller, M.S., 2014. Subduction-driven recycling of continental margin lithosphere. Nature 515, 253–256. https://doi.org/10.1038/nature13878

Leveau, P., 2012. Phénomènes météorologiques extrêmes et stratégies d'adaptation urbaine au Maghreb durant les premiers siècles de l'ère. Variabilités Environnementales, Mutations Sociales, Nature, Intensités, Échelles et Temporalités Des Changements 221–232.

Lister, G.S., Banga, G., Feenstra, A., 1984. Metamorphic core complexes of Cordilleran type in the Cyclades, Aegean Sea, Greece. Geology 12, 221–225. https://doi.org/10.1130/0091-7613(1984)12<221:MCCOCT>2.0.CO;2

Lonergan, L., White, N., Lonergan and White, 1997, Lonergan, L., White, N., 1997. Origin of the Betic-Rif mountain belt. Tectonics 16, 504–522. https://doi.org/10.1029/96TC03937

Loreto, M.F., Zitellini, N., Ranero, C.R., Palmiotto, C., Prada, M., 2021. Extensional tectonics during the Tyrrhenian back-arc basin formation and a new morpho-tectonic map. Basin Research 33, 138–158.

Lowe, D.G., 1999. Object recognition from local scale-invariant features. Proceedings of the Seventh IEEE International Conference on Computer Vision. Ieee, 1150–1157.

Lucazeau, F., Dhia, H. Ben, 1989. Preliminary heat-flow density data from Tunisia and the Pelagian Sea. Canadian Journal of Earth Sciences 26, 993–1000.

Lucente, F.P., Margheriti, L., Piromallo, C., Barruol, G., 2006. Seismic anisotropy reveals the long route of the slab through the western-central Mediterranean mantle. Earth and Planetary Science Letters 241, 517–529. https://doi.org/https://doi.org/10.1016/j.epsl.2005.10.041

Mahdi, D., Abdallah, R. Ben, Hatira, N., Tlili, A., Chaftar, H.R., Jamoussi, F., 2013. Burial

history determination of the Triassic succession of Central and Northern Tunisia using clay minerals. Arabian Journal of Geosciences 6, 4347–4355.

Mancilla, F. de L., Booth-Rea, G., Stich, D., Pérez-Peña, J.V., Morales, J., Azañón, J.M., Martin, R., Giaconia, F., 2015. Slab rupture and delamination under the Betics and Rif constrained from receiver functions. Tectonophysics 663, 225–237. https://doi.org/https://doi.org/10.1016/j.tecto.2015.06.028

Mannaï-Tayech, B., 2006. Miocene silicoclastic series from North-Eastern to South-Western of Tunisia: Standpoint. Geobios 39, 71–84. https://doi.org/10.1016/j.geobios.2004.08.003

Mantovani, M., Devoto, S., Forte, E., Mocnik, A., Pasuto, A., Piacentini, D., Soldati, M., 2013. A multidisciplinary approach for rock spreading and block sliding investigation in the north-western coast of Malta. Landslides 10, 611–622.

Mantovani, M., Devoto, S., Piacentini, D., Prampolini, M., Soldati, M., Pasuto, A., 2016. Advanced SAR interferometric analysis to support geomorphological interpretation of slow-moving coastal landslides (Malta, Mediterranean Sea). Remote Sensing 8, 443.

Manunta, M., De Luca, C., Zinno, I., Casu, F., Manzo, M., Bonano, M., Fusco, A., Pepe, A., Onorato, G., Berardino, P., 2019. The parallel SBAS approach for sentinel-1 interferometric wide swath deformation time-series generation: Algorithm description and products quality assessment. IEEE Transactions on Geoscience and Remote Sensing 57, 6259–6281.

Martínez-Martínez and Azañón, 1997. Mode' of extensional tectonics in the southeastern Betics (SE Spain): Implications for the tectonic evolution of the peri-Alborn orogenic system. Tectonics 16, 205–225.

Martínez-Martínez, J.M., Booth-Rea, G., Azañón, J.M., Torcal, F., 2006. Active transfer fault zone linking a segmented extensional system (Betics, southern Spain): Insight into heterogeneous extension driven by edge delamination. Tectonophysics 422, 159–173. https://doi.org/https://doi.org/10.1016/j.tecto.2006.06.001

Martínez-García, P., Comas, M., Lonergan, L., Watts, A.B., 2017. From extension to shortening: Tectonic inversion distributed in time and space in the Alboran sea, western Mediterranean. Tectonics 36, 2777–2805.

Martínez-Martínez, J.M., Soto, J.I., Balanyá, J.C., 2002. Orthogonal folding of extensional detachments: structure and origin of the Sierra Nevada elongated dome (Betics, SE Spain). Tectonics 21, 1–3.

Martins, B.H., Suzuki, M., Yastika, P.E., Shimizu, N., 2020. Ground Surface Deformation Detection in Complex Landslide Area—Bobonaro, Timor-Leste—Using SBAS DInSAR, UAV Photogrammetry, and Field Observations. Geosciences 10, 245.

Marzougui, W., Melki, F., Arfaoui, M., Houla, Y., Zargouni, F., 2014. Major faults, salt structures and paleo-ridge at tectonic nodes in Northern Tunisia: contribution of tectonics and gravity analysis. Arabian Journal of Geosciences 8, 7601–7617. https://doi.org/10.1007/s12517-014-1698-y

Masrouhi, A., Bellier, O., Koyi, H., 2014. Geometry and structural evolution of Lorbeus diapir , northwestern Tunisia : polyphase diapirism of the North African inverted passive margin. International Journal of Earth Sciences 103, 881–900. https://doi.org/10.1007/s00531-013-0992-3

Masrouhi, A., Bellier, O., Koyi, H., Vila, J.M., Ghanmi, M., 2013. The evolution of the Lansarine-Baouala salt canopy in the North African cretaceous passive margin in Tunisia. Geological Magazine 150, 835–861. https://doi.org/10.1017/S0016756812000763

Masrouhi, A., Ghanmi, M., Youssef, M. Ben, Vila, J.M., Zargouni, F., 2007. Definition of a thrust nappe with two Palaeogene units in the Lansarine plateau (northern Tunisia): A new structural element of the Tunisian Atlas and revaluation of the Tertiary compression phases. Comptes Rendus - Geoscience 339, 441–448. https://doi.org/10.1016/j.crte.2007.03.007

Masrouhi, A., Koyi, H.A., Masrouhi, A., Koyi, H.A., 2012. Submarine 'salt glacier' of Northern Tunisia, a case of Triassic salt mobility in North African Cretaceous passive margin. Geological Society, London, Special Publications 363, 579–593. https://doi.org/10.1144/SP363.29

Mateos, R.M., Ezquerro, P., Azañón, J.M., Gelabert, B., Herrera, G., Fernández-Merodo, J.A., Spizzichino, D., Sarro, R., García-Moreno, I., Béjar-Pizarro, M., 2018. Coastal lateral spreading in the world heritage site of the Tramuntana Range (Majorca, Spain). The use of PSInSAR monitoring to identify vulnerability. Landslides 15, 797–809.

Mauffret, A., 2007. The Northwestern (Maghreb) boundary of the Nubia (Africa) Plate. Tectonophysics 429, 21–44. https://doi.org/10.1016/j.tecto.2006.09.007

Maury, R.C., Fourcade, S., Coulon, C., Bellon, H., Coutelle, A., Ouabadi, A., Semroud, B., Megartsi, M., Cotten, J., Belanteur, O., 2000. Post-collisional Neogene magmatism of the Mediterranean Maghreb margin: a consequence of slab breakoff. Comptes Rendus de l'Académie Des Sciences-Series IIA-Earth and Planetary Science 331, 159–173.

McClay,& Buchanan, P.G., 1992. Thrust faults in inverted extensional basins. Springer Science & Business Media. https://doi.org/https://doi.org/10.1007/978-94-011-3066-0_8

McClusky, S., Reilinger, R., Mahmoud, S., Ben Sari, D., Tealeb, A., 2003. GPS constraints on Africa (Nubia) and Arabia plate motions. Geophysical Journal International 155, 126–138. https://doi.org/10.1046/j.1365-246X.2003.02023.x

McIntosh, K., Silver, E., Shipley, T., 1993. Evidence and mechanisms for forearc extension at the accretionary Costa Rica Convergent Margin. Tectonics 12, 1380–1392. https://doi.org/10.1029/93TC01792

Mejri, L., Regard, V., Carretier, S., Brusset, S., Dlala, M., 2010a. Evidence of Quaternary active folding near Utique (Northeast Tunisia) from tectonic observations and a seismic profile. Comptes Rendus - Geoscience 342, 864–872. https://doi.org/10.1016/j.crte.2010.06.006

Mejri, L., Regard, V., Carretier, S., Brusset, S., Dlala, M., 2010b. Plissement quaternaire d'Utique (nord-est de la Tunisie) mise en évidence par des observations tectoniques et une ligne sismique. Comptes Rendus - Geoscience 342, 864–872. https://doi.org/10.1016/j.crte.2010.06.006

Melki, F., Alouani, R., Boutib, L., Zargouni, F., & Tlig, S., 2002. Carte géologique de la Tunisie au 1/50.000, la feuille n° 2 de Bizerte. Office National Des Mines, Tunis, Tunisie.

Melki, F., Zouaghi, T., Ben, M., Bdir, M., Zargouni, F., Chelbi, M. Ben, 2012. Role of the NE-SW Hercynian Master Fault Systems and Associated Lineaments on the Structuring and Evolution of the Mesozoic and Cenozoic Basing of the Alpine Margin, Northern Tunisia. Tectonics - Recent Advances 131–168. https://doi.org/10.5772/2620

Melki, F., Zouaghi, T., Chelbi, M. Ben, Bédir, M., Zargouni, F., 2010. Tectono-sedimentary events and geodynamic evolution of the Mesozoic and Cenozoic basins of the Alpine Margin, Gulf of Tunis, north-eastern Tunisia offshore. Comptes Rendus Geoscience 342, 741–753. https://doi.org/10.1016/j.crte.2010.04.005

Melki, F., Zouaghi, T., Harrab, S., Sainz, A.C., Bédir, M., Zargouni, F., 2011. Structuring and evolution of Neogene transcurrent basins in the Tellian foreland domain, north-eastern Tunisia. Journal of Geodynamics 52, 57–69.

Merriman, R.J., Peacor, D.R., 1998. Very low-grade metapelites: mineralogy, microfabrics and measuring reaction progress. Low-grade Metamorphism 10–60.

Merriman, R.J., Roberts, B., 1985. A survey of white mica crystallinity and polytypes in pelitic rocks of Snowdonia and Llŷn, North Wales. Mineralogical Magazine 49, 305–319.

Molin, P., Pazzaglia, F.J., Dramis, F., Molin et al., 2004. Geomorphic expression of active tectonics in a rapidly-deforming forearc, Sila massif, Calabria, southern Italy. American Journal of Science 304, 559–589.

Monié, P., Maluski, H., Saadallah, A., Gaby, R., 1988. New39Ar-40Ar ages of Hercynian and Alpine thermotectonic events in Grande Kabylie (Algeria). Tectonophysics 152, 53–69. https://doi.org/10.1016/0040-1951(88)90029-7

Moragues, L., Rea, G.B., Ruano, P., Azañón, J.M., Gaidi, S., Peña, J.V.P., 2018. Middle Miocene

extensional tectonics in southeast Mallorca Island (Western Mediterranean). Revista de La Sociedad Geologica de Espana 31.

Morata, D., Aguirre, L., Puga, E., 1994. Na-metamorphic pyroxenes in low-grade metabasites from the External Zones of the Betic Cordilleras (southern Spain): influence of rock chemical composition on their formation. Andean Geology 21, 269–283.

Morgan, P., James, D.E., 1989. Heat flow in the earth. Encyclopedia of Solid Earth Geophysics: Van Nostrand Reinhold, New York 634–646.

Mourabit, T., Elenean, K.M.A., Ayadi, A., Benouar, D., Suleman, A. Ben, Abou Elenean, K.M., Ayadi, A., Benouar, D., Ben Suleman, A., Bezzeghoud, M., Cheddadi, A., Chourak, M., ElGabry, M.N., Harbi, A., Hfaiedh, M., Hussein, H.M., Kacem, J., Ksentini, A., Jabour, N., Magrin, A., Maouche, S., Meghraoui, M., Ousadou, F., Panza, G.F., Peresan, A., Romdhane, N., Vaccari, F., Zuccolo, E., 2014. Neo-deterministic seismic hazard assessment in North Africa. Journal of Seismology 18, 301–318. https://doi.org/10.1007/s10950-013-9375-2

Mzali, H., Zouari, H., 2006. Caractérisation géométrique et cinématique des structures liées aux phases compressives de l'Éocène au Quaternaire inférieur en Tunisie : exemple de la Tunisie nord-orientale. Comptes Rendus - Geoscience 338, 742–749. https://doi.org/10.1016/j.crte.2006.05.003

Naouali, B.S., Guellala, R., Bey, S., Inoubli, M.H., 2017. Gravity data contribution for petroleum exploration domain: Mateur case study (Saliferous Province, Northern Tunisia). Arabian Journal for Science and Engineering 42, 339–352.

Negro et al, 2007. Tectonic and metamorphic evolution of the Temsamane units , External Rif (northern Morocco): implications for the evolution of the Rif and the Betic – Rif arc. 164, 829–842.

Nieto, F., 1997. Chemical composition of metapelitic chlorites; X-ray diffraction and optical property approach. Eur J Mineral 9, 829–841.

Nieto, F., Mata, M.P., Bauluz, B., Giorgetti, G., Arkai, P., Peacor, D.R., 2005. Retrograde diagenesis, a widespread process on a regional scale. [Serial] Clay Minerals 40, 93–104.

Nocquet, J.-M., 2012. Present-day kinematics of the Mediterranean: A comprehensive overview of GPS results. Tectonophysics 579, 220–242.

Notti, D., Herrera, G., Bianchini, S., Meisina, C., García-Davalillo, J.C., Zucca, F., 2014. A methodology for improving landslide PSI data analysis. International Journal of Remote Sensing 35, 2186–2214.

Ouazaa, N.L., Casas, L., Álvarez, A., Fouzai, B., Moreno-Vide, M., Vidal, L., Sihem, R.,

Sonzogni, C., Borschneck, D., 2013. Provenance of marble sculptures from the National Museum of Carthage (Tunisia). Journal of Archaeological Science 40, 1602–1610. https://doi.org/https://doi.org/10.1016/j.jas.2012.10.035

Ouchi, S., 1985. Response of alluvial rivers to slow active tectonic movement. Geological Society of America Bulletin 96, 504–515. https://doi.org/10.1130/0016-7606(1985)96<504:ROARTS>2.0.CO;2

Oueslati, A., 1989. Propositions pour une chronologie du Quaternaire continental inférieur et moyen de Tunisie par l'étude de l'arrière-pays du golfe d'Hammamet. , ,. Comptes Rendus de l'Académie Des Sciences. Série 2, Mécanique, Physique, Chimie, Sciences de l'univers, Sciences de La Terre 309, 1833–1838.

Ould Bagga, M.A., Abdeljaouad, S., Mercier, E., 2006. The Tunissian "zone des nappes": a slightly inverted mesocenozoic continental margin (Taberka/Jendouba; northwestern Tunisia). Bulletin de La Société Géologique de France 177, 145–154. https://doi.org/10.2113/gssgfbull.177.3.145

Pánek, T., Hradecký, J., Smolková, V., Šilhán, K., 2008. Gigantic low-gradient landslides in the northern periphery of the Crimean Mountains (Ukraine). Geomorphology 95, 449–473. https://doi.org/10.1016/j.geomorph.2007.07.007

Paskoff, R., Sanlaville, P., 1986. Oscillations climatiques en Tunisie littorale depuis le dernier interglaciaire jusqu'au début de l'Holocène. Quaternaire 23, 78–83.

Pasuto, A., Soldati, M., 2013. 7.25 Lateral Spreading. Treatise on Geomorphology 7, 239–248. https://doi.org/10.1016/B978-0-12-374739-6.00173-1

Pasuto, A., Soldati, M., 1996. En: Landslide recognition: identification, movement and courses (R. Dikau, D. Brunsden, L. Schrott y ML Visen, Eds.).

Pedrera, A., Pérez-Peña, J.V., Galindo-Zaldívar, J., Azañón, J.M., Azor, A., 2009. Testing the sensitivity of geomorphic indices in areas of low-rate active folding (eastern Betic Cordillera, Spain). Geomorphology 105, 218–231. https://doi.org/10.1016/J.GEOMORPH.2008.09.026

Penven, M.-J., Zimmermann, J.-L., 1986. Mise en évidence, par la méthode potassium-argon, d'un âge Langhien pour le plutonisme calco-alcalin de la Kabylie de Collo (Algérie). Comptes Rendus de l'Académie Des Sciences. Série 2, Mécanique, Physique, Chimie, Sciences de l'univers, Sciences de La Terre 303, 403–406.

Pérez-Peña, J.V., Azor, A., Azañón, J.M., Keller, E.A., 2010. Active tectonics in the Sierra Nevada (Betic Cordillera, SE Spain): Insights from geomorphic indexes and drainage pattern analysis. Geomorphology 119, 74–87.

https://doi.org/10.1016/j.geomorph.2010.02.020

Pérez-Peña, J. V., Azañón, J.M., Azor, A., Azan, J.M., Pe, J. V, 2009a. Computers & Geosciences CalHypso : An ArcGIS extension to calculate hypsometric curves and their statistical moments . Applications to drainage basin analysis in SE Spain $. Computers and Geosciences 35, 1214–1223. https://doi.org/10.1016/j.cageo.2008.06.006

Pérez-Peña, J. V., Azañón, J.M., Booth-Rea, G., Azor, A., Delgado, J., 2009b. Differentiating geology and tectonics using a spatial autocorrelation technique for the hypsometric integral. Journal of Geophysical Research: Earth Surface 114, 1–15. https://doi.org/10.1029/2008JF001092

Pérez-Valera, L.A., Rosenbaum, G., Sánchez-Gómez, M., Azor, A., Fernández-Soler, J.M., Pérez-Valera, F., Vasconcelos, P.M., 2013. Age distribution of lamproites along the Socovos Fault (southern Spain) and lithospheric scale tearing. Lithos 180–181, 252–263. https://doi.org/https://doi.org/10.1016/j.lithos.2013.08.016

Perron, J.T., Royden, L., 2013. An integral approach to bedrock river profile analysis. Earth Surface Processes and Landforms 38, 570–576. https://doi.org/10.1002/esp.3302

Perthuisot, V., 1981. Diapirism in northern Tunisia. Journal of Structural Geology 3, 231–235.

Perthuisot, V., 1978. Dynamique et pétrogenèse des extrusions triasiques en Tunisie septentrionale.

Perthuisot, V., 1974. L'ACCIDENT EL ALIA-TEBESSA DANS LA REGION DE TEBOURSOUK.

Perthuisot, V., Rouvier, H., Smati, A., 1998. Style et importance des déformations anté-vraconnienes dans le Maghreb oriental: exemple du diapir du Jebel Sfilata. Bulletin de La Société Géologique de France 8, 389–398.

Piqué, A., Brahim, L.A., Maury, R.C., Bellon, H., Semroud, B., 1998. Le poinçon maghrébin: contraintes structurales et géochimiques. Comptes Rendus de l'Académie Des Sciences-Series IIA-Earth and Planetary Science 326, 575–581.

Piromallo, C., Morelli, A., 2003. *P* wave tomography of the mantle under the Alpine-Mediterranean area. Journal of Geophysical Research: Solid Earth 108, 1–23. https://doi.org/10.1029/2002JB001757

Platt, J.P., 1998. Comment on "Alternating contractional and extensional events in the Alpujarride nappes of the Alboran Domain (Betics, Gibraltar Arc)" by Juan C. Balanyá et al. Tectonics 17, 973–976. https://doi.org/10.1029/1998TC900005

Platt, J.P., Allerton, S., Kirker, A., Mandeville, C., Mayfield, A., Platzman, E.S., Rimi, A., 2003. The ultimate arc: Differential displacement, oroclinal bending, and vertical axis rotation in

the External Betic-Rif arc. Tectonics 22.

Platt, J.P., Vissers, R.L.M., 1989. Extensional collapse of thickened continental lithosphere: A working hypothesis for the Alboran Sea and Gibraltar arc. Geology 17, 540–543. https://doi.org/10.1130/0091-7613(1989)017<0540:ECOTCL>2.3.CO;2

Polonia, A., Torelli, L., Artoni, A., Carlini, M., Faccenna, C., Ferranti, L., Gasperini, L., Govers, R., Klaeschen, D., Monaco, C., Neri, G., Nijholt, N., Orecchio, B., Wortel, R., 2016. The Ionian and Alfeo–Etna fault zones: New segments of an evolving plate boundary in the central Mediterranean Sea? Tectonophysics 675, 69–90. https://doi.org/https://doi.org/10.1016/j.tecto.2016.03.016

Prada, M., Ranero, C.R., Sallarès, V., Zitellini, N., Grevemeyer, I., 2016. Mantle exhumation and sequence of magmatic events in the Magnaghi–Vavilov Basin (Central Tyrrhenian, Italy): New constraints from geological and geophysical observations. Tectonophysics 689, 133–142. https://doi.org/https://doi.org/10.1016/j.tecto.2016.01.041

Puga, E., de Fliert, V., Torres-Roldán, R.L., Sanz de Galdeano, C., 1988. Attempts of whole-rock K/Ar dating of Mesozoic volcanic and hypabissal igneous rocks from the Central Subbetic (Southern Spain): A case of differential Argon loss related to very low-grade metamorphism.

Rabaute, A., Chamot-Rooke, N., 2014. Active tectonics of the Africa–Eurasia boundary from Algiers to Calabria (1/500 000).

Radi, Z., Yelles-Chaouche, A., Corchete, V., Guettouche, S., 2017. Crust and upper mantle shear wave structure of Northeast Algeria from Rayleigh wave dispersion analysis. Physics of the Earth and Planetary Interiors 270, 84–89.

Ramzi, A., Ali, K., Lassaad, C., 2015. Neogene tectonic evolution in Northern Tunisia : case of Chaouat-Mannouba area . Palaeoseismic event associated. 8911–8925. https://doi.org/10.1007/s12517-015-1789-4

Ramzi, A., Lassaad, C., 2017. Superposed folding in the Neogene series of the northeastern Tunisia : precision of the upper Miocene compression and geodynamic significance. International Journal of Earth Sciences 106, 1905–1918. https://doi.org/10.1007/s00531-016-1394-0

Recanati, A., Missenard, Y., Leprêtre, R., Gautheron, C., Barbarand, J., Abbassene, F., Abdallah, N., Ouabadi, A., Derder, M.E.M., Boukari, C., Pinna-Jamme, R., Haurine, F., 2019. A Tortonian onset for the Algerian margin inversion: Evidence from low-temperature thermochronology. Terra Nova 31, 39–48. https://doi.org/10.1111/ter.12367

Redhaounia, B., Aktarakçi, H., Ilondo, B.O., Gabtni, H., Khomsi, S., Bédir, M., 2015. Hydro-

geophysical interpretation of fractured and karstified limestones reservoirs: A case study from Amdoun region (NW Tunisia) using electrical resistivity tomography, digital elevation model (DEM) and hydro-geochemical approaches. Journal of African Earth Sciences 112, 328–338.

Research group for lithospheric structure in Tunisia, n.d. Research group for lithospheric structure in Tunisia (1992). Tectonophy, 245–267.

Reston, T.J., Leythaeuser, T., Booth-Rea, G., Sawyer, D., Klaeschen, D., Long, C., 2007. Movement along a low-angle normal fault: The S reflector west of Spain. Geochemistry, Geophysics, Geosystems 8. https://doi.org/10.1029/2006GC001437

Riahi.S, M., Kamel, B., Ismail, B., Kmar, L., Stow, D., Sami, K., Mourad, B., Kmar, B.I.L., Stow, D., Sami, K., Mourad, B., 2010. Stratigraphy, sedimentology and structure of the Numidian Flysch thrust belt in northern Tunisia. Journal of African Earth Sciences 57, 109–126. https://doi.org/10.1016/j.jafrearsci.2009.07.016

Riahi, S., 2010. Paleogeographic and geodynamic Miocene evolution of the Tunisian Tell (Numidian and Post-Numidian Successions): bearing with the Maghrebian Chain. 831–855. https://doi.org/10.1007/s00531-012-0824-x

Riahi, S., Riahi,Sami, Soussi, M., Kamel, B., Ismail, B., Kmar, L., Stow, D., Sami, K., Mourad, B., Kmar, B.I.L., Stow, D., Sami, K., Mourad, B., Belayouni, H., Guerrera, F., Martı, M., Riahi, S., Soussi, M., Ben, K., Lattrache, I., 2010. AGE , IN TER NAL STRATI GRAPHIC AR CHI TEC TURE AND STRUC TURAL STYLE OF THE OLIGOCENE – MIO CENE NU MIDI AN FOR MA TION OF NORTH ERN TUNISIA. Journal of African Earth Sciences 85, 345–370. https://doi.org/10.1016/j.jafrearsci.2009.07.016

Riahi, S., Soussi, M., Lattrache, K.B.I., 2015. Age, internal stratigraphic architecture and structural style of the Oligocene–Miocene Numidian Formation of northern Tunisia. Annales Societatis Geologorum Poloniae. 345–370.

Röder, G., 1988. Numidian Marble and Some of its Specialities. In: Herz, N., Waelkens, M. (Eds.), Classical Marble: Geochemistry, Technology, Trade. Springer Netherlands, Dordrecht, 91–96. https://doi.org/10.1007/978-94-015-7795-3_10

Rodríguez-Fernández, J., Roldán, F.J., Azañón, J.M., García-Cortés, A., 2013. El colapso gravitacional del frente orogénico alpino en el Dominio Subbético durante el Mioceno medio-superior: El Complejo Extensional Subbético. Bol. Geol. Min 124, 477–504.

Rodríguez-Fernández, J., Azor, A., Miguel Azañón, J., 2011. The Betic intramontane basins (SE spain): stratigraphy, subsidence, and tectonic history. Tectonics of Sedimentary Basins: Recent Advances 461–479.

Roure, F., Casero, P., Addoum, B., 2012. Alpine inversion of the North African margin and delamination of its continental lithosphere. Tectonics 31, 1–28. https://doi.org/10.1029/2011TC002989

Rouvier, 1977, 1977. Géologie de l'extrême Nord-Tunisien: tectoniques et paléogéographie superposées à l'extrémité orientale de la chaîne Nord-Maghrebine. Unpublished PhD thesis. Université Pierre et Marie Curie.Paris, 856 France.

Rouvier, H., 1993. Carte géologique de la Tunisie au 1/50.000, la feuille n◦ 24 de Fernena.Tunis, Tunisie. Office National Des Mines.

Rouvier, H., 1992. Carte géologique de la Tunisie au 1/50.000, la feuille n◦ 19 d'Ain Drahem.Tunis, Tunisie. Office National Des Mines.

Rouvier, H., 1990. Carte géologique de la Tunisie au 1/50.000, la feuille n° 17 de Zahret Medien. Office National Des Mines, Tunis, Tunisie.

Rouvier, H., 1987. Carte géologique de la Tunisie au 1/50.000, la feuille n° 10 de Nefza. Office National Des Mines, Tunis, Tunisie.

Rouvier, H., 1977. Gelogie de l'Extreme-Nord tunisien: tectoniques et paleogeographies superposees a l'extremite orientale de la chaine nord-maghrebine. These Doctorat Es Sc., Univ. Pierre et Marie Curie.

Ruano, P., 2004. Striated and pitted pebbles as paleostress markers : an example from the central transect of the Betic Cordillera (SE Spain). Tectonophysics 379, 183–198. https://doi.org/10.1016/j.tecto.2003.11.001

Saadallah, A., Caby, R., 1996. Alpine extensional detachment tectonics in the Grande Kabylie metamorphic core complex of the Maghrebides (northern Algeria). Tectonophysics 267, 257–273. https://doi.org/10.1016/S0040-1951(96)00101-1

Sàbat, F., Gelabert, B., Rodríguez-Perea, A., Giménez, J., 2011. Geological structure and evolution of Majorca: Implications for the origin of the Western Mediterranean. Tectonophysics 510, 217–238.

Saïd, A., Baby, P., Chardon, D., Ouali, J., 2011a. Structure, paleogeographic inheritance, and deformation history of the southern Atlas foreland fold and thrust belt of Tunisia. Tectonics 30.

Saïd, A., Chardon, D., Baby, P., Ouali, J., 2011b. Active oblique ramp faulting in the Southern Tunisian Atlas. Tectonophysics 499, 178–189. https://doi.org/10.1016/j.tecto.2011.01.010

Salaj, J., B. Van Houten, F., 1988. Cenozoic palaeogeographic development of northern Tunisia, with special reference to the stratigraphic record in the miocene trough. Palaeogeography, Palaeoclimatology, Palaeoecology 64, 43–57. https://doi.org/https://doi.org/10.1016/0031-

0182(88)90141-1

Sami, R., Soussi, M., Kamel, B., Kmar, B.I.L., Stow, D., Sami, K., Mourad, B., 2010. Stratigraphy, sedimentology and structure of the Numidian Flysch thrust belt in northern Tunisia. Journal of African Earth Sciences 57, 109–126.

Sassi, F.P., Scolari, A., 1974. The bo value of the potassium white micas as a barometric indicator in low-grade metamorphism of pelitic schits. Contributions to Mineralogy and Petrology 45, 143–152.

Savelli, C., 2002. Time–space distribution of magmatic activity in the western Mediterranean and peripheral orogens during the past 30 Ma (a stimulus to geodynamic considerations). Journal of Geodynamics 34, 99–126.

Schumm, S.A., Dumont, J.F., Holbrook, J.M., 2000. Active tectonics and alluvial rivers. Cambridge university press Cambridge.

Scotti, V.N., Molin, P., Faccenna, C., Soligo, M., Casas-sainz, A., 2014. Geomorphology The in fl uence of surface and tectonic processes on landscape evolution of the Iberian Chain (Spain): Quantitative geomorphological analysis and geochronology. Geomorphology 206, 37–57. https://doi.org/10.1016/j.geomorph.2013.09.017

Seitz, S.M., Curless, B., Diebel, J., Scharstein, D., Szeliski, R., 2006. A comparison and evaluation of multi-view stereo reconstruction algorithms. 2006 IEEE Computer Society Conference on Computer Vision and Pattern Recognition (CVPR'06). IEEE, 519–528.

Selverstone, J., 1988. Evidence for east-west crustal extension in the Eastern Alps: Implications for the unroofing history of the Tauern window. Tectonics 7, 87–105. https://doi.org/10.1029/TC007i001p00087

Semyonov, D., 2011. Algorithms used in photoscan. Agisoft PhotoScan Forum.

Sibson, R.H., 1987. Earthquake rupturing as a mineralizing agent in hydrothermal systems. Geology 15, 701–704. https://doi.org/10.1130/0091-7613(1987)15<701:ERAAMA>2.0.CO;2

Siddiqui, S., Soldati, M., 2014. Appraisal of active tectonics using DEM-based hypsometric integral and trend surface analysis in Emilia-Romagna Apennines, northern Italy. Turkish Journal of Earth Sciences 23, 277–292. https://doi.org/10.3906/yer-1306-12

Soldati, M., Devoto, S., Prampolini, M., Pasuto, A., 2019. The spectacular landslide-controlled landscape of the northwestern coast of Malta. Landscapes and Landforms of the Maltese Islands. Springer, 167–178.

Soumaya, A., Ayed, N. Ben, Rajabi, M., Meghraoui, M., Ben Ayed, N., Rajabi, M., Meghraoui, M., Delvaux, D., Kadri, A., Ziegler, M., Maouche, S., Braham, A., 2018. Active Faulting

Geometry and Stress Pattern Near Complex Strike-Slip Systems Along the Maghreb Region : Constraints on Active Convergence in the Western Mediterranean. Tectonics 37, 3148–3173. https://doi.org/10.1029/2018TC004983

Soumaya, A., Ben Ayed, N., Delvaux, D., Ghanmi, M., 2015. Spatial variation of present-day stress field and tectonic regime in Tunisia and surroundings from formal inversion of focal mechanisms: Geodynamic implications for central Mediterranean. Tectonics 34, 1154–1180. https://doi.org/10.1002/2015TC003895

Soumaya, A., Ben Ayed, N., Khayati Ammar, H., Tayech, M., Ghanmi, M., 2016. Seismotectonic and seismic hazard map of Tunisia. AGU Fall Meeting Abstracts. T13A-2672.

Soumaya, A., Kadri, A., Ben Ayed, N., Kim, Y.-S., Dooley, T.P., Rajabi, M., Braham, A., 2020. TEMPORARY REMOVAL: Deformation styles related to intraplate strike-slip fault systems of the Saharan-Tunisian Southern Atlas (North Africa): New kinematic models. Journal of Structural Geology 104175. https://doi.org/https://doi.org/10.1016/j.jsg.2020.104175

Spakman, W., Chertova, M. V, van den Berg, A., van Hinsbergen, D.J.J., 2018. Puzzling features of western Mediterranean tectonics explained by slab dragging. Nature Geoscience 11, 211–216.

Spakman, W., Wortel, R., 2004. A tomographic view on western Mediterranean geodynamics. The TRANSMED Atlas-The Mediterranean Region from Crust to Mantle 31–52. https://doi.org/10.1007/978-3-642-18919-7_2

Strahler, A.N., 1952. Geological Society of America Bulletin. https://doi.org/10.1130/0016-7606(1952)63

Strzerzynski, P., Déverchère, J., Cattaneo, A., Domzig, A., Yelles, K., Mercier de Lépinay, B., Babonneau, N., Boudiaf, A., 2010. Tectonic inheritance and Pliocene-Pleistocene inversion of the Algerian margin around Algiers: Insights from multibeam and seismic reflection data. Tectonics 29.

Talbi, F., Jaafari, M., Tlig, S., 2005. Magmatisme néogène de la Tunisie septentrionale: pétrogénèse et événements géodynamiques. Revista de La Sociedad Geologica de España 18, 241–252.

Thiele, S.T., Grose, L., Samsu, A., Micklethwaite, S., Vollgger, S.A., Cruden, A.R., 2017. Rapid, semi-automatic fracture and contact mapping for point clouds, images and geophysical data. Solid Earth 8, 1241–1253.

Tricart, P., Torelli, L., Argnani, A., Rekhiss, F., Zitellini, N., 1994. Extensional collapse related to compressional uplift in the Alpine Chain off northern Tunisia (Central Mediterranean).

Tectonophysics 238, 317–329.

Troudi, H., Tari, G., Alouani, W., Cantarella, G., 2017. Styles of Salt Tectonics in Central Tunisia : An Overview, Permo-Triassic Salt Provinces of Europe, North Africa and the Atlantic Margins: Tectonics and Hydrocarbon Potential. Elsevier Inc. https://doi.org/10.1016/B978-0-12-809417-4.00026-4

Ullman, S., 1979. The interpretation of visual motion. Massachusetts Inst of Technology Pr.

Van der Beek, P., & Braun, J., 1998. Numerical modelling of landscape evolution on geological time-scales: A parameter analysis and comparison with the southeastern highlands of Australia. , ,. Basin Research 10(1), 49-68.

van der Meer, D.G., van Hinsbergen, D.J.J., Spakman, W., 2018. Atlas of the underworld: Slab remnants in the mantle, their sinking history, and a new outlook on lower mantle viscosity. Tectonophysics 723, 309–448. https://doi.org/https://doi.org/10.1016/j.tecto.2017.10.004

van Hinsbergen et al, 2014. Origin and consequences of western Mediterranean subduction, rollback, and slab segmentation. 393–419. https://doi.org/10.1002/tect.20125.Received

Vidal, O., Lanari, P., Muñoz, M., Bourdelle, F., de Andrade, V., 2016. Deciphering temperature, pressure and oxygen-activity conditions of chlorite formation. Clay Minerals 51, 615–633. https://doi.org/10.1180/claymin.2016.051.4.06

Vila et al, 1996. A large submarine middle Albian "'salt glacier'" in north-western Tunisia (250 km(2): The Triassic rocks of Ben Gasseur " 'diapir'" and of El Kef anticline. Cr Acad Sci Ii A 322(3), 221–227.

Vila, J.M., 1995. First Terrestrial Study of a Large Submarine Salt Glacier - the Eastern Part of the Ouenza-Ladjebel-Meridef Structure (Algerian Tunisian Confines) - Proposal for an Emplacement Scenario and Comparisons. B Soc Geol Fr 166(2), 149–167.

Vila, J.M., Ghanmi, M., Ben Youssef, M., Jouirou, M., 2002. Les 'glaciers de sel'sous marins des marges continentales passives du nord-est du Maghreb (Algérie-Tunisie) et de la Gulf Coast (USA): comparaisons, nouveau regard sur les "glaciers de sel" composites, illustré par celui de Fedj el Adoum (Nord-Ouest tunis. Eclogae Geologicae Helvetiae 95, 347–380.

Wang, Y., Zheng, D., Pang, J., Zhang, H., Wang, W., Yu, J., Zhang, Z., Zheng, W., Zhang, P., Li, Y., 2018. Using slope-area and apatite fission track analysis to decipher the rock uplift pattern of the Yumu Shan: New insights into the growth of the NE Tibetan Plateau. Geomorphology 308, 118–128. https://doi.org/10.1016/j.geomorph.2018.02.006

Warr, L.N., Ferreiro-Mahlmann, R., 2015. Recommendations for Kübler Index standardization. Clay Minerals 50, 283–286. https://doi.org/10.1180/claymin.2015.050.3.02

Warr, L.N., Rice, A.H.N., 1994. Interlaboratory standardization and calibration of clay mineral

crystallinity and crystallite size data. Journal of Metamorphic Geology 12, 141–152.

Whipple, K.X., DiBiase, R.A., Crosby, B.T., 2013. Bedrocks Rivers. Treatise on Geomorphology 9, 550–573. https://doi.org/10.1016/B978-0-12-374739-6.00254-2

Whipple, K.X., Tucker, G.E., 1999. Dynamics of the stream-power river incision model: Implications for height limits of mountain ranges, landscape response timescales, and research needs. Journal of Geophysical Research: Solid Earth 104, 661–674. https://doi.org/10.1029/1999jb900120

Willett, S.D., McCoy, S.W., Perron, J.T., Goren, L., Chen, C.Y., 2014. Dynamic reorganization of river basins. Science 343, 1248765. https://doi.org/10.1126/science.1248765

Willgoose, C., Hancock, G., Willgoose, G., Hancock, G., 1998. REVISITING THE HYPSOMETRIC CURVE AS AN INDICATOR OF FORM AND PROCESS IN TRANSPORT-LIMITED CATCHMENT. Earth Surface Processes and Landforms 623, 611–623. https://doi.org/10.1002/(SICI)1096-9837(199807)23:7<611::AID-ESP872>3.0.CO;2-Y

Wobus, C., Whipple, K.X., Kirby, E., Snyder, N., Johnson, J., Spyropolou, K., Crosby, B., Sheehan, D., 2006. Tectonics from topography: procedurses, promise, and pitfalls. Geological Society of America Special Paper 398, 55–74. https://doi.org/10.1130/2006.2398(04).

Wortel and Spakman, 2000. Subduction and Slab Detachment in the Mediterranean-Carpathian Region. Geophysics.

Zargouni, F. et Ruhland, M., 1981. Style de déformation du Quaternaire récent lié au coulissement de la faille de Gafsa et chronologie des phases tectoniques de l'Atlas méridional tunisien. CR Acad. Sci. Paris 292, 912-915.

Zargouni.F, 1984. Style et chronologie des déformations des structures de l'Atlas tunisien méridional, évolution récente de l'accident sud-atlasique. C. R. Acad, 71– 76.

Zargouni, F., 1978. Analyse structurale de la chaîne de Lansarine (zone des diapirs, Atlas tunisien). Bulletin de La Société Des Sciences Naturelles, Tunisie 13, 97–104.

Zitellini, N., Ranero, C.R., Loreto, M.F., Ligi, M., Pastore, M., D'Oriano, F., Sallares, V., Grevemeyer, I., Moeller, S., Prada, M., 2020. Recent inversion of the Tyrrhenian Basin. Geology 48, 123–127. https://doi.org/10.1130/G46774.1

Zouaghi, T., Bédir, M., Melki, F., Gabtni, H., Gharsalli, R., Bessioud, A., Zargouni, F., 2011. Neogene sediment deformations and tectonic features of northeastern Tunisia: evidence for paleoseismicity. Arabian Journal of Geosciences 4, 1301–1314. https://doi.org/10.1007/s12517-010-0225-z